Universidade de Aveiro Departamento de Biologia
2011

Maria Fátima da Fonseca

Carbapenemases de *Serratia fonticola* UTAD54

Carbapenemases of *Serratia fonticola* UTAD54

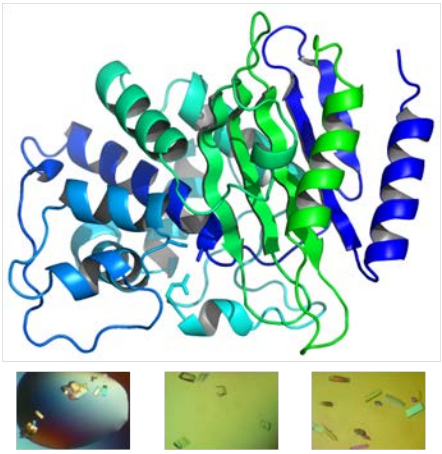

Universidade de Aveiro Departamento de Biologia
2011

Maria Fátima da Fonseca

Carbapenemases de *Serratia fonticola* UTAD54

Dissertação apresentada à Universidade de Aveiro para cumprimento dos requisitos necessários à obtenção do grau de Doutor em Bioquímica, realizada sob a orientação científica do Prof. Doutor António Carlos Matias Correia, Professor Catedrático do Departamento de Biologia da Universidade de Aveiro e do Prof. Doutor James Spencer, Professor do Department of Cellular and Molecular Medicine da Universidade de Bristol (UK).

Apoio financeiro do POPH-QREN, comparticipado pelo FSE, através da Bolsa de Doutoramento da FCT com a referência SFRH/BD/30490/2006

UNIÃO EUROPEIA
Fundo Social Europeu

PROGRAMA OPERACIONAL POTENCIAL HUMANO

To my husband for his endless love and care.

o júri

Presidente

Prof. Doutor José Carlos da Silva Neves
professor Catedrático do Departamento de Electrónica da Universidade de Aveiro

Prof. Doutor Jean-Denis Docquier
professore Aggregato do Dipartimento di Biotecnologie da Universidade de Siena

Prof. Doutor Francisco Manuel Lemos Amado
professor Associado do Departamento de Química da Universidade de Aveiro

Prof. Doutora Ana Cristina de Fraga Esteves
professora Auxiliar Convidada do Departamento de Biologia da Universidade de Aveiro

Doutor João Morais-Cabral
investigador Principal do Instituto de Biologia Molecular e Celular da Universidade do Porto

Prof. Doutora Maria José Félix Saavedra
professora Associada com Agregação do Departamento de Ciências Veterinárias da Universidade de Trás-os-Montes e Alto Douro

Prof. Doutor James Spencer
professor da School of Cellular and Molecular Medicine da Universidade de Bristol

Prof. Doutor António Carlos Matias Correia
professor Catedrático do Departamento de Biologia da Universidade de Aveiro

agradecimentos

I feel this is the last part of a long but, at the same time, remarkable journey.

This project was developed in the Department of Biology at University of Aveiro and in the School of Cellular and Molecular Medicine at University of Bristol. I wish to thank both Institutions and their staff for providing me access to their facilities, and FCT for funding this work (PhD grant SFRH/BD/30490/2006).

During these years I have met and worked with numerous people and therefore there are many to thank for valuable help and support.

I am deeply grateful to my supervisors, Dr. António Correia and Dr. James Spencer who offered me the opportunity to work in this project.
I would like to thank Dr. António Correia for his encouragement, constant enthusiasm and guidance, and Dr. James Spencer for introducing me the field of protein crystallography, his extensive knowledge and valuable advice, as well as his careful reading of this dissertation.
In addition, I enjoyed their kindness and patience; they never quit believing in my ability to accomplish this task, even when I doubted it myself.
Also important, I thank their friendship.

I would like to acknowledge my colleagues and friends in the lab during the years, for the wonderful atmosphere lived there and for supporting me whenever I needed.

I am particularly indebted to Isabel who helped in many ways and shared her knowledge of molecular biology, and to Cristina, who introduced me the amazing protein world, for helpful discussions and suggestions.

I am as well thankful to my colleagues and friends from D60 and C-floor in Bristol, for their generous help and support in the lab, and Alex, Zoe and Aisha for the great moments outside the lab.

Further, I wish to express my gratitude to all the collaborators of this project and co-authors of my manuscripts for their great assistance and skilful comments that greatly contributed to the improvement of this work. I would like to thank Chris Arthur (University of Bristol), and Bart Samyn and Pablo Moerman (Ghent University) for performing mass spectrometry and protein sequencing experiments, and Beth Bromley (University of Bristol) for assisting me with the CD measurements.

Also my friends who have accompanied me throughout the years were important to my success ... Thank you all! I will never forget Madams coffee break; it was revitalizing and helped keeping me sane (as possible).

The most special thanks is to my family for their unconditional love, kindness and encouragement during the years of my study, and particularly to my husband Fernando for his endless love, enduring support and understanding through all the time of my absence and the preparation of this dissertation.

palavras-chave

Beta-lactamases, mecanismos de resistência a antibióticos, antibióticos β-lactâmicos, carbapenemos, metalo-β-lactamases, carbapenemases.

resumo

As carbapenemases, serínicas e metalo-β-lactamases (MBLs), formam um grupo cada vez mais importante de β-lactamases capazes de tornar as bactérias resistentes a antibióticos β-lactâmicos, incluindo carbapenemos utilizados como antibióticos de último recurso no tratamento de infecções causadas por bactérias multirresistentes. De modo a compreender melhor a relação estrutura-função deste grupo de enzimas, prosseguimos com a caracterização bioquímica e estrutural das carbapenemases SFC-1 e Sfh-I específicas de *Serratia fonticola* UTAD54, uma estirpe ambiental isolada previamente de águas de consumo não tratadas no Nordeste de Portugal. Ambas as β-lactamases foram sobre-expressas em *Escherichia coli* e purificadas por cromatografia líquida. A SFC-1 recombinante, uma carbapenemase serínica, hidrolisa eficientemente antibióticos β-lactâmicos de todas as classes e exibe, comparativamente a enzimas relacionadas (ex. KPC), uma maior eficiência contra a ceftazidima e uma menor susceptibilidade aos inibidores convencionais das β-lactamases. As estruturas do cristal da SFC-1 nativa e de complexos de mutantes, obtidos por mutagénese dirigida, com o meropenemo não hidrolisado e na forma de acetilenzima foram determinados por substituição molecular utilizando cristalografia de raios-X. A estrutura da SFC-1 contém todas as características conservadas do centro activo das carbapenemases de classe A. Nas estruturas dos mutantes o meropenemo aparece orientado no centro activo por Thr236 e Thr238, posicionando-o próximo da Ser130 para a transferência do protão. Nas enzimas de classe A inibidas por carbapenemos, a interacção com a Arg244 impõe uma orientação diferente do meropenemo ligado, prejudicando a transferência do protão. Estas constituem as primeiras estruturas de uma carbapenemase de classe A com um carbapenemo no centro activo e revelam que estas enzimas alteram a orientação do meropenemo ligado para promover a catálise, sem alteração significativa da estrutura geral. A Sfh-I, tal como as outras MBLs da subclasse B2, apresenta um perfil de substratos reduzido, que inclui maioritariamente os carbapenemos. A Sfh-I hidrolisa imipenemo e meropenemo com um k_{cat} de 51 e 109 s^{-1} e um K_M de 79 e 215 μM, respectivamente. A Sfh-I liga um equivalente de zinco, como demonstrado por espectrometria de massa. Contrariamente a enzimas da subclasse B2 previamente caracterizadas, a Sfh-I hidrolisa a cefepima, mostrando que a Sfh-I é uma MBL da subclasse B2 com propriedades únicas. Por espectroscopia de fluorescência mostrou-se que a Sfh-I é capaz de ligar até 3 equivalentes de zinco (K_{d2} = 95 μM; K_{d3} = 2.3 mM). A estrutura do cristal da Sfh-I, determinada por substituição molecular utilizando a CphA como modelo, é a primeira para uma MBL da subclasse B2 não ligada. Esta estrutura revela a disposição das moléculas de água no centro activo corroborando um mecanismo catalítico para as MBLs da subclasse B2 no qual a His118, em vez do Asp120 proposto anteriormente, activa a molécula de água nucleofílica.

keywords

Beta-lactamases, antibiotic resistance mechanisms, β-lactam antibiotics, carbapenems, metallo-β-lactamases, carbapenemases.

abstract

Carbapenemases, both serine and metallo-β-lactamases (MBLs) constitute an increasingly important group of β-lactamases that render bacteria resistant to β-lactam-containing antibiotics, including carbapenems used as last resort antibiotics in treatment of multidrug resistant bacteria. In order to better understand the structure-function relationship among this group of enzymes we pursued the biochemical and structural characterization of SFC-1 and Sfh-I both carbapenemases specific to *Serratia fonticola* UTAD54, an environmental strain previously isolated from untreated drinking waters in Northeast Portugal. Both β-lactamases were over-expressed in *Escherichia coli* and purified by liquid chromatography.

Recombinant SFC-1, a serine carbapenemase, efficiently hydrolyses β-lactams of all classes and exhibits, as compared to related enzymes (e.g. KPC), an increased activity towards ceftazidime but a decreased sensitivity to conventional β-lactamase inhibitors. Crystal structures of wild-type SFC-1 and of complexes of site-directed mutants with the meropenem in unhydrolysed and acylenzyme intermediate forms were solved by molecular replacement using X-ray crystallography. Wild-type SFC-1 has all the conserved features of the class A carbapenemases active site. In the mutants structures meropenem is shown to be oriented in the active site by Thr236 and Thr238, placing it close to Ser130 for proton transfer. In the carbapenem-inhibited class A enzymes interaction with Arg244 imposes a different orientation on bound meropenem, impairing proton transfer. These first structures of a class A carbapenemase with bound carbapenem reveal that these enzymes change the orientation of bound meropenem to promote catalysis, without gross distortion of overall structure.

Sfh-I, like other subclass B2 MBLs, has a narrow substrate profile which mostly include carbapenems. Sfh-I hydrolyses imipenem and meropenem with a k_{cat} of 51 and 109 s^{-1} and K_M of 79 and 215 μM, respectively. Purified Sfh-I binds one equivalent of zinc, as shown by mass spectrometry. Unlike previously characterised subclass B2 enzymes, Sfh-I hydrolyzes cefepime showing that Sfh-I is a subclass B2 MBL with unique properties. Fluorescence spectroscopy shows that Sfh-I is able to bind up to 3 zinc equivalents (K_{d2} = 95 μM; K_{d3} = 2.3 mM). The Sfh-I crystal structure, solved by molecular replacement using CphA as search model, is the first of an unliganded B2 MBL. This structure reveals the disposition of water molecules in the active site supporting a catalytic mechanism for subclass B2 MBLs in which His118, rather than the previously proposed Asp120, activates the nucleophilic water molecule.

CONTENTS

CHAPTER 1: GENERAL INTRODUCTION

CHAPTER 2: SCOPE OF THIS DISSERTATION

CHAPTER 3: BIOCHEMICAL CHARACTERISATION OF RECOMBINANT SFC-1

CHAPTER 4: CRYSTALLOGRAPHIC STRUCTURE OF SFC-1: INSIGHTS INTO CARBAPENEMASE ACTIVITY IN CLASS A β-LACTAMASES

CHAPTER 5: OVER-EXPRESSION, PURIFICATION AND BIOCHEMICAL CHARACTERISATION OF Sfh-I

CHAPTER 6: STRUCTURAL CHARACTERISATION OF Sfh-I: EVIDENCE FOR CATALYTIC MECHANISM IN SUBCLASS B2 MBLs

PUBLICATIONS

Most results of the work here presented have been published (or waiting for publication) in the following articles:

Fonseca F., Sarmento A. C., Henriques I., Samyn B., van Beeumen J., Domingues P., Domingues M. R., Saavedra M. J., and Correia A. (2007) Biochemical characterization of SFC-1, a class A carbapenem-hydrolyzing β-lactamase. Antimicrobial Agents and Chemotherapy. 51: 4512-4514.

Fonseca F., Correia A., and Spencer J. High resolution crystal structures of SFC-1 and acyl-intermediate in complex with meropenem: structural basis for carbapenemase activity in class A β-lactamases (manuscript in preparation).

Fonseca F., Arthur C. J., Bromley E. C. H., Samyn B., Moerman P., Saavedra M. J., Correia A, and Spencer J. Biochemical characterization of Sfh-I, the subclass B2 metallo-β-lactamase from *Serratia fonticola* UTAD54. Antimicrobial Agents and Chemotherapy (accepted for publication).

Fonseca F., Bromley E. C. H., Saavedra M. J., Correia A., and Spencer J. Crystal structure of *Serratia fonticola* Sfh-I: activation of the nucleophile in the catalytic mechanism of mono-zinc metallo-β-lactamases. Journal of Molecular Biology (in press).

LIST OF FIGURES

LIST OF TABLES

ABBREVIATIONS

CD	Circular dichroism
DAP	Diaminopimelate
EDTA	Etilenodiaminotetracetic acid
ESBLs	Extended spectrum β-lactamases
EXAFS	Extended X-Ray Absorption Fine Structure
GES	Guiana extended spectrum
HEPES	N-(2-hydroxyethyl)-piperazine-N'-2-ethanesulfonic acid
HPLC	High-performance liquid chromatography
IPTG	Isopropyl β-D-1-thiogalactopyranoside
IRTs	Inhibitor resistant TEMs
KPC	*Klebsiella pneumoniae* carbapenemase
LB	Luria-Bertani
MBLs	Metallo-β-lactamases
MES	2-(N-morpholino)ethanesulfonic acid
MIC	Minimal inhibitory concentration
NAG	N-acetylglucosamine
NAM	N-acetylmuramic acid
OD	Optical density
OMPs	Outer membrane proteins
PBP	Penicillin binding protein
PCR	Polimerase chain reaction
PDB	Protein Data Bank

PEG	poly (ethylene glycol)
pI	Isoelectric point
PTH	Phenylthiohydantoin
QM−MM	Quantum mechanics − molecular mechanics
r.m.s.d.	Root mean square deviation
RND	Resistance nodulation division
Rpm	Rotations per minute
SDS	Sodium dodecyl sulfate
SDS-PAGE	Sodium dodecyl sulfate polyacrylamide gel electrophoresis
TEM	Temoniera β-lactamase
TEMED	n', n', n', n'- Tetramethylethylenediamine
Tris	tris(hydroxymethyl)aminomethane
WT	Wild-type

1. General Introduction

1.1 Antimicrobial agents and bacterial resistance

"Antibiotics, compounds that are literally "against life", are typically antibacterial drugs that interfere with some structure or process that is essential to bacterial growth or survival without harming the eukaryotic host that harbour's the bacterial infection" (WALSH, 2000). Introduced in human therapy for more than 60 years, antibiotics constitute one of the most important medical inventions, reducing human morbidity and mortality.

Antibiotics display differing modes of action. They are considered to be bactericides if they effectively kill bacteria or bacteriostatic if the ability of the bacterium to grow is impaired. There are several classes of antimicrobials available to clinicians. These compounds can target vital microbial processes such as cell wall biosynthesis (e.g. β-lactam antibiotics and glycopeptides such as vancomycin), protein synthesis (e.g. aminoglycosides, tetracyclines, macrolides) and bacterial DNA replication and repair (e.g. fluoroquinolones, rifampicin) (LEVY and MARSHALL, 2004; WALSH, 2000).

Antimicrobials have been successfully employed for therapy of bacterial infections for more than six decades, leading to a rise in average life expectancy in the last century. However their use is now threatened by the emergence of resistant pathogenic strains. Antibiotic resistance is now well recognized as a major problem in the treatment of infections in hospitals and, with increasing and alarming frequency, in the community (LEVY and MARSHALL, 2004; LIVERMORE, 2007).

Antibiotic resistance confers an advantage for bacterial survival. Resistant bacteria are selected by exposure to antibiotics as a product of Darwinian selection: resistant strains are selected while susceptible strains are inhibited or eliminated (SYKES, 2010). In order to survive an organism has to be intrinsically resistant or acquire resistance after the introduction of drugs in the bacterial environment (LEVY and MARSHALL, 2004; MAZEL and DAVIES, 1999). Intrinsic resistance means that each member of an entire bacterial group (genus or species) is resistant without any additional genetic alteration. For example, in Gram-negative bacteria the presence of a relatively impermeable outer membrane is a barrier to antibiotics such as glycopeptides and macrolides, making these bacteria intrinsically resistant to these drugs (WRIGHT and BEGLEY, 2007). Also mycoplasma bacteria, lacking a cell wall, are intrinsically resistant to β-lactam antibiotics as well as other antibiotics targeting the cell wall components (BEBEAR and PEREYRE, 2005). On the other hand,

resistance to antibiotics can result from selection of spontaneous mutations that lead to activation or modification of chromosomal determinants or from acquisition of resistance genes localized on mobile genetic elements (FROST *et al.*, 2005) such as transposons, plasmids (BENNETT, 2008), and ISCR elements (TOLEMAN *et al.*, 2006), which can be exchanged among bacteria of a wide range of genera. Although they are not considered to be mobile genetic elements, integrons (HALL and COLLIS, 1998) also play an important role in the transfer and dissemination of resistance genes and are most often associated with mobile genetic elements (MOURA *et al.*, 2010). The rapid generation time of bacteria allows them to evolve quickly, becoming resistant to antimicrobials within a short time of their introduction (SYKES, 2010; WRIGHT and BEGLEY, 2007).

Although used in human therapy, antimicrobial drugs are also used inappropriately in animal husbandry for prophylaxis, chemotherapy and growth promotion (COLLIGNON, 2004; WEGENER, 2003; WITTE, 1998). The ultimate fate of these drugs is the soil and aquatic environments (ALLEN *et al.*, 2010; XI *et al.*, 2009) where bacteria can exchange their genetic material through horizontal gene transfer (FROST *et al.*, 2005). Selective pressure can promote the transmission of resistant traits to pathogenic bacteria and ultimately to humans via the food chain (QIN *et al.*, 2006; RHODES *et al.*, 2000).

Antibiotic use by humans plays an important role in selection and evolution of resistance in pathogenic bacteria. However antibiotic resistance genes are likely to have originated in natural microbial communities (DAVIES, 1994). Indeed, many antibiotics are produced by environmental strains (NAGARAJAN *et al.*, 1971; SYKES *et al.*, 1981) so it is possible that these organisms could be the origin of antibiotic resistance genes, used to protect themselves from the antimicrobials they produce (PANG *et al.*, 1994; TAHLAN *et al.*, 2007).

Recent studies by D'Costa and collaborators (2006) and Dantas and colleagues (2008) have demonstrated that soil bacteria are both antibiotic producers that are resistant to antimicrobials, and sources of resistance determinants. Moreover the antibiotics tested included not only "older" compounds but also some that have been just recently approved and resistance was observed to all antibiotics in these strains of soil bacteria (D'COSTA *et al.*, 2006).

Also evidence shows that bacterial multidrug efflux pumps are common in environmental bacteria, where their primary functions are not associated with

antibiotic resistance but rather detoxification of the cell, virulence, cell homeostasis and intercellular signal trafficking (LIN *et al.*, 2006; MARTINEZ *et al.*, 2009).

Relatively few studies are available concerning the role(s) of antibiotic resistance genes in the environment. However, it is clear that natural environments constitute important reservoirs of antibiotic resistance microorganisms and resistance genetic determinants (ALLEN *et al.*, 2010; D'COSTA *et al.*, 2006; SAAVEDRA *et al.*, 2003). Once available, resistance genes are picked up from these reservoirs and propagated into pathogenic microbes upon use of antimicrobial agents either in medicine or agriculture posing a serious problem in human therapy (MARTINEZ, 2009). For example, the genes encoding CTX-M β-lactamases, enzymes that compromise the activity of clinically important antibiotics and constitute a major clinical problem (CANTON and COQUE, 2006), have been shown to originate from environmental *Kluyvera* species that are not recognized as antibiotic producers (POIREL *et al.*, 2002).

1.2 β-lactam antibiotics

The first antibiotic was penicillin, discovered accidentally from a mould culture of *Penicillium* by Alexander Fleming in 1928 (FLEMING, 1929). This discovery revolutionized the treatment of infectious diseases and marks the start of modern medicine. Florey and Chain developed the purification method (CHAIN *et al.*, 1940) and used it to treat bacterial infections during the Second World War, regarded as a "magic bullet". Penicillin was first used in patients in 1942. Alexander Fleming, Howard Florey and Boris Chain were awarded the Nobel Prize of Medicine and Physiology in 1945 for the discovery and application of penicillin. Further studies on this important molecule by Dorothy Hodgkin led to the determination of the structure of penicillin using X-ray crystallography (HODGKIN, 1949) and identified the β-lactam ring as the key functional group. The β-lactams remain a cornerstone of antimicrobial chemotherapy.

β-lactam antibiotics comprise natural or semi synthetic compounds that can be divided into four main groups based on their structure: penicillins, cephalosporins, monobactams and carbapenems (Figure 1.1). These antibiotics possess, as a common feature, a highly reactive β-lactam ring constituted by three carbon atoms and one nitrogen, but differ in the presence of additional rings to

which the β-lactam ring may be fused (DEMAIN and ELANDER, 1999). For example, β-lactam ring is fused to a five-membered thiazolidine ring in the penicillins but to a six-membered dihydrothiazine ring in the cephalosporins. Monobactams have no additional ring. Carbapenems have a β-lactam ring fused to a ring that is similar to that of penicillins but is unsaturated and the sulphur atom is substituted by a carbon. Different antibiotics within the same group are distinguished by the nature of one or more side chains (DEMAIN and ELANDER, 1999).

Carbapenem antibiotics were originally developed from thienamycin, a natural product identified in culture filtrates of *Streptomyces cattleya* (BIRNBAUM *et al.*, 1985). The thienamycin molecule was chemically unstable and was never used for therapy. However, its structural scaffold was used to produce similar drugs with adequate properties for chemotherapy. Imipenem, meropenem, ertapenem, and doripenem are the carbapenems approved for human use so far (BAUGHMAN, 2009). The carbapenems exhibit the broadest spectrum of activity among the β-lactam antimicrobials, providing safe and efficacious therapies in the treatment of serious infections, caused by multidrug-resistant Gram-positive, Gram-negative, and anaerobic pathogens (BAUGHMAN, 2009; MANDELL, 2009).

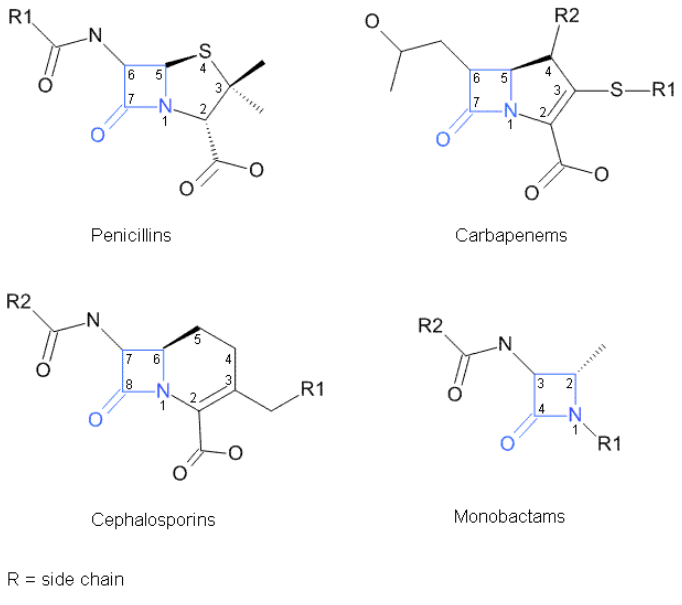

Figure 1.1 The core structures of β-lactam antibiotics with the numbering scheme shown.

The discovery and subsequent development of β-lactam antibiotics was very important both for drug development and medicine. Today several hundred β-lactam

molecules structurally different from the four subclasses are available and most of them are prescribed for medical use. The antibacterial effect of all β-lactam antibiotics is dependent on their ability to cross the cellular membrane, the affinity of the antibiotic to target proteins and the stability to bacterial degradation (KOTRA and MOBASHERY, 1999).

The β-lactams are among the most safe and efficient of all antibiotics. These drugs are also characterised by an absence of secondary effects in eukaryotes. Due to these characteristics and their relatively low cost and ease of delivery, β-lactam antibiotics are the most important antimicrobial agents in the treatment of bacterial infections, accounting for over 50% of antibiotic prescriptions in many countries (MOLSTAD *et al.*, 2002; THERRIEN and LEVESQUE, 2000).

Antimicrobial agents from the β-lactam class are still the first choice for treatment of infections in critically ill patients caused by multidrug resistant Gram-negative bacteria where other options may be limited. Among these organisms are *Pseudomonas aeruginosa*, *Acinetobacter baumannii*, and the *Enterobacteriacea*, all of which may be responsible for a wide range of infections, particularly hospital acquired infections of immunocompromised patients (LIVERMORE, D., 2009; PELEG and HOOPER, 2010). In particular, the spread of resistance to other antibiotic classes, including cephalosporins, means that carbapenems are increasingly used routinely for these infections, rather than being in held in reserve in case of failure of other treatments (MASTERTON, 2009).

1.2.1 Mechanism of action

β-lactam antibiotics exert their bactericidal activity primarily by inactivation of bacterial cell wall synthesis. The cell wall is a protective layer located externally to the cytoplasmic membrane and composed of an inner layer of peptidoglycan that is surrounded by an outer membrane in Gram-negative bacteria.

Peptidoglycan is the main component of the bacterial cell wall. It is a complex polymer composed of peptide chains and sugars that are linked by covalent bonds and is responsible for bacterial cell wall strength and resistance to osmotic pressure from cytoplasm (SCHLEIFER and KANDLER, 1972; WALSH, 2000).

The basic repeating unit is a disaccharide consisting of alternating residues of N-acetylglucosamine (NAG) and N-acetylmuramic acid (NAM) (Figure 1.2). A five amino-acid stem peptide chain of variable sequence, according to bacterial species, is terminated by a D-alanine, D-alanine moiety and attached to each NAM unit. It normally contains L-alanine, D-glutamic acid, mesodiaminopimelic acid (which may be substituted by other amino acids including L-lysine in Gram positive bacteria), and two residues of D-alanine (VOLLMER *et al.*, 2008). The peptidoglycan polymer is constructed using two kinds of covalent bonds: β 1-4 glycosidic bonds link the sugar rings while the amino acid side chains are joined by peptide bonds. These peptide bonds are formed in the final transpeptidation step of cell wall synthesis which results in the cross-linking of the peptide chains of two neighbouring sugar strands by peptide bridges to form a three-dimensional network. This reaction is catalyzed by a series of transpeptidase enzymes that are also known as penicillin binding proteins (PBPs) due to their ability to bind to penicillin molecules (JEAN-MARIE, 1997; MACHEBOEUF *et al.*, 2006).

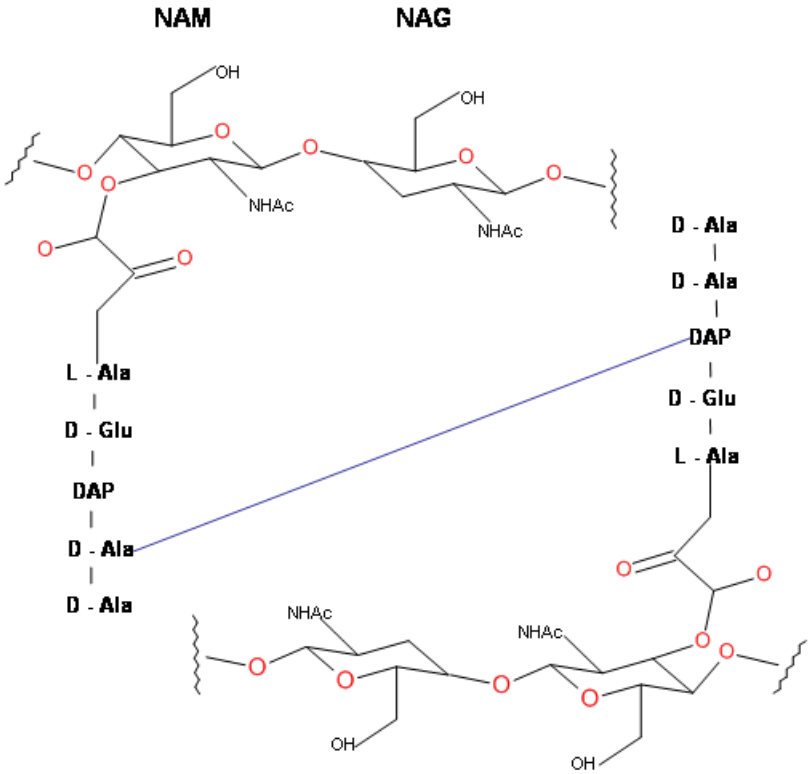

Figure 1.2 Schematic representation of peptidoglycan cross-linking in Gram-negative bacteria.

Tipper and Strominger (1965) suggested that the nucleus of β-lactam antibiotics mimics the terminal of D-alanyl-D-alanine of the linear stem peptide (Figure 1.3) and inhibits transpeptidation by reacting with the substrate binding site of PBPs. PBPs are active-site serine enzymes that catalyse the transpeptidation reaction via a covalent acylenzyme intermediate. In the initial step an acylenzyme complex is formed by reaction of the active site serine hydroxyl with the terminal D-Ala-D-Ala, leading to cleavage of the last D-Ala residue. This is followed by a second reaction, involving the transfer of the acylenzyme to an amino group of a neighbouring chain, cross-linking individual peptidoglycan strands to establish a unifying network (TIPPER and STROMINGER, 1965). Cross-linking of the glycan strands generally occurs between the carboxyl group of D-Ala at position 4 and the amino group of the diamino acid at position 3, either directly in Gram-negative bacteria (Figure 1.2) or through a short peptide bridge (Gram-positive bacteria) (VOLLMER *et al.*, 2008).

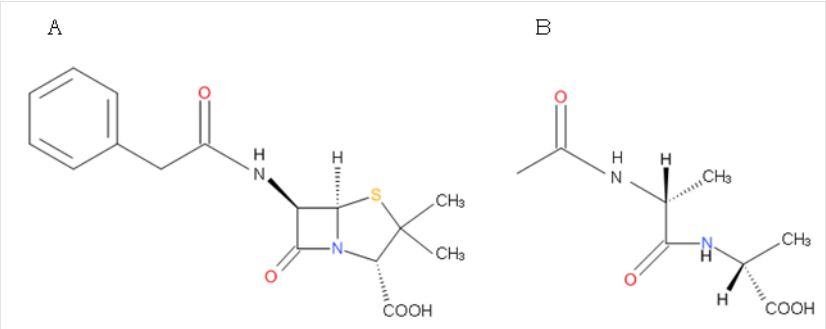

Figure 1.3 Structural similarities between penicillin G (A) and D-alanyl-D-alanine (B).

β-lactam antibiotics bind to PBPs, promoting the formation of an acylenzyme complex with the PBP by acylating the essential serine residue of the active site (Figure 1.4) (LEE *et al.*, 2001). Once acylated by a β-lactam, the PBP deacylates very slowly, leading to irreversible inhibition of PBP catalysis and rendering them unable to catalyse the transpeptidation reaction (FISHER and MOBASHERY, 2009). This causes an incomplete biosynthesis of bacterial cell wall that triggers peptidoglycan autolysin action, resulting in osmotic lysis and ultimately cell death (BAYLES, 2000). However, the specific details of how this occurs are not yet known. The high specificity and absence of secondary effects is thus explained as molecules similar to peptidoglycan precursors do not exist in eukaryotic cells (MACHEBOEUF *et al.*, 2006).

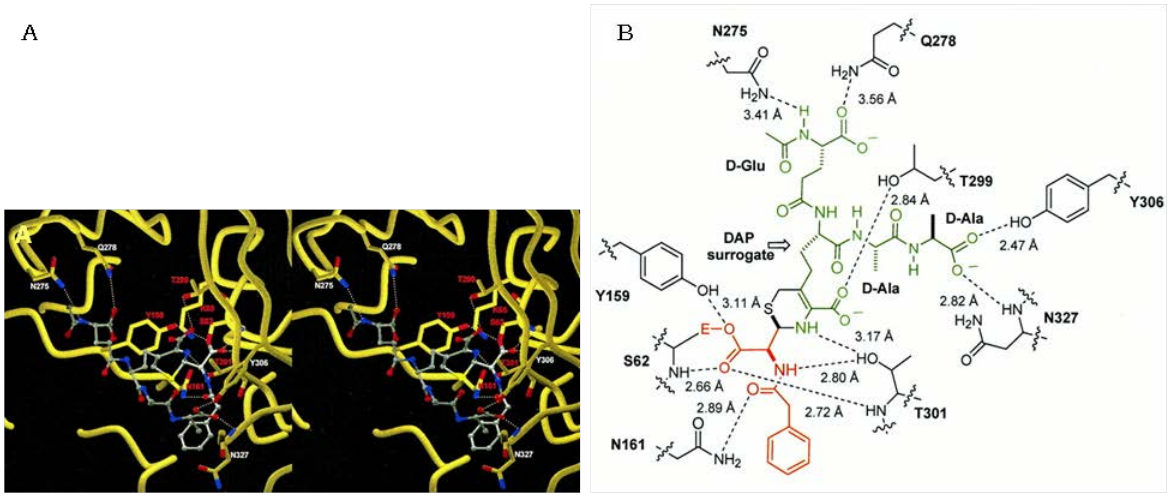

Figure 1.4 A. Stereoview of the active site of *Streptomyces* R61 DD-carboxypeptidase/transpeptidase acylated by a cephalosporin. The ligand is rendered as ball and stick with CPK atom colours. Hydrogen bonds between the enzyme and the ligand are shown as dotted white lines. Residues labeled in red are conserved among PBPs and β-lactamases. **B.** A schematic of interactions shown in A; the cephalosporin backbone (red) mimics the terminal acyl-D-Ala-D-Ala portion of the peptide branch of the first strand of the peptidoglycan. The cephalosporin acylates the active site serine of the transpeptidase, as would the peptide from the first strand of peptidoglycan, concomitant with the departure of the terminal D-Ala. The β-lactam nitrogen and its adjacent carbon and carboxylate collectively serve as a substitute for the departing D-Ala. The acyl-enzyme species depicts the first enzyme-bound "peptidoglycan" strand (shown in red) poised to receive the amine of DAP from the second strand of peptidoglycan (shown in green). Figure and legend were adapted from Lee *et al.*, (2001).

1.2.2 Resistance mechanisms

In order to exert their antimicrobial action, antimicrobial compounds must enter the cell, accumulate to inhibitory concentrations, and interact with their targets. Antibiotic resistance can arise from alterations to any of these processes, through a number of changes in the cell. Bacteria have developed escape strategies against all antimicrobials drugs and β-lactams are no exception. Resistance to these agents is common to Gram-positive and Gram-negative bacteria and is mediated by four mechanisms: alteration of the target (i.e. PBPs) (LAMBERT, 2005), reduction of the entry of the antibiotic to the cell by decreased permeability and/or efflux mechanisms (KUMAR and SCHWEIZER, 2005; POOLE, 2007) and inactivation of the antibiotic by hydrolytic enzymes before it can reach the target (FISHER *et al.*, 2005).

In Gram-negative bacteria a synergy between resistance mechanisms is frequently used not only to increase but also to broaden resistance profile. The most commonly observed combinations are a reduction in outer membrane permeability together with active efflux and β-lactamase expression (BONOMO and SZABO, 2006; QUALE *et al.*, 2006).

The subject of this dissertation is the study of β-lactamases; therefore just a brief overview of other resistance mechanisms to β-lactams will be presented, while β-lactamases will be covered in more detail.

1.2.2.1 Target alteration

Resistance to β-lactam antibiotics due to PBP alteration occurs either by mutations in the chromosomal genes that code for PBPs or acquisition of supplementary genes that code for new PBPs with reduced affinity for the antibiotics (GEORGOPAPADAKOU, 1993). In *Streptococcus pneumoniae* resistance to β-lactams occurs almost entirely from modified versions of their own PBPs, mainly 2X, 2B, and 1A, that are poorly acylated by β-lactams (GREBE and HAKENBECK, 1996; SMITH *et al.*, 2005). The altered proteins from penicillin-resistant isolates are encoded by mosaic genes that have arisen by interspecies recombination events (HAKENBECK *et al.*, 2001; LAIBLE *et al.*, 1991).

Resistance to penicillin and methicillin in *Staphylococcus aureus* has been known for a long time. Resistance to penicillin, reported soon after its introduction as a therapeutic agent, is due to expression of the "penicillinase" PC1 (RICHMOND, 1963). More importantly, shortly after the clinical use of methicillin, a semi-synthetic penicillin introduced to restore β-lactam activity, methicillin-resistant *S. aureus* (MRSA) strains were identified (Barber, 1961). Methicillin-resistance is mediated by the acquisition of an altered PBP, encoded by the *mecA* gene that is designated as PBP2a or PBP2' (DE LENCASTRE *et al.*, 1994; HARTMAN and TOMASZ, 1984), and shows reduced affinity for all β-lactams (FUDA *et al.*, 2005).

PBP alteration is an important resistance mechanism to β-lactam antibiotics in Gram-positive cocci such as *S. aureus* and *S. pneumoniae* but is observed less frequently in Gram-negative bacteria (GEORGOPAPADAKOU, 1993). However, in

Neisseria gonorrhoeae, the causative agent of gonorrhoea, the production of modified PBP2 plays a major role in resistance to these agents, including extended-spectrum cephalosporins (OCHIAI *et al.*, 2007; OHNISHI *et al.*, 2010). Recently, it has been reported that modification of native PBPs also accounts for β-lactam resistance in other Gram-negative multi-resistant species such as *A. baumannii* (RUSSO *et al.*, 2009) and *P. aeruginosa* (ZAMORANO *et al.*, 2010).

1.2.2.2 Decreased permeability

As stated above, Gram-negative bacteria have an impermeable outer membrane surrounding the peptidoglycan layer. This membrane functions as a barrier, preventing the access of several toxic compounds to the cell interior. Therefore, the transport of nutrients and other substances, including β-lactam antibiotics, across the outer membrane is achieved by water-filled channel-forming proteins known as porins (NIKAIDO, 2003). Resistance to β-lactams among Gram-negative bacteria can be attained by altered (reduced) permeability through change in porin copy number or selectivity. This mechanism is often combined with active efflux to enable bacteria acquire high level resistance to many antibiotics (KUMAR and SCHWEIZER, 2005).

One of the mechanisms responsible for carbapenem resistance in important human oportunistic pathogens such as *Klebsiella pneumoniae*, *P. aeruginosa* and *A. baumannii* is the loss of specific porins which generally occurs in combination with other resistance mechanisms. In *K. pneumoniae* for example, it has been reported that resistance to carbapenems can arise via combination of AmpC or ESBLs enzymes that display very low carbapenemase activity, together with loss of the porins OmpK35 and/or OmpK36 (CHIA *et al.*, 2010; SONG *et al.*, 2009). Recently García-Fernández and co-workers (2010) described an ertapenem-resistant *K. pneumoniae* isolate that did not produce the OmpK35 porin due to a nonsense mutation, but expressed an altered OmpK36 along with the ESBLs SHV-12 and CTX-M-15. Although this clone remained susceptible to meropenem and imipenem, the loss of OmpK36 expression in two isolates of the same clone converted these to an imipenem and meropenem-resistant phenotype (GARCIA-FERNANDEZ *et al.*, 2010).

P. aeruginosa also contains specific porins involved in antibiotic resistance. Apart from the expression of carbapenemases (LIVERMORE and WOODFORD, 2006), carbapenem resistance in *P. aeruginosa* is attributed to an interplay between low

permeability, activity of the efflux pump MexAB-OprM and an inducible or derepressed chromosomal AmpC β-lactamase (QUALE *et al.*, 2006). In these bacteria derepressed expression of the OprD porin is important to achieve resistance to carbapenems (RODRIGUEZ-MARTINEZ *et al.*, 2009; WANG *et al.*, 2010). In a recent study, the loss of OprD proved to be the main mechanism of resistance to carbapenems (RODRIGUEZ-MARTINEZ *et al.*, 2009).

The decreased expression of some OMPs (outer membrane proteins) has also been reported to be associated with antimicrobial resistance in *A. baumannii* (MUSSI *et al.*, 2005; TOMAS *et al.*, 2005). Although there is not much data available on decreased permeability in *A. baumannii*, carbapenem resistance has been specifically correlated with loss of porins including CarO (LIMANSKY *et al.*, 2002; MUSSI *et al.*, 2005), and additional OprD-like (DUPONT *et al.*, 2005) and 33- to -36 kDa proteins (TOMAS *et al.*, 2005). In these studies no other mechanism is associated with carbapenem resistance, in contrast to the *K. pneumonia* and *P. aeruginosa* described above.

1.2.2.3 Active efflux

β-lactam antibiotics must pass through the cell membrane to reach their targets in order to exert their bactericidal action on bacterial cells. Bacteria can become resistant to β-lactam antibiotics by reducing the effective intracellular antibiotic concentration by means of increased energy-dependent (or active) efflux, expelling the antimicrobials out of the cell interior (KUMAR and SCHWEIZER, 2005; POOLE, 2007).

Efflux pumps are membrane-bound proteins working as transporters of antibiotics (and other toxic substrates) to the outside of the cell. Efflux pumps can be single- or multi-component. Gram-positive bacteria, which have only a cytoplasmic membrane, use single component pumps to transport their substrates, while Gram-negative bacteria use these pumps to export drugs across their inner membranes. By way of contrast, multi-component pumps found in Gram-negative organisms transport molecules across both the inner and the outer membranes and comprise an inner membrane transporter associated with a periplasmic membrane fusion protein component and an outer membrane protein component, thus effluxing substrates across the entire cell envelope (KUMAR and SCHWEIZER, 2005).

Efflux systems are divided into five classes according to their number of pump components, energy source used and type of substrate (POOLE, 2007). The RND (resistance-nodulation-division) family of efflux systems accommodates a variety of clinically significant antibiotics, including β-lactams, and is therefore one of the most relevant efflux mechanisms of multidrug resistance in Gram-negative bacteria. RND systems are multi-component pumps constituted by the transporter protein in the inner membrane, a periplasmic membrane fusion protein and an outer membrane protein (POOLE, 2007). Such a pump can expel antibiotics from both the cytoplasm and the periplasmic space.

The RND efflux pumps that have been studied in most detail are the MexAB-OprM from *P. aeruginosa* and AcrAB-TolC from *Escherichia coli*. MexAB-OprM from *P. aeruginosa* is constitutively expressed, accounting for intrinsic resistance of these bacteria, and often confer multidrug resistance due to a broad substrate specificity (LLANES *et al.*, 2004; MASUDA *et al.*, 2000). MexAB-OprM is able to acomodate a wide range of β-lactam antibiotics including penems (faropenem), carbapenems (meropenem and panipenem), penicillins (carbenicillin and azlocillin), moxalactam and extended-spectrum cephalosporins (cefepime, cefotaxime, cefoxitin) (LI *et al.*, 1995; MASUDA *et al.*, 2000; OKAMOTO *et al.*, 2001). Additionally this pump also recognizes other clinically relevant antibiotics such as quinolones, macrolides, tetracyclines, and chloramphenicol (MASUDA *et al.*, 2000). Quale and colleagues reported that carbapenem resistance in clinical isolates of *P. aeruginosa* is achieved by interplay between increased expression of chromosomal AmpC and of efflux systems, and reduced expression of OprD (QUALE *et al.*, 2006).

Recent studies also show that the efflux system AcrAB-TolC plays a key role in the β-lactam uptake and susceptibility in clinical isolates of *K. pneumoniae* (PADILLA *et al.*, 2010; PAGES *et al.*, 2009).

1.3 β-lactamases

The most common resistance mechanism to β-lactam antibiotics, particularly among Gram-negative bacteria, is the production of β-lactamases (β-lactam hydrolases EC.3.5.2.6). β-lactamases are efficient enzymes that cleave the amide bond of the four-membered β-lactam ring rendering these drugs microbiologically inactive (LIVERMORE, D. M., 2009) (Figure 1.5).

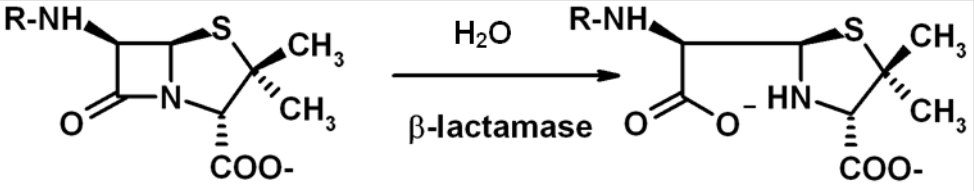

Figure 1.5 β-lactamase attack on penicillin with formation of inactive penicilloic acid.

Once expressed β-lactamases produced by Gram-positive bacteria are bound to the cytoplasmic membrane or secreted into the extracellular milieu while those produced by Gram-negative organisms are concentrated in the periplasmic space. Many β-lactamases are structurally related to PBPs and probably evolved from these enzymes (MASSOVA and MOBASHERY, 1998).

The production of penicillinase by *E. coli*, described even before the widespread clinical use of penicillin, represents the first reported resistance mechanism to β-lactam antibiotics (ABRAHAM and CHAIN, 1940). Since then, these enzymes, now known as β-lactamases, have been described in Gram-negative, Gram-positive and mycobacteria (LIVERMORE, D. M., 2009).

β-lactamases are found encoded on the chromosome or on plasmids and are frequently associated with other mobile genetic elements such as transposons and more recently ISCRs (FROST *et al.*, 2005; TOLEMAN *et al.*, 2006). More than 890 β-lactamases have been described so far and this number continues to grow ((BUSH and JACOBY, 2010), http://www.lahey.org/studies/). The production of β-lactamases constitutes the most important and widespread antimicrobial resistance mechanism among important human pathogens. The ability of bacteria to acquire β-lactamases with a broad range of substrate specificities is a major concern, making

bacteria resistant to almost all β-lactams (QUEENAN and BUSH, 2007). The situation gets even more dramatic with the rapid spread of β-lactamase-encoding genes by the transmission by mobile genetic elements (BENNETT, 2008; SYKES, 2010).

Bacteria resistant to new β-lactam antibiotics are being selected in a relatively short time after their introduction for chemotherapy. In order to overcome β-lactam resistance and restore the antibacterial activity of these antibiotics, several strategies have been employed: the search of new antibiotics from microbial sources, chemical alteration of 'old' or first generation antibiotic structures to obtain new compounds with decreased sensitivity to resistance mechanisms and/or improved pharmacology (e.g. cephalosporins), and the use of β-lactamase inhibitors, such as clavulanic acid or sulbactam, in combination with an older antibiotic (e.g amoxicillin, piperacillin) (ABBANAT *et al.*, 2008; CLARDY *et al.*, 2006; DONADIO *et al.*, 2010; DRAWZ and BONOMO, 2010).

1.3.1 Classification

Due to the diversity of enzymatic features of the β-lactamases identified so far, several attempts have been made to classify this group of enzymes. These classifications are based on functional and biochemical characteristics such as substrate profile and isoelectric point (RICHMOND and SYKES, 1973; SYKES and MATTHEW, 1976) or on the amino acid sequences of the enzymes (AMBLER, 1980).

The Ambler classification initially separated the serine enzymes, designated as class A, from the metallo-β-lactamases or class B. It was completed with the subsequent inclusion of class C (JAURIN and GRUNDSTROM, 1981) and class D enzymes as their sequences became available (HUOVINEN *et al.*, 1988; OUELLETTE *et al.*, 1987).

With the emergence of new β-lactamases it was possible to develop a classification system that relates substrate/inhibitor specificity with molecular structure (BUSH, 1989). This classification was later updated (BUSH, 2010; BUSH *et al.*, 1995) and nowadays is the most used classification scheme. Table 1.1 shows the most used classification schemes with representative enzymes of each group.

Table 1.2 Classification and properties of β-lactamases (adapted from Bush *et al.*, 1995).

Functional group (Bush *et al.*, 1995)	Molecular class	Substrate profile	Inhibition AC[a]	Inhibition EDTA	Representative enzymes
1	C	Cephalosporins penicillins cephamycins monobactams	–	–	AmpC, CMY variants, FOX, ACT-1, LAT-1, MIR-1, DHA-
2a	A	Penicillins	+	–	PC1 (Gram-positive bacteria)
2b	A	Penicillins cephalosporins	+	–	TEM-1, TEM-2, SHV-1
2be	A	Penicillins cephalosporins monobactams	+	–	TEM, SHV, CTX-M and GES/IBC variants, PER-1 –2, VEB-1
2br	A	Penicillins	–	–	TEM-30 –41, TEM-44 –45, TEM-51, 54
2c	A	Penicillins carbenicillins	+	–	PSE-1, PSE-3, PSE-4
2d	D	Penicillins cloxacillins	±	–	OXA variants
2e	A	Cephalosporins	+	–	Cephalosporinase from *Proteus vulgaris*
2f	A	Penicillins cephalosporins carbapenems	+	–	NMC-A, Sme-1-3, IMI-1, KPCs
3	B	All β-lactams except monobactams	–	+	BcII, L1, CphA, ImiS, IMP, VIM, SPM-1
4	Unknown	Penicillins			Penicillinase from *Burkholderia* (formerly *Pseudomonas) cepacia*

[a] Clavulanic acid

1.3.2 Serine β-lactamases

The serine β-lactamase group includes enzymes belonging to molecular classes A, C and D. This is a rather heterogeneous group that requires an active-site serine residue to catalyse the opening of the β-lactam ring. They are mostly penicillinases and cephalosporinases, including TEM, SHV and CTX-M-type enzymes that do not hydrolyse carbapenems (JACOBY and MUNOZ-PRICE, 2005), although increasing numbers of such enzymes with carbapenemase activity have now been reported (WALTHER-RASMUSSEN and HOIBY, 2007).

The interaction between serine β-lactamases (and related serine penicillin-recognizing enzymes) and β-lactams comprises three steps: non-covalent binding to form a Michaelis complex ($\boldsymbol{k_{-1}/k_1}$), acylation ($\boldsymbol{k_2}$), and deacylation ($\boldsymbol{k_3}$) (Scheme 1.1) (HERZBERG and MOULT, 1987).

$$E + S \underset{k_{-1}}{\overset{k_1}{\longleftrightarrow}} ES \xrightarrow{k_2} ES^* \xrightarrow[H_2O]{k_3} E + P$$

Scheme 1.1

In scheme 1.1 **E** represents a β-lactamase, **S** the β-lactam substrate, **ES** is the noncovalent Michaelis complex, **ES*** is the covalent acylenzyme complex, where the antibiotic is covalently bound to the active-site serine residue, and **P** is the released hydrolysed β-lactam. In general, β-lactamases efficiently catalyze the deacylation step (high k_3 value) which regenerates the active enzyme (E) and releases a biologically inactive product (P). By contrast, in the PBPs the hydrolysis of the acylenzyme ester bond is slow. Compared with the deacylation rate constant displayed by the β-lactamases, the same rate in PBPs is up to six orders of magnitude slower (KNOX *et al.*, 1996).

The reaction mechanism of serine β-lactamases consists of two main steps: acylation of an active site serine by the β-lactam antibiotic, followed by deacylation and release of the inactive compound (Figure 1.6).

The first step involves activation of the serine residue in the active site, the nucleophile, by a general base. Upon activation this serine performs a nucleophilic

attack on the carbonyl of the β-lactam ring creating a tetrahedral intermediate that is stabilized by hydrogen bonding between the carbonyl oxygen and an oxyanion hole formed by the enzyme active site. Protonation of the β-lactam nitrogen and cleavage of the C-N bond in the β-lactam ring leads to the formation of a covalent acylenzyme intermediate. In the second step, a base-activated water molecule attacks the covalent complex with formation of a tetrahedral deacylation intermediate. Cleavage of this intermediate by hydrolysis of the bond between the serine oxygen and the carbonyl of the β-lactam, releases the inactive (hydrolysed) β-lactam and the active enzyme.

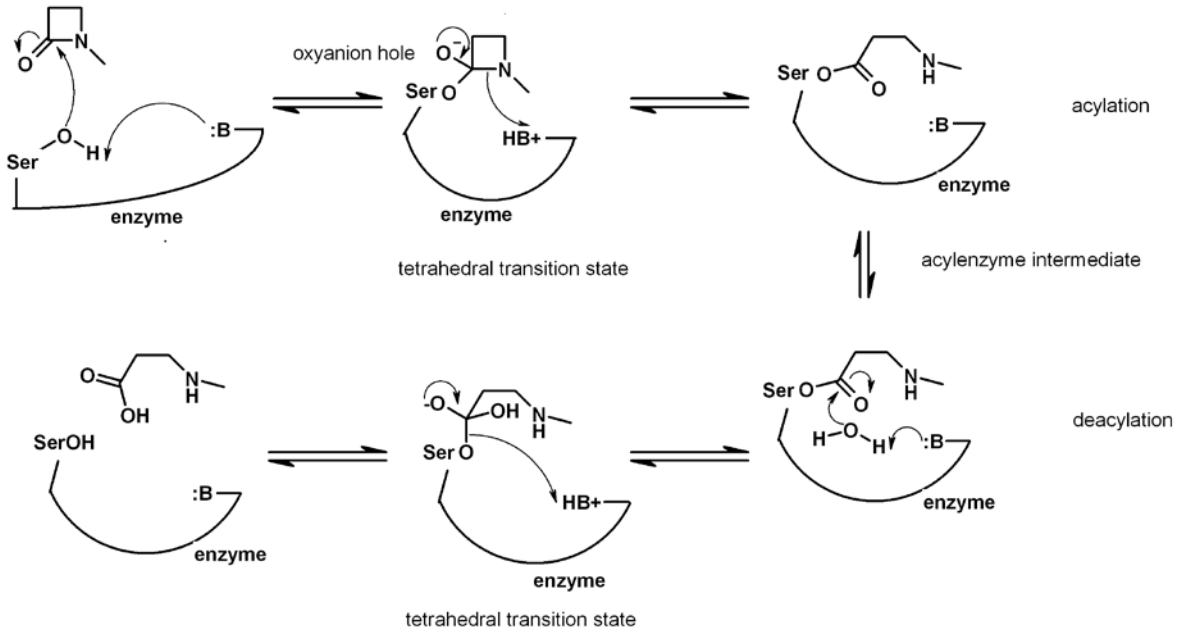

Figure 1.6 Schematic reaction mechanism for a β-lactam substrate and a serine β-lactamase. The acylation and deacylation transition states of the reaction pathway are shown, where B represents the general base and it is not necessarily the same residue for both acylation and deacylation.

The differences between the catalytic mechanisms of serine β-lactamases from molecular classes A, C and D are largely focussed on the identity of the residues used as general base for acylation and deacylation (DRAWZ and BONOMO, 2010; FISHER *et al.*, 2005). In enzymes from molecular class A it is well accepted that Glu166 acts as the general base for the deacylation reaction, while the precise

mechanism by which the catalytic Ser70 is activated remains the subject of long-term debate (see discussion in section 1.3.3).

Studies of the crystal structure of the *C. freundii* class C enzyme have suggested that the conserved residue Tyr150 activates the active site Ser64 for nucleophilic attack on the β-lactam ring (OEFNER *et al.*, 1990), and is involved in the deacylation step by accepting a proton from the deacylation water (OEFNER *et al.*, 1990). However, recent data indicate that Tyr150 is protonated throughout the reaction coordinate, disfavouring mechanisms that involve a stable tyrosinate as the general base for deacylation (CHEN *et al.*, 2006). These authors propose a role for Tyr150 in coordinate activation of the deacylating water in cooperation with the lactam nitrogen of the substrate itself (substrate-assisted catalysis), although it does not rule out, in itself, the alternative Lys67-Tyr150 coordinate base mechanism.

Class D enzymes display the unique feature of activation of their β-lactamase activity by CO_2. In these enzymes Lys70 (the structural equivalent of Lys73 and Lys67 of class A and class C β-lactamases, respectively) is N-carboxylated by addition of the lysine side chain amine to CO_2 (GOLEMI *et al.*, 2001; MAVEYRAUD *et al.*, 2000). Structural analysis shows that the resulting carbamate anion forms a hydrogen bond with the nucleophilic Ser67, suggesting that this carboxy-lysine may be the agent that activates the attacking groups, Ser67 and the hydrolytic water, in both the acylation and deacylation reactions, respectively (GOLEMI *et al.*, 2001; MAVEYRAUD *et al.*, 2002; MAVEYRAUD *et al.*, 2000).

From this point, the discussion in this dissertation will focus on the class A and class B β-lactamases as these are the most relevant to the work here presented.

1.3.3 Structure and mechanism of class A β-lactamases

Among the four Ambler classes of β-lactamases, class A enzymes are largely plasmid encoded, the most numerous and widespread among Gram-positive and Gram-negative bacteria.

The study of three dimensional structures of several β-lactamases from molecular class A showed remarkable similarities with the penicillin-binding proteins (PBPs). The first class A β-lactamase crystal structure to be determined was that of PC1 from *S. aureus* (HERZBERG and MOULT, 1987) followed by the class A β-

lactamases of *Streptomyces albus* G (DIDEBERG *et al.*, 1987), *Bacillus licheniformis* 749/C (MOEWS *et al.*, 1990) and *E. coli* (TEM-1) (JELSCH *et al.*, 1992; JELSCH *et al.*, 1993). By the same time Strynadka and collaborators solved the crystal structure of the TEM-1 mutant Glu166Asn as an acylenzyme complex with benzylpenicillin (STRYNADKA *et al.*, 1992). Since then numerous structures of wild-type, mutants and substrate and inhibitor complexes have been determined for class A β-lactamases (FISHER *et al.*, 2005).

Comparison of these structures revealed that molecular class A β-lactamases consist of two structural domains: an all α domain consisting of eight α helices and an α/β domain formed by three α helices and five β sheets. The active site pocket is located at the interface of the two domains (HERZBERG and MOULT, 1987). Along with the similarity in the three dimensional structures, a high degree of similarity is also found in the relative positions of four highly conserved motifs (Figure 1.7).

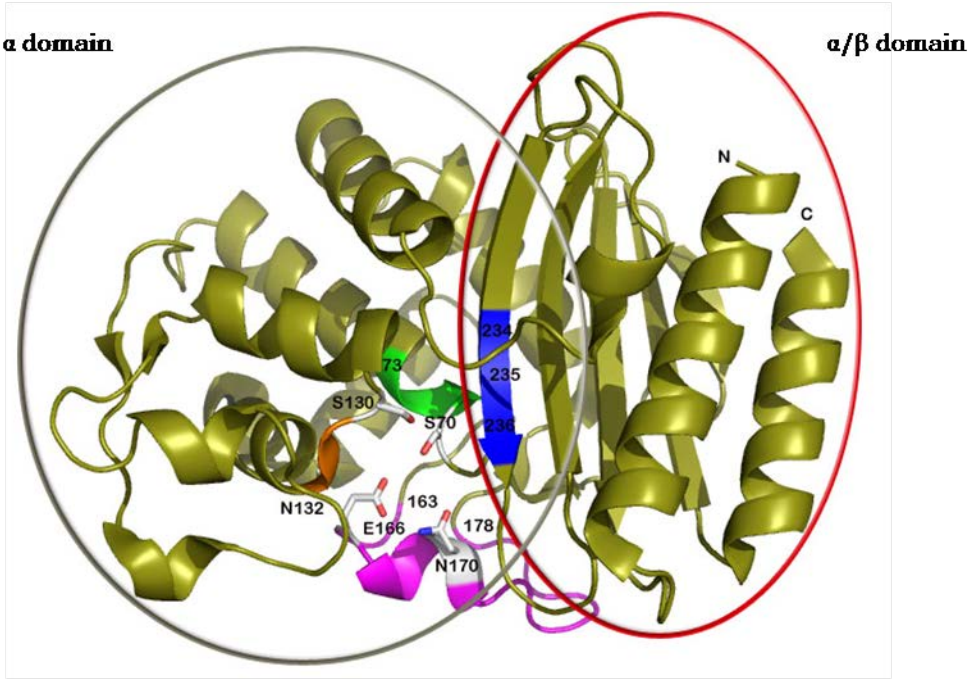

Figure 1.7 Overall structure of the class A β-lactamase TEM-1 (PDB accession 1ZG4) with the two domains labelled. The conserved motifs of class A β-lactamases are shown in different colours. The first motif (S70-K73) in the active site is in green; the second motif (S130-N132) is in orange; the third motif (K234-G236) and the omega loop (residues 163 to 178) are shown in blue and magenta, respectively. The catalytic S70, and S130, E166 and N170, some of the residues involved in the catalytic mechanism, are shown as a stick model with grey carbon atoms, red oxygen atoms, and blue nitrogen atoms.

The first motif extends from Ser70 to Lys73 (SXXK) (residue numbering according to Ambler *et al.*, (AMBLER *et al.*, 1991)) and includes the critical serine that is activated to undergo acylation. This residue is located near the N-terminus of a helix (Figure 1.7) thus facilitating its activation as a nucleophile (HERZBERG and MOULT, 1987; MOEWS *et al.*, 1990). Replacement of the active-site serine with other residues abolishes enzyme activity, providing evidence that Ser70 is involved in the β-lactam hydrolysis (CHEN *et al.*, 1996; DALBADIE-MCFARLAND *et al.*, 1986). Lys73 is located in the same helix and points into the active site, however its role in the catalytic mechanism is still under discussion. Mutagenesis studies have shown experimentally that Lys73 is involved in the acylation reaction (CHEN *et al.*, 1996), probably through stabilization of Ser70 during its deprotonation (CHEN *et al.*, 1996).

The second element, situated on a short loop, contains Ser130 to Asn132 (SXN) and forms one side of the active site groove (Figure 1.7). Ser130 is an important residue in the catalytic mechanism and is thought to be required to transfer a proton from its hydroxyl group to the nitrogen atom of the β-lactam substrate after formation of the tetrahedral intermediate (LAMOTTE-BRASSEUR *et al.*, 1991).

A triad composed of residues Lys234-Thr(Ser)235-Gly236 composes the third motif and forms the opposite wall of the active site cavity (Figure 1.7). Lys234 is considered to be involved in stabilization of Ser130 (in the SXN motif) through hydrogen bonding (MATAGNE *et al.*, 1998).

A fourth element, found in class A β-lactamases, extends from Glu163 to Asn178 and forms the bottom of the active site cavity (HERZBERG and MOULT, 1987; JELSCH *et al.*, 1993) (Figure 1.7). This element is known as the Ω loop and contains the essential Glu166, involved in deacylation. Involved in a dense hydrogen-bonding network, the conserved residues Glu166 and Asn170 are essential to position the conserved deacylating water molecule close to Ser70 (LAMOTTE-BRASSEUR *et al.*, 1991). During deacylation Glu166 activates this water molecule that then attacks the carbonyl carbon of the acylenzyme intermediate. Transfer of a proton to the catalytic Ser70 regenerates the enzyme (HERZBERG and MOULT, 1987). The study of Glu166 mutants confirmed the involvement of this residue in substrate hydrolysis (ADACHI *et al.*, 1991; DELAIRE *et al.*, 1991) while the decrease

in the deacylation rate with the E166A mutant is consistent with Glu166 acting as a general base to activate water in the deacylation step (ESCOBAR *et al.*, 1991).

Although the mechanism for deacylation is well established, the identity of the residue involved in the activation of the active serine (Ser70) in the acylation step has been subject of controversy. Two residues, Glu166 and Lys73 have been proposed as candidates to act as the general base in the acylation mechanism, i.e. abstracting the hydroxyl proton of the active serine and increasing its nucleophilicity. Strynadka and co-workers proposed that Lys73 acts as a general base, abstracting a proton from Ser70 and transferring it to the nitrogen atom of the β-lactam amide of the substrate via Ser130, assuming that the lysine is unprotonated (STRYNADKA *et al.*, 1992). However, a NMR study suggested that Lys73 is positively charged in the free enzyme, with a pK_a value above 10 (Damblon et al. 1996). Also, Lietz and collaborators studied the role of Lys73 in the acylation reaction using the mutant K73A from *B. licheniformis* β-lactamase (LIETZ *et al.*, 2000). According to these authors, a decreased turnover rate and catalytic efficiency was observed, but also a significant shift in pK_a to higher pH, consistent with the removal of the positive ammonium group of the lysine from the proximity of Glu166. These data provide indication that Lys73 does not act as the general base in the activation of the serine hydroxyl group but is most likely involved in both acylation and deacylation through electrostatic effects on neighbouring residues (LIETZ *et al.*, 2000).

In an alternative mechanism, Glu166 is proposed to act as the general base in both acylation and deacylation (Figure 1.8), activating Ser70 by way of a water molecule that is situated between the two residues (LAMOTTE-BRASSEUR *et al.*, 1991). Several mutagenesis studies support this hypothesis: with the El66C mutant both acylation and deacylation are decreased by several orders of magnitude (Escobar, 1994); mutants E166N in TEM-1 and E166H in the *S. albus G* β-lactamases were shown to form stable acylenzymes with β-lactam antibiotics but with a reduced acylation rate when compared to the wild-type enzymes (GUILLAUME *et al.*, 1997). In addition, ultra-high resolution crystal structures of TEM-1 in complex with an acylation transition-state analogue (MINASOV *et al.*, 2002) and of CTX-M-9 (CHEN *et al.*, 2007) together with theoretical simulations of the reaction coordinates (HERMANN *et al.*, 2009) suggest that Glu166 acts through a water molecule to activate Ser70 for nucleophilic attack on the β-lactam ring of the substrate.

Taken together these studies strongly support the conclusion that Glu166 functions as a general base catalyst in both formation and hydrolysis of the acylenzyme intermediate as originally proposed by Lamotte-Brasseur and collaborators (1991).

Over the course of the reaction pathway, tetrahedral transition-state intermediates are formed in which the β-lactam carbonyl oxygen is negatively charged (B and D in Figure 1.8). In order to stabilize this charge, hydrogen-bonding interactions are made with an "oxyanion hole" formed by the main chain amino groups of Ser70 and Ala237 (HERZBERG and MOULT, 1987; STRYNADKA *et al.*, 1992).

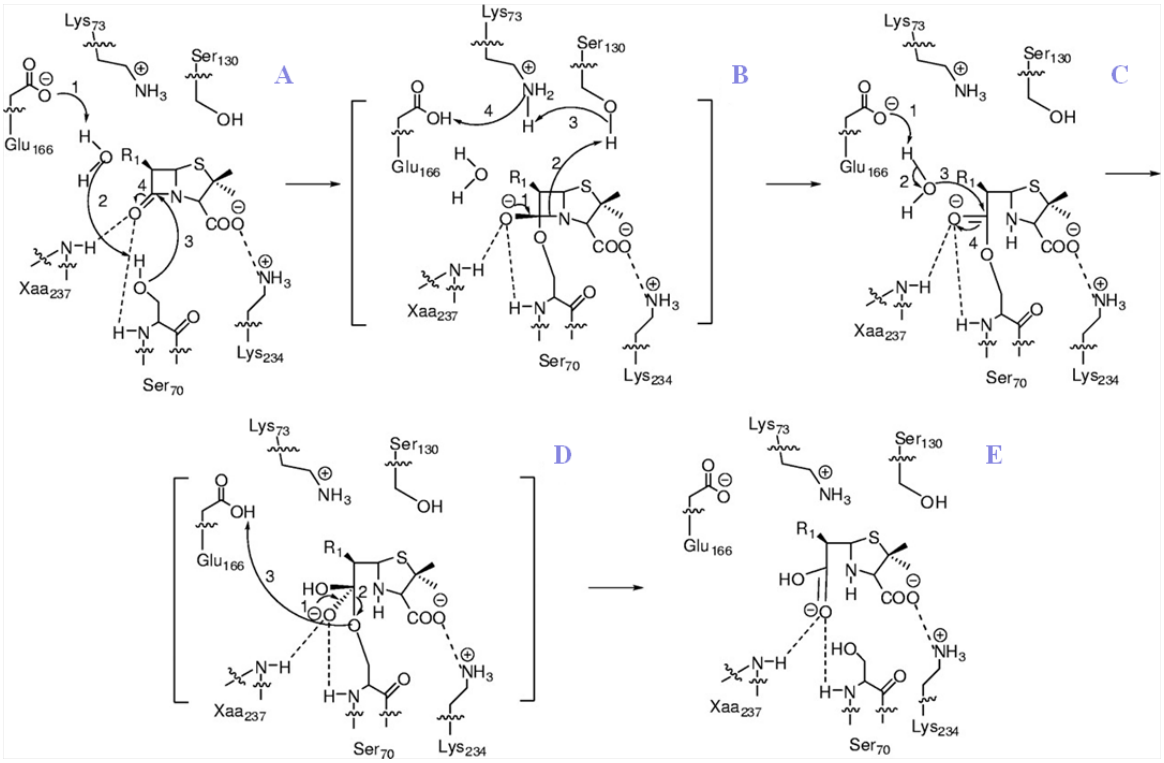

Figure 1.8 Proposed reaction mechanism for a penicillin β-lactam substrate and a class A serine β-lactamase in which Glu166 participates in activating a water molecule for both acylation and deacylation. Dashed lines represent hydrogen bonds. Following activation of the hydroxyl group, Ser70 performs a nucleophilic attack on the carbonyl group of the β-lactam antibiotic (A), resulting in a high-energy acylation intermediate (B). Protonation of the β-lactam nitrogen leads to cleavage of the C-N bond and formation of the covalent acyl-enzyme (C), which adopts a lower energy state. Attack by a catalytic water leads to a high-energy deacylation intermediate (D), with

subsequent hydrolysis of the bond between the β-lactam carbonyl and the oxygen of Ser70 (E). Deacylation regenerates the active enzyme and releases the inactive β-lactam. Adapted from Drawz and Bonomo (2010).

1.3.4 Evolution of class A β-lactamases

Penicillin-resistant staphylococci were observed shortly after the introduction of penicillin, threatening the treatment of infectious diseases (BARBER, 1947). In order to restore penicillin activity, pharmaceutical companies developed new generations of penicillins, including methicillin and oxacillin. Methicillin was introduced to the clinic in 1959, but by 1961 strains of methicillin resistant *S. aureus* (MRSA) had emerged (JEVONS, 1961) due to the production of altered PBPs as described earlier (see section 1.2.2.1).

To fight pathogenic bacteria able to produce penicillinases, particularly Gram-negative organisms, new β-lactams, aimed at resisting the hydrolytic action of β-lactamases and further increasing their spectrum of activity, were developed (ABBANAT *et al.*, 2008). Among these "β-lactamase-stable" antibiotics are modified penicillins (e.g. ampicillin), third (e.g. cefotaxime and ceftazidime) and fourth generation cephalosporins (cefepime), cephamycins (cefoxitin), oxacephamycins (moxalactam), monobactams (aztreonam) and carbapenems (e.g. imipenem). Another strategy employed to retain the effectiveness of β-lactam antibiotics is the discovery and use of compounds that inactivate the β-lactamases (DRAWZ and BONOMO, 2010; FISHER *et al.*, 2005). Clavulanate, a natural product of *Streptomyces clavuligerus*, was the first inhibitor to be identified (BROWN *et al.*, 1976). Subsequent modifications to its structure lead to the development of two other inhibitors, sulbactam and tazobactam (CARTWRIGHT and COULSON, 1979; ENGLISH *et al.*, 1978). Although they share structural similarity with β-lactam antibiotics, generally these inhibitors do not have antimicrobial activity on their own, and are formulated with a β-lactam antibiotic (e.g. amoxicillin-clavulanate and ampicillin-sulbactam) to act as shields against β-lactamases (DRAWZ and BONOMO, 2010). The three commercially available β-lactamase inhibitors described above are directed mainly to class A β-lactamases and are usually less effective against other β-lactam resistant enzymes (BUYNAK, 2006). Still, bacteria have always evolved to counteract the action of new β-lactam drugs and β-lactam inhibitor combinations as these are introduced into clinical use (LIVERMORE, D. M., 2009).

The plasmid-encoded β-lactamases TEM-1, TEM-2 and SHV-1 are the most frequently found β-lactamases in clinical isolates of *E. coli* and *Klebsiellae*, respectively, and confer resistance to penicillins and first generation cephalosporins. The introduction of third and fourth generation cephalosporins in the early 1980s has driven the evolution of extended-spectrum TEM and SHV β-lactamases (ESBLs) that are characterised by the ability to hydrolyse second and third generation cephalosporins and aztreonam, but not cefoxitin or carbapenems (PATERSON and BONOMO, 2005; PEREZ *et al.*, 2007). These ESBLs result from one to four aminoacid substitutions compared with their parent enzymes, usually at positions located close to the active site cavity. The mutations associated with the ESBL activity occur at positions Glu104 (TEM), Ala146 (SHV), Gly156 (SHV), Arg164 (TEM), Leu169 (SHV), Asp179 (SHV and TEM), Arg205 (SHV), Ala237 (TEM), Gly238 (TEM and SHV), and Glu240 (TEM and SHV) (KNOX, 1995; MATAGNE *et al.*, 1998).

The most frequent substitutions occurring in both TEM and SHV-derived ESBLS are those of Gly238 for serine and Glu240 for lysine (http://www.lahey.org/studies). Mutagenesis studies on TEM and SHV ESBLs determined that the G238S and E240K mutations were the primary cause for ceftazidime resistance and that an increased catalytic efficiency towards cefotaxime was observed only with G238S mutants (HULETSKY *et al.*, 1993; VENKATACHALAM *et al.*, 1994). Cantu and Palzkill (1998) proposed that a steric conflict with the S238 side chain affects the displacement of the Ω loop and that an intramolecular hydrogen bond between S238 side chain and N170 main chain carbonyl group in the Ω loop is required to stabilize the Ω loop in a new location. This would allow extended-spectrum cephalosporins greater access to the active site cavity and consequently improves the catalytic efficiency of the enzyme for these substrates (CANTU and PALZKILL, 1998). The crystal structure of SHV-2, a naturally occurring G238S mutant of SHV-1, has shown a significant displacement of part of the β-sheet strand S3 (residues 234-237), and of the short loop connecting S3 and S4 (residues 238-243), as well as a conformational rotation in the 240–241 region in this loop (NUKAGA *et al.*, 2003b). The structure of TEM-52 (E104/M182T/G238S) reports the movement of loop 238-243 with respect to its position in TEM-1, widening the opening of the active site and causing a reorganization of adjacent loops (ORENCIA *et al.*, 2001). Consequently, the carboxylate group of E240 is shown to be removed from the active site and oriented over the strand S3, decreasing the possibility of any interference with substrate side chain (ORENCIA *et al.*, 2001). These structural changes at the β-sheet are caused by the insertion of the larger S238 side-chain

between the strand S3 and the Ω loop. The displacement of strand S3 away from the Ω loop results in an expansion of the β-lactam binding site so that it is better able to accommodate the bulky, rigid R1 substituents of the oxyimino cephalosporins, as previously suggested by Huletsky and collaborators (HULETSKY *et al.*, 1993).

More recently (since 1995) a new family of plasmid-mediated ESBLs has emerged that preferentially hydrolyse cefotaxime, the CTX-M-type enzymes. CTX-M enzymes are more active against cefotaxime and ceftriaxone than against ceftazidime and are now the most frequently observed ESBLs (BONNET, 2004). These enzymes are not related to TEM or SHV β-lactamases but probably originate from chromosome-encoded class A β-lactamases from environmental *Kluyvera* species with an inherited intrinsic ESBL activity (POIREL *et al.*, 2002). In contrast to the enlarged active site observed in the TEM and SHV mutant ESBLs, thought to be responsible for their specificity (NUKAGA *et al.*, 2003b; ORENCIA *et al.*, 2001), CTX-M enzymes have small active sites (CHEN *et al.*, 2005).

Crystallographic data for CTX-M ESBLs provided insight for understanding the structure-activity relationship in these β-lactamases (CHEN *et al.*, 2005; DELMAS *et al.*, 2008). According to these studies, the increased activity against the bulky third-generation cephalosporins, especially ceftazidime, results from an enhanced flexibility of the β-sheet strand S3 of the active site. This increased flexibility is correlated with higher ceftazidimase activity, but costs a reduction in enzyme stability. The improved activity towards ceftazidime is related with the substitution Asp240Gly. In CTX-M-16 (Val231Ala/Asp240Gly), an enzyme that is significantly more active against both cefotaxime and ceftazidime compared to the CTX-M-9 (Val231Ala), the substitutions that occur at strand S3 create structural defects, apparently loosening the strand in a coordinated way that is linked to a decreased internal stability (CHEN *et al.*, 2005). This relation between activity and stability is also common in TEM and SHV-ESBLs and IRTs (inhibitor resistant TEMs) (KNOX, 1995). Recently, it was reported that the substrate binding site in CTX-M-16 is not enlarged and that the residue at position 240 is unable to interact with ceftazidime (DELMAS *et al.*, 2008), in clear contrast to the situation observed with TEM and SHV ESBLs (NUKAGA *et al.*, 2003b). Molecular dynamics simulations showed that in CTX-M-16 G240 promotes the coordinated vibration of strand S3 along with the catalytic S70 and residues 167 to 170 located in the Ω loop. These coordinated vibrations improve interactions between residues 237 and 235 and the

side chain of ceftazidime, favouring the accommodation of the bulky antibiotic (DELMAS *et al.*, 2008).

The ESBLs are mostly plasmid-encoded and thus easily spread through horizontal gene transfer. They are now found worldwide, not only in the hospitals but also in the community. These enzymes are able to hydrolyse β-lactam antibiotics from several classes resulting in resistance to penicillins, cephalosporins and aztreonam. Since the 1980s, they have been known to cause nosocomial outbreaks and have been on the increase in recent years (CANTON and COQUE, 2006; PEREZ *et al.*, 2007).

1.3.5 Metallo-β-lactamases

Not all β-lactamases use a serine residue for catalytic activity. The metallo-β-lactamases (MBLs) or molecular classe B β-lactamases are classified in functional group 3 (BUSH and JACOBY, 2010) and constitute a subset of zinc hydrolases with the ability to hydrolyse the amide bond of the β-lactam ring of a number of β-lactam antibiotics. The metallo-β-lactamase group includes a small number of enzymes when compared to serine β-lactamases, but their numbers are still increasing.

The first metallo-β-lactamase to be described was the BcII enzyme isolated from B*acillus cereus* in 1966 (SABATH and ABRAHAM, 1966). For two decades it was the only example of an MBL and was regarded as a biochemical curiosity as *B. cereus* was not considered to be a serious clinical pathogen. Later these enzymes were described in several species of bacteria that occur naturally, such as *Bacteroides fragilis*, *Chryseobacterium* spp., *Legionella gormanii*, *Stenotrophomonas* spp., and several species of *Aeromonas*. In these environmental bacteria MBLs are encoded in the chromosome (QUEENAN and BUSH, 2007). The zinc-dependent enzymes were only regarded as potential threats when found to be transferable (WATANABE *et al.*, 1991). Since 1991 a dramatic increase in acquired and transferable MBLs has been observed among major Gram-negative pathogens, including various *Acinetobacter*, *P. aeruginosa* and the *Enterobacteriaceae* (WALSH *et al.*, 2005). The majority of transferable metallo-β-lactamases are included in common families: IMP, VIM, GIM, SPM and SIM, members of which are associated with several genetic platforms such as integrons, plasmids, transposons and ISCRs. Some of these are mobile, facilitating the transfer of MBLs among bacteria (WALSH *et al.*, 2005).

1.4 Carbapenemases

The treatment of infectious diseases by penicillins and cephalosporins is increasingly challenged by the emergence and dissemination of numerous CTX-M, TEM and SHV mutants with a broad spectrum of activity (PEREZ *et al.*, 2007). Of all β-lactams, carbapenems are the least prone to β-lactamase activity, being stable against ESBLs and AmpC β-lactamases. This β-lactamase stability, together with the rapid penetration to the target site and strong PBP affinity, gives carbapenems the broadest spectrum of activity of any β-lactams (BONFIGLIO *et al.*, 2002). Unlike most other antibiotics, most carbapenems are effective against clinically-significant, Gram-negative non-fermenters (e.g., *P. aeruginosa*, *Burkholderia cepacia* and *Acinetobacter* spp.) (BETRIU *et al.*, 2010; CASTANHEIRA *et al.*, 2009) and anaerobes (GOLDSTEIN and CITRON, 2009). Moreover, these β-lactam compounds also behave as irreversible inhibitors of most serine-β-lactamases (BEADLE and SHOICHET, 2002; NUKAGA *et al.*, 2003a). As is the case of the other β-lactamase inhibitors, carbapenems can give rise to a tetrahedral acylenzyme intermediate that resists deacylation and permanently inactivates the β-lactamase (BEADLE and SHOICHET, 2002).

Therefore, carbapenems have traditionally been reserved to treat the most serious infections, being considered last resource antibiotics in the hospital, used against bacterial strains that exhibit resistance to other β-lactams. However, their clinical use has increased over the last 20 years as the prevalence of resistance to penicillins, cephalosporins, fluoroquinolones and aminoglycosides has increased (BAUGHMAN, 2009). Although carbapenems are susceptible to serine carbapenemases and metallo-β-lactamases, so far these resistance mechanisms are less common; nevertheless they are increasing worldwide, selected by the treatment of infections caused by ESBL-producing pathogens. Their dissemination severely limits the options for treatment of producing organisms (QUEENAN and BUSH, 2007; WALTHER-RASMUSSEN and HOIBY, 2007).

According to Poirel and Nordmann, carbapenemases can be defined as β-lactamases that significantly hydrolyse at least imipenem and/or meropenem; additionally most of these enzymes are also active against other β-lactams such as penicillins, oxyimino-cephalosporins and cephamycins (POIREL and NORDMANN, 2002). Carbapenemases are a diverse group including enzymes from molecular classes A, B and D (QUEENAN and BUSH, 2007).

Occasionally overproduction of AmpC enzymes can confer clinically relevant resistance to carbapenems, if this is associated with other resistance mechanisms such as porin loss (MAMMERI *et al.*, 2008).

1.4.1 Oxacillinases

The class D β-lactamases are also referred as oxacillinases because they hydrolyse oxacillin and cloxacillin much faster than classical penicillins. A limited number of oxacillinases with weak carbapenemase activity have been described, mainly in *A. baumannii* (BERTINI *et al.*, 2006; CARRER *et al.*, 2010), but also occur in *P. aeruginosa* (GIRLICH *et al.*, 2004) and *Enterobacteriaceae* (GÜLMEZ *et al.*, 2008; POIREL *et al.*, 2004b). The OXA carbapenemases are very diverse enzymes that can be divided into subgroups such as OXA-23-like, OXA-24-like, OXA-48, OXA-51-like, and OXA-58-like. OXA carbapenemase genes are located on both chromosomes and plasmids (WALTHER-RASMUSSEN and HØIBY, 2006).

The substrate specificities of the OXA-type carbapenemases are diverse, but generally the enzymes have measurable hydrolytic activity against the penicillins (benzylpenicillin, ampicillin, piperacillin and ticarcillin), some cephalosporins (cefalotin and cefaloridine) and imipenem while the extended-spectrum β-lactams, ceftazidime, cefotaxime and aztreonam, are not or only very poorly hydrolysed (WALTHER-RASMUSSEN and HOIBY, 2007). In general, imipenem hydrolysis, which is faster than meropenem hydrolysis, is slow, with the highest k_{cat} values for the OXA-54 and OXA-48 enzymes at 1 s^{-1} and 2 s^{-1}, respectively (POIREL *et al.*, 2004a; POIREL *et al.*, 2004b). The K_m values for imipenem are also low, ranging from 2 to 20 μM, indicating that the OXA enzymes have very high affinity for these substrates (QUEENAN and BUSH, 2007).

Class D β-lactamases are usually not inhibited by clavulanic acid, tazobactam, and sulbactam, whereas their activities may be inhibited *in vitro* by sodium chloride (NaCl) (WALTHER-RASMUSSEN and HOIBY, 2007). Inhibition by NaCl is attributed to the presence of a Tyr residue in the Tyr144-Gly-Asn motif (HERITIER *et al.*, 2003).

Most of the OXA-type carbapenemases exhibit low catalytic efficiency for the carbapenems *in vitro*; however the association with other resistance mechanisms such as reduced permeability (MUSSI *et al.*, 2005; POIREL *et al.*, 2004b) or

expression of efflux pumps (HERITIER *et al.*, 2005; LEE *et al.*, 2010) usually results in high-level resistance to carbapenems in the resistant strains.

1.4.2 Class A carbapenemases

Class A β-lactamases with activity against carbapenems were considered uncommon. These were first described in the 1980s in some *Enterobacteriaceae* (NORDMANN *et al.*, 1993; YANG *et al.*, 1990). However, they are now widespread as result of the transmission of plasmid-mediated carbapenemases (LIVERMORE, D. M., 2009). The class A carbapenemases belong to functional group 2f, are inhibited, to varying degrees, by β-lactamase inhibitors (but not EDTA), and still represent a relatively small group of β-lactamases. However, they are increasing in number, due primarily to the increasing identification of the plasmid-mediated enzymes KPC (*Klebsiella pneumoniae* carbapenemase) and GES (Guiana extended spectrum) (BUSH and JACOBY, 2010). These enzymes have been described in isolates that also have AmpC-type cephalosporinases, thereby broadening their substrate profile to a wide variety of β-lactam compounds (RASMUSSEN and BUSH, 1997).

As mentioned earlier, carbapenems are able to irreversibly inhibit most class A β-lactamases including ESBLs (BEADLE and SHOICHET, 2002; NUKAGA *et al.*, 2003a). However, so far, the mechanism by which class A carbapenemases escape inhibition and hydrolyse these antibiotics remains unclear.

The group of class A carbapenem-hydrolysing β-lactamases consists of a small number of chromosomal enzymes including NMC-A and IMI-1 from *E. cloacae* (NORDMANN *et al.*, 1993; RASMUSSEN *et al.*, 1996), Sme-1 to -3 from *S. marcescens* (enzymes differing by one to two amino acid substitutions) (QUEENAN *et al.*, 2006; QUEENAN *et al.*, 2000; YANG *et al.*, 1990), SFC-1 from *S. fonticola* (HENRIQUES *et al.*, 2004) and the recently described BIC-1 from *P. fluorescens* (GIRLICH *et al.*, 2010). In addition, class A carbapenemases also include plasmid-mediated enzymes, the most important being the carbapenemases from *K. pneumoniae* (KPCs), and some GES β-lactamases (POIREL *et al.*, 2001; YIGIT *et al.*, 2001).

The chromosomal enzymes NMC-A, Sme and IMI-1 share a similar spectrum of hydrolysis that includes penicillins, early cephalosporins, carbapenems and aztreonam. Imipenem is hydrolysed faster than meropenem and they display, if detected, a very low activity against extended-spectrum cephalosporins. These

enzymes are inhibited by the β-lactamase inhibitors clavulanic acid, tazobactam and sulbactam (MARIOTTE-BOYER *et al.*, 1996; QUEENAN *et al.*, 2000; RASMUSSEN *et al.*, 1996). The expression of these β-lactamases is inducible and regulated by a LysR-type regulator (NAAS *et al.*, 1995; NAAS and NORDMANN, 1994). In two reports IMI-2 has been identified in plasmids associated with transposable elements (AUBRON *et al.*, 2005; YU *et al.*, 2006).

The plasmid-mediated class A carbapenemases KPC were first described in *Klebsiellae* (KPC-1 to KPC-3 differing by one to two point mutations), and were later reported in other members of the *Enterobacteriaceae* family (QUEENAN and BUSH, 2007; YIGIT *et al.*, 2001). KPC enzymes display a similar hydrolytic profile, exhibiting resistance to carbapenems, penicillins, cephalosporins and aztreonam and inhibition by the β-lactamase inhibitors clavulanic acid and tazobactam. Cephamycins and ceftazidime are weakly hydrolysed (WOODFORD *et al.*, 2004; YIGIT *et al.*, 2001; YIGIT *et al.*, 2003). In contrast to most chromosomal carbapenemases, expression of KPC enzymes is not inducible (YIGIT *et al.*, 2001). The KPC family has a great potential for spread due to its location on plasmids. KPC enzymes were recently reported in non-fermenters such as *P. aeruginosa* (VILLEGAS *et al.*, 2007) and *Acinetobacter* spp. (ROBLEDO *et al.*, 2010). To date, nine different KPC variants (KPC-2 to -10) have been identified that differ by one or two amino acid substitutions (ROBLEDO *et al.*, 2010). Of great concern is the concomitant occurrence of KPC enzymes with multiple plasmid-mediated enzymes, most often TEM-1 and SHV-11 (GIANI *et al.*, 2009; YANG *et al.*, 2010). More worrisome is the co-expression of KPCs and metallo-carbapenemases (YANG *et al.*, 2010) and additionally common ESBLs such as CTX-M-15 (POURNARAS *et al.*, 2010). This fact, together with their current spread worldwide, makes KPCs a potential threat to the antibiotic-based treatments currently available.

The GES family is the most recently reported group of class A carbapenemases. The first enzyme to be described with carbapenemase activity was GES-2, a point mutant derivative (G170N) of the extended-spectrum β-lactamase GES-1 (POIREL *et al.*, 2001). GES-2 is an ESBL with the substrate profile extended to imipenem but with hydrolysis rates lower than those of other carbapenem-hydrolyzing class A β-lactamases (POIREL *et al.*, 2001). Subsequently, three other variants with similar carbapenemase activity have been described (GES-4, GES-5, and GES-6), displaying the amino acid substitution G170S in the Ω-loop of the catalytic site (VOURLI *et al.*, 2004; WACHINO *et al.*, 2004). The genes encoding GES

β-lactamases were found in the variable region of class 1 integrons carried on self-transferable plasmids from different geographical locations (POIREL *et al.*, 2001; WACHINO *et al.*, 2004).

1.4.2.1 Tertiary structure

Class A carbapenemases comprise a peculiar group of enzymes as they are very broad spectrum β-lactamases able to efficiently hydrolyse not only classical penicillins and cephalosporins but also β-lactam substrates that are usually considered resistant to the activity of class A enzymes (QUEENAN and BUSH, 2007; WALTHER-RASMUSSEN and HOIBY, 2007).

To date crystal structures of class A carbapenemases have been determined for NMC-A, Sme-1, KPC-2 and GES-2 showing that all share an overall structural organization and catalytic residues similar to those of other class A β-lactamases (FRASE *et al.*, 2011; KE *et al.*, 2007; SOUGAKOFF *et al.*, 2002; SWARÉN *et al.*, 1998) (Figure 1.9A and B).

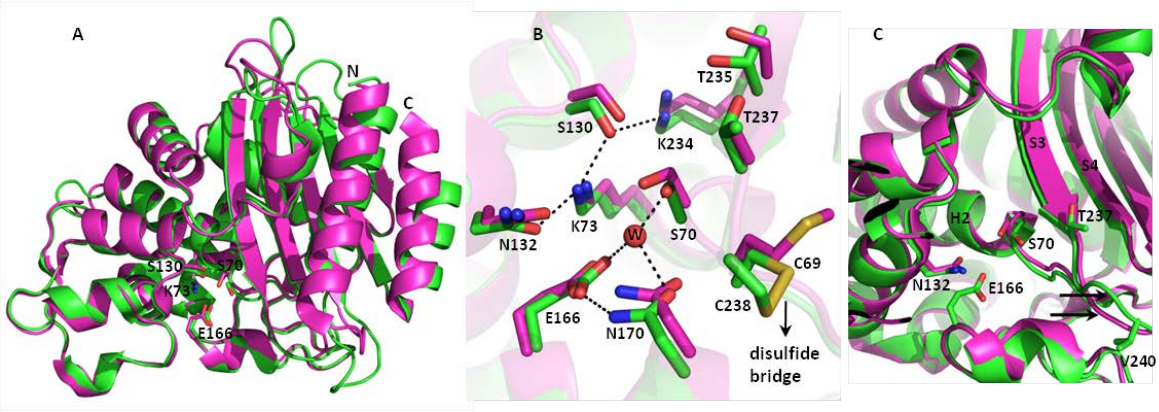

Figure 1.9 Superposition of a class A carbapenemase (KPC-2, green; PDB accession 2OV5) and a non-carbapenemase (TEM-1, magenta; PDB accession 1ZG4). A) Overall structure with some conserved residues depicted to position the active site. B) Active site of carbapenemase KPC-2 with β-lactamase TEM-1 as reference. Hydrogen bonds are shown as dashed lines and the deacylation water as a red sphere (W). C) Change in structure between β-sheets strands S3 and S4 (black arrows).

At the structural level, one of the most striking features of class A carbapenemases is the unique disulfide bond between Cys69 and Cys238, located

near the active site (Figure 1.9B), and absent in the other class A β-lactamases (KE *et al.*, 2007; RAQUET *et al.*, 1997; SOUGAKOFF *et al.*, 2002; SWARÉN *et al.*, 1998). Homology modelling studies with NMC-A and Sme-1 suggested that this disulfide bridge connects and constrains the two structural domains, significantly modifying the position of the S3 β-strand and consequently, the active site geometry (RAQUET *et al.*, 1997). According to these authors, the altered active site geometry allows a better interaction of the β-lactam carbonyl of imipenem with the oxyanion hole of Sme-1 than is possible with that of TEM-1 (RAQUET *et al.*, 1997). However, site-directed mutagenesis experiments have shown that the disulfide bond is required for hydrolysis of all β-lactams by Sme-1 and therefore, although important, it does not uniquely provide carbapenemase activity. These data suggest that the disulfide bond is necessary for the structural organization, or to stabilize, the enzyme (MAJIDUDDIN and PALZKILL, 2003; SOUGAKOFF *et al.*, 2002). On the other hand, some GES variants, such as GES-1, have cysteine at positions 69 and 238 but have poor carbapenemase activity while hydrolysing extended-spectrum cephalosporins (WALTHER-RASMUSSEN and HOIBY, 2007). This is evidence that other features are necessary for carbapenem hydrolysis.

The structure of NMC-A revealed a number of structural differences in the proximity of the active site in comparison to other class A β-lactamases (SWARÉN *et al.*, 1998). Apart from the disulfide bond discussed above, the conformation adopted by C238 induces a change in conformation of β-sheet strand S3 between residues 237 and 240 (Figure 1.9C), potentially increasing the access of substrate to the active site. In addition, positional differences were observed at N132 (Figure 1.9B); this residue is shifted away from strand S3 by 1.0 Å in NMC-A compared to the acylenzyme complex TEM-1-6α-hydroxymethyl penicillanic acid, and provides additional space in the substrate-binding cavity. This modification was proposed to allow the accommodation of the 6α-1R-hydroxyethyl substituent of carbapenems (SWARÉN *et al.*, 1998).

In the crystal structure of Sme-1 however, N132 occupies a position that is almost identical to that observed in TEM-1 (SOUGAKOFF *et al.*, 2002). In Sme-1 the most remarkable structural feature is the short distance (1.4 Å) separating the side chains of residues S70 and E166 in the active site cleft, compared with NMC-A and TEM-1. This leads to a lack of space to accommodate the catalytic water molecule found in that position in the other class A β-lactamases (SOUGAKOFF *et al.*, 2002). The authors hypothesized that a water molecule situated in the oxyanion hole of

Sme-1 can serve as the deacylating agent of the acylated enzyme (SOUGAKOFF *et al.*, 2002).

A Ser237Ala mutation in Sme-1 resulted in a marked decrease in catalytic activity against imipenem and cephalosporin substrates, showing that S237 contributes to the carbapenemase activity (SOUGAKOFF *et al.*, 1999). In another site-directed mutagenesis study of Sme-1, it was possible to recognize that several positions are important for hydrolysis of β-lactam antibiotics, but no single position was found to uniquely contribute to carbapenem hydrolysis (MAJIDUDDIN and PALZKILL, 2005). Taken together, these data support the idea that the carbapenemase activity of the group 2f carbapenemases is due to the important conserved residues that contribute together to form an active site that can accommodate and hydrolyse the carbapenems (MAJIDUDDIN and PALZKILL, 2005).

The structure of KPC-2 shows several active site alterations that are unique among carbapenemases. A shift of the catalytic S70 residue (Figure 1.9B) renders the active sites of the carbapenemases shallower, likely allowing easier access of the bulkier substrates. Further multiple active site adjustments including shifts in N132 and N170 (Figure 1.9B) are likely to collectively provide additional room to accommodate the α-substituents present in carbapenems and cephamycins (KE *et al.*, 2007).

Apart from the disulfide bridge, no major structural differences have been observed between class A carbapenemases and non-carbapenemases. Moreover, the structures of the class A carbapenemases solved so far did not provide a precise mechanism for the carbapenem hydrolysis in these enzymes. The structure of a class A carbapenemase complexed with a β-lactam molecule would provide useful information to definitely establish the catalytic mechanism of these threatening enzymes.

1.4.3 Metallo- β-lactamases

Most of the carbapenemases described so far belong to the metallo-β-lactamase (MBL) group. These are part of a superfamily of metallo-hydrolases with wide catalytic diversity (including oxydoreductases, glyoxylases, phosphoryl cholinesterase, etc.) (BEBRONE, 2007). The MBLs are unique among β-lactamases in requiring divalent cations (usually Zn (II)) in the active site for activity and constitute

the only family of β-lactamases whose carbapenemase activity is prevalent (QUEENAN and BUSH, 2007). A major characteristic of most MBLs is that they catalyse the hydrolysis of nearly all β-lactams used for therapeutic purposes. These enzymes have a very broad spectrum of activity exhibiting high activity towards carbapenems, cephamycins, third-generation cephalosporins and penicillins. Monobactams are the sole β-lactam antibiotics to be poorly recognized (FELICI *et al.*, 1993), however MBLs are often identified in isolates that also produce an ESBL able to hydrolyse aztreonam (POURNARAS *et al.*, 2010). Metallo-β-lactamases are resistant to the clinically available class A β-lactamase inhibitors such as clavulanic acid, but are susceptible to chelating agents such as EDTA, dipicolinic acid or 1,10-phenanthroline (QUEENAN and BUSH, 2007).

1.4.3.1 Classification

Based on DNA sequence alignments, protein structure, activity profile and metal ion requirements, MBLs are classified into three subclasses: B1, B2, and B3 (GALLENI *et al.*, 2001; GARAU *et al.*, 2004).

Subclass B1 includes several chromosomally encoded enzymes such as BcII from *B. cereus* (HUSSAIN *et al.*, 1985), CcrA from *B. fragilis* (RASMUSSEN *et al.*, 1990), BlaB from *Elizabethkingia meningoseptica* (ROSSOLINI *et al.*, 1998), as well as the plasmid-encoded IMP (WATANABE *et al.*, 1991), VIM (LAURETTI *et al.*, 1999), SPM (TOLEMAN *et al.*, 2002), and GIM (CASTANHEIRA *et al.*, 2004)-type enzymes. The acquired MBL genes located on plasmids are usually embedded in class 1 integrons, which can contain additional gene cassettes, and are easily disseminated among clinical isolates (HU and ZHAO, 2009; TATO *et al.*, 2010). The most recent examples of transferable B1 enzymes are DIM-1 from *P. stutzeri* (POIREL *et al.*, 2010b) and NDM-1, originally described in a *K. pneumoniae* isolate (YONG *et al.*, 2009) but rapidly spreading in India, Pakistan, the UK (KUMARASAMY *et al.*, 2010), Australia (POIREL *et al.*, 2010a) and a rapidly growing number of other countries (NORDMANN *et al.*, 2011).

The subclass B2 includes the enzymes produced by different *Aeromonas* species (CphA (MASSIDDA *et al.*, 1991), ImiS (WALSH *et al.*, 1998) and AsbM1 (YANG and BUSH, 1996)) and the Sfh-I β-lactamase from *S. fonticola* (SAAVEDRA *et al.*, 2003). These MBLs are considered as “true” carbapenemases due to their high

specificity for hydrolyzing carbapenems, and cannot effectively be detected with the use of nitrocefin (QUEENAN and BUSH, 2007).

Subclass B3 includes the MBLs L1 from *S. maltophilia* (WALSH *et al.*, 1994), GOB from *E. meningoseptica* (BELLAIS *et al.*, 2000), FEZ-1 from *L. gormanii* (BOSCHI *et al.*, 2000), THIN-B produced by *Janthinobacterium lividum* (ROSSOLINI *et al.*, 2001), Mbl1b (SIMM *et al.*, 2001) and CAU-1 (DOCQUIER *et al.*, 2002) from *Caulobacter crescentus*, and BJP-1 from *Bradyrhizobium japonicum* (STOCZKO *et al.*, 2006). Most of the organisms cited above are environmental species, of which some can cause opportunistic infections (such as *S. maltophilia* and *L. gormanii*) whereas others are not pathogenic. Apart from L1 enzyme from *S. maltophilia*, reported to exist as a tetramer (CROWDER *et al.*, 1998), all the MBLs are monomeric enzymes.

MBLs included in both subclasses B1 and B3 have a broad substrate profile exhibiting high hydrolytic activity for all β-lactams except aztreonam (FELICI *et al.*, 1993) and require two bound zinc atoms for full activity; however, these enzymes differ in the amino acids involved in zinc binding in the active site (GALLENI *et al.*, 2001; GARAU *et al.*, 2004). In contrast, the enzymes belonging to subclass B2 behave as strict carbapenemases, efficiently hydrolyzing only carbapenems, and display weak hydrolytic activity towards penicillins and cephalosporins (FELICI *et al.*, 1993; WALSH *et al.*, 1996). Another distinctive feature of this subclass is that these MBLs require only one Zn (II) for its maximal enzymatic activity and are considered to be inactivated by a second Zn (II) (COSTELLO *et al.*, 2006; VALLADARES *et al.*, 1997)

1.4.3.2 Structure of MBLs

The three-dimensional structures of several B1 enzymes (BcII (CARFI *et al.*, 1995; FABIANE *et al.*, 1998), CcrA (CONCHA *et al.*, 1996), IMP-1 (CONCHA *et al.*, 2000), SPM-1 (MURPHY *et al.*, 2006), VIM-2 (GARCIA-SAEZ *et al.*, 2008) and IND-7 (YAMAGUCHI *et al.*, 2010)), one B2 enzyme (CphA (GARAU *et al.*, 2005)) and a few B3 enzymes (L1 (ULLAH *et al.*, 1998), FEZ-1 (GARCIA-SAEZ *et al.*, 2003) and BJP-1 (DOCQUIER *et al.*, 2010)) have been solved by X-ray crystallography. Despite the generally low degree of sequence similarity between the different subclasses, the MBLs share a similar folding pattern (Figure 1.10).

Metallo-β-lactamases exhibit a common αββα fold, known as the metallo-β-lactamase fold, which includes a compact core of two β sheets sandwiched by five α helices on the external faces (CARFI *et al.*, 1995) (Figure 1.10). The active site, containing one or two Zn (II) ions, is located within a shallow groove formed by the interface of the two αβ domains (CARFI *et al.*, 1995). The MBLs have a conserved structural metal-binding sequence, the amino acid sequence $H^{116}XH^{118}XD^{120}...H^{196}...C^{221}...H^{263}$ and are able to bind up to two metal ions in their active site (CROWDER *et al.*, 2006).

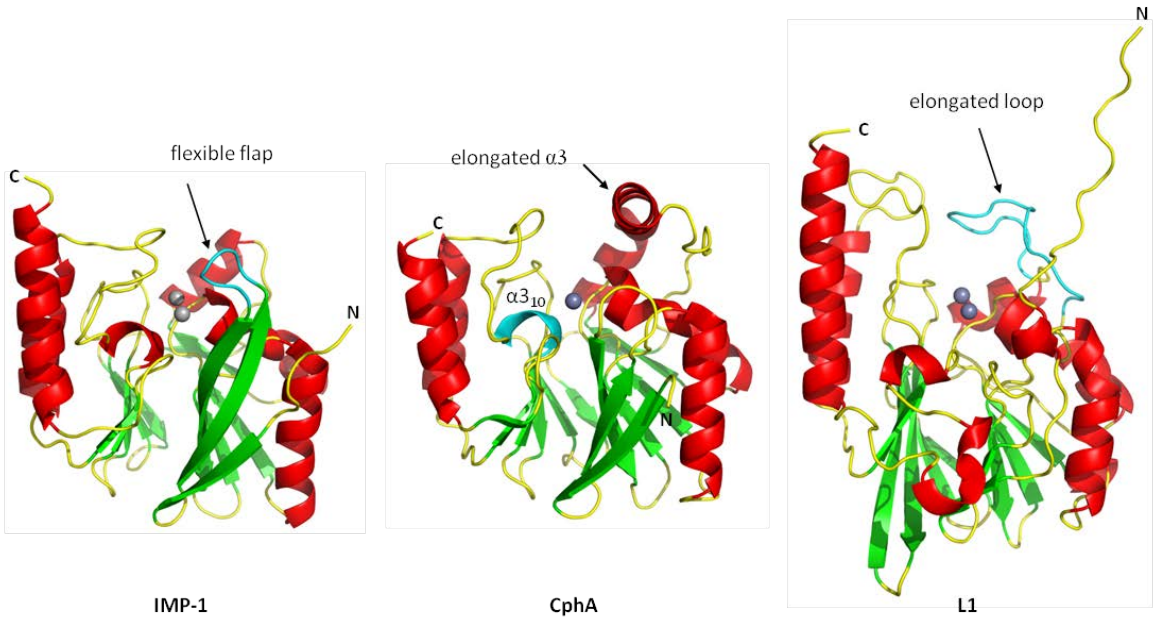

Figure 1.10 Metallo-β-lactamase overall fold, showing a representative of each subclass: IMP-1 from *P. aeruginosa* (B1; PDB accession 1DDK), CphA from *A. hydrophila* (B2; PDB accession 1X8G) and L1 from *S. maltophilia* (B3; PDB accession 1SML). The helices are coloured red, the β-sheets are green and loops are yellow. Zinc ions are represented as grey spheres. Non-conserved secondary structural elements among subclasses are labelled and/or shown in cyan.

Although the first structure determined for BcII revealed one zinc ion bound (CARFI *et al.*, 1995), subsequent structures of enzymes from the B1 and B3 subclasses, including BcII, show a dinuclear metal center (FABIANE *et al.*, 1998). In these enzymes, one Zn (II) ion (Zn1) is tetrahedrally coordinated to three histidine ligands, His116, His118, and His196 and a bridging water/hydroxide (Figure 1.11), while the second Zn (II) ion (Zn2) displays a trigonal bipyramidal coordination geometry (CONCHA *et al.*, 1996; FABIANE *et al.*, 1998; ULLAH *et al.*, 1998). In B1

enzymes the second metal ion-binding site consists of Asp120, Cys221, His263, the bridging water/hydroxide and an additional solvent molecule. In B2 enzymes this site represents the active site species in the mono-zinc form (CRAWFORD *et al.*, 2005; GARAU *et al.*, 2005). The B1 Zn2 ligand Cys221 is substituted by His121 in B3 enzymes affecting the geometry of this site; thus the metal ion is bound to Asp120, His121 and His263, and one or two water molecules. The serine residue present at position 221 in B3 MBLs does not act as a metal ligand (ULLAH *et al.*, 1998) (Figure 1.11). The other exception to the consensus metal-binding site is the single mutation of His116 to Asn116 in the Zn1 binding site among B2 enzymes (GALLENI *et al.*, 2001) (Figure 1.11).

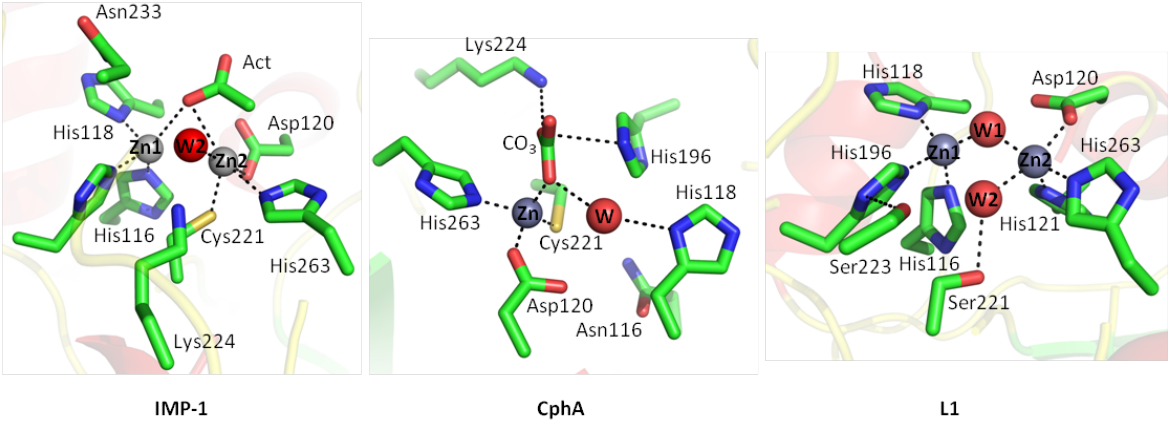

Figure 1.11 Metallo-β-lactamase active sites from the three subclasses: IMP-1 (B1), CphA (B2) and L1 (B3) (PDB accessions are as in Figure 1.9). Zinc ions (Zn) and water molecules (W) are represented as grey and red spheres, respectively. Coordination bonds are shown as dashed lines. Act (IMP-1, left) represents an acetate molecule that occupies the place of a water molecule.

The structure of B1 MBLs is characterised by a mobile loop or flap spanning residues 61-65 covering the active site (Figure 1.10), believed to be involved in substrate recognition and binding (CONCHA *et al.*, 2000; MOALI *et al.*, 2003). Mutagenesis studies showed that a large percentage of residues in the flap have a limited tolerance for substitutions further supporting the key role of the flap in the structure and function of IMP-1 (MATERON and PALZKILL, 2001). The mobile loop is disordered in the structure of native enzymes but in the presence of an inhibitor, the loop is stabilized (CONCHA *et al.*, 2000; GARCÍA-SÁEZ *et al.*, 2003). Deletion of the flap from IMP-1 resulted in a loss of catalytic efficiency dependent on the substrate tested, with almost no effect over carbapenems (MOALI *et al.*, 2003). The structure of

SPM-1, however, reveals the lack of the mobile flap, suggesting a different mechanism of β-lactam recognition by this enzyme compared with related enzymes (MURPHY *et al.*, 2006).

The 61-65 mobile flap is absent in MBLs from subclasses B2 and B3. In CphA, a B2 enzyme, an elongated α3 helix is present (Figure 1.10) and shows a kink about Trp150 that enables α3 to follow the surface curvature of the protein and provide a hydrophobic face that contributes to binding of carbapenem substrates (GARAU *et al.*, 2005). Crystal structures of B3 enzymes showed that there is an elongated loop between residues 150 and 168 extending over the active site (Figure 1.10) which is absent in the better characterised subclass B1 enzymes (GARCIA-SAEZ *et al.*, 2003; ULLAH *et al.*, 1998). Modelling studies have predicted that two residues of this flexible loop, Ile164 and Phe158, make significant contacts with large hydrophobic substituents of penicillins, cephalosporins, or carbapenems (ULLAH *et al.*, 1998). However, mutagenesis studies revealed that these residues are not essential for tight substrate binding (CARENBAUER *et al.*, 2002).

A unique feature is observed in the structure of B3 enzymes: a single intramolecular disulphide bridge links two cysteines, Cys256 and Cys290 in L1 and FEZ-1 (GARCIA-SAEZ *et al.*, 2003; ULLAH *et al.*, 1998) while in the recently solved structure of BJP-1 a single disulphide bridge is also present but in a different region of the structure (between Cys200 and Cys220) (DOCQUIER *et al.*, 2010).

1.4.3.3 Catalytic mechanism

As for serine β-lactamases, β-lactam hydrolysis in metallo-β-lactamases occurs by a nucleophilic attack on the carbonyl group of the β-lactam ring, followed by the cleavage of the amide bond and protonation of the bridging nitrogen atom (CROWDER *et al.*, 2006). However, in contrast to serine enzymes, in the MBL mechanism no covalent intermediate is formed. Although the number of metal ions required for hydrolysis, and the role of each metal site in the hydrolysis of β-lactams by MBLs, are still under debate, there is a general consensus that the Zn1-bound water molecule, or hydroxide, is the nucleophile for the reaction of mono- and dinuclear B1 and B3 MBLs (CROWDER *et al.*, 2006).

The structures of enzyme-product complexes of hydrolysed moxalactam with the subclass B3 MBL L1 (SPENCER *et al.*, 2005) and hydrolysed and rearranged biapenem with the subclass B2 MBL CphA (GARAU *et al.*, 2005) have suggested a

common role for Zn2 in MBLs. In both cases, the Zn2 site displays strong interactions with the bridging nitrogen of the hydrolysed β-lactam ring and the carboxylate moiety of the antibiotic. These studies indicate that Zn2 may be involved in C–N bond cleavage by stabilization of the development of negative charge in the β-lactam nitrogen atom, and may also play a role in substrate binding (LLARRULL *et al.*, 2007; SPENCER *et al.*, 2005). A quantum mechanical–molecular mechanical (QM–MM) reaction modelling report postulates that Zn2 orients a water molecule to act as a proton donor in the rate-determining step (DAL PERARO *et al.*, 2007).

Based on the crystal structures and models of β-lactams bound to the active site, a catalytic mechanism has been proposed for dinuclear MBLs, such as B1 and B3 enzymes (CONCHA *et al.*, 2000; SPENCER *et al.*, 2005; ULLAH *et al.*, 1998). Following substrate binding, one of the Zn ions, together with enzyme residues, polarizes the β-lactam carbonyl for attack by the metal-bridging hydroxyl group that is additionally positioned and oriented by hydrogen bonding to Asp120. This creates an unstable tetrahedral species that undergoes C-N bond cleavage to generate an intermediate in which the β-lactam nitrogen is anionic. This species is resolved by proton transfer to the nitrogen followed by product dissociation from the enzyme active site. The source of the proton may be Asp120 or a water molecule (DAL PERARO *et al.*, 2007). The unprotonated anionic intermediate is not necessarily highly populated- while in some cases (such as hydrolysis of the chromogenic cephalosporin nitrocefin by the CcrA or L1 enzymes (MCMANUS-MUNOZ and CROWDER, 1999; SPENCER *et al.*, 2001; WANG, ZHIGANG *et al.*, 1999)) this species accumulates to high levels, in others (e.g. hydrolysis of cephalosporins by BcII (RASIA and VILA, 2004)) it does not and hydrolysis effectively occurs in a single step.

A different mechanism, however, has been proposed for the B2 MBL CphA based on the crystal structures of the native enzyme and of a product complex with hydrolysed biapenem (GARAU *et al.*, 2005). Nucleophilic attack is performed by a water molecule that is activated by a general base, His118 or Asp120, and is not coordinated to zinc (GARAU *et al.*, 2005; XU *et al.*, 2006). This water molecule attacks the β-lactam carbonyl to generate a tetrahedral intermediate. The single Zn ion (Zn2) is thought to promote C-N bond cleavage by coordination to the β-lactam nitrogen as described above for the binuclear enzymes (XU *et al.*, 2006). An incoming solvent molecule that replaces the water used in the nucleophilic attack protonates the amide nitrogen, followed by release of the final product. However, a recently published computational study of the complete reaction mechanism of CphA

proposes a single-step mechanism involving two water molecules in the active site (SIMONA *et al.*, 2009). One water molecule (Wat1) performs the nucleophilic attack to the β-lactam carbonyl carbon, and another Zn-bound water (Wat2) simultaneously protonates the β-lactam nitrogen (Figure 1.12). This work also highlights a role for His118 in the orientation of the catalytic water as well as acting as the general base. Despite significant effort aimed at identifying the general base in the catalytic mechanism of the B2 MBLs, this remains controversial with studies pointing to either Asp120 (XU *et al.*, 2006) or His118 (SIMONA *et al.*, 2009) as the likely candidates.

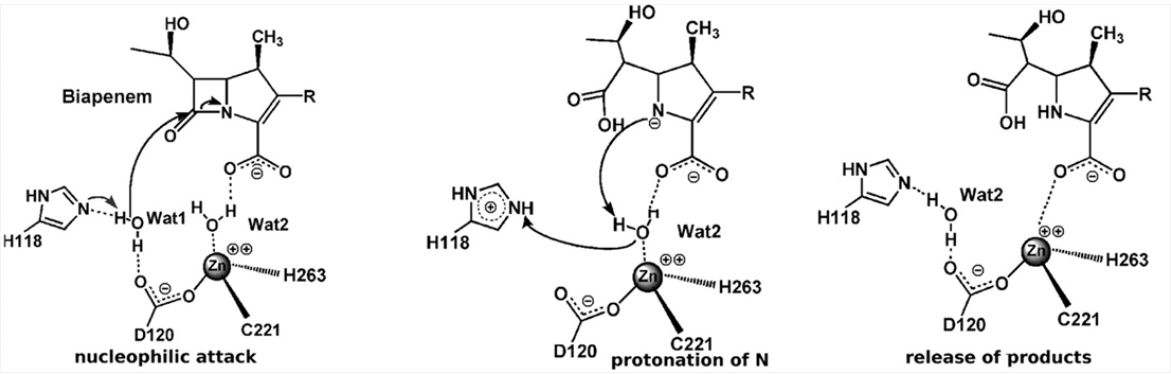

Figure 1.12 Schematic representation of the proposed reaction mechanism of B2 MBL CphA involving two water molecules (Wat). In the Henry-Michaelis complex, the interaction of the substrate with the zinc ion is mediated by Wat1 and Wat2. Wat1 is activated by a general base (His118 in the scheme) to perform the nucleophilic attack. The zinc-bound Wat2 acts as a proton donor to the lactam nitrogen. Figure and legend were modified from Simona *et al.*, (2009).

Until recently, the identification of the second, inhibitory zinc binding site in B2 enzymes was a matter of debate. Spectroscopic studies of cobalt-substituted ImiS from *A. veronii* suggested that the inhibitory zinc binds in a site distinct from the active site, involving both His118 and Met146 as ligands (COSTELLO *et al.*, 2006; CRAWFORD *et al.*, 2005). However, a mutagenesis study that aimed to investigate the potential zinc binding sites in CphA indicated that the position of the second zinc is similar to the tri-histidine site (see above) of subclasses B1 and B3 MBLs, with His118 and His196 as potential ligands (BEBRONE *et al.*, 2008). This hypothesis was confirmed by determination of the structure of the dizinc form of CphA (BEBRONE *et al.*, 2009). The structure shows that the first zinc binds in the cysteine site, as previously determined, and that the second zinc occupies a modified histidine site. In

CphA the second zinc ion is coordinated by His118 and His196 where a sulfate ion and a water molecule complete the metal coordination, with the sulfate ion acting as a bridging species between the two zinc ions (BEBRONE *et al.*, 2009).

2. Scope of this dissertation

2.1 *Serratia fonticola* UTAD54

Currently bacterial resistance to β-lactam antibiotics constitutes a very serious threat to the clinical community. Resistance to this class of antibiotics is primarily due to the expression of several serine and metal-containing β-lactamases that hydrolyse the amide bond of the β-lactam rings, resulting in antibiotic inactivation. Of utmost importance are the carbapenemases, β-lactamases that are able to hydrolyse the carbapenems (i.e. imipenem and meropenem), drugs considered to be the last resort agents to treat infections caused by multiresistant pathogens.

The study here presented consists of a biochemical characterisation of SFC-1 and Sfh-I, both carbapenemases of *Serratia fonticola* UTAD54. In this work the three-dimensional structures of the two β-lactamases were also determined.

The strain *S. fonticola* UTAD54 is an environmental strain that was isolated in 2002 during a study in Northeastern Portugal investigating the susceptibility of bacterial populations of untreated drinking waters to antimicrobial agents, including carbapenems. This new strain was resistant to penicillins, cephalothin, cefuroxime and carbapenems, antibiotics to which other strains of the same species were susceptible (SAAVEDRA *et al.*, 2003). Research upon carbapenem resistance mechanisms in *S. fonticola* UTAD54 led to the characterisation of a new gene coding for a metallo-β-lactamase, Sfh-I, that was assigned to subclass B2.

However, this β-lactamase alone could not explain the complete resistance profile of *S. fonticola* UTAD54. Further investigation lead to the identification of a new gene coding for a class A β-lactamase designated SFC-1 (HENRIQUES *et al.*, 2004). At the primary structure level, SFC-1 has high homology with the class A carbapenemases, the closest relative being KPC-1 (62% identical), a clinically important carbapenemase described in *K. pneumoniae* and other nosocomial pathogens. As reported for KPC-1, no transcriptional regulator controlling the expression of bla_{SFC-1} was found. SFC-1 is active against penicillins, cephalothin and aztreonam but has reduced susceptibility to meropenem and imipenem. The activity of SFC-1 is inhibited by β-lactamase inhibitors (e.g. clavulanic acid, tazobactam). The hydrolytic profile of SFC-1 is thus typical of the class A carbapenemases already described (HENRIQUES *et al.*, 2004).

2.2. Goals

Compared to other β-lactamases, a relatively low number of class A carbapenemases have been identified and characterised. Thus, the first goal of the work here presented was the kinetic characterisation of SFC-1.

A further aim was then to investigate the molecular basis of carbapenemase activity in SFC-1, in particular, and by implication of class A carbapenemases in general, by determining the three-dimensional structure of this enzyme.

There was considered to be both a lack of structural data on the interactions between β-lactamases and β-lactams while the mechanism of hydrolysis of carbapenems by class A carbapenemases remains unclear. A further objective of this project was thus to use structures of β-lactam complexes to establish a basis for the mechanism and specificity of SFC-1, especially with respect to carbapenem hydrolysis.

Given the divergent amino acid sequence of Sfh-I relatively to those of other B2 enzymes (50%), and the generally lower level of characterisation of these enzymes when compared to B1 and B3 MBLs, an initial aim for studies on this Sfh-I was to overexpress the *bla*$_{\text{Sfh-I}}$ gene in *E. coli* to facilitate purification and kinetic characterisation of the recombinant β-lactamase.

Considering that there is little consensus about the catalytic mechanism of the metallo-β-lactamases, in particular for subclass B2 enzymes, the final goal of this work was to determine the crystal structure of Sfh-I in order to establish a basis for the mechanism and specificity of this group of enzymes.

3. Biochemical characterisation of recombinant SFC-1 from *Serratia fonticola* UTAD54

3.1 Introduction

β-lactam antibiotics are among the safest, most efficient and most frequently prescribed antibacterial agents available (BUSH, 2002; MOLSTAD *et al.*, 2002). The intensive use of stable β-lactams in activities such as animal farming and medicine has resulted in the large spread of resistant bacterial strains (WEGENER, 2003; WITTE, 1998). The most efficient and prevalent mechanism of resistance to β-lactams is the production of β-lactamases, which inactivate the antibiotics by hydrolysis of the β-lactam ring (FISHER *et al.*, 2005; THOMSON and BONOMO, 2005).

Considering that carbapenems are broad spectrum β-lactams and are less prone to the hydrolytic action of most of the β-lactamases, a serious threat is posed by carbapenem-hydrolysing enzymes (QUEENAN and BUSH, 2007). Although comparatively rare, the frequency of carbapenemase containing-bacterial species has been increasing (QUEENAN and BUSH, 2007; WALTHER-RASMUSSEN and HOIBY, 2007). Previously characterised carbapenem-hydrolysing enzymes were included into Ambler molecular classes A, B and D (POIREL and NORDMANN, 2002; RASMUSSEN and BUSH, 1997). Class A carbapenemases belonging to functional group 2f (WALTHER-RASMUSSEN and HOIBY, 2007) are uncommon and comprise the chromosomally encoded β-lactamases NMC-A and IMI-1 from *E. cloacae* (NORDMANN *et al.*, 1993; RASMUSSEN *et al.*, 1996), Sme-1 to -3 from *S. marcescens* (QUEENAN *et al.*, 2006; QUEENAN *et al.*, 2000; YANG *et al.*, 1990), SFC-1 from *S. fonticola* (HENRIQUES *et al.*, 2004) and BIC-1 from *P. fluorescens* (GIRLICH *et al.*, 2010); and the plasmid mediated enzymes KPC-2 to -3 initially found in *K. pneumoniae* (SMITH MOLAND *et al.*, 2003; WOODFORD *et al.*, 2004; YIGIT *et al.*, 2001) but later described in other *Enterobacteriaceae* (BUSH, 2010) and non-fermenters (ROBLEDO *et al.*, 2010; VILLEGAS *et al.*, 2007) performing a total of 9 different variants (KPC-2 to -10).

Most of the strains included in the species *Serratia fonticola* express both a chromosomally encoded extended-spectrum class A β-lactamase and a species-specific AmpC β-lactamase (PEDUZZI *et al.*, 1997; STOCK *et al.*, 2003). Previous studies have shown that *S. fonticola* UTAD54 additionally expresses a metallo-enzyme (Sfh-I) (SAAVEDRA *et al.*, 2003) and a class A carbapenem-hydrolyzing β-lactamase (SFC-1) (HENRIQUES *et al.*, 2004). Both enzymes are chromosomally

encoded and are absent from other *S. fonticola* strains. The deduced amino acid sequence of SFC-1 displays considerable similarity to those of class A carbapenemases already described and the expression of the bla_{SFC-1} gene in *E. coli* confers on the host an antibiotic resistance profile typical of class A carbapenemases (HENRIQUES *et al.*, 2004).

In order to further characterise this class A carbapenemase, the gene encoding SFC-1 from *S. fonticola* UTAD54 was cloned and the protein was over-expressed in *E. coli*. After purification, the recombinant protein was characterised by kinetic and biochemical techniques.

3.2 Materials and methods

3.2.1 Bacterial strains and plasmid

E. coli XL-2 Blue (Stratagene Inc., La Jolla, CA, USA) and *E. coli* BL21 (DE3) (Novagen Inc., Madison, WI, USA) were respectively used as hosts for bla_{SFC-1} cloning and expression experiments. Plasmid pET-26b (Novagen, Inc.) was used as the cloning and expression vector.

E. coli bacterial cultures were routinely grown aerobically in LB medium at 37ºC, unless otherwise specified. Transformed cells were selected for the presence of plasmids using 50 µg/ml kanamycin. *S. fonticola* UTAD54 was grown aerobically in LB medium at 30ºC.

3.2.2 Antimicrobial agents

Antibiotics were provided as powders by GlaxoSmithKline (ceftazidime), Atral Laboratories (piperacillin), Hoeport Pharmaceutical Products (cefotaxime), Eurobio (ampicillin), Sigma (aztreonam, cephalothin, clavulanic acid, tazobactam), Sequoia Research Products (meropenem) and Merck Sharp & Dohme Co (cefoxitin). Sulbactam and imipenem were kindly provided by Pfizer Inc. and Merck Sharp & Dohme Co, respectively.

3.2.3 Plasmid construction

Genomic DNA was extracted from *S. fonticola* UTAD54 with the Genomic DNA Purification kit (MBI Fermentas, Vilnius, Lithuania) following the manufacturer's recommendations. All restriction enzymes were from Roche (Roche Diagnostics, Meylan, France).

The open reading frame encoding the mature SFC-1 polypeptide without the leader sequence was amplified by PCR using the following primers containing restriction sites (underlined) for *BspLu11*I and *Xho*I:

SFCexp2_for: 5'-GGA TCC ACA TGT CAC GCA CCG GTC GAC TG-3'

SFCexp2_rev: 5'-GTG CTC GAG TTA GAA GCCGAT AGA CTT TCC-3'

PCR was carried out in an iCycler Thermal Cycler (Bio-Rad Laboratories, Richmond, CA, USA) using *Taq* polymerase, nucleotides and buffers purchased from MBI Fermentas (Vilnius, Lithuania). PCR was performed in 50 µl mixtures containing 0.5x PCR buffer with $(NH4)_2SO_4$, 0.5x PCR buffer without $MgCl_2$, 3 mM $MgCl_2$, 200 µM deoxynucleoside triphosphates, 15 pmol of each primer, 1 U of *Taq* polymerase, and 50-100 ng of purified DNA from *S. fonticola* UTAD54. The temperature profile was as follows: initial denaturation at 94ºC for 7 min; 30 cycles of denaturation at 94ºC for 1 min, annealing at 60ºC for 1 min, and extension at 72ºC for 1 min; and a final extension at 72ºC for 10 min. PCR products (5 µl) were analysed by electrophoresis on a 1% agarose gel to confirm the 900 bp bla_{SFC-1} amplification. The remaining PCR product was purified using the Concert Rapid PCR Purification System (Gibco BRL, Eggenstein, Germany).

The amplified fragment was digested with *BspLu11*I and *Xho*I and ligated with T4 ligase into the *Nco*I site of the pET-26b vector to produce the recombinant plasmid pMF13. This plasmid expressed SFC-1 as a fusion with the *pelB* leader sequence from the pET-26b vector. *E. coli* XL-2 Blue competent cells were transformed and recombinant clones were selected on LB agar plates supplemented with 50 µg/ml kanamycin and 5 µg/ml aztreonam.

Five colonies were picked into 10 ml LB medium supplemented with 50 µg/ml kanamycin and grown overnight at 37°C. Plasmid DNA was purified using the Concert High Purity Plasmid Miniprep System (Life Technologies Inc., Gaithersburg, MD, USA). The presence of inserts was confirmed by double digestion with *BspLu11*I and *Xho*I. The gene was sequenced in the forward direction to verify that bla_{SFC-1} was inserted in frame. Plasmid pMF13 was then transformed into the expression host *E. coli* BL21 (DE3).

3.2.4 Detection of β-Lactamase activity by SDS-PAGE

Crude cell extracts of the *E. coli* clone expressing the recombinant enzyme were prepared. Expression of the SFC-1 enzyme was confirmed by SDS-PAGE. β-lactamase activity was detected by incubation of SDS-PAGE gels with nitrocefin, according to Stock and collaborators (STOCK *et al.*, 2003). After the identification of the β-lactamase band, the gel was stained with Coomassie Brilliant Blue (Sigma). The Low Molecular Weight SDS Calibration Kit (GE Healthcare UK Limited, Buckinghamshire, UK) was used to estimate the molecular weight of the protein.

3.2.5 Optimization of the expression of recombinant SFC-1

SFC-1 production was tested in induced and non-induced cultures. Overnight cultures of *E. coli* BL21 (DE3) transformed with pMF13 were used to inoculate 100 ml LB medium supplemented with kanamycin, and grown at 37ºC to reach an OD_{600nm} of 0.6. At that point, the culture was split into 2 x 50 ml cultures: one was induced by addition of 1 mM IPTG and the other served as uninduced control. Different temperatures were tested: 25ºC, 30ºC and 37ºC. Aliquots (1 ml) were sampled at different times (2, 3, 5, 12, 18 and 24 h) and centrifuged (23,000 x g for 122 min at 4ºC). Cell pellets were suspended in 0.25 ml of 50 mM sodium phosphate (pH 7.0) and frozen overnight at -20ºC. Cells were disrupted by sonication and the debris was removed by centrifugation (23,000 x g, 15 min, 4ºC). The crude protein solution was stored at -20ºC until use. β-lactamase activities in cell extracts were determined spectrophotometrically using 100 µM aztreonam as substrate ($\Delta\varepsilon_{318nm}$ = – 640 $M^{-1}cm^{-1}$; (POIREL *et al.*, 2000)) in 50 mM sodium phosphate (pH 7.0).

3.2.6 Over-expression and purification of SFC-1

Recombinant SFC-1 was purified from an uninduced culture of *E. coli* BL21 (DE3) (pMF13) grown in 0.5 L of LB medium supplemented with kanamycin at 37°C to an OD_{600nm} of 0.6. The incubation was continued for 12 h at 25°C. Cells were harvested by centrifugation (23,000 x g, 5 min, 4°C) and resuspended in 5 ml of 10 mM sodium phosphate buffer (pH 7.0). Crude lysates were obtained as described above (section 2.2.5).

Clear supernatant containing β-lactamase activity was filtered through a 0.2-µm-pore-size filter and loaded onto a pre-equilibrated S-Sepharose column (Amersham Pharmacia Biotech) with 10 mM sodium phosphate buffer (pH 6.0). The proteins were eluted with a linear gradient of NaCl (0 to 1 M) in the same buffer, at a flow rate of 3 ml/min.

The fractions presenting β-lactamase activity, measured as initial rate of hydrolysis of 100 µM ampicillin ($\Delta\varepsilon_{232nm}$ = - 1070 M^{-1} cm^{-1}), were loaded onto a pre-equilibrated Superdex 75 column (Amersham Pharmacia Biotech) with 10 mM sodium phosphate buffer, pH 7.0. Elution was performed with the same buffer at a flow rate of 1 ml/min, and active fractions were collected.

The protein content of each sample was determined with the Pierce BCA protein assay using BSA as standard. The purification yield and the relative molecular mass of SFC-1 were estimated by SDS-PAGE on 12% gels (LAEMMLI, 1970).

3.2.7 IEF analysis

Isoelectric focusing (IEF) of crude β-lactamase extracts of *S. fonticola* UTAD54 and *E. coli* BL21 (DE3) (pMF13), as well as of purified SFC-1 was performed with commercially prepared polyacrylamide gel plates (pH 3 to 9; Amersham Pharmacia Biotech), on a Phast System apparatus (Amersham Pharmacia Biotech). Focused β-lactamases were detected by a 1 mM nitrocefin solution (Oxoid, Basingstoke, UK). The pI of SFC-1 was determined by comparison to those of β-lactamases TEM-2 (pI 5.6) and SHV-5 (pI 8.2).

3.2.8 N-terminal sequencing

Purified enzyme was subjected to electrophoresis in a 15% acrylamide gel (200 V, 1 h). Proteins were electroblotted onto a polyvinylidene difluoride (PVDF) membrane (Bio-Rad) for 4h at 100 mA. After transfer the membrane was stained with 0.1% Coomassie Brilliant Blue. SFC-1 bands were excised and N-terminal sequence analysis was performed in the gas-pulsed liquid phase using a model 476A protein sequencer with a micro reaction chamber and an on-line HPLC system for phenylthiohydantoin (PTH) analysis (Applied Biosystems, Foster City, California, USA). Absorbance was monitored at 269 nm. The first 7 residues were determined and compared with the deduced sequence.

3.2.9 Mass spectrometry

The exact mass of the SFC-1 enzyme was determined by electrospray ionization-mass spectrometry (ESI-MS) on a Q-TOF 2 mass spectrometer (Micromass, Manchester, UK). An aliquot (400 µg) of the purified enzyme was desalted by overnight dialysis against water and lyophilized. Before injection into the mass spectrometer, the sample was solubilised in 200 µl of 0.005% (v/v) trifluoroacetic acid (TFA) in methanol. Data acquisition was carried out with a Micromass MassLynkx 3.4 data system.

3.2.10 Determination of kinetic parameters

Initial hydrolysis rates were measured at 25°C in 50 mM sodium phosphate (pH 7.0) on an ULTROSPEC 2000 spectrophotometer (Amersham Pharmacia Biotech). The following antibiotics and inhibitors were used: ampicillin, piperacillin, cephalothin, cefoxitin, cefotaxime, ceftazidime, aztreonam, imipenem, meropenem, tazobactam, sulbactam, clavulanic acid and EDTA. The wavelengths and extinction coefficients of β-lactams have been described previously (POIREL *et al.*, 2000). Substrates were assayed at different days, with ampicillin included as a reference each day. Kinetic parameters were determined by recording the initial rates at different substrate concentrations and by fitting the experimental data to the Michaelis-Menten equation, using GraphPad Prism (GraphPad Software Inc., La Jolla, USA).

Inhibition was measured after a 10-min pre-incubation of enzyme with inhibitor in phosphate buffer (pH 7.0), using cephalothin (100 µM) as the reporter substrate. Fifty percent inhibitory concentrations (IC_{50}) were determined from inhibition graphs of percent control activity *versus* concentration of inhibitor.

3.3 Results and discussion

3.3.1 Over-expression of SFC-1 in *E. coli*

Over-expression of the *S. fonticola* bla_{SFC-1} gene in *E. coli* was carried out using the T7 promoter-based expression vector, pET-26b. SFC-1 is expressed without the leader sequence as a fusion with the *pelB* leader sequence from the pET-26b vector. The construct was transformed into *E. coli* BL21 (DE3), expressing T7 RNA polymerase.

In order to confirm the expression of the enzyme, separation of proteins by SDS-PAGE was performed. The crude cell extract of *E. coli* BL21 (DE3) (pMF13) revealed a unique β-lactamase band with an apparent molecular weight of around 30.5 kDa after staining with nitrocefin. This result was in agreement with the value of 30.7 kDa predicted for the mature SFC-1 protein (HENRIQUES *et al.*, 2004).

Conditions for large-scale production of recombinant SFC-1 were optimised by testing IPTG-induced and non-induced cultures at three different temperatures (37, 30 and 25ºC). Production of the SFC-1 enzyme is shown to be temperature-dependent (Figure 3.1).

Cultures grown at 37ºC yielded a β-lactamase activity of 43 $\mu M.min^{-1}.ml^{-1}$ when induced with 1 mM of IPTG. Lowering the temperature to 30ºC and 25ºC significantly increased the enzyme yield (to 55 and 234 $\mu M.min^{-1}.ml^{-1}$, respectively). It was also verified that the SFC-1 production was remarkably influenced by IPTG induction. In non-induced cultures the yield was significantly higher with β-lactamase activities of 333, 420 and 542 $\mu M.min^{-1}.ml^{-1}$ for the cultures grown at 37, 30 and 25ºC, respectively. After 24h SFC-1 activity was drastically reduced in the cell fraction. Since highest yields were obtained in uninduced cultures, grown at 25ºC, these conditions were adopted for larger-scale SFC-1 production and purification.

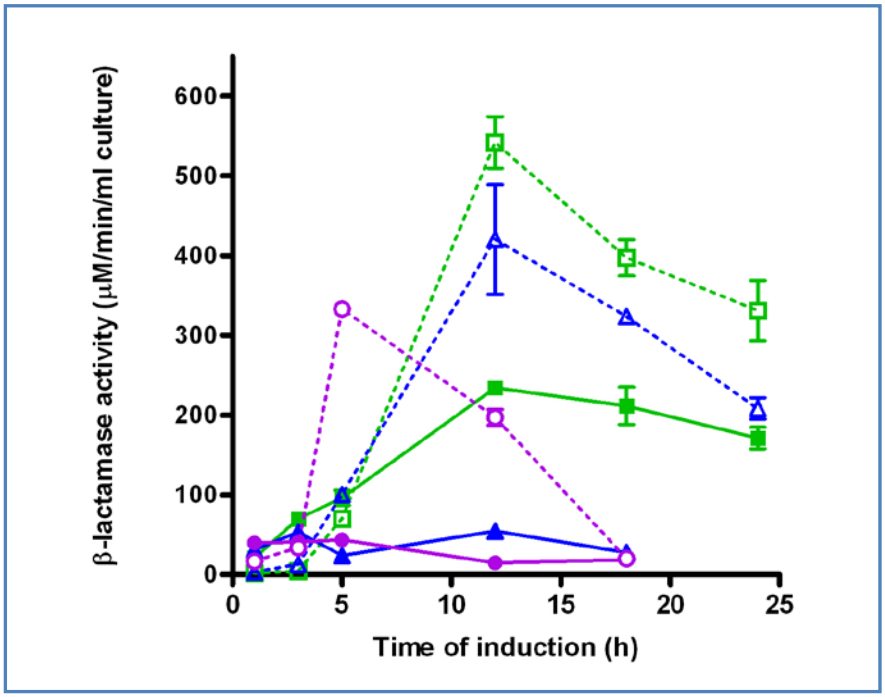

Figure 3.1 Influence of temperature and IPTG induction on the production of the SFC-1 β-lactamase. Production temperatures include 25°C (□), 30°C (Δ) and 37°C (○). In each case, time is post cell density equal to OD_{600nm} of 0.6. Cultures to which IPTG (1 mM) was added as inducer (—■—) and cultures not induced (--□--) are represented.

3.3.2 Purification and biochemical properties of SFC-1

Recombinant SFC-1 enzyme was purified from a 500 ml culture grown at 25°C for 12 h, by means of two chromatographic steps, as described in the Material and methods section 2.2.6. A summary of a typical purification experiment is shown in Table 3.1.

The initial SP-Sepharose chromatography step removed the majority of the contaminating proteins. Approximately 25 mg of purified enzyme was obtained per liter of culture using the described methodology. Protein was estimated to be >95% pure by sodium dodecyl sulfate-polyacrylamide gel electrophoresis (SDS-PAGE) (Figure 3.2) and the overall yield of the purification protocol was 82% (Table 3.1).

Table 3.1 Purification of the carbapenem-hydrolyzing β-lactamase SFC-1 produced by *E. coli* BL21 (DE3) (pMF13).

Purification step	Volume (ml)	Total protein (mg)	Specific activity[a] ($mM\ min^{-1}mg^{-1}$)	Total activity ($mM\ min^{-1}$)	Yield (%)	Purification (fold)
Crude extract	7.0	119.7	2.0	244	100	1
SP-Sepharose	15.5	16.4	12.7	208	85	6
Superdex 75	27.0	12.7	15.8	201	82	8

[a] β-lactamase activity of the different fractions was determined with 100 μM ampicillin as substrate.

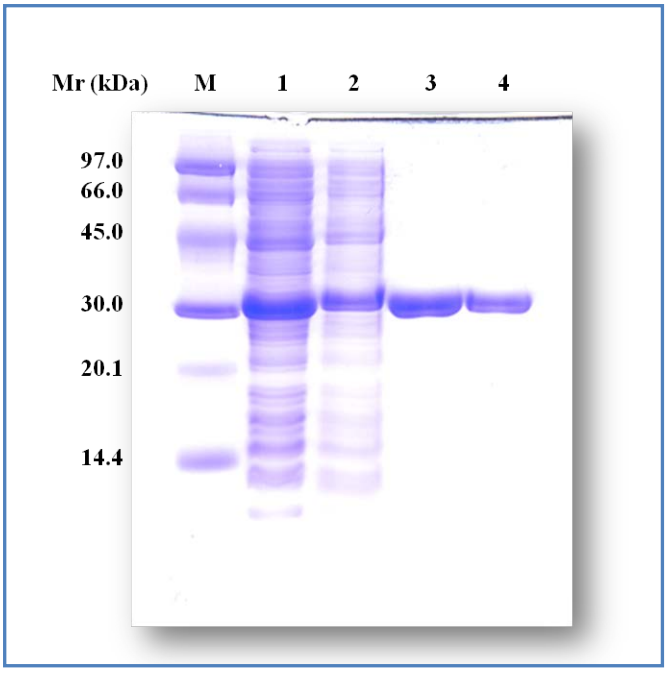

Figure 3.2 SDS-polyacrylamide gel of crude extract and of purified SFC-1 β-lactamase from *E. coli* BL21 (DE3)(pMF13). Lane M, molecular weight marker; lane 1, crude extract from *E. coli* BL21 (DE3)(pMF13); lane 2, crude extract 10 fold diluted; lane 3, cation exchange fraction with β-lactamase activity; lane 4, purified SFC-1. The gel was stained with Coomassie Brilliant Blue.

SDS-PAGE analysis showed that the purified SFC-1 migrates as a single band of approximately 30.5 kDa (Figure 3.2). However, isoelectric focusing revealed two forms of the purified SFC-1, with pIs of 7.6 and 8.2 (Figure 3.3).

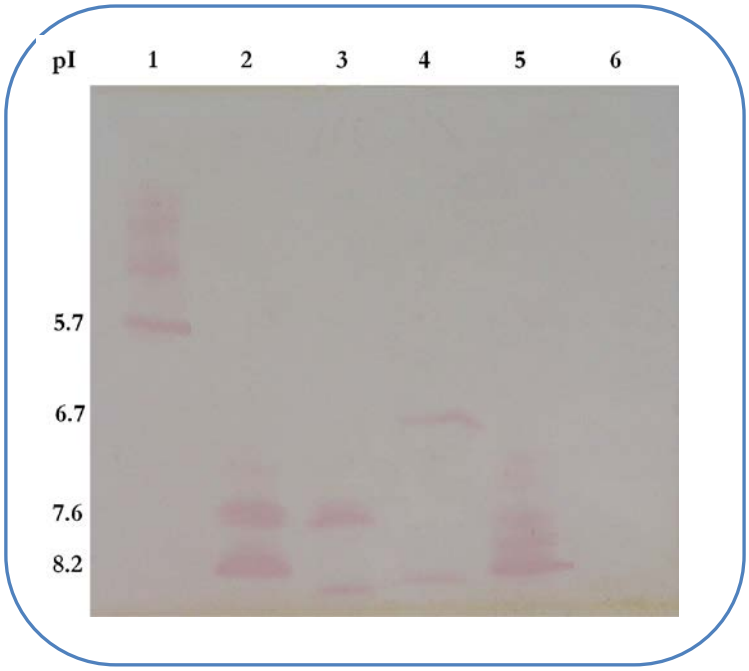

Figure 3.3 IEF patterns of crude extracts and purified SFC-1. Lanes 1 and 5, crude extracts from reference strains producing TEM-2 (pI 5.6) and SHV-5 (pI 8.2), respectively; lane 2, purified SFC-1; lane 3, crude extract from *S. fonticola* UTAD54; lane 4, crude extract from *S. fonticola* 7882^T; lane 6, crude extract from *E. coli* BL21 (DE3).

Mass spectrometry confirmed the presence of two molecular forms of the SFC-1 enzyme, with 30773 and 31083 Da (Figure 3.4). The value of 30773 Da is consistent with the predicted molecular mass of the mature protein (HENRIQUES *et al.*, 2004) and this form seems to be relatively more abundant in the purified product. Truncated forms of β-lactamases have been encountered in other bacteria, but those forms share similar hydrolytic properties and inhibitor activities (WALTHER-RASMUSSEN *et al.*, 1999).

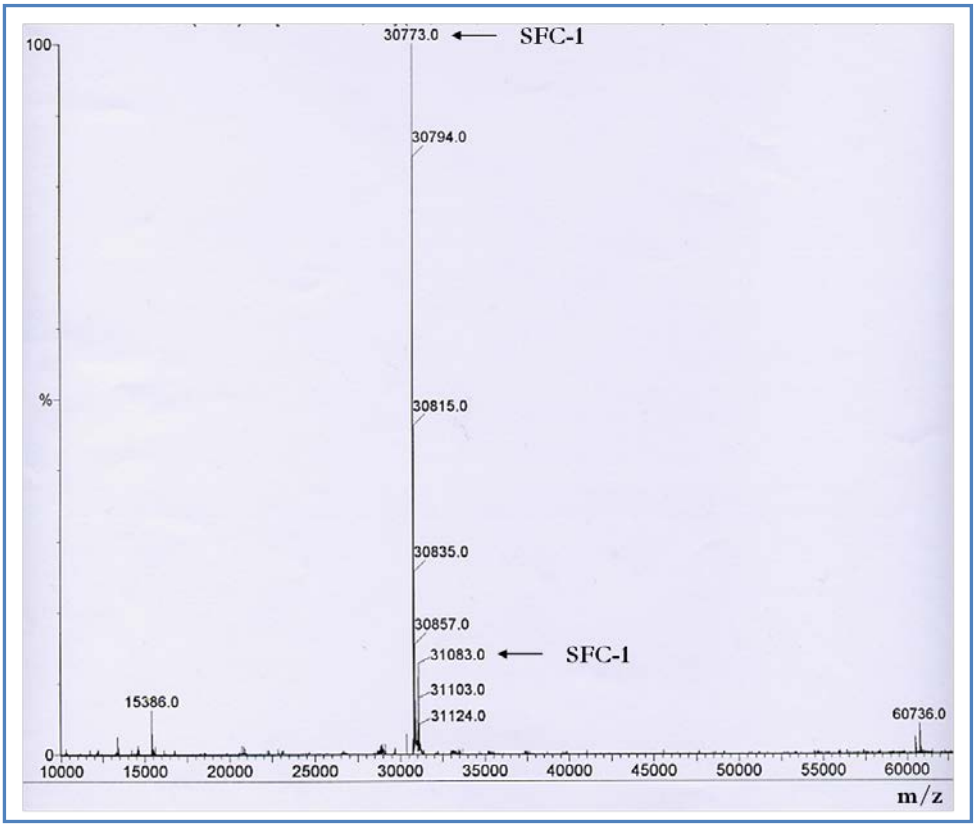

Figure 3.4 Q-TOF mass spectrogram of purified SFC-1, showing two forms of the carbapenem-hydrolysing β-lactamase.

The N-terminal sequence of the SFC-1 β-lactamase produced by *E. coli* was found to be ASQPPQV, showing that a 26-amino acid leader sequence is removed from the primary translation product during processing to generate the mature SFC-1 (HENRIQUES *et al.*, 2004). The mass difference of 310 Da between both forms of the purified protein may indicate the presence of an uncharacterised post-translational modification.

3.3.3 Kinetic properties of SFC-1

SFC-1 recognizes a variety of β-lactams (penicillin, cephalosporin, monobactam and carbapenem groups) as substrates, as summarized in Table 3.2. The activity against penicillins (ampicillin and piperacillin), narrow spectrum-cephalosporins (cephalothin) and aztreonam is very high, while the hydrolytic activities against extended-spectrum cephalosporins (cefotaxime, ceftazidime and

cefoxitin) are much lower, a feature shared by other class A carbapenem hydrolyzing β-lactamases (MARIOTTE-BOYER *et al.*, 1996; RASMUSSEN *et al.*, 1996; YANG *et al.*, 1990; YIGIT *et al.*, 2001).

The highest turnover rates were obtained for cephalothin (k_{cat}, 280 s^{-1}) followed by aztreonam (162 s^{-1}) and ampicillin (155 s^{-1}). Although SFC-1 showed a strong hydrolytic activity against aztreonam revealed by the value of k_{cat}, the enzyme has a relatively low affinity towards this substrate (K_m of 484 µM) and therefore a low catalytic efficiency was observed when compared to those obtained using penicillins, cephalothin and imipenem as substrates (Table 3.2).

The highest catalytic efficiency was observed with cephalothin and penicillins, while extended-spectrum cephalosporins appeared to be poor substrates. SFC-1 had the highest apparent affinity for meropenem and piperacillin (K_m, 26 µM and 38 µM, respectively). Among carbapenems, SFC-1 hydrolysed imipenem with a rate 8 times higher than that of meropenem (k_{cat}, 54 s^{-1} and 6.5 s^{-1}, respectively).

Analysis of the kinetic parameters for SFC-1 shows that this enzyme has a broad substrate profile, similar to that of other carbapenamases of group 2f (MARIOTTE-BOYER *et al.*, 1996; RASMUSSEN *et al.*, 1996; WOODFORD *et al.*, 2004; YANG *et al.*, 1990). However, SFC-1 exhibits catalytic efficiencies and turnover rates for ceftazidime and cefoxitin that are somewhat higher than those reported for IMI and KPC-1 (Table 3.2), the closest enzymes at the amino acid sequence level. The turnover rate for ceftazidime (k_{cat}, 2 s^{-1}) was approximately 300 and 20 times higher than those reported for IMI-1 and KPC-1 (0.0068 s^{-1} and 0.1 s^{-1}, respectively), resulting in much higher catalytic efficiencies (1730 and 40 times higher, respectively). SFC-1 hydrolysed cefoxitin more efficiently than IMI-1 and KPC-1 (8 and 27 times, respectively).

In the SFC-1 (and KPC) sequence(s) the serine residue at position 237 (as found in to Sme-1, NMC-A and IMI-1) is substituted by a threonine. This residue is known to be directly involved in imipenem hydrolysis and was also associated with higher hydrolytic efficiency against cephalosporins (SOUGAKOFF *et al.*, 1999). Yigit and co-workers reported that KPC-1 hydrolysed cefotaxime better than Sme-1, suggesting that Thr237 extends the activity of the enzyme to a broader array of cephalosporins (YIGIT *et al.*, 2001). Also, a site-directed mutagenesis study demonstrated that when random mutations of Sme-1 were selected for cefotaxime resistance only threonine was observed at position 237 (MAJIDUDDIN and

PALZKILL, 2005). A recent study of KPC-2 showed that T237 plays a role in the hydrolysis of carbapenems and selected cephalosporins (PAPP-WALLACE *et al.*, 2010b). In this report, of 19 aminoacid variants at position 237, only the T237S mutation maintains carbapenem resistance in KPC-2. Therefore, in agreement with previous reports, it is possible that threonine at position 237 contributes to the oxyimino-cephalosporinase activity observed in SFC-1. However, site-directed mutagenesis is required to confirm this hypothesis.

In addition, a valine found at position 240 may be involved in the increased hydrolytic activity against extended-spectrum cephalosporins displayed by SFC-1. KPC-1 also exhibits a valine at position 240 (YIGIT *et al.*, 2001) that is substituted by an alanine in the other carbapenem-hydrolysing β-lactamases. In the ESBLs, lysine or serine have usually been described at this position, suggesting that they are involved in the extension of the substrate profile (HULETSKY *et al.*, 1993; ORENCIA *et al.*, 2001). Interestingly, TEM-149 a β-lactamase with ESBL activity which displays, among other substitutions, a valine at position 240 has been recently characterised (PERILLI *et al.*, 2008). TEM-149 hydrolyses cefazolin, cefotaxime, ceftazidime, cefepime, aztreonam, and penicillins. Ceftazidime proved to be a better substrate than cefotaxime that behaved as an overall poor substrate. The authors suggested that the presence of a nonpolar residue, such as valine, at position 240 can facilitate the accommodation of the bulky oximino substituent of ceftazidime (PERILLI *et al.*, 2008). However, to our knowledge, the effect of a valine at this position has never been demonstrated and site-directed mutagenesis would be necessary to determine its precise effect in the specificity of β-lactamases.

The activity of SFC-1 was inhibited by the class A β-lactamase inhibitors clavulanic acid (IC_{50}, 73 µM), sulbactam (IC_{50}, 23 µM) and tazobactam (IC_{50}, 7 µM). In contrast to previously published data for IMI-1 and KPC-1, which are well inhibited by tazobactam (IC_{50}, 0.03 µM and 0.374 µM, respectively; (RASMUSSEN *et al.*, 1996; YIGIT *et al.*, 2001)), SFC-1 was not efficiently inhibited by any of the compounds tested, with IC_{50} > 1 µM. The weak inhibition displayed by SFC-1 could be hypothetically linked to the Asn276Asp substitution. This is one of the point mutations in TEM enzymes that lead to the inhibitor-resistant phenotype, occurring either alone, as in TEM-84 (LEFLON-GUIBOUT *et al.*, 2000), or in combination with other substitutions (usually at Met69) as in TEM-35 (IRT-4) and TEM-36 (IRT-7) (HENQUELL *et al.*, 1995; ZHOU *et al.*, 1994) (www.lahey.org/studies). Characterisation of an Asn276Asp TEM mutant showed that an asparte at position

276 plays a significant role in the resistance to clavulanic acid inhibition (SAVES *et al.*, 1995). According to Saves and co-workers this resistance would be explained by electrostatic interaction of the aspartate with arginine 244, together with the possible displacement of the water molecule involved in the inactivation process. However, a comparison of the amino acid sequence of SFC-1 with those of other class A carbapenemases revealed that these enzymes also have an aspartate at position 276. A recent study by Papp-Wallace *et al.*, (2010a) have shown that, in addition to its role in the hydrolysis of carbapenems and cephalosporins, T237 in the KPC-2 carbapenemase is implicated in the resistance to β-lactamase inhibitors. As proved for the class A carbapenemase KPC-2, the weak activity of the inhibitors tested against SFC-1 is most likely associated with threonine found at position 237.

As expected, no inhibition was observed when the enzyme was assayed with 10 mM EDTA.

Table 3.2 Kinetic parameters of purified SFC-1 and comparison to other class A carbapenem-hydrolysing β-lactamases. [a]

Substrate or inhibitor	k_{cat} (s^{-1})			K_m (μM)			k_{cat}/K_m ($mM^{-1} s^{-1}$)		
	SFC-1	IMI-1	KPC-1[b]	SFC-1	IMI-1	KPC-1	SFC-1	IMI-1	KPC-1
Substrates									
Ampicillin	155 ± 2	190	110	176 ± 17	780	130	881	240	850
Piperacillin	44.7 ± 1	6.1	24	38 ± 4	13	18	1190	470	1333
Cephalothin	280 ± 2	120	75	129 ± 14	130	53	2171	920	1400
Cefotaxime	8.3 ± 0.5	3.4	14	89 ± 16	190	160	93.3	18	90
Ceftazidime	2.1 ± 0.1	0.0068	0.1	52 ± 10	270	94	40.4	0.024	1
Cefoxitin	4.2 ± 0.2	0.3	0.26	77 ± 14.46	45	120	54.5	6.7	2
Aztreonam	162 ± 7	51	20	484 ± 78	93	310	334.7	550	70
Imipenem	54 ± 1	89	12	82 ± 5	170	81	659	520	150
Meropenem	6.5 ± 0.1	10	3	26 ± 2	26	12	250	380	250

[a] Kinetic values used for IMI-1 and KPC-1 were reported by Rasmussen *et al.*, (1996) and Yigit *et al.*, (2001), respectively. k_{cat}s and K_ms for SFC-1 are means ± standard deviations.

[b] KPC-1 is now KPC-2; KPC-1 designation is not used.

3.4 Concluding remarks

The over-expression of bla_{SFC-1} allowed us to obtain a large quantity of SFC-1 enzyme, enabling effective protein purification. Kinetic studies showed that purified SFC-1 exhibits a remarkably broad substrate range including β-lactams of all classes, and exhibits an increased efficiency against ceftazidime when compared to other class A (group 2f) carbapenemases. Moreover, SFC-1 is less inhibited by class A β-lactamase inhibitors than other characterised group 2f carbapenemases. These results confirm that SFC-1 is a member of β-lactamase group 2f, according to the Bush β-lactamase classification (BUSH *et al.*, 1995), with some unusual properties.

Tertiary structures for KPC-2, Sme-1 and NMC-A are already available (KE *et al.*, 2007; SOUGAKOFF *et al.*, 2002; SWARÉN *et al.*, 1998). It would be interesting to generate a crystal structure of the carbapenem-hydrolyzing β-lactamase SFC-1 and investigate biochemical/structural relationships of SFC-1 in comparison with these enzymes.

4. Crystallographic structure of SFC-1: insights into carbapenemase activity in class A β-lactamases

4.1 Introduction

The evolution of narrow spectrum β-lactamases (e.g. TEM-1, SHV-1) into so-called extended-spectrum β-lactamases (ESBLs) with the ability to hydrolyse oxyimino cephalosporins (e.g. cefotaxime and ceftazidime) in addition to penicillins and previous generations of cephalosporins (PATERSON and BONOMO, 2005; PEREZ *et al.*, 2007), has resulted in an increased use of carbapenems. Carbapenems were formerly reserved for treatment of severe infections by Gram-negative pathogens (BAUGHMAN, 2009), but are now increasingly viewed as front-line therapy for treatment of nosocomial infections by both *Enterobacteriaceae* and non-fermenting pathogens (MASTERTON, 2009). This growth in carbapenem use has led to an increase in the incidence of carbapenem-hydrolysing β-lactamases of classes A, B and D (QUEENAN and BUSH, 2007; WALTHER-RASMUSSEN and HOIBY, 2007).

In the case of the class A serine β-lactamases, several such enzymes (e.g. IMI, NMC, KPC and SFC-1) have been identified from environmental and pathogenic organisms. In particular, members of the KPC group are now endemic in *Enterobacteriaceae* in a number of locations (NORDMANN *et al.*, 2009) where their production results in organisms with reduced or abolished susceptibility to carbapenems and for which there are few other effective treatment options (BUSH, 2010). The situation is further complicated by the ability of many class A carbapenemases to resist the effect of mechanism based inhibitors such as clavulanic acid that are successful against the majority of class A β-lactamases (PAPP-WALLACE *et al.*, 2010a).

Carbapenems are able to inhibit the majority of class A β-lactamases through formation of a stable acylenzyme species that deacylates slowly. Carbapenems readily acylate enzymes such as TEM-1 and SHV-1 via nucleophilic attack of the active site serine, Ser70, upon the scissile β-lactam amide bond. However, kinetic (EASTON and KNOWLES, 1982), crystallographic (MAVEYRAUD *et al.*, 1998; NUKAGA *et al.*, 2008) and spectroscopic (KALP and CAREY, 2008) experiments demonstrate that the acylenzyme so formed can partition between two states, a deacylation-competent form in which the acylenzyme carbonyl oxygen occupies the oxyanion hole, and a deacylation-incompetent state in which this oxygen is displaced from the oxyanion hole. Thus two distinct acylenzyme species are observed in crystal

structures of complexes of TEM-1 with imipenem (MAVEYRAUD *et al.*, 1998) or SHV-1 with meropenem (NUKAGA *et al.*, 2008).

In order for class A β-lactamases to act as effective carbapenemases it is therefore likely that their interactions with carbapenems will differ substantially from those made by their carbapenem-inhibited counterparts. However, despite the determination of numerous crystal structures (KE *et al.*, 2007; SOUGAKOFF *et al.*, 2002; SWARÉN *et al.*, 1998) those properties that are responsible for carbapenemase activity in class A enzymes remain relatively obscure. Whilst it is clear that certain features (substitution of Arg244; possession of a disulfide bond between Cys69 and Cys238) are important, the close structural resemblance between the active sites of carbapenem-hydrolysing and carbapenem-inhibited enzymes has led to speculation that multiple subtle alterations are responsible for activity against carbapenem substrates. Moreover, to date there remains little information regarding the interactions between class A carbapenemases and their carbapenem substrates.

Therefore, in order to pursue this lack of structural information on carbapenem binding and hydrolysis in class A carbapenemases we investigated SFC-1, a close relative of KPC-type enzymes. Here we present crystal structures of wild-type SFC-1 and of complexes of site-directed mutants with the carbapenem meropenem in unhydrolysed and acylenzyme intermediate forms.

4.2 Materials and methods

4.2.1 Mutagenesis of SFC-1

The SFC-1 β-lactamase gene from *S. fonticola* UTAD54 (HENRIQUES *et al.*, 2004) was cloned into pET-26(b) and transformed into *E. coli* BL21(DE3) as described in Chapter 3. The recombinant plasmid harbouring SFC-1 (pMF13) was used as the DNA template for site-directed mutagenesis. The mutagenic oligonucleotide primers used in the PCR reactions are shown in Table 4.1.

SFC-1 mutants were generated using Quikchange™ Site-Directed Mutagenesis Kit (Agilent) according to the manufacturer's instructions, except for the PCR cycling parameters.

Briefly, the double stranded plasmid template pMF13 was initially denatured at 95ºC for 1 min and oligonucleotide primers containing the desired mutations were extended during 25 cycles of denaturation at 95ºC for 1 min, annealing at 55ºC for 2 min, and extension at 68ºC for 8 min by *PfuTurbo* DNA polymerase. Amplification products were digested by *Dpn* I (1h at 37ºC) to remove the parent strands and transformed into *E. coli* XL1-Blue. The transformation reaction was plated on LB agar plates supplemented with 50 µg/ml kanamycin and incubated at 37ºC overnight. Plasmid DNA containing the putative mutation was subsequently isolated from transformed XL1-Blue cells using the QIAprep Spin Miniprep Kit (Qiagen) and sequenced in order to ensure the introduction of the desired mutation. DNA sequencing was performed by The Sequencing Service (School of Life Sciences, University of Dundee, Scotland).

Table 4.1 Primers used to generate SFC-1 mutants.

Primer	Sequence 5' --- 3'
S70A_F	CGAGCGTTTTCCTCTCTGTGCTTCATTTAAAGGCTTCCTTG
S70A_R	CAAGGAAGCCTTTAAATGAAGCACAGAGAGGAAAACGCTCGT
E166A_F	CGTCTGGACCGATGGGCACTGGAGTTGAATTCC
E166A_R	GGA ATTCAACTCCAGTGCCCATCGGTCCAGACG

4.2.2 Protein expression and purification

In order to obtain a yield suitable for crystallisation trials, wild-type SFC-1 was purified from cells growing in 4 L LB supplemented with kanamycin and purified as described in Chapter 3 (section 3.3.6).

For protein expression mutant proteins were transformed into *E. coli* strain BL21 (DE3) and selected on LB agar plates containing 50 µg/ml kanamycin. Over-expression and purification of the mutant proteins were performed as described for the wild-type SFC-1 (Chapter 3). After purification proteins were stored at 4ºC until use.

Protein concentrations were determined by UV absorbance at 280 nm with molar extinction coefficients ε_{280} = 31840 M^{-1} cm^{-1}, estimated from the amino-acid

composition by the method of Gill and von Hippel (GILL and VON HIPPEL, 1989) using the Protean application of Lasergene (DNAStar Inc.)

4.2.3 β-Lactamase crystallisation

Wild-type or mutant SFC-1 in 10 mM phosphate buffer (pH 7.0) were concentrated by centrifugal filtration in Amicon Ultra-15 spin concentrators with a molecular weight cut off (MWCO) of 10 kD. For wild-type SFC-1, an initial screen of crystallisation parameters was performed by the sitting drop vapour diffusion method using protein concentrated to 12.3 and 6.15 mg/mL against the sparse-matrix screens Structure screen I & II HT-96 (JANCARIK and KIM, 1991), JCSG-*plus* HT-96 and PACT *premier* (NEWMAN *et al.*, 2005) (Molecular Dimensions) using a Phoenix crystallisation robot (Art Robbins Instruments) by mixing 0.5 µL protein solution with 0.5 µl screen solution. MRC two well crystallisation plates in the 96-well format (Hampton Research) were used. Plates were sealed with ClearSeal Film™ (Hampton Research) and incubated at 20 °C.

Within a week, plate-like crystals were observed in conditions F6 from Structure screen (no salt, 0.1 M Hepes pH 7.5, 4.3 M sodium chloride) and C10 from PACT *premier* (0.2 M magnesium chloride, 0.1 M Hepes pH 7.0, 20% w/v PEG 6000). Needle-like crystals were also obtained in condition F10 from the Structure screen (0.1 M MES pH 6.5, 1.6 M magnesium sulphate. These conditions were used to optimise crystal quality in 24-well XRL crystallisation plates (Molecular Dimensions) by hanging drop vapour diffusion using a wide range of approaches: varying salt and precipitant concentrations, pH, and the ratio of protein: crystallisation solution. Crystals obtained from these trials were taken to the Diamond synchrotron but no diffraction was observed probably due to their small size.

In subsequent experiments protein concentration was increased to 30 mg/mL and the Additive screen (Molecular Dimensions) was tried (additives were mixed either in the drops of protein solution or in the reservoir solution, depending on the additive, to a final concentration of 10%) but no single crystals were obtained. A new inspection of the initial screens lead us to test condition E7 from the PACT screen, consisting of 0.2 M sodium acetate and 20% w/v PEG 3350 with 15 and 30 mg/mL of protein. Crystals were reproducible and diffraction quality single crystals of wild-type SFC-1 were grown by mixing 1.5 µL of protein (30 mg/mL) with 1.5 µL of

reservoir solution and equilibrating the samples against 500 µL of reservoir solution. The reservoir solution contained 18-22% w/v PEG 3350 and 0.2 M sodium acetate.

Crystallisation of SFC-1 mutants was first attempted using the same condition as previously employed for the wild-type protein (17-22% w/v PEG 3350 and 0.2 M sodium acetate), using proteins concentrated to 15 and 30 mg/mL. The drops contained 1µL of protein and 1µL of reservoir solution and were equilibrated against 500 µL of reservoir solution. However this condition did not yield crystals. The proteins were then screened with JCSG-*plus* HT-96 and PACT *premier* (Molecular Dimensions) using the Phoenix robot with drops containing 0.5 µL of protein (10 and 20 mg/mL) and 0.5 µL of reagent. After one week the most promising crystallisation conditions for the mutant proteins were D5 from JCSG-*plus* HT-96 (0.1 M Hepes pH 7.5, 70% v/v MPD) for the E166A mutant and F5 from PACT *premier* (0.2 M sodium nitrate, 0.1 M Bis Tris propane pH 6.5, 20% w/v PEG 3350) for the S70A mutant. Reproducibility and optimisation (changing precipitant concentration, pH and use of the Additive screen) of the crystals using the above conditions failed. In most cases clear drops were obtained. Therefore, in order to obtain single crystals of diffraction quality, crystals of native SFC-1 were used for streak seeding. In this trial mutant proteins were used at a concentration of 30 mg/mL. Drops were prepared by mixing 1.5 µL of protein with 1.5 µL of well solution (0.2 M sodium acetate, 18-22% w/v PEG 3350). A good crystal of native protein was touched with a whisker that transferred seeds to the prepared drops containing mutant proteins. Crystals emerged after 1 day.

The crystals used for data collection were looped out from the cover slides using either nylon or litholoops (Molecular Dimensions) mounted on cryo-pins, dipped into the cryoprotectant solution for a few seconds and stored in liquid nitrogen until the diffraction experiments. Cryoprotectant solutions for crystals of both wild-type SFC-1 and mutant proteins consisted of mother liquor solution plus 20% ethylene glycol.

Acylenzyme-intermediates and complexes with unhydrolysed meropenem were prepared by soaking crystals of the mutant proteins, E166A and S70A respectively, in cryoprotectant solution containing 50 mM meropenem for 30 to 50 minutes before freezing in liquid nitrogen.

4.2.3 X-ray diffraction data collection and crystallographic refinement

Diffraction data were collected at 100 K on beamlines 10.1 of the SRS (Daresbury, UK) for wild-type enzyme, and IO2/IO3 of the Diamond Light Source (Didcot, UK) for mutant proteins.

The crystals diffracted to maximum resolutions of 1.35 Å (WT), 1.08 Å (S70A substrate complex) and 1.3 Å (E166A acylenzyme complex). Data were processed and scaled using the programs HKL2000 (OTWINOWSKI and MINOR, 1997) or MOSFLM (LESLIE, 2006) and SCALA (EVANS, 2006) as shown in Table 4.2. The crystals of wild-type SFC-1 belong to the monoclinic space group $P2_1$ with two SFC-1 molecules in the asymmetric unit, while the space group of crystals from mutant proteins was $P2_12_12_1$ with one molecule in the asymmetric unit.

Structures were determined by molecular replacement with PHASER (MCCOY *et al.*, 2007) using chain A of the KPC-2 β-lactamase (PDB ID 2OV5) (KE *et al.*, 2007) (wild-type enzyme) or the wild-type structure (mutant enzymes) as the initial search model. Model building and refinement were performed with the programs COOT and REFMAC, respectively (EMSLEY *et al.*, 2010), (MURSHUDOV *et al.*, 1997). Ligand restraints were generated using the CCP4i monomer sketcher (POTTERTON *et al.*, 2003) and the PRODRG server (SCHUTTELKOPF and VAN AALTEN, 2004).

The models were further refined using conjugate gradient minimization in SHELXL (SHELDRICK, 2008). The program mtz2hkl (GRUNE, 2008) was used in the transition from REFMAC refinement to SHELXL. The refinement with SHELXL started with the lowest resolution data (to 2.5 Å resolution) and remaining data was added in steps to the highest resolution (Table 4.2). Anisotropic B-factors were introduced with the highest resolution data and produced a 1−3% drop in the R_{free} values, depending on the dataset's resolution. In all the structures it was possible to model alternative side chains in numerous residues. The progress of crystallographic refinement was monitored using the MOLPROBITY server (CHEN *et al.*, 2010) and the quality of the final structures was verified with PROCHECK (LASKOWSKI *et al.*, 1993).

4.3 Results and discussion

4.3.1 Structure of the SFC-1 carbapenemase

Crystals of the wild-type SFC-1 were obtained by the hanging drop vapour diffusion technique using 30 mg/ml protein and 18-22% w/v polyethylene glycol 3350, 0.2M sodium acetate. Crystals of SFC-1 mutants were obtained by the same technique using streak seeding with crystals of the wild-type protein and the same protein concentration (Figure 4.1).

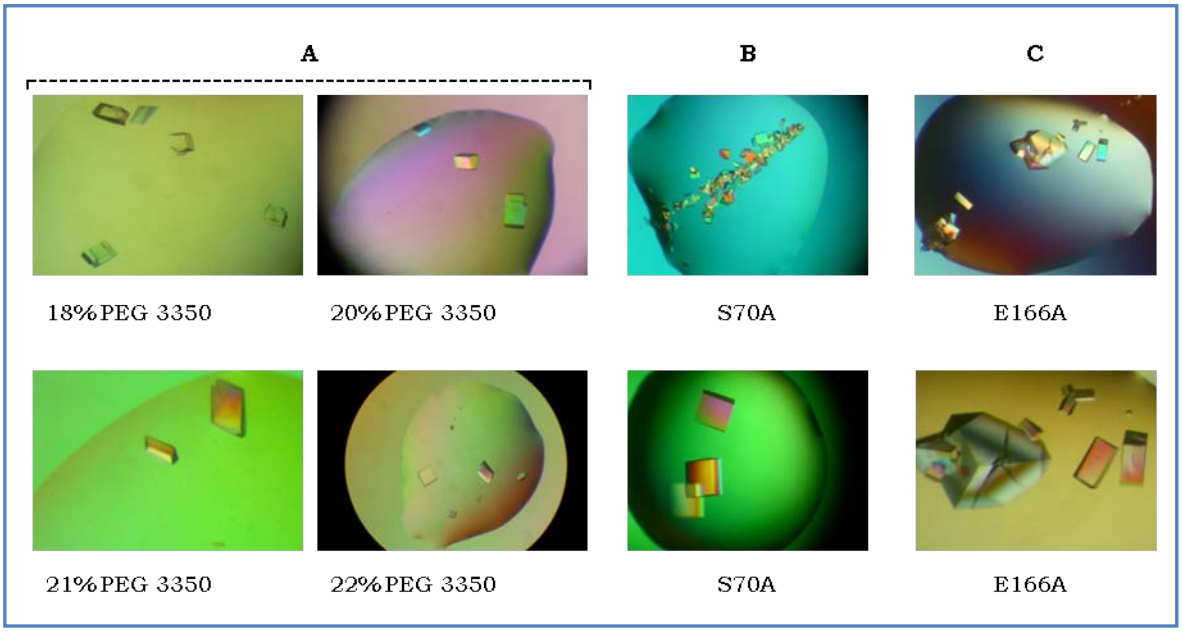

Figure 4.1 A, SFC-1 crystals growing in 0.2 M sodium acetate with different concentrations of PEG 3350 (w/v); **B** and **C**, SFC-1 S70A and E166A mutant crystals after seeding, respectively.

The crystal structure of SFC-1 was determined to 1.35 Å resolution by molecular replacement using the coordinates of the structure of the β-lactamase KPC-2 from *K. oxytoca* as a search model (KE *et al.*, 2007). The SFC-1 crystal reveals two molecules per asymmetric unit, which were refined in space group $P2_1$ to a final crystallographic *R*-factor and R_{free} values of 11.6 and 16.0 %, respectively.

The crystallographic and model statistics for the native and SFC-1 mutant-complexes structures are reported in Table 4.2.

Table 4.2 Data collection and refinement statistics for native and SFC-1 mutant-complexes structures.

Dataset	**Native**	**E166A**	**S70A**
Processing	HKL2000	MOSFLM/SCALA	MOSFLM/SCALA
Beamline	SRS 10.1	DLS I03	DLS I02
Space Group	P 2_1	P 2_1 2_1 2_1	P 2_1 2_1 2_1
Cell Dimensions (Å)	a = 42.33 b = 85.46 c= 70.29 β = 103.26°	a = 59.17 b = 61.95 c= 79.11	a = 59.06 b = 61.91 c= 79.01
Wavelength (Å)	1.117	0.9763	0.9702
Resolution (Å)	50 – 1.35 (1.40 – 1.35)a	37.64 – 1.49 (1.57 – 1.49)a	22.52 – (1.08) (1.14 - 1.08)a
Total reflections	355 336	678 589	840 706
Unique reflections	102 989 (8 012)[a]	48 468 (7 000)[a]	123 610 (17 824)[a]
Completeness (%)	96.6 (75.5)[a]	100 (100)[a]	99.5 (99.5)[a]
Redundancy	3.5 (2.0)[a]	14 (13.4)[a]	6.8 (6.6)[a]
I / (sig. I)	18.6 (1.69)[a]	28.9 (14.0)[a]	16.9 (5.1)[a]
R_{merge} (%)	6.1 (50.7)[a]	9.0 (17.4)[a]	7.0 (28.5)[a]
Refinement (SHELXL)			
Resolution range (Å)	∞-1.35	∞-1.30	∞-1.08
No. of reflections used	97807	64944	116903
R-factor/R_{free} (%)	11.6/ 16.0	11.1/ 14.8	11.0/ 13.2
R_{total} (%)			
Ramachandran plot (%)			
favored/allowed	98.0/ 2.0	98.9/ 1.1	98.5/ 1.5
disallowed	0	0	0
RMSD values			
bond lengths (Å)	0.01	0.014	0.015
bond distances (Å)	0.04	0.031	0.031
Mean B-factor (Å^2)			
protein	14.744	12.150	11.205
substrate	---	15.348	11.865
ethylene carbonate	9.864	---	---
water molecules	27.435	28.743	30.517
all atoms	15.733	13.673	13.193

[a] The values in parentheses are for the highest-resolution shell used in refinement. One crystal was used for the data collection of each dataset.

The final model contains two independent molecules: molecule A comprising residues Ser23–Ala294 (numbering according to the standard Ambler scheme; AMBLER et al., 1991) of the mature polypeptide and molecule B comprising residues Ser23–Arg296 with 13 and 10 residues not observed in molecules A and B, respectively, due to disorder.

The Ramanchandran plot shows that 97.8% of the residues have φ and ψ angles in the most favoured regions with no residues in the disallowed regions. When compared, the two monomers are very similar with an r.m.s. deviation in atomic positions of 0.5 Å for 270 aligned Cα atoms, using the secondary structure matching (SSM) algorithm (KRISSINEL and HENRICK, 2004) as implemented in COOT.

The SFC-1 active site is located in the cavity generated at the interface of the two domains and contains conserved residues that are known to play a role in substrate binding and/or catalysis in class A β-lactamases (Figure 4.2). Such residues include the catalytic Ser70, Lys73, Ser130, Asn132, Glu166, Asn170, Lys234, Thr235 and Thr237, as well as the Cys69-Cys238 disulphide bridge (Figure 4.3). This disulphide bridge is a feature unique to class A carbapenemases and is thought to play a role in the stabilization of the protein fold (RAQUET *et al.*, 1997; WALTHER-RASMUSSEN and HOIBY, 2007). The oxyanion hole is formed by the backbone nitrogen atoms of Ser70 and Thr237.

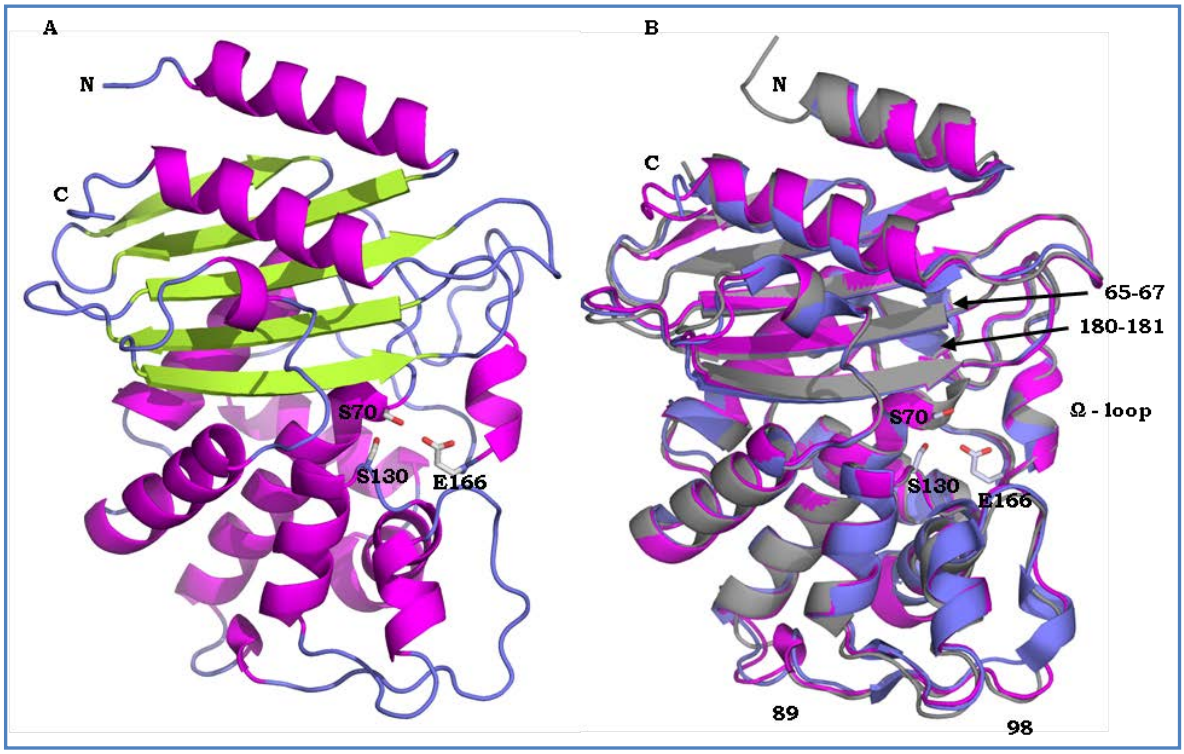

Figure 4.2 Overall fold of class A carbapenemases. A) Ribbon secondary structure representation of the SFC-1 structure; α-helices are shown in magenta and β-strands in limon. B) Superposition of SFC-1 structure (magenta) with serine carbapenemases NMC-A (gray; PDB accession 1BUE) and KPC-2 (blue, PDB accession 2OV5). The labelled catalytic residues Ser70, Ser130 and Glu166 (shown as gray model sticks) and the Ω-loop localize the active site. This and all subsequent figures were generated using the program Pymol (DELANO, 2008).

Unexpectedly a cyclic adduct, modelled as ethylene carbonate (EC), was shown to be present in the SFC-1 active site (Figure 4.3), and is observed in the active sites of both SFC-1 molecules in the asymmetric unit. The electron density found close to the catalytic Ser70 during model building did not correspond to any compound used in protein purification or crystallisation but resembled a five-membered ring. In the literature there is a precedent for a similar interaction. Indeed, a structure of the recombinant (−) γ-lactamase from an *Aureobacterium* species was determined in complex with a cyclic ethylene carbonate molecule covalently bound to the catalytic serine residue (LINE *et al.*, 2004). Therefore an ethylene carbonate molecule was built into the positive electron density and refined, and a good fit to the electron density maps was achieved. Moreover, in the final model, the B-factors of the ligand (mean less than 10 Å^2) were comparable to those displayed by neighbouring amino acid residues, indicative of a good assignment of the ligand modelled into the active site of native SFC-1.

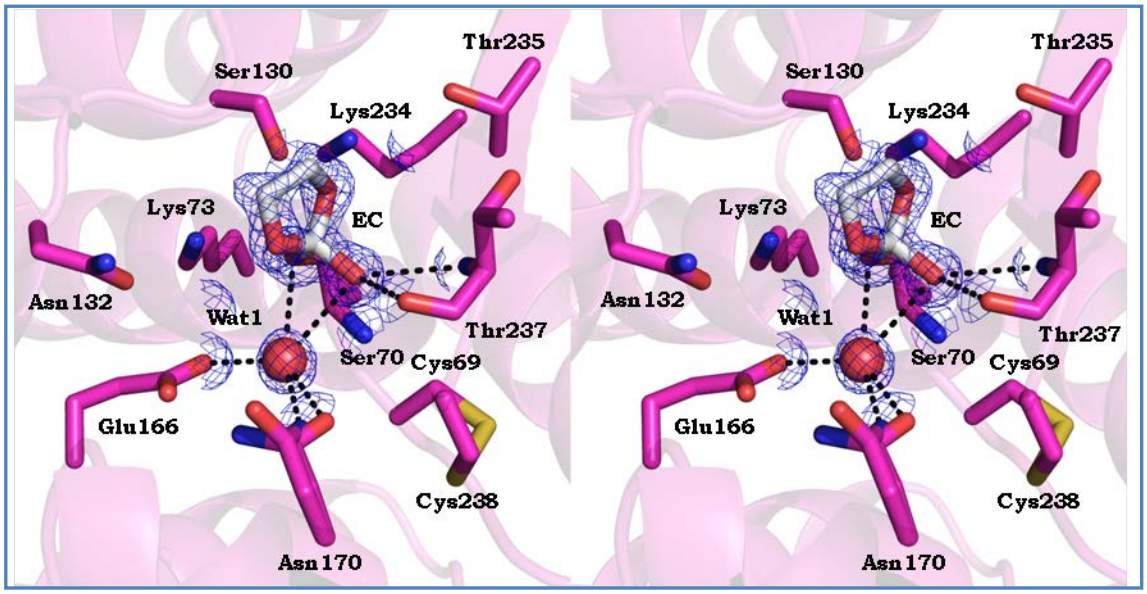

Figure 4.3 Stereoview of the SFC-1 active site with labelled conserved residues shown as stick models. 2mFo − DFc electron density maps (blue) surrounding catalytic water molecule (Wat1) and the cyclic ethylene carbonate (EC; carbon atoms coloured grey) are contoured at 1.5σ. Hydrogen bonding interactions (black dashed lines) of the active site water molecule (red sphere) and the carbonyl group of ethylene carbonate are displayed.

The ethylene carbonate forms a tetrahedral complex with the catalytic Ser70 as described for the (−) γ-lactamase (LINE *et al.*, 2004). It is also involved in hydrogen bonding with two other active site residues, namely Ser130 and Thr237. Interestingly, the carbonyl group of ethylene carbonate sits in the oxyanion hole formed by the main chain nitrogen atoms of Ser70 and Thr237, in the position usually occupied by a water molecule (Wat2) in class A β-lactamases (CHEN *et al.*, 2005; STEC *et al.*, 2005; SWARÉN *et al.*, 1998). This water molecule is also missing in the structure of carbapenemase KPC-2 due to the positioning of Ser70 side chain, partially blocking the oxyanion hole (KE *et al.*, 2007). The carbonyl group of ethylene carbonate is hydrogen bonded to the backbone carbonyl (2.74 Å) and nitrogen (2.95 Å) of Thr237 and to the deacylation/catalytic water (Wat1) (Figure 4.3).

In contrast to the class A carbapenemase Sme-1 (SOUGAKOFF *et al.*, 2002) the putative deacylating water molecule (Wat1) is observed in the structure of SFC-1 and establishes a hydrogen bonding network with residues Glu166, Asn170 and Ser70, as described in other class A β-lactamases (STEC *et al.*, 2005; SWARÉN *et al.*, 1998), and with the carbonyl group of ethylene carbonate (Figure 4.3).

The superposition of the SFC-1 structure on to other available structures of class A serine carbapenemases such as NMC-A (SWARÉN *et al.*, 1998) and KPC-2 (KE *et al.*, 2007) points to the existence of some elements of difference between the three carbapenemases as shown in Figure 4.2. These comprise loops near residues 88 and 98, and two secondary elements in NMC-A and KPC-2 near residues 87 and 180 which are absent in SFC-1. However, all of these regions are distant from the active site and are therefore unlikely to explain the unusual spectrum of activity of SFC-1.

When compared to other class A β-lactamases, the main differences in SFC-1 are seen at the entrance of the catalytic cavity. Pro104 in SFC-1 and KPC-2 is substituted with Tyr and Phe in Sme-1 and NMC-A, respectively, and Glu in TEM-1 (STEC *et al.*, 2005), indicating that the residue at Ambler position 104 is not conserved among class A β-lactamases. In the structure of SHV-1, Asp was found at this position and it was observed that the substrate binding cavity was wider when compared to TEM-1 β-lactamase (KUZIN *et al.*, 1999). As described for SHV-1, it can be proposed that the small nonpolar residue Pro104 that is present in KPC-2 and SFC-1 contributes to an enlarged entry to the active site in these enzymes, resulting in increased activity against ceftazidime and cefotaxime. A site saturation mutagenesis study at position 104 in the SHV-1 and SHV-2 β-lactamases (BETHEL *et al.*, 2006) showed that the SHV-1 Asp104Pro variant expressed in *E. coli* DH10B increased resistance to cefotaxime (MIC range, 0.06 to 0.125 μg/ml) while ampicillin resistance was fourfold decreased. In the SHV-2 Asp104Pro variant, however, resistance to all β-lactams tested (ampicillin, cephalothin, cefotaxime and ceftazidime) was twofold increased (BETHEL *et al.*, 2006).

Adjacent to Pro104 is residue His105 which in SFC-1 (chain A) adopts a completely different orientation when compared to other class A β-lactamases. In chain A of the SFC-1 structure the side chain of His105 is rotated more than 90° in the direction of the entrance of the binding cavity but away from Ser130. In contrast, the side chains of residues at position 105 in Sme-1 and NMC-A (His), KPC-2 (Trp) and TEM-1 (STEC *et al.*, 2005), SHV-1 (KUZIN *et al.*, 1999) and CTX-M-16 (CHEN *et al.*, 2005) (Tyr) are directed towards the active site pocket making hydrogen bonds to the main chain carbonyl of the residue at position 129 (Met or Tyr in the enzymes referred above). This interaction is absent in SFC-1 whose His105 side chain and the backbone carbonyl of Tyr129 are hydrogen bonded to water molecules. This probably results in a widened active site cavity in SFC-1, which is able to recognize and

accommodate the large oxyimino-cephalosporins, possibly explaining the higher hydrolytic activity of SFC-1 against the third generation cephalosporins cefotaxime and ceftazidime (FONSECA *et al.*, 2007). Doucet *et al.*, (2004) previously reported a site saturation mutagenesis study of Tyr105 in TEM-1 β-lactamase; their results suggest that Tyr105 is important in substrate recognition and stabilization rather than hydrolysis. Moreover, this study shows that the conformation of the residue at Ambler position 105 prevents unfavourable steric interactions with the substrate in the active site pocket (DOUCET *et al.*, 2004).

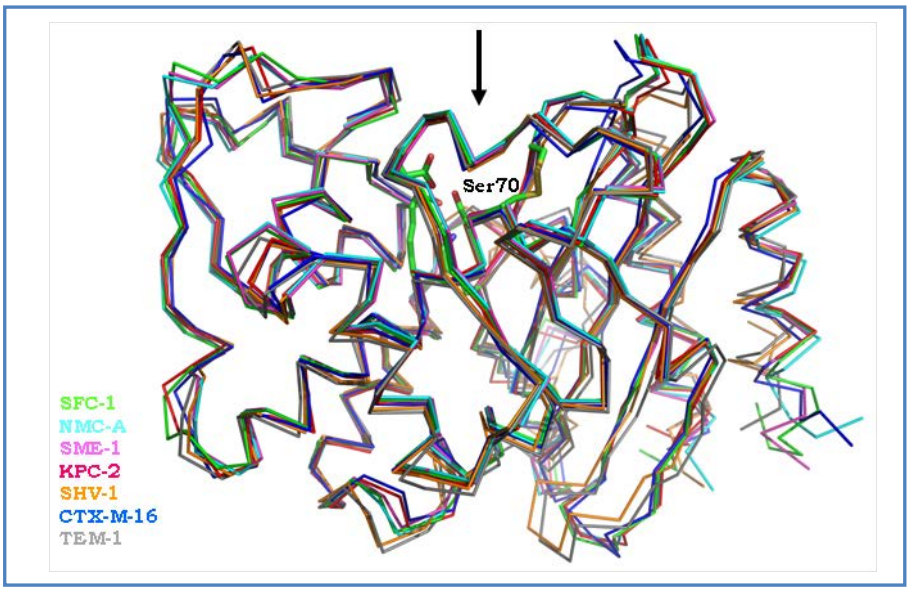

Figure 4.4 Superposition of the Cα trace of class A carbapenemases (SFC-1, NMC-A, SME-1, KPC-2) and carbapenem-inhibited enzymes (SHV-1, CTX-M-16, TEM-1). Arrow shows active site with key SFC-1 residues (Ser70, Glu166, Ser130 and the Cys69-Cys238 disulphide bridge) represented as sticks.

Despite the drastic differences in the ability to hydrolyse carbapenems among carbapenemases and non-carbapenemase enzymes, the overall folds of class A β-lactamases are shown to be closely conserved, as depicted in Figure 4.4. The comparison between the crystallographic structures of class A carbapenem-hydrolysing β-lactamases such as SFC-1, KPC-2, NMC-A and SME-1, and those of TEM-1, SHV-1 and CTXM-16, does not provide an unambiguous basis for the enhanced catalytic activity of class A carbapenemases against carbapenem substrates. The same conclusion was found by Ke and collaborators when analysing the structure of KPC-2 (KE *et al.*, 2007). Therefore, the basis for the unusual spectrum of activity of SFC-1 and related enzymes is somewhat to be expected in

subtle active site rearrangements, together with altered enzyme dynamics, rather than in gross structural changes.

To date there is no structural data on the interaction between class A carbapenemases and carbapenems, although a number of class A β-lactamase structures with bound inhibitors or acyl intermediates are available (DELMAS *et al.*, 2008; MAVEYRAUD *et al.*, 1998; NUKAGA *et al.*, 2008). To investigate how carbapenems achieve hydrolysis by these β-lactamases, mutational techniques were used to determine atomic resolution structures of SFC-1 active site bound with the carbapenem meropenem, in both the Michaelis complex and the covalent acyl intermediate. The results provided relevant structural data on the recognition and hydrolysis of carbapenems by SFC-1, that can be extended to other class A carbapenemases.

4.3.2 The SFC-1 S70A-meropenem complex structure

In this study two catalytic-deficient mutants of SFC-1 were engineered. Mutating conserved active site residues, specifically the acylating nucleophile Ser70 and Glu166 (responsible for the activation of the catalytic water molecule during deacylation), to alanine residues generates class A β-lactamases with impaired ability to complete the acylation or deacylation steps of the reaction, respectively. This strategy, previously employed by several researchers to maximize the possibility of trapping class A β-lactamase acylenzyme intermediates for crystallographic analysis (CHEN and HERZBERG, 2001; IBUKA *et al.*, 1999; PADAYATTI *et al.*, 2004; SHIMAMURA *et al.*, 2002; TREMBLAY *et al.*, 2010), enabled us to obtain the first structures of a class A carbapenemase bound to an intact carbapenem (meropenem) (mutant S70A) and of an acylenzyme intermediate (meropenem complex of the E166A mutant).

The crystal structure of the SFC-1 S70A mutant in complex with the carbapenem meropenem was determined to a resolution of 1.08 Å by molecular replacement using chain A of the previously solved wild-type SFC-1 structure as the starting model. The complex crystallized in space group $P2_12_12_1$ with one molecule per asymmetric unit and was refined to final *R*-factor and R_{free} values of 10.9 and

13.1%, respectively (Table 4.2). The refined structure of the S70A mutant is essentially similar to that of the wild-type, with an r.m.s. deviation of 0.47 Å between the Cα atoms of the two structures. Regardless of the better-diffracting crystals, it was not possible to model the position of all 283 residues of the mature protein in the electron density map, with 13 residues not observed at the C-terminus of the current structure due to disorder. The final model also contains a meropenem molecule located in the active site, seven sodium ions, four ethylene glycol molecules, and 550 water molecules.

Initial difference electron density maps contoured at 3σ clearly revealed the presence of meropenem bound in the active site of the mutant enzyme. Meropenem was readily fitted into the 2Fo-Fc maps and electron density for the entire antibiotic is complete, indicating that no fragmentation of the molecule occurred during soaking procedures. Indeed, the drug refines with an occupancy of 1.0 and temperature factors varying from less than 8.0 Å^2 (from the hydroxyl to sulphanyl moieties) to more than 20.0 Å^2 for atoms in the R' side chain beyond the sulphur, where the electron density is less intense and no interaction with protein residues is observed. For comparison, the CB atom of the side chain of the mutated residue Ala70 has a B factor of 6.13 Å^2, confirming a good fit of the bound antibiotic in the model.

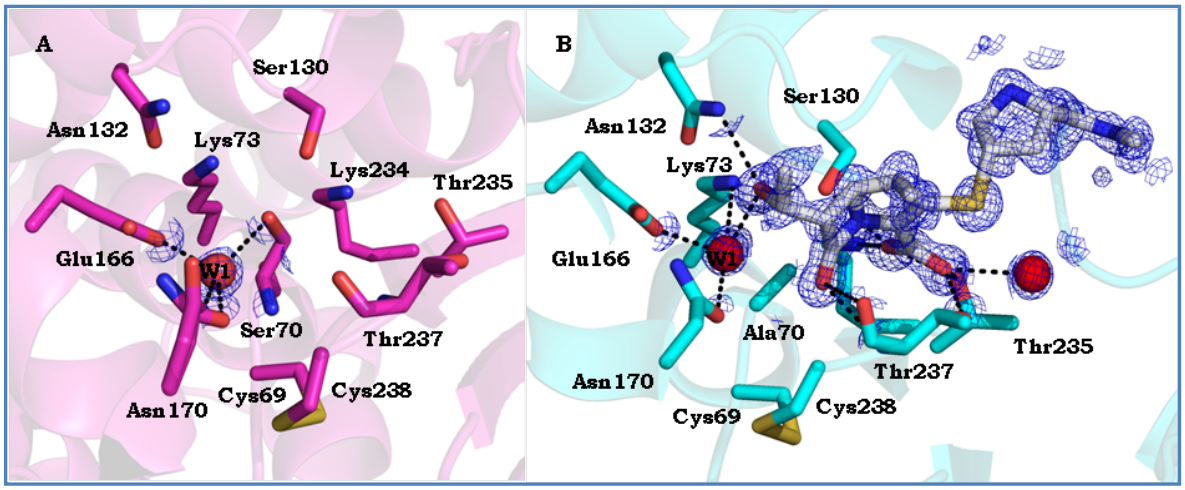

Figure 4.5 Binding of unhydrolysed meropenem in SFC-1 active site. A) Wild-type SFC-1; ethylene carbonate molecule is omitted for clarity. B) SFC-1 S70A mutant showing bound meropenem (carbon atoms in gray). Sigma-A weighted electron densities displayed are contoured at 1.0σ.

In the substrate complex, the β-lactam carbonyl oxygen of meropenem is hydrogen bonded by the backbone nitrogen and carbonyl group of Thr237 (Figure 4.5) at 2.84 and 3.08 Å respectively. The hydrogen bonds formed by the carbonyl oxygen help to polarise this bond and increase its susceptibility to hydrolytic attack.

The hydroxyl oxygen of the β-lactam interacts, also through hydrogen bonds, with the ND2 atom of Asn132 (2.95 Å) and the catalytic water molecule (Wat1, 2.69 Å). Additionally, hydrogen bonding interactions are observed between the meropenem carboxylate and the side chain hydroxyl groups of Thr235 (2.84 Å), Thr237 (2.70 Å) and Ser130 (2.84 Å). The carboxylate is also hydrogen bonded to the side chain of Lys234 (3.04 Å) and a water molecule (2.89 Å) as shown in Figure 4.5.

4.3.3 The SFC-1 E166A-meropenem acylenzyme structure

The SFC-1 E166A mutant in complex with hydrolysed meropenem (acylenzyme) was crystallized and its structure determined by molecular replacement as described for the S70A mutant. The acylenzyme complex crystallised in space group $P2_12_12_1$ with one molecule in the asymmetric unit, and clear electron density was observed for residues 32–292 in the initial maps. A total of 269 ordered residues, one hydrolysed meropenem molecule, four ethylene glycol molecules, and 510 water molecules were refined to a resolution of 1.30 Å with a crystallographic *R*-factor of 11.1% and an R_{free} of 14.8% (Table 4.2). No electron density was found for 13 residues in the C-terminal of the protein that were assumed to be disordered in the crystal structure. Electron density for meropenem, introduced during the soaking process, was observed in the active site pocket of the protein, whereas electron density for ethylene glycol, the cryoprotectant used for crystal freezing, was found mostly on the surface of the protein.

The overall structure of the SFC-1 E166A acylenzyme is very similar to that of native SFC-1. In fact, the two proteins can be superimposed with an r.m.s.d. of 0.48 Å for 268 structurally aligned Cα positions. Upon alignment of SFC-1 E166A acylenzyme and S70A mutant with bound meropenem, an r.m.s.d. of 0.14 Å was determined for all Cα atoms, demonstrating the strong similarity throughout the entire proteins.

In the structure of the E166A acylenzyme, an uninterrupted electron density connects the active site catalytic residue Ser70 with the β-lactam ring-opened form of meropenem, showing that the enzyme and the antibiotic have been covalently linked. This corresponds to the covalent acylenzyme intermediate formed upon attack of the conserved serine nucleophile (Ser70 in class A β-lactamases) on the carbonyl carbon of the β-lactam ring. The electron density of the covalent acylenzyme intermediate is displayed in Figure 4.6B.

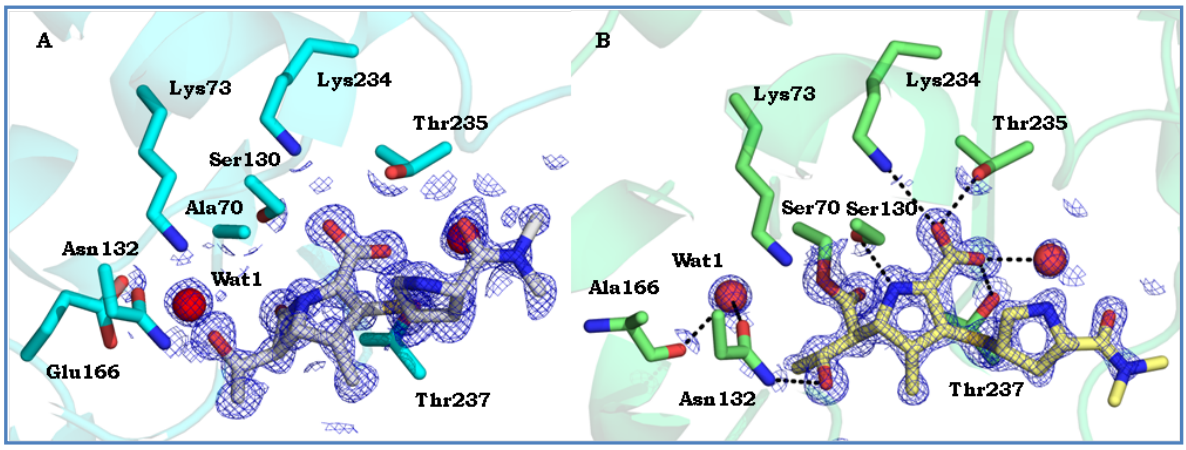

Figure 4.6 A) Binding of unhydrolysed meropenem (gray carbons) in the active site of SFC-1 S70A, shown for comparison. B) Binding and interactions of hydrolysed meropenem (yellow carbons) and catalytic water molecule (Wat1) in the active site of SFC-1 E166A. The sigma-A weighted electron density maps shown are contoured at 1.0σ.

An overlay of the S70A mutant-meropenem complex with the crystal structure of the E166A acylenzyme reveals that the β-lactam ring carbonyl oxygen is placed deeper into the oxyanion hole in the structure of the E166A acylenzyme. In the meropenem complex the β-lactam ring carbonyl oxygen was not hydrogen bonded to the Ala70 backbone amide (Figure 4.5B) and the distance to the Thr237 backbone amide nitrogen was 2.84 Å. In the acylenzyme, the β-lactam ring carbonyl oxygen establishes hydrogen bonding contacts with the backbone amide nitrogen atoms of both Ser70 and Thr237 (2.82 Å) (Figure 4.6B). Originally at a distance of 3.15 Å from the side chain carbon atom of Ala70 (in the S70A mutant-meropenem complex), the β-lactam ring carbonyl carbon shifts position coming closer to Ser70 (2.7 Å to side chain carbon atom) to form a covalent bond (1.35 Å) with the hydroxyl group (in the structure of the E166A acylenzyme), generating the ester bond and opening the β-lactam ring. Along with these changes, also the meropenem carboxylate is closer to

the side chain hydroxyl of Thr237 and Thr235 (shifts from 2.76 to 2.66 Å and 3.02 to 2.54 Å, respectively), whereas the existing hydrogen bond with Ser130 hydroxyl group is lost, although its position remains unchanged.

In the crystal structure of the E166A acylenzyme the 6α-hydroxyethyl substituent of meropenem is rotated nearly 90° about the C6−C61 axis keeping its hydrogen bond with Asn132 while bonding with the deacylating water molecule (Wat1) disappeared (Figure 4.6). The deacylating water molecule forms two hydrogen bonds, one with backbone oxygen of Ala166 (2.8 Å) and another with the side chain oxygen atom of Asn132 (3.0 Å). However, in crystal structures of class A carbapenem-inhibited enzymes with carbapenems covalently bound, a hydrogen bond is observed between the hydrolytic water molecule and the carbapenem's hydroxyethyl substituent, an interaction considered to weaken the nucleophilicity of this important water molecule and thus contribute to the stability of carbapenems in the acylenzyme form in TEM-1 and SHV-1 β-lactamases (MAVEYRAUD *et al.*, 1998; NUKAGA *et al.*, 2008).

Superimposing the SFC-1 E166A-meropenem complex on the crystal structure of class A carbapenem-inhibited class A β-lactamases complexed with carbapenems such as TEM-1 (PDB 1BT5) and SHV-1 (PDB 2ZD8) (Figure 4.7), reveals some modifications in active site residues and binding of the carbapenem. SFC-1 binds meropenem in a single, well-defined orientation (Figure 4.5B, Figure 4.6). Two isomers of the carbapenems, Δ^1 and Δ^2-pyrroline that differ in the position of the double bond about the carbapenem nucleus have been observed in the active site of the β-lactamase SHV-1 (KALP and CAREY, 2008). According to this work, the Δ^1 acyl-enzyme is a long-lived, hydrolytically inert species, while the Δ^2 acyl-enzyme is the reactive species that undergoes deacylation. Although it is not possible to visualize the tautomer in the crystal structure, the collinear positioning of the thioether sulfur atom in line with the N1, C2, C3, and C4 bonds is indicative of the presence of the reactive Δ^2-pyrroline ring in SFC-1. This contrasts with the two orientations that have been observed for carbapenems bound to SHV-1 (NUKAGA *et al.*, 2008) (Figure 4.7A). Moreover, the structure of SHV-1 acylated with meropenem showed that the carbonyl oxygen of the acyl group was "flipped outside" the oxyanion hole in one of the conformers, whereas in the SFC-1 structure the carbonyl oxygen is hydrogen bonded to the amide nitrogens of Ser70 and Thr237 that form the oxyanion hole. Also in the TEM-1: imipenem complex the carbonyl group was found outside the oxyanion hole (MAVEYRAUD *et al.*, 1998).

Nukaga and collaborators reported that Ser130 is reoriented in the complex, when compared to the apo structure of SHV-1, with the hydroxyl group directed towards the amino group of Lys234 rather than to Lys73 (apo structure). A similar conformation is seen in the TEM-1: imipenem structure (Figure 4.7). In the structures of SFC-1, both the apo and meropenem complexes, Ser130 is in the same orientation and resembles that observed in the apo structure of SHV-1 (PDB 1SHV) (KUZIN *et al.*, 1999). In SFC-1 the hydroxyl group of Ser130 interacts, via hydrogen bonds, with the amino groups of both Lys73 (2.79 Å) and Lys234 (2.92 Å) and, in the structure of the acylenzyme, the amide nitrogen (N4) of meropenem (2.88 Å). This nitrogen is also hydrogen bonded to the hydroxyl of catalytic Ser70 (2.84 Å). By contrast, no interactions are observed between the carbapenem amide nitrogen and protein residues in the TEM-1 and SHV-1 structures. This suggests that Ser130 is involved not only in the acylation step by proton transfer to the amide nitrogen (N4), but also in the deacylation step by helping to position the carbapenem in an orientation favourable to catalysis.

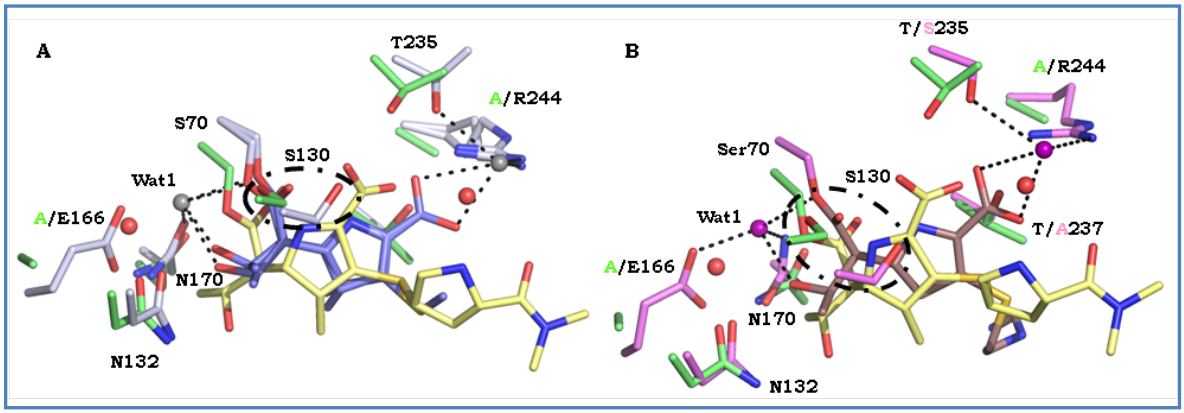

Figure 4.7 A) Superposition of SFC-1 E166A: meropenem and SHV-1: meropenem (blue: silver; PDB 2ZD8). B) Superposition of SFC-1 E166A: meropenem and TEM-1: imipenem (pink: brown; PDB 1BT5). In both schemes, active site residues of SFC-1 E166A and meropenem are coloured green and yellow, respectively and water molecules represented as red spheres; active site water molecules and their interactions are shown for SHV-1 (A) and TEM-1 (B). Black circles locate the side chains of active site Ser130.

Interestingly, the structures of carbapenem-inhibited enzymes complexed with carbapenems can be distinguished from that of the SFC-1 acylenzyme by the position and interaction of the carbapenem's 6α-hydroxyethyl substituent. In the

acylenzymes of TEM-1 and SHV-1 the hydroxyl group of the substituent is directed towards the active site groove, interacting with the hydroxyl group of Ser70, the side chain oxygen of Asn132 and the deacylating water molecule. In SFC-1 the hydroxyl group of the 6α substituent is oriented in the opposite way, directed away from the active site and hydrogen bonded to the amide group of Asn132 and a water molecule. In class A carbapenemases the active site residue Asn132 is shifted away from the active site, enlarging the substrate binding cavity (SWARÉN *et al.*, 1998). This rearrangement in the active site, along with increases in the hydrogen bonding distance between the meropenem hydroxyl group and Asn132 side chain (shifts from around 2.70 Å in TEM-1 and SHV-1 complexes to 2.86 Å in SFC-1) may possibly allow the hydrolytic water to approach the ester carbonyl of the acylenzyme species resulting in deacylation of active site bound carbapenems, as occurs in class A carbapenemases. In other class A β-lactamases (MAVEYRAUD *et al.*, 1998; NUKAGA *et al.*, 2008) the reorientation of the hydroxyethyl substituent in the acylenzyme reduces the reactivity of the deacylating water molecule, thus stabilising the covalently bound carbapenem intermediate.

An arginine at position 244 is observed in most class A β-lactamases, known to interact strongly with the substrate carboxylate in these enzymes (NUKAGA *et al.*, 2008; STRYNADKA *et al.*, 1992) (Figure 4.7) and has been shown to be important in the tautomerization of the Δ^2- to Δ^1-pyrroline acylenzyme involved in carbapenem inhibition by these enzymes (KALP and CAREY, 2008; ZAFARALLA and MOBASHERY, 1992). However, in class A carbapenemases an alanine is found replacing the arginine. Instead, the side chain of an arginine at position 220 is projected into the active site occupying a position similar to that of Arg244 of non-carbapenemases. Although this doesn't change the architecture of the active site, the anchoring of the substrate's carboxylate is different in the two groups of enzymes. Indeed, in the SFC-1 complex meropenem carboxylate is anchored by Thr237, Thr235 and Lys234 while in TEM-1 and SHV-1 acylenzymes, carboxylate is hydrogen bonded to Arg244, Ser235 and water molecules. Consequently in TEM-1 and SHV-1 β-lactamases, bound carbapenem adopts a different orientation due to interaction with Arg244, which results in flexible binding at a distance from Ser130 (Figure 4.7). It has been proposed that in the deacylation mechanism the leaving group lactam nitrogen is activated by accepting a proton from Ser130 (MINASOV et al., 2002). However, in the former β-lactamases Ser130 is rotated away from the amide nitrogen

(N4), impairing proton transfer. By contrast in the SFC-1 E166A acylenzyme structure reported here, the interaction of the amide nitrogen with Ser130 (Figure 4.7) maintains the hydrolytically active tautomer and allows the proton transfer from Ser130, essential for an efficient deacylation. Therefore, the results shown here provide evidences to explain the carbapenemase activity exhibited by SFC-1 and related enzymes.

4.3.4 Concluding remarks

Here is reported the atomic structures of mutants and native SFC-1, a class A carbapenemase that is closely related, at the amino acid sequence level, to the clinically relevant KPC enzymes. These data show, for the first time, the interaction of carbapenems with class A carbapenemases, both in the unhydrolysed form and the acylenzyme intermediate, by X-ray crystallography.

The overall structure of SFC-1 closely resembles those of other known class A β-lactamases. However, these first structures of a class A carbapenemase with bound carbapenem and carbapenem acylenzyme suggest that, in SFC-1, and likely other class A carbapenemases, tight interaction with Ser130 maintains bound meropenem, in a conformation suitable to carbapenem hydrolysis, without gross distortion of the overall structure.

The SFC-1: meropenem complex reveals important differences in the interaction with meropenem when compared to carbapenem-inhibited enzymes, providing information on the mechanism of carbapenem hydrolysis by class A β-lactamases.

5. Over-expression, purification and biochemical characterisation of Sfh-I

5.1 Introduction

Carbapenems are broad spectrum β-lactams that are insusceptible to the hydrolytic action of most β-lactamases, and consequently are growing in importance as treatments for infection by opportunist Gram-negative bacterial pathogens (MASTERTON, 2009). As other treatment options for such organisms are frequently limited, carbapenem-hydrolyzing β-lactamases pose a serious threat to the effective resolution of such infections (QUEENAN and BUSH, 2007; WALSH, 2008). Although they remain comparatively rare, the frequency of carbapenemase containing-bacterial species continues to increase (HAWKEY and JONES, 2009). Carbapenemase activity has now been reported for β-lactamases of all four Ambler classes (A-D) (KIM *et al.*, 2006; QUEENAN and BUSH, 2007).

Ambler class B or metallo-β-lactamases (MBLs) require zinc as a cofactor and are not susceptible to serine β-lactamase inhibitors (e.g. clavulanic acid) in clinical use (CROWDER *et al.*, 2006). MBLs are divided, according to their sequence, metal requirement and substrate specificity, into three subclasses (GALLENI *et al.*, 2001). Subclasses B1 and B3 generally bind two zinc equivalents and exhibit a broad spectrum of activity, hydrolyzing all classes of β-lactams except monobactams (CROWDER *et al.*, 2006). By contrast, subclass B2 MBLs, such as CphA (SEGATORE *et al.*, 1993; VALLADARES *et al.*, 1997), ImiS (CRAWFORD *et al.*, 2004; WALSH *et al.*, 1996) and AsbM1 (YANG and BUSH, 1996) from *Aeromonas* spp., are monozinc enzymes with a strong preference for carbapenem substrates, and are inhibited upon binding of a second zinc ion (VALLADARES *et al.*, 1997; YANG and BUSH, 1996). These are the least studied MBLs.

Serratia fonticola are *Enterobacteriaceae* found mainly in aquatic and other environmental samples (GAVINI *et al.*, 1979; MÜLLER *et al.*, 1995; MÜLLER *et al.*, 1986) and are generally considered as nonpathogenic, but have also been described as occasional human pathogens associated with respiratory tract infections or as infectious agents in wounds (BOLLET *et al.*, 1991; FARMER *et al.*, 1985; GORRET *et al.*, 2009; PFYFFER, 1992). Previously characterised *S. fonticola* strains are intrinsically resistant to β-lactams due to the expression of both a chromosomally encoded extended-spectrum class β-lactamase and a species-specific AmpC β-lactamase (PEDUZZI *et al.*, 1997; STOCK *et al.*, 2003).

However, it was previously established that UTAD54, a *S. fonticola* strain isolated from a natural water source, also expresses a metallo-β-lactamase, Sfh-I (SAAVEDRA *et al.*, 2003) and a class A carbapenem-hydrolysing β-lactamase, SFC-1 (FONSECA *et al.*, 2007; HENRIQUES *et al.*, 2004), that are both absent from other *S. fonticola* strains. The Sfh-I amino acid sequence diverges markedly (approximately 50% identity) from those of previously described B2 MBLs originating from *Aeromonas* strains (SAAVEDRA *et al.*, 2003).

In order to further characterise the Sfh-I metallo-enzyme, the gene encoding Sfh-I from *S. fonticola* UTAD54 was cloned and over-expressed in *E. coli*. This chapter describes the purification and biochemical characterisation of the recombinant enzyme.

5.2 Materials and methods

5.2.1 Antimicrobial agents and reagents

Antibiotics were obtained as powders from Sigma-Aldrich (ampicillin, benzylpenicillin, carbenicillin, cefepime, cefotaxime, cefoxitin, ceftazidime, cephalothin, cephaloridine, moxalactam, piperacillin), Merck Sharp & Dohme Co (imipenem), Sequoia Research Products (meropenem) and Becton-Dickinson (nitrocefin).

General reagents and buffers were purchased from Sigma-Aldrich or Merck Sharp & Dohme Co and were of analytical quality.

5.2.2 Cloning and over-expression of Sfh-I

Molecular biology procedures followed manufacturers' protocols except where stated.

Initially Sfh-I was expressed as the mature protein, i.e. without its own predicted leader peptide, using the *pelB* sequence leader from the expression vector pET-26b (Novagen) that encodes a signal sequence aimed to direct expressed recombinant proteins to the periplasmic space. The same procedure was used to

obtain a high yield of recombinant SFC-1 (FONSECA *et al.*, 2007) (Chapter 3). For that, *bla*$_{Sfh-I}$ was PCR-amplified from the genomic DNA of *Serratia fonticola* UTAD54 using the methodology described in Chapter 3 (see section 3.2.3) and primers SfhFv2 and SfhRv2 (Table 5.1; the *Nco*I and *Xho*I recognition sequences are underlined), obtained from STAB VIDA (Caparica, Portugal). PCR products were purified with the JETQUICK PCR Purification Spin Kit (GENOMED). Purified products and vector were digested with *Nco*I and *Xho*I (Roche) and cloned into the corresponding site of the pET-26b expression vector. The recombinant plasmid (pSfh-Iv2) was transformed into *E. coli* TOP10 (Invitrogen) and the presence of unwanted mutations in the expression plasmid was confirmed by sequencing.

Table 5.1 Primers used to clone *bla*$_{Sfh-I}$.

Primer	Sequence 5' --- 3'
SfhFv2	GGATCCACCATGGCTTCTGAAAAAAACTTAACG
SfhRv2	GTGCTCGAGTTACTTAGGCGCCTTCTCAAGC
SfhFv3	GGATCCCATATGTCTGAAAAAAACTTAACGCTTACC
SfhFv4	GGATCCCATATGAATATTAAATATTTATTTACGGCTG

Underlined sequences represent restriction endonuclease sites.

Recombinant protein was expressed from E*. coli* BL21 (DE3) (Novagen). The expression of the recombinant β-lactamase was optimised in a small scale (50 mL) by decreasing the post-induction temperature (26ºC, 20ºC, 15ºC) and concentration of the inducing agent (IPTG, 1 mM and 0.5 mM), analysing expression under different time-course of induction (1h, 3h, 5h, 12h, 24h) and using a range of different culture media in a commercially available Media Optimization Kit™ (AthenaES™).

Several attempts were made to solubilise this material, either using the BugBuster® Protein Extraction Reagent (Novagen) or strong denaturants (6M Guanidine-HCl, 8M Urea and CAPS pH 11), with refolding of the target protein *in vitro*, by dilution of supernatant (after centrifugation, 15000 g for 15 minutes) into 50 mM Tris pH 7.5, 100 μM $ZnCl_2$ (4ºC, with gentle swirling).

With the purpose of obtaining soluble active recombinant Sfh-I two further constructs were made lacking the *pelB* leader sequence of the pET-26b expression

vector. Primers SfhFv4 (Sigma-Aldrich) (*Nde*I restriction site underlined) and SfhRv2 (Table 5.1) were used to amplify the complete Sfh-I open reading frame (including its own predicted leader sequence; Sfh-Iv4). To obtain a construct encoding Sfh-I without the predicted periplasmic leader sequence (i.e. nucleotides 55 – 759; Sfh-Iv3), primers SfhFv3 (Sigma-Aldrich) and SfhRv2 (Table 5.1) were used.

Sfh-I-containing DNA fragments were amplified from *S. fonticola* UTAD54 genomic DNA using *Pfu* polymerase (Fermentas) and purified from agarose electrophoresis gels using the QIAEX II Gel Extraction Kit (QIAGEN). Purified PCR products were digested overnight with *Nde*I and *Xho*I (New England Biolabs) at 37ºC and ligated, using the Quick Ligation Kit™ (New England Biolabs) according to the manufacturer protocol, into the *Nde*I − *Xho*I site of digested pET-26b. The recombinant plasmids (pSfh-Iv4 and pSfh-Iv3) were transformed into *E. coli* TOP10 and plated into LB agar containing 50 mg/ml kanamycin. Positive clones were identified by colony PCR procedures using the following protocol: 5 to 10 colonies were picked and resuspended in 5 µl of sterile water, and incubated 10 minutes at 100ºC; 4 µl of the supernatant solution were used as template DNA in the PCR reactions carried out with the T7 primers (Sigma-Aldrich). Plasmid DNA was purified, for the clones whose insert was amplified, using the QIAprep Spin Miniprep Kit (Qiagen). The cloned inserts were further characterised by restriction enzyme analysis of purified plasmid DNA using *Xho*I followed by agarose gel electrophoresis. The integrity of the Sfh-I DNA sequence was ensured by complete sequencing of the inserts in both recombinant plasmids.

5.2.3 β-lactamase production and purification

For β-lactamase expression recombinant plasmids (pSfh-Iv4 and pSfh-Iv3) were transformed into *E. coli* BL21 Star (DE3) (Invitrogen). Recombinant Sfh-Iv3 and Sfh-Iv4 were produced following procedures previously developed for production of recombinant SFC-1 (FONSECA *et al.*, 2007) (Chapter 3) except that expression was induced by using 1mM IPTG overnight at 25°C. Protein extracts were loaded onto a 40ml Q-Sepharose column (GE Healthcare) pre-equilibrated in Tris-HCl buffer (50 mM, pH 8.5) containing $ZnCl_2$ (100 µM) and bound proteins eluted on a 400ml 0 to 500 mM NaCl linear gradient.

Fractions with β-lactamase activity, identified by hydrolysis of the chromogenic β-lactam antibiotic nitrocefin, were concentrated by centrifugal filtration (Amicon Ultra, Millipore) and further purified on a 300ml Superdex 75 column (GE Healthcare) running in HEPES buffer (50 mM, pH 7.0). Active fractions were collected and concentrated. The presence and purity of protein at each stage of the purification process was confirmed by SDS-PAGE (LAEMMLI, 1970).

5.2.4 Determination of kinetic parameters

Kinetic parameters, k_{cat} and K_M, for the hydrolysis of a range of β-lactam antibiotics were calculated from initial hydrolysis rates measured at 25°C in HEPES buffer (50 mM, pH 7.0) in UV-transparent 96-well plates (BD Biosciences) at appropriate wavelengths (LARAKI *et al.*, 1999), using a SpectraMax 190 plate-reader (Molecular Devices) as described previously (SAMUELSEN *et al.*, 2008). Stock substrate concentrations were determined from measurements of complete hydrolysis using previously reported extinction coefficients (LARAKI *et al.*, 1999).

Typically, experiments were conducted in which data points were recorded every 3-4 seconds for 20 - 30 minutes. Substrate and enzyme concentrations employed were adjusted to ensure that the evolution of product remained linear over a substantial fraction of the total time recorded across the whole range of substrate concentrations under investigation, i.e. that the reaction was taking place under steady-state conditions and that initial rates were indeed being recorded. Results obtained from experiments conducted in an independent laboratory with a conventional spectrophotometer using a subset of substrates (M.N. Lisa and A.J. Vila, personal communication) were in good agreement with those reported here, giving us further confidence in the accuracy of plate reader data. Kinetic parameters (k_{cat} (s^{-1}) and K_M (μM)) were determined by non-linear least squares fitting of the initial velocity of hydrolysis *versus* substrate concentration plots using GraphPad Prism (version 5.01, GraphPad Software Inc., La Jolla, USA). For cephalothin, the K_m was determined as the inhibition constant, K_i, calculated by nonlinear global fitting of initial velocity *versus* [nitrocefin] curves obtained at multiple cephalothin concentrations using the competitive inhibition model contained within GraphPad Prism. Reactions were initiated by addition of Sfh-I (final concentration 1.5 μM) to

pre-mixed nitrocefin and cephalothin and data recorded immediately (i.e. there was no pre-incubation of Sfh-I with cephalothin).

5.2.5 Time- and concentration-dependence of Sfh-I inhibition by cephalothin

In assays of the time-dependence of inhibition, 1.5 μM Sfh-I was incubated with a 1:5 molar ratio of cephalothin for 0.5−1200 minutes in 50 mM HEPES buffer pH 7.0 at room temperature. 100 μl samples were withdrawn at appropriate time intervals and residual activity was assayed by introducing these into a 1 ml cuvette containing nitrocefin as reporter substrate at a final concentration of 200 μM. Initial hydrolysis rates for the reporter substrate were measured using a Lambda 35 spectrophotometer (Perkin-Elmer). Extinction coefficients and wavelengths used were as described (LARAKI *et al.*, 1999). Hydrolysis of cephalothin under these conditions was monitored in parallel in a 1 ml sample by continuously recording absorbance at 265 nm in another spectrophotometer.

In order to determine the reversibility of inhibition, Sfh-I was incubated with cephalothin as above for a time sufficient to inhibit the enzyme, and the mixture was then dialyzed overnight at 4ºC against 50 mM HEPES buffer pH 7.0. A control sample of protein incubated in the absence of inhibitor was treated identically and used for comparison. The recovery of enzymatic activity was determined by measuring the residual activity as described above.

5.2.6 Inactivation of Sfh-I by hydrolysed antibiotics

The antibiotics here studied as putative Sfh-I inactivators (cephalothin, cefoxitin and moxalactam) (2 mM) were hydrolysed by IMP-1 (LARAKI *et al.*, 1999) in 50 mM HEPES pH 7.0, as monitored spectrophotometrically. After complete hydrolysis, the products were separated from the enzyme by centrifugal filtration (Amicon Ultra-4 – 10,000 NMWL; Millipore) and stored on ice until use. Hydrolysed antibiotics at a concentration of 1 mM were used to inactivate 3.6 mM Sfh-I at 4ºC. Inactivation was followed by measuring the residual activity as described above.

5.2.7 Mass spectrometry

The molecular mass and metal content of Sfh-I were determined by electrospray mass spectrometry. Sfh-I (200 μM) was dialysed into ammonium acetate buffer (25 mM, pH 7.0) and mass spectra were recorded under both native and denaturing conditions. Samples were delivered at nanolitre per minute flow rates using a Nanomate source (0.3psi, 1.4kV) and mass spectra were recorded on a QStar XL qTOF instrument in positive ion mode.

Inhibition of Sfh-I by cephalothin was studied by liquid chromatography mass spectrometry (LC-MS). A sample of 500 pmols of a mixture (5:1 or 15:1) of cephalothin and Sfh-I (200 μM) incubated for 30 minutes was run on a Zorbax C3 column with a linear gradient of 1:1 (v/v) water-acetonitrile containing 0.06% formic acid. Eluent was fed directly into a Q-TOF I (Micromass) mass spectrometer and mass spectra were acquired.

The sample containing a 5:1 ratio of cephalothin-SfhI was incubated with trypsin (1:50 substrate ratio) for 3h at 37°C and analysed by MALDI mass spectrometry.

5.2.8 Zinc binding

Fluorescence emission spectra of the enzyme (1 μM) in the presence of increasing amounts of Zn^{2+} were recorded on a FluoroLog® spectrofluorometer (Horiba Jobin Yvon) using excitation and emission wavelengths of 280 and 341 nm, respectively. Slits were set to a band pass width of 5 nm. Assays were conducted at 25°C in 50 mM HEPES buffer, pH 7.0, in a 1 ml cuvette with continuous mixing provided by a magnetic stirrer. The dissociation constants (K_d) for zinc binding to Sfh-I were estimated by plotting the measured change in fluorescence (Y) against zinc concentration ($[Zn^{2+}]$) and nonlinear fitting to a two-site hyperbola model:

$$Y=Y1*[Zn^{2+}]/(K_{d1}+[Zn^{2+}]) + Y2*[Zn^{2+}]/(K_{d2}+[Zn^{2+}])$$

where Y1 and Y2 are the maximal fluorescence changes associated with the binding events described by K_{d1} and K_{d2}, respectively.

5.2.9 Zinc concentration dependence of Sfh-I activity

Zinc dependence assays of Sfh-I activity were conducted in 96-well plate format under the conditions described above using nitrocefin and imipenem as reporter substrates and a range of $ZnCl_2$ concentrations (0-500 μM). Reactions were initiated by addition of Sfh-I (1.5 μM with nitrocefin and 1.0 nM with imipenem) to pre-mixed nitrocefin and zinc and data recorded immediately. Apparent k_{cat} and K_M values were determined as described above in the presence of increasing concentrations of zinc. The ratio k_{cat}/k_{cat0} (where k_{cat0} is the value of k_{cat} measured in the absence of added zinc) was plotted against zinc concentration and the resulting hyperbola was fitted to Equation 5.1:

$$k_{cat}/k_{cat0} = (K_{d2} + \alpha*[Zn^{2+}]) / ([Zn^{2+}] + K_{d2}) \qquad \text{Equation 5.1}$$

by non-linear regression analysis using GraphPad Prism where α is the value of the k_{cat}/k_{cat0} ratio when zinc concentration is saturating. K_{d2} represents the dissociation constant for the second zinc ion.

Circular dichroism (CD) spectroscopy was used to give information about the effect of zinc on the secondary structure of Sfh-I. For these studies, the buffer of the Sfh-I solution was exchanged to 20 mM sodium phosphate pH 7.0, by dialysis overnight at 4°C, using Slide-A-Lyzer® Dialysis Cassettes (10K MWCO, Pierce). CD spectra were recorded on a Jasco J-815 spectropolarimeter in the range 260-190 nm using 8.5 μM Sfh-I in a 1 mm cuvette. Temperature was set to 20°C. For each sample four spectra were collected and averaged. Baselines of phosphate buffer without protein were subtracted from the samples to yield the contribution of the protein component. Thermal stability spectra were measured at 220 nm with temperature stepwise increased from 20°C to 90°C at an interval of 5°C. Four scans were obtained for each sample and averaged.

5.3 Results and Discussion

5.3.1 Over-expression and purification of Sfh-I

The production of *S. fonticola* Sfh-I in *E. coli* BL21 (DE3), from the T7 promoter-based expression vector pET-26b, was tested with 3 different constructs.

The first construct of Sfh-I was prepared as previously described for production of recombinant SFC-1 (Chapter 3), i.e. the open reading frame encoding the mature Sfh-I polypeptide without the leader sequence was expressed as a fusion with the *pelB* leader sequence from the pET-26b vector. Although high-level expression was attained in *E. coli* (Figure 5.1A), the majority of the recombinant protein aggregated inside the cells in insoluble inclusion bodies (BANEYX and MUJACIC, 2004; VILLAVERDE and MAR CARRIÓ, 2003) (Figure 5.1B).

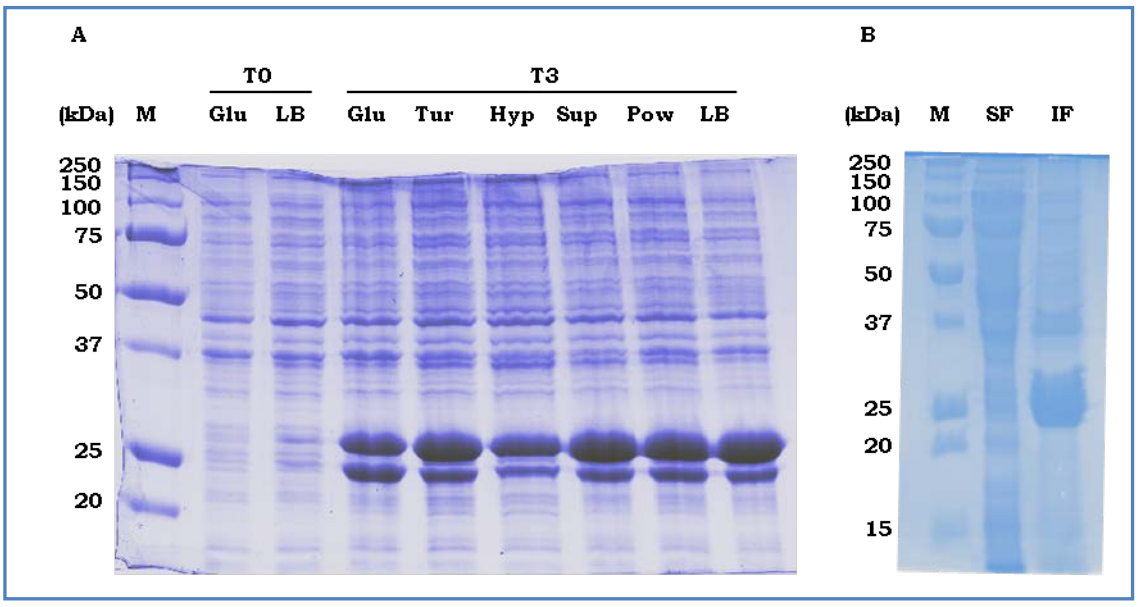

Figure 5.1 Analysis of recombinant Sfh-Iv2 expression in *E. coli* BL21 (DE3) by SDS-PAGE (12%), stained with Coomassie Blue. A) Lane 1, marker proteins (Precision Plus Protein™ all blue standards – Bio-Rad;); lanes 2-3, total protein from uninduced cultures grown in Glucose M9Y and LB broth, respectively; lanes 4-9, total protein from induced cultures (1 mM IPTG) grown at 37°C in different culture media including Glucose M9Y, Turbo, Hyper, Super, Power and LB broth (lanes 4-9, respectively) 3h post-induction. B) marker proteins (lane 1), soluble (lane 2) and insoluble (lane 3) fractions of *E. coli* BL21 (DE3) host cells containing the pSfh-Iv2 plasmid induced with 1 mM IPTG (37°C for 3h). Protein was extracted using the BugBuster® Protein Extraction Reagent.

An extensive expression optimization was carried out to improve solubility by testing a number of parameters. These included growth temperature, culture media composition (Figure 5.1A), time-course of induction and the concentration of the inducing agent. However, the improvement in the solubility of the recombinant enzyme was not significant as only a small quantity of soluble protein was achieved. In an effort to obtain soluble protein from this construct, the solubilisation and refolding of the insoluble material was attempted. Nonetheless, the efficiency of the procedures used to solubilise/refold the insoluble protein proved to be very low, as revealed by the activity assays (data not shown).

Two other constructs were designed and cloned into pET-26b using the *Nde*I (and *Xho*I) restriction site(s) such that the *pelB* leader sequence was no longer present. Both the constructs pSfh-Iv3, which encodes a version from which the signal peptide is deleted, and pSfh-Iv4, which encodes a form that contains the original signal peptide, produced soluble recombinant protein.

When evaluated the expression of the two constructs without the *pelB* leader sequence by SDS-PAGE (Figure 5.2), mature Sfh-I (Sfh-Iv3) was generated in higher yields and was accordingly purified and used for kinetic experiments.

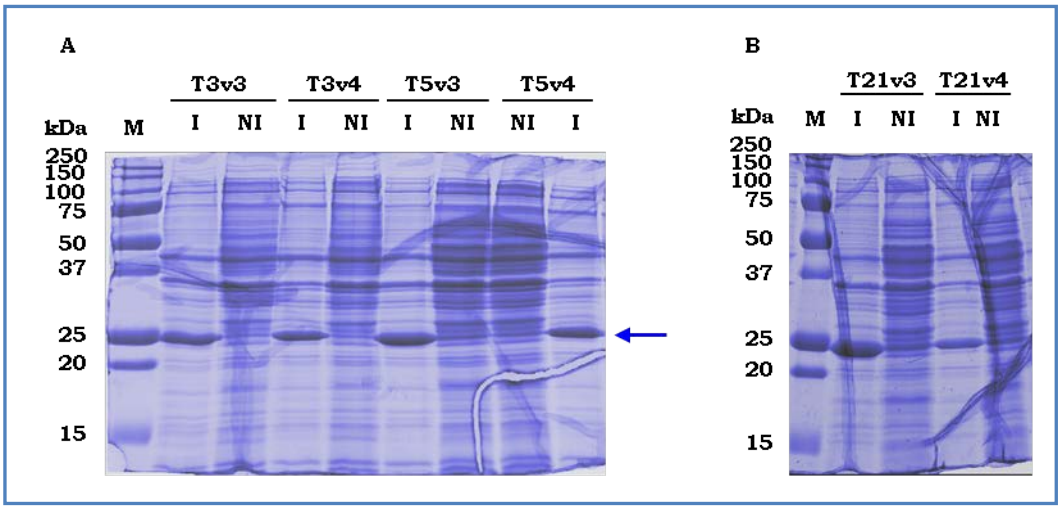

Figure 5.2 Analysis of recombinant Sfh-Iv3 (v3) and Sfh-Iv4 (v4) expression in *E. coli* BL21 (DE3) by SDS-PAGE (12%), stained with Coomassie Blue. A) Lane 1, protein ladder; lanes 2-9, soluble fraction from induced (1 mM IPTG, I) and uninduced (NI) cultures grown in LB media at 25°C. Cells were collected at 3h (T3) and 5h (T5) post-induction. B) As described in A) except cells were grown up to 21h after induction. The blue arrow shows the position of a protein band with the expected size of Sfh-I. Protein was extracted using the BugBuster® Protein Extraction Reagent.

Recombinant Sfh-I was readily purified from induced (1 mM IPTG) cultures of *E. coli* BL21 (DE3) cells containing the pSfh-Iv3 plasmid grown overnight at 25ºC. The optimised purification protocol consists of two chromatographic steps: an anionic exchange (Q-Sepharose) run with 50 mM Tris buffer pH 8.5 containing 100 μM $ZnCl_2$ and eluted with a linear gradient (0-25 %) of 1 M NaCl (Figure 5.3A), followed by a gel filtration (Superdex 75).

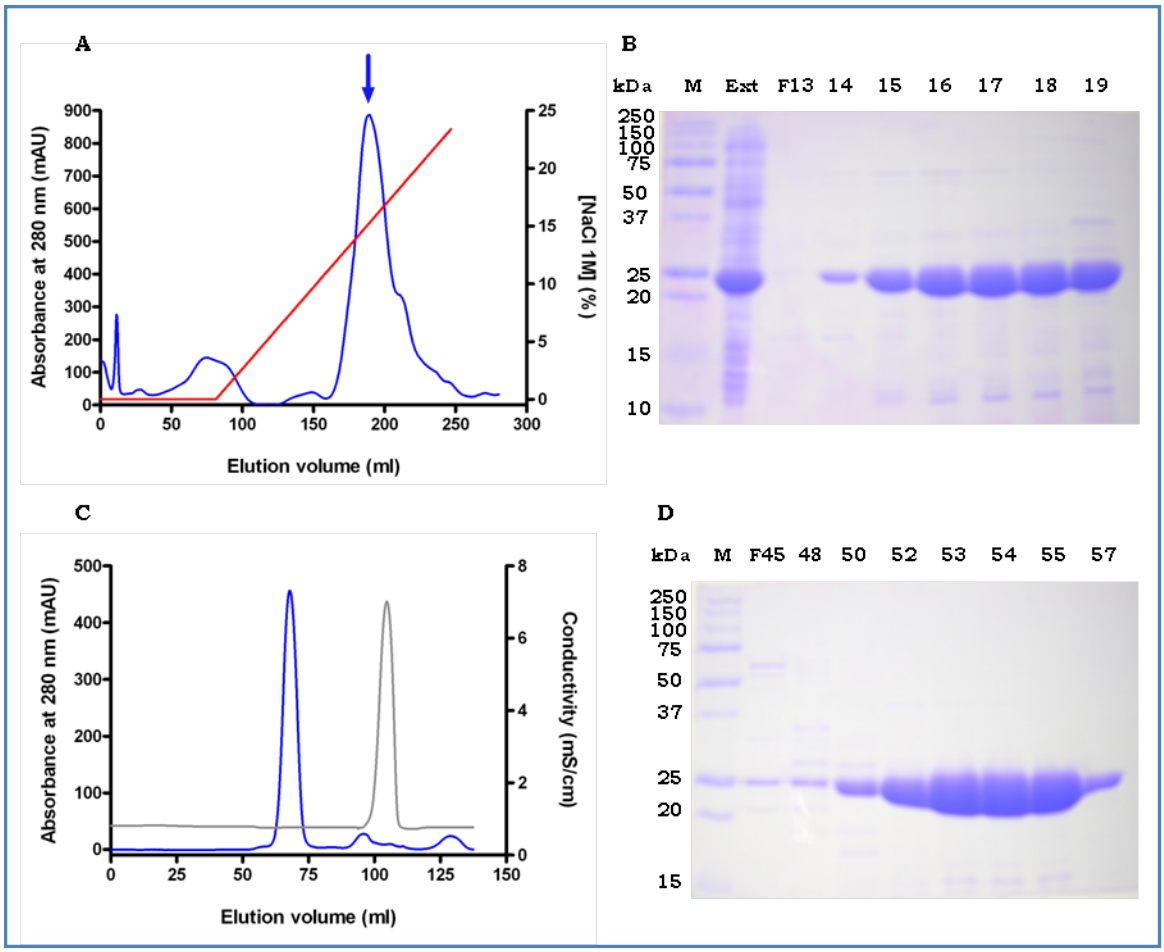

Figure 5.3 Optimised purification of recombinant Sfh-Iv3. A) and C) Chromatograms obtained from an extract of culture of *E. coli* BL21 (DE3) cells containing the pSfh-Iv3 plasmid applied to a Q-Sepharose™ anionic exchange column with β-lactamase active peak indicated by an arrow, and from the fraction pointed in A) applied to a Superdex™ 75 gel filtration column, respectively. B) and D) Analysis of the purification by SDS-PAGE (12%) stained with Coomassie Blue. B) Soluble extract of *E. coli* culture (lane 2) and fractions from anionic exchange (lanes 3-9). D) Protein fractions from gel filtration chromatography. M is the protein ladder.

The active fractions recovered from the anionic exchange were applied to the gel filtration column and elution was performed with 50 mM Hepes buffer pH 7.0 (Figure 5.3C). This step allows excess zinc and salt to be washed from the purified protein (peak in the conductivity scale; silver line in Figure 5.3C) as well as a change in the pH promoting a higher stability of the protein during storage. The analysis of purified protein by SDS-PAGE confirmed the purification of recombinant Sfh-I to homogeneity (Figure 5.3D). The purification procedure used enabled to yield 50 mg/liter of purified protein at a purity of >95% as adjudged by SDS-PAGE (Figure 5.3).

The interpretation of electrospray mass spectrometry experiments (in particular the native spectrum) is complicated by multiple peaks that may arise from bound salt and/or water molecules. However, the mass of 26 136 Da obtained under denaturing conditions (Figure 5.4A) is consistent with removal of the N-terminal methionine from Sfh-Iv3 and in agreement with the value predicted from sequence (26 134 Da). A similar result for the Sfh-Iv4 construct confirms previous predictions that Sfh-I is expressed with a 21-amino-acid signal peptide that is cleaved between Ala and Ser to generate the mature form of the enzyme (SAAVEDRA *et al.*, 2003).

5.3.2 Sfh-I is isolated as a monozinc enzyme

In the native spectrum (Figure 5.4B) peaks at 26 201 Da (26 136 + 65 Da); 26 218 Da (26 152 + 66 Da) and 26 239 Da (26 170 + 69 Da) all indicate addition of one equivalent of zinc (65 Da) to species found under denaturing conditions. These results, together with the size exclusion analysis, confirm that as isolated Sfh-I exists primarily in the mononuclear form, consistent with the assignment, from sequence, of Sfh-I as a B2 MBL (SAAVEDRA *et al.*, 2003). The same zinc content was reported from previous investigations of the CphA and ImiS enzymes (CRAWFORD *et al.*, 2004; VALLADARES *et al.*, 1997).

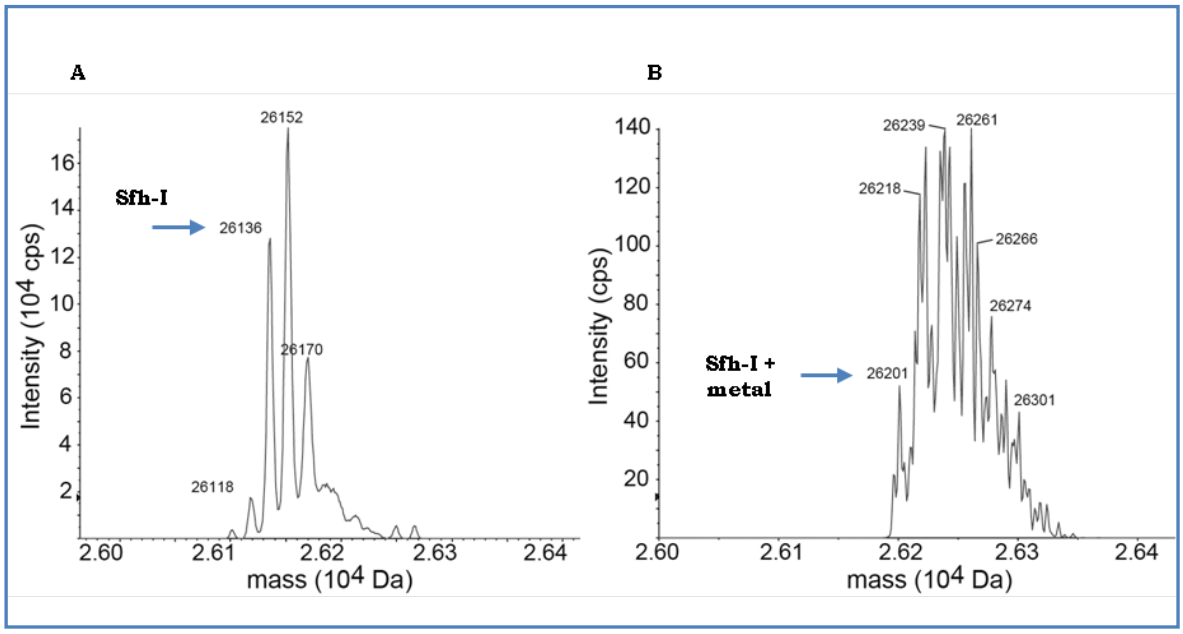

Figure 5.4 Electrospray mass spectra of purified Sfh-I showing molecular mass of 26 136 Da (A) and binding of one zinc equivalent (Mr = 65) per protein molecule under non-denaturing conditions (B).

5.3.3 Kinetic parameters of Sfh-I

Hydrolysis of a representative set of β-lactam antibiotics by Sfh-I was investigated under steady-state conditions (Table 5.2). Sfh-I efficiently hydrolyses carbapenems (imipenem, meropenem) but exhibits low affinity (K_M > 300μM) for many penicillins (ampicillin, carbenicillin and benzylpenicillin) and some cephalosporins (cefotaxime, ceftazidime). This behaviour is broadly similar to that previously reported for other *Aeromonas* B2 enzymes (FELICI and AMICOSANTE, 1995; FELICI *et al.*, 1993; SEGATORE *et al.*, 1993; VANHOVE *et al.*, 2003; WALSH *et al.*, 1996; YANG and BUSH, 1996). However, compared to *A. hydrophila* CphA, Sfh-I shows higher K_M values (indicative of lower affinity) for penicillins (with the exception of ampicillin) and significantly increased turnover rates (k_{cat}) for ampicillin. For cephalosporins such as cefoxitin, nitrocefin and cephaloridine, K_M values are reduced (indicative of higher affinity) compared to those reported for CphA (Table 5.2). With respect to CphA, catalytic efficiency (k_{cat}/K_M) is thus increased for all non-carbapenem substrates except carbenicillin and cephaloridine. In the case of ampicillin this increase is almost four orders of magnitude. Sfh-I hydrolysed the cephalosporins cefotaxime and ceftazidime, as well as the serine-β-lactamase

inhibitor sulbactam, but plots of hydrolysis rate against substrate concentration were linear and we were consequently unable to derive kinetic parameters for these substrates.

Unexpectedly, and in contrast to the poor hydrolysis of many other cephalosporins, Sfh-I (0.01 μM) hydrolysed cefepime with relatively high efficiency (3.02×10^3 $M^{-1}s^{-1}$) when compared to that of CphA for other cephalosporin substrates. Felici and Amicosante have previously reported that 0.5 μM CphA shows no detectable activity towards cefepime (FELICI and AMICOSANTE, 1995). Compared to the other less well characterised subclass B2 MBLs from other *Aeromonas* species, Sfh-I is distinguished by its faster hydrolysis of penicillins and differs from AsbM1, but resembles ImiS, in its relatively low affinity towards penicillins. Faster hydrolysis (higher k_{cat}) but weaker K_M values for meropenem compared to imipenem appears to be a shared property of all of these enzymes.

Table 5.2 Kinetic parameters of purified Sfh-I β-lactamase and comparison with other B2 metallo-β-lactamases.[a]

Substrate or inhibitor	k_{cat} (s^{-1})				K_M (μM)				k_{cat}/K_M ($M^{-1}s^{-1}$)			
	Sfh-I	CphA	AsbM1	ImiS	Sfh-I	CphA	AsbM1	ImiS	Sfh-I	CphA	AsbM1	ImiS
Ampicillin	9.53	<0.01[b]	0.13	1.1	676	2500[b]	65	510	1.41×10^4	<4[b]	7.5×10^3	2.2×10^4
Benzylpenicillin	ND	0.03	1.2	0.53	>1500	870	160	250	ND	35	2.0×10^3	2.1×10^3
Carbenicillin	9.15	10[d]	0.44	0.5	1280	500[d]	28	260	7.18×10^3	2.0×10^{4}[d]	1.6×10^4	2.1×10^3
Nitrocefin	0.06	0.0028	≤0.02	0.024[g]	106	1200	ND	51[g]	5.67×10^2	2.5	ND	4.0×10^{3}[g]
Cephaloridine	8.21×10^{-5}	<0.006	≤0.06	NH	334	~6000	ND	NH	2.46×10^{-1}	<1	ND	NH
Cephalothin	ND	NR	NR	NR		NR	NR	NR	ND	NR	NR	NR
Cefotaxime	ND	0.009[b]	NR	NH	>1000	1000[b]	NR	NH	ND	9[b]	NR	NH
Ceftazidime	ND	NR	NR	NR	>500	NR	NR	NR	ND	NR	NR	NR
Cefoxitin	0.032	0.02[e]	≤0.06	NH	99	615[e]	ND	NH	3.23×10^2	33[e]	ND	NH
Cefepime	0.61	NH[c]	NR	NR	202	NH[c]	NR	NR	3.16×10^3	NH[c]	NR	NR
Moxalactam	0.017	NR	NR	NH	91	NR	NR	NH	1.87×10^2	5.6[e]	NR	NH
Imipenem	51	1200	71	350[f]	79	340	230	100[f]	6.42×10^5	3.5×10^6	3.1×10^5	9.1×10^{5}[f]
Meropenem	109	3100	220	296[g]	215	1340	630	308[g]	5.05×10^5	2.3×10^6	3.5×10^5	3.3×10^{6}[g]

[a] Kinetic data displayed for CphA, AsbM1 and ImiS as reported by Vanhove *et al.* (2003), Yang *et al.* (1996) and Walsh *et al.* (1996), respectively, except where indicated.

[b] Bebrone *et al.* (2005), [c] Felici and Amicosante (1995), [d] Segatore *et al.*, (1993), [e] Zervosen *et al.* (2001), [f] Sharma *et al.* (2006) [g] Crawford *et al.* (2004).

ND, values could not be determined; NH, no hydrolysis detected; NR, not reported.

5.3.4 Inhibition of Sfh-I by cephalothin

Previous workers (ZERVOSEN *et al.*, 2001) have reported that *A. hydrophila* CphA may be inactivated by the cephamycin cefoxitin and the oxacephem moxalactam, as well as by other cephalosporin antibiotics with good 3' leaving groups. Similarly, the degradation products of various cephalosporins have been shown to inhibit the subclass B1 MBL BcII from *Bacillus cereus* (BADARAU *et al.*, 2005). Accordingly, we investigated the interactions of Sfh-I with the hydrolysis products of cefoxitin, cephalothin and moxalactam.

Incubation (18 h; 25°C) of Sfh-I (3.6 μM) with each of these hydrolysis products (1 mM) resulted in reductions in hydrolytic activity against imipenem (200 μM) of 13% (cefoxitin), 36% (cephalothin) and 94% (moxalactam). These results suggest that, similarly to CphA, Sfh-I is inhibited by the degradation products of certain cephalosporins and related compounds, although in no case were we able to obtain complete inactivation.

As the reactions of CphA with hydrolysed cefoxitin and moxalactam have been extensively described (ZERVOSEN *et al.*, 2001), but those with cephalothin have not, we investigated the Sfh-I:cephalothin interaction in more detail. Experiments in which Sfh-I was preincubated with cephalothin, or its hydrolysis product, and aliquots removed and assayed for nitrocefin hydrolysis at a range of time points, confirmed that both of these compounds inactivate the enzyme in a time-dependent fashion. Experiments in which absorbance at 265 nm (reporting breakdown of cephalothin during incubation with Sfh-I) was monitored in parallel with measurements of enzyme activity suggested that loss of Sfh-I activity correlates with cephalothin hydrolysis (Figure 5.5), indicating that the hydrolysis product is the likely inhibitory species. Activity of cephalothin-treated samples remained 54% that of control samples, even after overnight dialysis was performed to remove unbound cephalothin and/or its degradation products, suggesting that inactivation results from a modification of the enzyme.

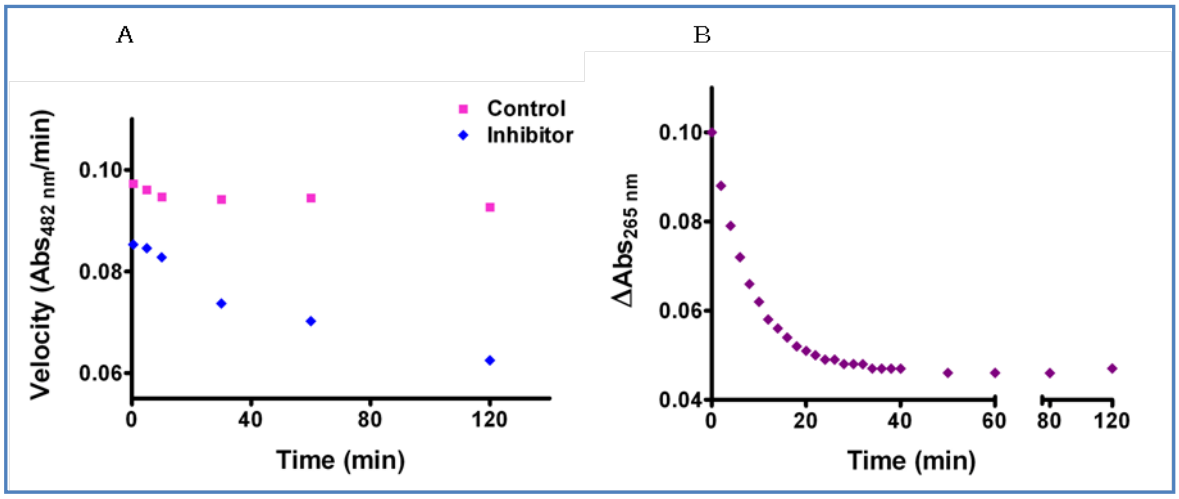

Figure 5.5 Effect of cephalothin on Sfh-I activity. A) Activity of Sfh-I (1.5 μM) after incubation with cephalothin (7.5 μM) assayed in the presence of 200 μM nitrocefin; the control sample was submitted to the same treatment but without cephalothin added in the incubation mixture. B) Hydrolysis of cephalothin measured as a decrease in absorbance monitored at 265 nm.

Zervosen and co-workers have suggested that the moxalactam, and probably cefoxitin, hydrolysis products form covalent bonds to the free thiol of the conserved cysteine, Cys221, in the B2 MBL active site (ZERVOSEN *et al.*, 2001). Similar inactivation mechanisms, in which Cys221 could interact either with the thiol generated by opening the dihydrothiazine ring of the hydrolysed cephalosporin (BADARAU *et al.*, 2005), or by addition to the exo-methylene formed after elimination of the 3' leaving group, could also explain inactivation of Sfh-I by cephalothin. Accordingly we incubated Sfh-I with cephalothin, used trypsin to degrade the sample and analysed the resulting peptide mixture by MS/MS. Unfortunately, while all expected Sfh-I-derived peptides were detected, we were unable to observe any modified fragments, suggesting that the inhibitory complex is labile under the conditions employed.

5.3.5 The effect of excess Zn^{2+}

Previous studies have revealed that CphA binds a single zinc ion tightly (K_{d1} < 20 nM) and is most active as a mono-zinc enzyme, but can bind a second, inhibitory zinc ion more weakly (K_{d2}= 46 μM) (VALLADARES *et al.*, 1997). As shown by mass spectrometry (Figure 5.4), in the absence of added zinc Sfh-I is already in a monozinc

form, as is the case for ImiS and CphA (CRAWFORD *et al.*, 2004; VALLADARES *et al.*, 1997).

Monitoring fluorescence emission during a titration of Sfh-I with excess zinc (Figure 5.6) shows two distinct transitions, demonstrating that the enzyme is able to bind 2 further zinc ions with dissociation constants for the second (K_{d2}) and third (K_{d3}) zinc equivalents calculated as 95 ± 14 μM and 2300 ± 870 μM, respectively. The value that we obtained for K_{d2} is broadly comparable to that reported for binding of a second zinc ion to CphA. The crystal structure of CphA determined in the presence of excess zinc (BEBRONE *et al.*, 2009) shows that CphA can bind a third zinc ion on the protein surface at a site distinct from the active site. Similarly, our results indicate that binding of a third zinc equivalent by Sfh-I is weak (very high K_{d3}) and accordingly is unlikely to be of physiological relevance.

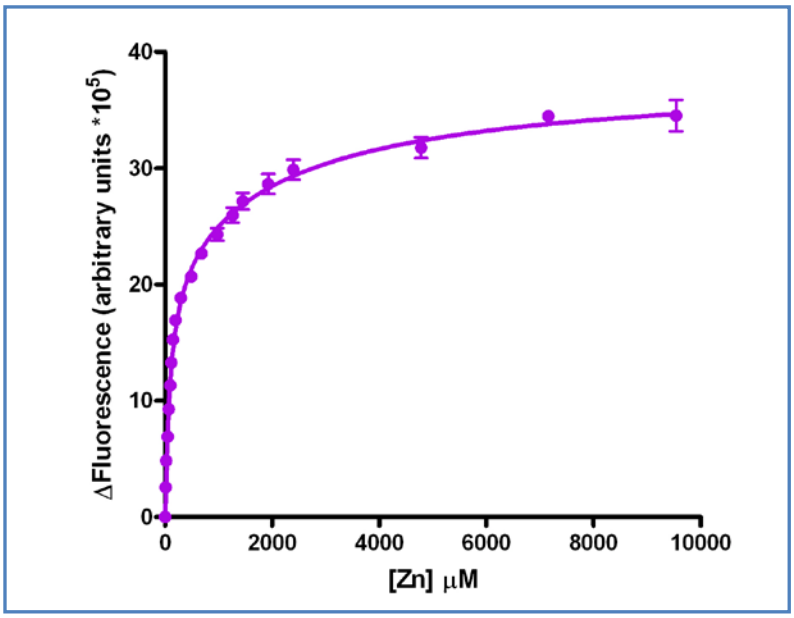

Figure 5.6 Variation in fluorescence emission intensity of Sfh-I (1 μM) as a function of the concentration of added zinc monitored at 341 nm. The data were background subtracted and analysed by nonlinear fitting using two site binding analysis in GraphPad Prism.

Other members of subclass B2 are known to be active as monozinc enzymes, whereas the binding of a second zinc ion results in non-competitive inhibition (CRAWFORD *et al.*, 2004; VALLADARES *et al.*, 1997; YANG and BUSH, 1996).

To investigate the effect of added zinc on Sfh-I activity, hydrolysis of the substrates nitrocefin and imipenem was measured in the presence of increasing concentrations of zinc (Figure 5.7). The activity of Sfh-I against imipenem was essentially unaffected in the presence of zinc up to 400 μM, in clear contrast to reports for related enzymes. Previous studies revealed that the highest imipenem hydrolysis activity was observed when ImiS, CphA, or AsbM1 bind one equivalent of zinc and the activity of the enzyme decreases as the more zinc is added (CRAWFORD *et al.*, 2004; VALLADARES *et al.*, 1997; YANG and BUSH, 1996). Surprisingly, nitrocefinase activity increased (3.7 fold) with the increase in zinc concentration (Figure 5.7), due to increases in k_{cat} with little effect on K_M (Table 5.3). It was shown for CphA that added zinc did not influence the activity of the enzyme with nitrocefin as substrate (BEBRONE *et al.*, 2005) but an increase in activity was observed for some CphA mutants. These results, together with the substrate-dependent activity of Sfh-I in the presence of added zinc, reinforce the idea of a different mechanism for hydrolysis of imipenem and nitrocefin, as already suggested for CphA mutants (BEBRONE *et al.*, 2005; VANHOVE *et al.*, 2003). Although Sfh-I and CphA have the functional (active site) residues conserved, the two enzymes overall share just 50% identity, so the differences in activity described here can most likely be attributed to a combination of substitutions.

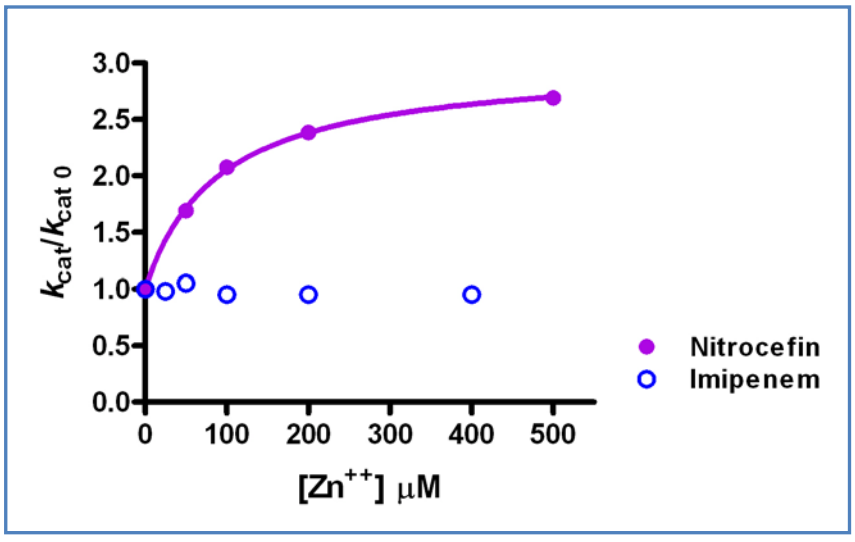

Figure 5.7 Effect of added zinc on k_{cat}/k_{cat0} (ratio of k_{cat} at a given zinc concentration to k_{cat0} determined in the absence of excess zinc) for hydrolysis of nitrocefin (filled circles) and imipenem (open circles). Solid line is a fit of nitrocefin data to Equation 5.1.

Table 5.3 Influence of added zinc on k_{cat} and K_M values of nitrocefin hydrolysis by Sfh-I.

Antibiotic	Added zinc (μM)	k_{cat} (s^{-1})	K_M (μM)	K_{d2} (μM)
Nitrocefin	0	0.13	250	90
	50	0.22	160	
	100	0.27	190	
	200	0.31	200	
	500	0.35	190	

To study the effect of added zinc on Sfh-I secondary structure and stability, circular dichroism (CD) wavelength scans and temperature melts were acquired (Figure 5.8).

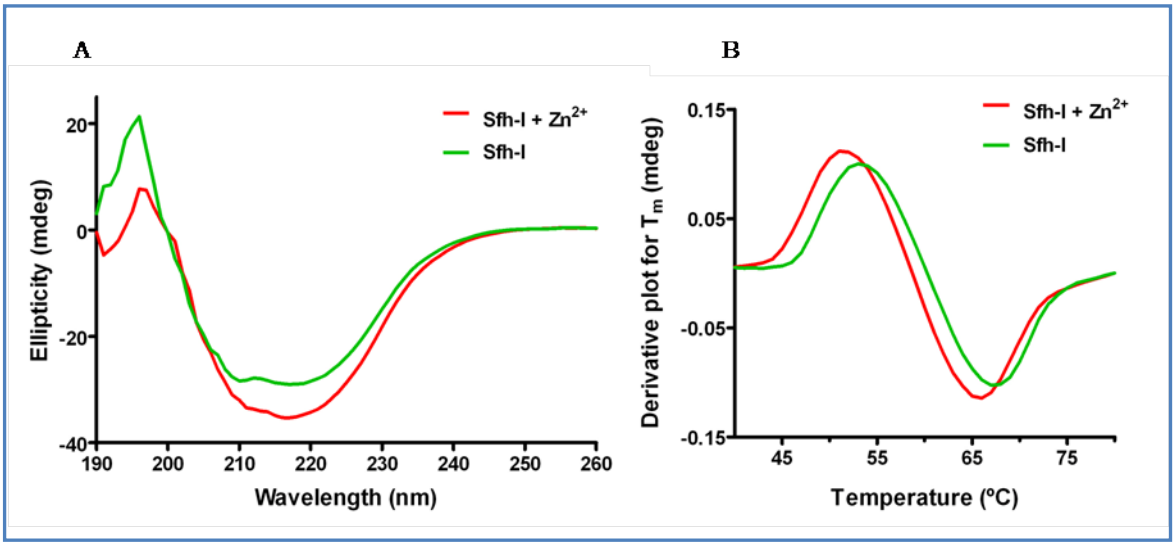

Figure 5.8 Effect of additional zinc on Sfh-I. A) Far-UV circular dichroism spectra of Sfh-I measured in the absence (green line) and presence (red line) of 1 mM Zn^{2+}. B) Second derivatives of plots of ellipticity at 220nm against temperature for thermal unfolding of Sfh-I in the absence (green line) and presence (red line) of 1 mM Zn^{2+}.

The CD spectra obtained for Sfh-I in the presence and absence of 1 mM Zn^{2+} reveals that the addition of zinc does not cause major structural rearrangements, inducing a small increase in Sfh-I secondary structure (Figure 5.8A). The thermal stability monitored by CD spectroscopy showed no significant difference between the midpoint for thermal unfolding of Sfh-I in the absence (60°C) and in the presence of additional Zn^{2+} (58°C) (Figure 5.8B), indicating that the addition of Zn^{2+} to the Sfh-I enzyme does not significantly affects its thermal stability.

5.3.6 Concluding remarks

We show here that Sfh-I is readily produced from recombinant *E. coli* and that the purified protein is a monozinc enzyme with a strong preference for carbapenem substrates. These properties confirm Sfh-I to be a member of the B2 MBL subgroup, previously known to contain only enzymes from *Aeromonas* spp.

Our kinetic characterisation, however, shows that Sfh-I differs significantly from CphA, the best characterised B2 MBL, in its activity towards a range of substrates including cephalosporins (cefepime) and sulbactam.

Fluorescence and activity measurements suggest that, while isolated as a predominantly monozinc enzyme, Sfh-I is able to bind up to three zinc ions with varying affinities, and that the effect of added zinc on enzyme activity is substrate-dependent. Further investigation of the recombinant enzyme is needed to establish the basis for these differences.

6. Structural characterisation of Sfh-I: mechanism for subclass B2 metallo-β-lactamases

6.1 Introduction

Class B β-lactamases are zinc-dependent enzymes that are also known as metallo-β-lactamases (MBLs) (CROWDER *et al.*, 2006)). These enzymes are able to inactivate almost all β-lactams, including the carbapenems, drugs of increasing importance in treatment of infections by multidrug resistant Gram-negative bacteria (MASTERTON, 2009), and are resistant to the clinical β-lactamase inhibitors (e.g. clavulanic acid, sulbactam) currently available. Despite the increasing importance of the MBLs, clinically useful inhibitors are not yet available.

MBLs are divided into subclasses B1, B2 and B3, based on their primary sequences, substrate specificity, and metal-ion requirement (GALLENI *et al.*, 2001). Subclasses B1 and B3 include the most extensively studied enzymes, display activity against a wide range of β-lactam substrates and generally bind two zinc ions (FELICI *et al.*, 1993), (SPENCER *et al.*, 2001). In these enzymes the binuclear zinc centre comprises a tetrahedral site (Zn1) with three histidine ligands (His116, His118, His196), and a five-coordinate site (Zn2) with cysteine (Cys221) – histidine (His263) - aspartate (Asp120; subclass B1) or histidine (His121) – histidine (His263) - aspartate (Asp120; B3) ligands. Coordination is completed by two water molecules, one bridging the two metal ions and the other situated in the Zn2 site (CROWDER *et al.*, 2006; WALSH *et al.*, 2005).

A number of crystal structures for representatives of subclasses B1 and B3 are currently available (CARFI *et al.*, 1995; CONCHA *et al.*, 2000; CONCHA *et al.*, 1996; MURPHY *et al.*, 2006; ULLAH *et al.*, 1998). In contrast, the best characterised representatives of subclass B2, CphA and ImiS from *Aeromonas* sp., efficiently hydrolyse carbapenems but have poor activity against penicillins and cephalosporins (FELICI *et al.*, 1993; WALSH *et al.*, 1996). These enzymes lack the Zn1 ligand His116 and are fully active with one bound zinc ion, located in the Zn2 (Cys – His – Asp) site, but are noncompetitively inhibited upon binding of a second zinc equivalent (CRAWFORD *et al.*, 2004; VALLADARES *et al.*, 1997).

Despite efforts to characterise B2 MBLs with regard to substrate specificity, zinc binding and catalytic mechanism, (WALSH *et al.*, 1996), (COSTELLO *et al.*, 2006), (BEBRONE *et al.*, 2008), (SHARMA *et al.*, 2006; SIMONA *et al.*, 2009; XU *et al.*, 2006), these remain the least studied MBLs. To date the only structures available for B2 MBLs are of CphA from *A. hydrophila*, including a CphA mutant in complex

with the hydrolysis product of the carbapenem biapenem (BEBRONE *et al.*, 2009; GARAU *et al.*, 2005). The mechanism of action of B2 MBLs is also incompletely understood (GARAU *et al.*, 2005; SHARMA *et al.*, 2006; SIMONA *et al.*, 2009; XU *et al.*, 2006).

Previously determined crystal structures (BEBRONE *et al.*, 2009; GARAU *et al.*, 2005) all contain small molecule ligands such as bicarbonate or sulphate and the origin and mechanism of activation of the water nucleophile essential to the hydrolytic reaction, and the identity of the proton donor to the β-lactam amide nitrogen, thus remain to be unambiguously established. Computational studies have proposed two possible candidates: His118 (SIMONA *et al.*, 2009) or Asp120 (XU *et al.*, 2006) for the general base that activates the nucleophilic water molecule in subclass B2 MBLs.

Sfh-I, a member of the B2 MBL subclass, was previously described. Sfh-I possesses 60% sequence identity to *A. hydrophila* CphA (mature polypeptides) and is specific to *Serratia fonticola* strain UTAD54 (SAAVEDRA *et al.*, 2003). Like previously characterised B2 MBLs, Sfh-I efficiently hydrolyses carbapenems but displays reduced activity against penicillins and cephalosporins (Chapter 5). However, Sfh-I also displays some distinctive properties when compared to other B2 enzymes, showing some hydrolytic activity against the cephalosporin cefepime and being only weakly inhibited by excess zinc in a substrate-dependent fashion (Chapter 5). Sfh-I is thus the most divergent member of the B2 MBL subgroup that has been identified to date.

This Chapter presents crystal structures of Sfh-I determined at two different resolutions in the presence and absence of a bound glycerol ligand. The glycerol complex structure results from attempts at ligand soaking. These data reveal, for the first time, the architecture of water molecules in the B2 MBL active site and strongly suggest that the catalytic water nucleophile is associated with His118, rather than the active site zinc ion or Asp120. Based on these results, a catalytic mechanism for B2 MBLs is offered.

6.2 Materials and methods

6.2.1 Purification and crystallisation

Wild-type Sfh-I was produced in *Escherichia coli* BL21 (DE3) cells harbouring the pSfh-Iv3 recombinant plasmid and purified by liquid chromatography as described in Chapter 5. Following purification protein fractions showing >99% purity by SDS–PAGE were concentrated by Amicon Ultra-15 spin concentrators with a molecular weight cut off (MWCO) of 10 kD, stored at 4ºC, and used in crystallisation trials. Purified Sfh-I was quantified spectroscopically by absorbance at 280 nm using a molar extinction coefficient of 35995 $M^{-1}cm^{-1}$ calculated from the amino acid composition using the method of Gill and von Hippel (1989) as implemented in the software Protean (Lasergene Software, DNAStar Inc.).

Initial crystallisation trials of native Sfh-I were performed by the sitting drop vapour diffusion method using Molecular Dimensions Structure screen I & II HT-96 (JANCARIK and KIM, 1991), JCSG-*plus* HT-96 and PACT *premier* screens (NEWMAN *et al.*, 2005). Drops were set up using a Phoenix liquid-handling system (Art Robbins Instruments) and 96-well MRC two well crystallisation plates (Hampton Research). Crystallisation drops consisted of 1 µL of both the protein, concentrated to 11 and 22 mg/mL, and reservoir solutions. Plates were sealed with ClearSeal Film™ (Hampton Research) and placed at 20ºC.

The initial crystallisation conditions were optimised in 24-well XRL crystallisation plates (Molecular Dimensions) using a gradient of PEG and salt concentration, by the hanging drop vapour diffusion method. The drops resulted from a 1:1 mixture of protein solution at 15 mg/mL and reservoir solution (1 µl each component). Samples were equilibrated against 500 µL of reservoir solution. Conditions derived from C3 (0.2 M ammonium nitrate, 20% polyethylene glycol (PEG) 3350) and H6 (0.1 M ammonium acetate, 0.1 M Bis Tris pH 5.5, 17% PEG 10000) were further refined using an Additive Screen (Molecular Dimensions) with protein concentrated to 15 mg/mL. The most promising crystals of Sfh-I were observed in drops consisting of 0.1 M ammonium nitrate and 25% PEG 3350 with several additives (calcium chloride, strontium chloride, dioxane, isopropanol) at a final concentration of 10%. Using these crystals higher quality crystals were obtained by streak seeding (Figure 6.1A).

The best crystals of native Sfh-I grew in 0.1 M ammonium nitrate, 3% v/v isopropanol, 25% w/v PEG 3350. Crystals appeared after 2-3 days at 20°C, in a variety of morphologies from flattened hexagonal rods to rhombohedral crystals.

Prior to data collection crystals were briefly soaked in reservoir solution supplemented with 30% v/v ethylene glycol as cryoprotectant and flash-cooled in liquid nitrogen.

Further screening was carried out with the aim of obtaining diffraction-quality crystals of Sfh-I in complex with excess zinc (1 mM), cefepime or cephalothin at different concentrations. This included co-crystallisation using commercial screens as above with substrate/zinc as additives, seeding to new drops containing the additive with additional refinement of some of the conditions and adding β-lactam powder to drops containing crystals. Although data sets from several crystals were collected, no complex was obtained. However, this screening established that superior crystals could be generated by mixing 2.5 µl of protein (15 mg/mL), 2 µL of reservoir solution (0.2 M sodium acetate, 27% w/v PEG 3350) and 0.5 µl 30% glycerol (Figure 6.1B) and equilibrating against a 500 µl reservoir in hanging-drop format in XRL crystallisation plates (Molecular Dimensions). 20% v/v PEG 400 was used as a cryoprotectant.

6.2.2 Data collection and crystallographic refinement

Diffraction data were collected at Diamond Light Source beamline IO4 and processed with HKL2000 (OTWINOWSKI and MINOR, 1997) (apo Sfh-I) or MOSFLM (LESLIE, 2006) and SCALA (EVANS, 2006) (glycerol complex) (Table 6.1) from the CCP4 program suite (COLLABORATIVE COMPUTATIONAL PROJECT, 1994). Structures were solved by molecular replacement using the programs AMoRe (NAVAZA, 2001) (apo Sfh-I) or PHASER (MCCOY *et al.*, 2007) (glycerol complex) and the three-dimensional structure of *A. hydrophila* CphA (GARAU *et al.*, 2005) (PDB ID 1X8G) as a search model.

Table 6.1 Data Collection Statistics[a]

	Native	**Glycerol complex**
X-ray Source	DIAMOND IO4	DIAMOND IO4
Wavelength (Å)	0.9529	0.9795
Data processing	HKL2000	MOSFLM/SCALA
Space group	P21	P21
Asymmetric unit	2 molecules	2 molecules
Cell dimensions		
a, b, c (Å)	a = 32.92 b = 72.17 c = 86.46	a = 32.83 b = 87.28 c = 72.57
α, β, γ (°)	β = 90.12º	β = 90.85º
Resolution (Å)	50 – 1.8 (1.86 – 1.8)	33.5 – 1.37 (1.45 – 1.37)
R_{merge}	0.076 (0.500)	0.056 (0.55)
No. reflections (total)	109 572 (9 549)	603 317 (84 447)
No. reflections (unique)	36 421 (3 537)	84 788 (12 336)
I / σI	13.2 (1.9)	18.0 (3.3)
Completeness (%)	97.3 (95.3)	99.8 (100)
Redundancy	3.0 (2.7)	7.1 (6.8)

*Values in parentheses are for the highest resolution shell.

Models were refined iteratively using positional refinement in REFMAC5 (MURSHUDOV *et al.*, 1997) followed by manual rebuilding into $2mF_o-dF_c$ electron density maps using the program COOT (EMSLEY *et al.*, 2010). Water molecules were added to the models at positions showing large positive peaks in F_o-F_c electron density. During iterative rebuilding residue geometries, van der Waals contacts and hydrogen bonds were monitored using the MOLPROBITY server (CHEN *et al.*, 2010). Statistics from structure refinement are shown in Table 6.2.

Table 6.2 Refinement Statistics[a]

	Native	Glycerol complex
Resolution (Å)	27.70 – 1.80 (1.847 – 1.800)	26.23 – 1.37 (1.41 – 1.37)
No. reflections	34 573 (2 482)	80 514 (5 932)
R_{work} / R_{free}	18.7/23.6 (23.5/33.8))	16.3/19.6 (26.5/30.2)
No. atoms		
Protein	3 662	3 878
Ligand/ion	2	14
Water	266	436
B-factors		
Protein	13.42	15.40
Ligand/ion	28.91	22.95
Water	19.50	27.02
R.m.s deviations		
Bond lengths (Å)	0.0128	0.0101
Bond angles (°)	1.338	1.322

[a]Values in parentheses are for the highest resolution shell.

6.2.3 Circular Dichroism (CD)

Circular dichroism (CD) spectroscopy was employed to compare the secondary structure, and the conformational stability of both Sfh-I and ImiS by increasing the temperature. ImiS is the *Aeromonas veronii* subclass B2 MBL, with a sequence 98% identical to that of CphA (differing at only seven amino acids) (WALSH *et al.*, 1998). ImiS was used as a comparator as an over-expressing construct was readily available.

ImiS was over-expressed and purified as previously reported (CRAWFORD *et al.*, 2004). Briefly, 4 x 1L flasks of LB containing 50 µg/mL kanamycin were inoculated with an overnight culture of *E. coli* BL21 DE3 containing the pET26b*imiS* plasmid and incubated at 37°C until an optical density of 0.6 was reached. At this point cell cultures were induced with 1 mM IPTG and allowed to grow at 37°C for 3

hours. Cells were collected by centrifugation (4000 rpm, 30 minutes at 4°C), resuspended in 40 mL of cold, 50 mM Tris 100 μM $ZnCl_2$, pH 7.0, and lysed by sonication followed by centrifugation (18000 rpm, 30 min at 4°C). The supernatant with protein solution was dialyzed overnight at 4°C *versus* 2 L of 50 mM Tris 100 μM $ZnCl_2$, pH 7.0. The dialyzed crude extract was centrifuged (18000 rpm, 30 min at 4°C) and the cleared supernatant was loaded onto a pre-equilibrated SP-Sepharose column with 50 mM Tris 100 μM $ZnCl_2$, pH 7.0. Elution was performed with a linear gradient of 0 to 50 mM NaCl in 50 mM Tris 100 μM $ZnCl_2$, pH 7.0. Fractions containing ImiS were identified by SDS-PAGE (bands of approximately 25 kDa), concentrated by Amicon Ultra-15 spin concentrators (MWCO of 10 kDa) and loaded onto a Superdex 75 gel filtration column. ImiS was eluted in 50 mM Tris, pH 7.0 and protein fractions were analysed by SDS-PAGE. ImiS fractions with purity greater than 95% were pooled and concentrated.

For CD studies, protein samples, both Sfh-I and ImiS, were dialyzed overnight at 4°C *versus* 1 L of 20 mM sodium phosphate pH 7.0 using Slide-A-Lyzer® Dialysis Cassettes (10K MWCO, Pierce). The concentration of ImiS was determined from absorbance at 280 nm using the extinction coefficient, $\Delta\varepsilon$ = 37250 $M^{-1}cm^{-1}$, estimated previously by Crawford and co-workers (2004).

CD spectra were recorded at 20°C on a Jasco J-815 CD spectropolarimeter using 8.5 μM protein in 20 mM sodium phosphate, pH 7.0. The wavelength range scanned was 260-190 nm. For each sample four spectra were collected and averaged. Baselines of phosphate buffer without protein were subtracted from the samples to yield the contribution of the protein component. Thermal stability spectra were measured at 220 nm with temperature stepwise increased from 20°C to 90°C at an interval of 5°C. Four scans were obtained for each sample and averaged.

6.2.4 Accession numbers

The coordinates and structure factors for the two Sfh-I structures have been deposited in the Protein Data Bank (PDB) with accession numbers 3Q42 (unliganded structure) and 3Q6V (glycerol complex).

6.3 Results and Discussion

6.3.1 Sfh-I overall structure

From the initial crystallisation trials of native Sfh-I using commercial screens, the most promising conditions, containing plate-like crystals or small crystals, were identified as conditions C3 (0.2 M ammonium nitrate, 20% w/v PEG 3350), H6 (0.1 M ammonium acetate, 0.1 M Bis Tris pH 5.5, 17% w/v PEG 10000), H7 (0.2 M ammonium sulphate, 0.1 M Bis Tris pH 5.5, 25% w/v PEG 3350) and H9 (0.2 M lithium sulphate, 0.1 M Bis Tris pH 5.5, 25% w/v PEG 3350) from JCSG-*plus* HT-96.

Upon optimisation of initial conditions, crystals of apo Sfh-I grew by hanging drop vapour diffusion from 15 mg/ml protein and 0.1 M ammonium nitrate, 25% (w/v) PEG3350 with isopropanol as additive (3% v/v). Streak seeding was employed to improve crystal quality for X-ray diffraction experiments (Figure 6.1A). Crystals grown in conditions such as 0.2 M sodium acetate, 27% (w/v) PEG 3350, 3% glycerol and 0.2 M lithium chloride, 0.1 M Hepes pH 7.0, 28% (w/v) PEG 3350 (Figure 6.1B and 6.1C) were also used to collect diffraction data. However, crystals recovered from the lithium chloride solution proved to be highly mosaic and these data were not used for the determination of the Sfh-I structure.

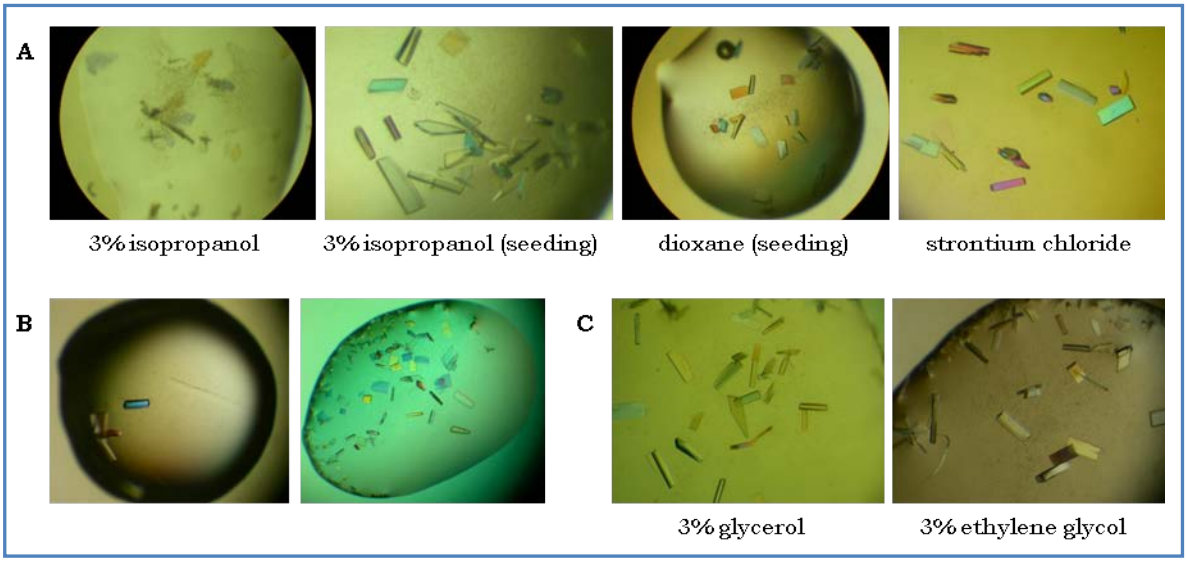

Figure 6.1 Crystals of native Sfh-I. **A.** Individual panels showing the effect of additives on Sfh-I crystallisation in 0.1 M ammonium nitrate, 25% (w/v) PEG3350. **B.** and **C.** Native crystals grown in 0.2 M sodium acetate, 27% (w/v) PEG 3350, 3% glycerol and in 0.2 M lithium chloride, 0.1 M Hepes pH 7.0, 28% (w/v) PEG 3350 with additives (glycerol and ethylene glycol), respectively.

Two crystal structures of recombinant Sfh-I were determined by molecular replacement, using the structure of *A. hydrophila* CphA (GARAU *et al.*, 2005) as a search model. An unliganded structure was obtained to a resolution of 1.8 Å, and a structure with glycerol bound in the active site to a resolution of 1.4 Å.

Both structures contain 228 amino acids (residues 41-304 using the BBL numbering system (GALLENI *et al.*, 2001)). The overall fold of Sfh-I (Figure 6.2) conforms to the αβ/βα sandwich structure characteristic of MBLs and related enzymes, with the active site located in a shallow cleft formed by the interface of the two β-sheets. The two Sfh-I structures are almost identical (root mean square deviation (r.m.s.d.) of 0.279 Å between Cα atoms for molecule A in the respective structures as determined using SSM (KRISSINEL and HENRICK, 2004)).

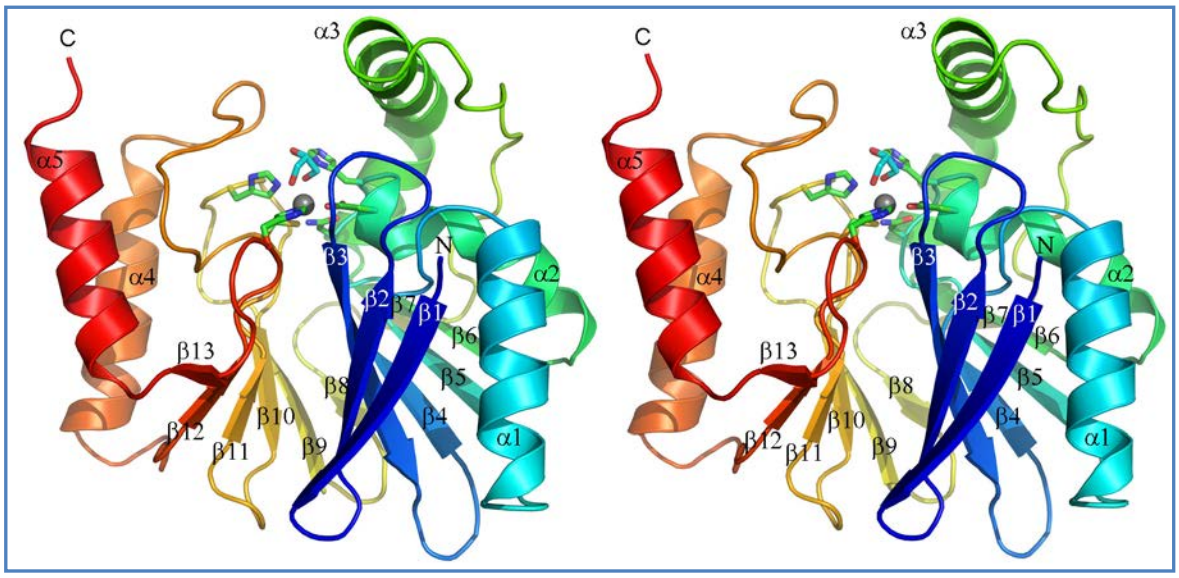

Figure 6.2 Stereo ribbon diagram of the Sfh-I structure (glycerol complex). The polypeptide chain is colour-ramped from N- (blue) to C- (red) terminus. Zinc ion is rendered as a grey sphere and zinc ligands shown as sticks (atom colours as standard, carbons in green). Bound glycerol is shown as a stick model with carbon atoms in cyan. This figure and Figures 6.3, 6.5 and 6.6A were generated using PyMol (DELANO, 2008).

Comparison with *A. hydrophila* CphA (Figure 6.3A) shows the two B2 MBL structures to be closely superimposable (Cα r.m.s.d. 0.646 Å) with the major difference between them the extended loop between helix α4 and strand β12 arising from the presence of a 4-amino acid insertion (BBL residues 254a-d) in the Sfh-I sequence relative to that of CphA.

The Sfh-I crystal structure, the second for a B2 MBL, thus confirms that the elongated and kinked α3 helix, and the absence of extended mobile loops between strands β2 and β3 (as in B1 MBLs) or between α3 and strand β7 (as in B3 MBLs) are likely to be general structural features that distinguish B2 MBLs from those of subclasses B1 and B3 (GARAU *et al.*, 2005).

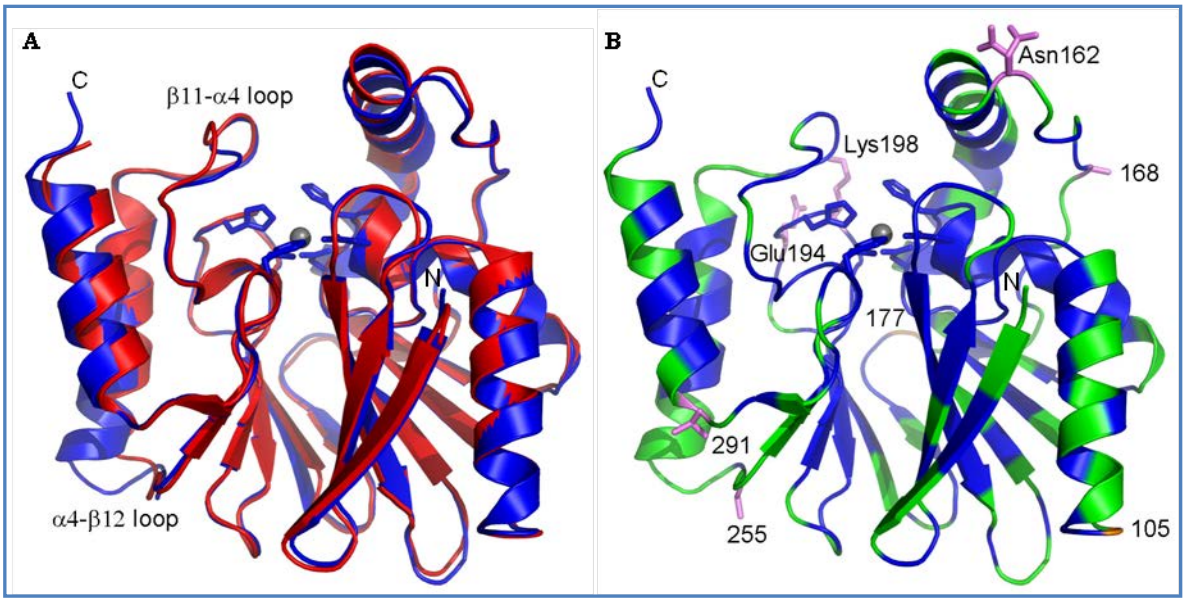

Figure 6.3 A. Overlay of Sfh-I (blue) and *A. hydrophila* CphA (red; pdb accession 1X8G) (GARAU *et al.*, 2005) structures. Positions of loops (β11–α4; α4–β12) whose conformations vary between the two structures are marked. **B.** Ribbon diagram of Sfh-I structure (blue) highlighting (green) positions of residues that differ between Sfh-I and CphA. Positions of alterations involving proline residues are numbered and coloured magenta (proline deletions in Sfh-I relative to CphA) or orange (proline insertions in Sfh-I relative to CphA). Proline substitutions in the vicinity of the Sfh-I active site (positions 162, 194 and 198) are labelled and depicted in stick form.

In CphA the conformation of the loop connecting β11 and α4 varies between the uncomplexed and biapenem-bound structures, enabling Asn233 to make H-bonding contacts with the C3 carboxylate of bound biapenem (GARAU *et al.*, 2005). In both of our Sfh-I structures this loop adopts the "closed" conformation associated with the biapenem-bound CphA structure, rather than that observed in the uncomplexed enzyme. However, in the unliganded structure the Asn233 side chain adopts either a dual conformation (molecule A of the 2 molecules in the asymmetric unit), or points away from, rather than towards, the zinc centre, indicating that some mobility at this position is required to permit interactions with bound β-lactam substrates.

Sfh-I, like other subclass B2 MBLs and unlike the enzymes of subclasses B1 and B3, displays a strong preference for carbapenem substrates and has only weak activity against β-lactams of other classes (e.g. penicillins and cephalosporins). However, Sfh-I has some limited activity against certain substrates, for example the cephalosporin cefepime, against which CphA is entirely inactive (Chapter 5). Accordingly, the positions where the Sfh-I and CphA sequences differ onto the Sfh-I structure were mapped in an effort to identify substitutions likely to affect the spectrum of activity of Sfh-I (Figure 6.3B). While the majority of the substitutions are in surface-exposed regions, such as α-helices 1, 2, 4 and 5 and at the ends of β-strands, that are not expected to influence catalytic activity, it is noticeable that Sfh-I contains 4 fewer proline residues than does CphA. In particular, two of these substitutions, CphA Pro194Glu and CphA Pro198Lys, are at positions that define a loop (linking strands β12 and β13) that bears the conserved active site residue His196; and the CphA Pro168Glu substitution is located at the end of the extended α3 helix.

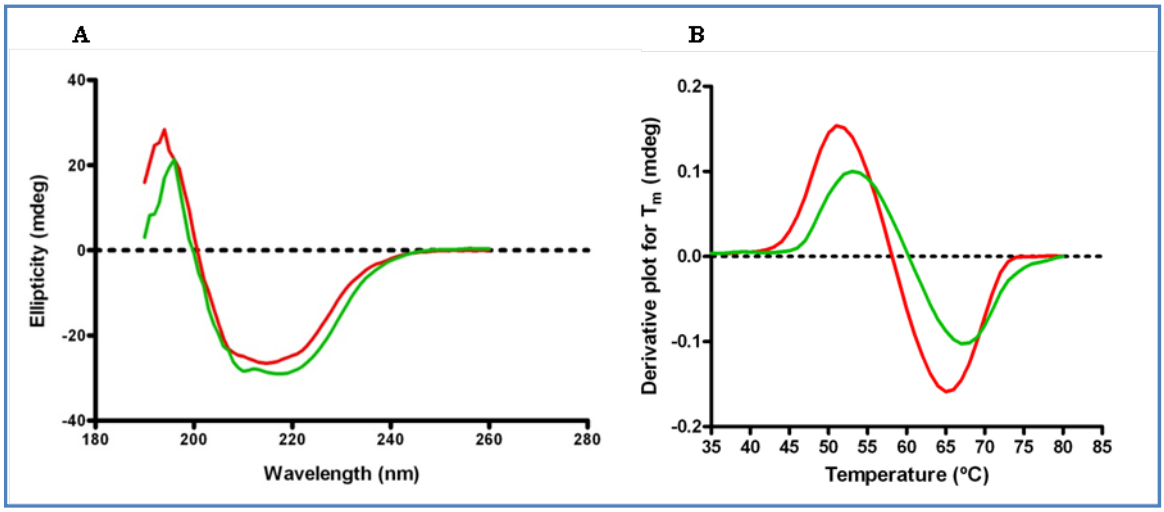

Figure 6.4 Circular dichroism (CD) spectroscopy of Sfh-I (green) and ImiS (red) **A.** CD spectra from 8.5 μM protein in 20 mM phosphate buffer, pH 7.0 at 20°C. **B.** Thermal unfolding of the metallo-β-lactamases by stepwise increasing the temperature, measured by CD at 222 nm.

It is possible that these substitutions may increase the flexibility of the Sfh-I active site with respect to that of CphA (or ImiS), potentially enabling it to adjust to accommodate some additional substrates. In order to explore possible collective impact of these substitutions on protein secondary structure and stability, circular

dichroism (CD) wavelength scans and temperature melts were carried out for Sfh-I and ImiS (Figure 6.4). The CD spectra produced for each of the purified enzymes were nearly superimposable (Figure 6.4A), revealing a very similar secondary structure. Moreover, the thermal stability monitored by CD spectroscopy indicated no significant difference between the midpoint for thermal unfolding of Sfh-I (60°C) compared to that of ImiS (58°C) (Figure 6.4B) or that reported for CphA (58.7°C; (BEBRONE *et al.*, 2009)), demonstrating that these substitutions do not impose a stability cost on the Sfh-I enzyme.

6.3.2 Active site

The active site of uncomplexed Sfh-I (Figure 6.5) contains a single zinc ion coordinated by the three conserved protein ligands: Asp120 (one oxygen; 1.98 Å, distances are for chain A), Cys221 (2.39 Å) and His263 (2.01 Å) that comprise the Zn2 site. Similar to CphA, but unlike the Zn2 sites of B1 or B3 MBLs, the Zn2 site adopts a tetrahedral, rather than trigonal bipyramidal, geometry. Coordination is completed by a single water molecule (Wat1; 2.24 Å) that occupies a similar position to the amide nitrogen (N1) of bound biapenem in the CphA complex structure; i.e. a location distinct from those of water molecules found in B1 or B3 MBL active sites.

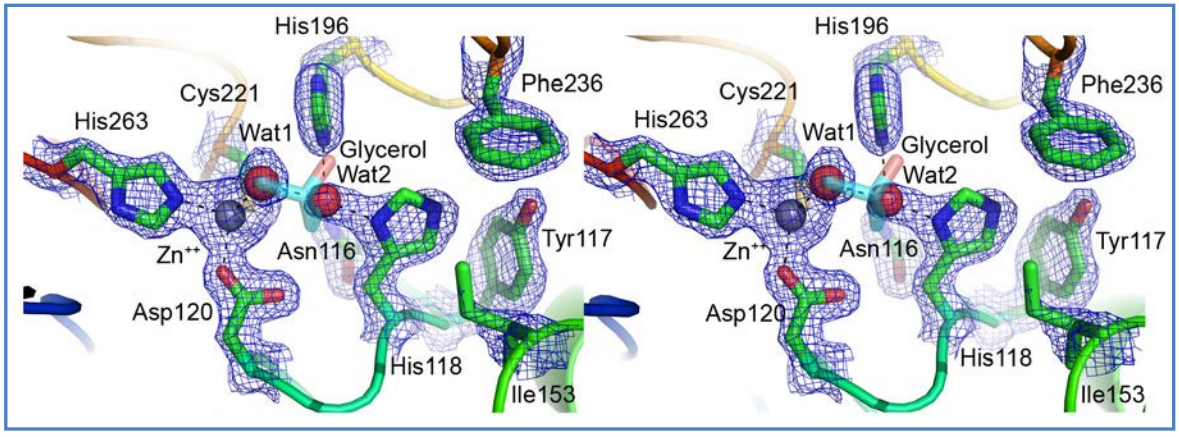

Figure 6.5 Stereo view of uncomplexed Sfh-I active site. Electron density shown is |2Fo|-|Fc|. ϕ_{calc}, contoured at 1.2σ. Zinc ion is rendered as a grey and water molecules as red spheres. Protein is colour-ramped from N- (blue) to C- (red) terminus; side chain atom colouring is as standard excepting carbon atoms are rendered in green. Hydrogen and coordination bonds are depicted as dashed lines. Bound glycerol, positioned by overlaying the complex structure, is rendered semitransparent with carbon atoms in cyan.

In common with other B2 MBLs, Sfh-I lacks the Zn1 ligand His116 and consequently binds a second zinc equivalent with greatly reduced affinity (Chapter 5). In Sfh-I structure the Zn1 site is instead occupied by a second water molecule (Wat2) that is tightly bound (2.00 Å) by His118 and makes weaker interactions with both His196 (2.50 Å) and Wat1 (2.52 Å). Importantly, Wat2 is comparatively far (3.82 Å) from the unbound oxygen of Asp120. In the complex structure, the positions of glycerol oxygen atoms superimpose upon those of Wat1 and Wat2 (Figure 6.5). Taken together, these two structures thus define two favoured positions for protein:ligand interactions in the Sfh-I active site.

6.3.3 Implications for catalytic mechanism

The catalytic mechanism of B2 MBLs has been the subject of considerable debate (GARAU *et al.*, 2005; SHARMA *et al.*, 2006; SIMONA *et al.*, 2009; XU *et al.*, 2006). Available CphA crystal structures (BEBRONE *et al.*, 2009; GARAU *et al.*, 2005) all contain small molecule ligands (biapenem, sulphate or bicarbonate), and the disposition of water molecules in the B2 active site, and thus the likely means by which the water nucleophile is activated, have consequently remained uncertain. The identification of bound water molecules in the Sfh-I active site therefore provides new insights into B2 MBL mechanism.

Previous crystal structures, including that of the CphA biapenem complex (GARAU *et al.*, 2005), and spectroscopic studies (SHARMA *et al.*, 2006) suggest interaction between Zn2 and the β-lactam amide nitrogen during the catalytic cycles of all MBL subclasses (GARRITY *et al.*, 2004; SPENCER *et al.*, 2005; TIONI *et al.*, 2008). These data indicate that Wat1 is displaced by substrate during the catalytic cycle and we thus consider Wat2 to be the most likely nucleophile. Computational studies have suggested that either Asp120 (XU *et al.*, 2006) or His118 (SIMONA *et al.*, 2009) may activate a water nucleophile (Wat2) located in the B2 Zn1 site. The location of Wat2 in the structure of metallo-β-lactamase Sfh-I strongly supports the proposal that His118 fulfils this function: Wat2 makes a tight interaction with His118 but a much weaker contact with Asp120.

Inspection of both the Sfh-I and CphA crystal structures further supports the idea that His118, while completely conserved across all three MBL subclasses, fulfils a different function in B2 MBLs (activating the hydrolytic water molecule) compared

to subclasses B1 and B3, where it is a Zn1 ligand. In B1 MBLs His118 is H-bonded to a conserved acidic residue (Asp or Glu) at position 236 (Figure 6.6A). In available crystal structures of B3 enzymes this interaction is maintained, although the sequence position of the interacting carboxylic acid varies. Such second shell interactions between histidine zinc ligands and aspartate or glutamate side chains have been proposed to promote catalysis by enzyme zinc centres through a range of effects that include enhancing the reactivity of the metal-bound hydroxide nucleophile (LIN *et al.*, 2005). By way of contrast, in the Sfh-I and CphA structures, the residue at position 236 is a phenylalanine, and the His118 side chain is not strongly H-bonded, but instead occupies a hydrophobic pocket formed by the side chains of Tyr117, Ile153 and Phe236 (Figure 6.6A).

By virtue of its tight association with His118, Wat2 is therefore part of an electron-rich environment that, we believe, will enhance its nucleophilicity. Additional interactions with Wat1 and with the His196 side chain will then serve to appropriately orient Wat2 for nucleophilic attack upon the carbonyl carbon of incoming β-lactam substrate.

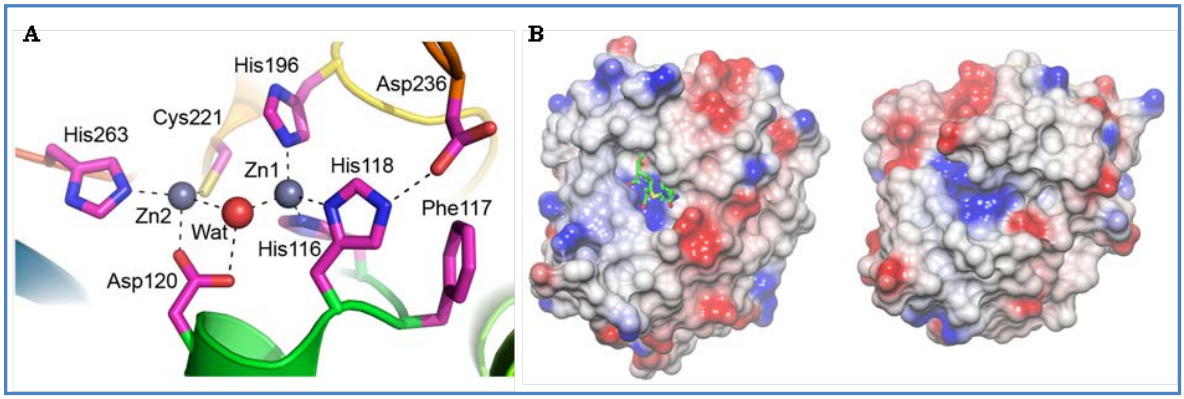

Figure 6.6 A. Active site of VIM-2 (GARCIA-SAEZ *et al.*, 2008) (PDB accession 1KO3) showing altered second shell ligands of His118. Protein is colour-ramped from N- (blue) to C- (red) terminus; side chain atom colouring is as standard excepting carbon atoms that are rendered in magenta. Hydrogen and coordination bonds are depicted as dashed lines. **B.** Molecular surfaces of uncomplexed Sfh-I (left) and VIM-2 (right) coloured by electrostatic potential. A molecule of meropenem (atom colours as standard; carbons in green) is manually placed in the Sfh-I structure to highlight the occluded Sfh-I active site. Figure 6.6B was generated using CCP4MG (POTTERTON *et al.*, 2004).

6.3.4 Proposed catalytic mechanism

Based upon these and previously published observations, a catalytic mechanism for Sfh-I and, by inference, for other B2 MBLs is therefore proposed (Scheme 6.1).

Scheme 6.1. Hydrolysis of the carbapenem meropenem by subclass B2 metallo-β-lactamases. Zinc: ligand interactions (omitted for clarity in lower panels) are shown as dotted lines.

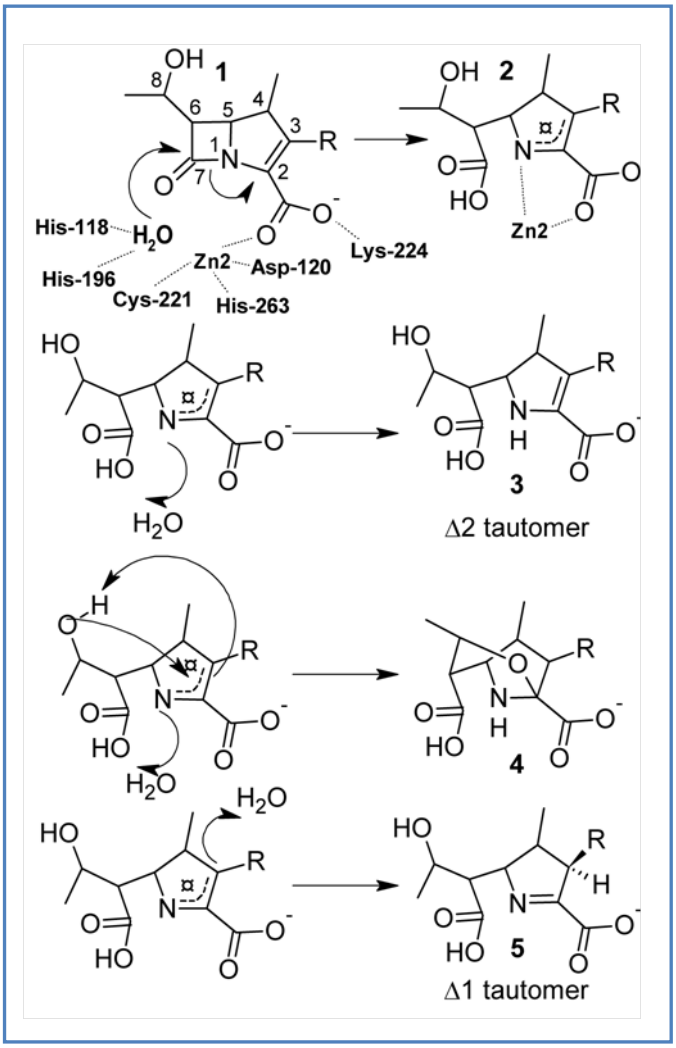

Incoming carbapenem substrate **1** displaces Wat1 from the Sfh-I active site to interact directly with the zinc ion through the C2 carboxylate group. The second carboxylate oxygen contacts the side chain of Lys224, as observed in the CphA:biapenem complex (GARAU *et al.*, 2005). Replacement of Lys224 by Thr decreases carbapenemase activity of the related ImiS enzyme (SHARMA *et al.*, 2006). This mode of binding positions Wat2, activated as described by contact with His118, to make a nucleophilic attack upon the carbonyl carbon of the β-lactam amide.

The consequent electronic rearrangement results in opening of the β-lactam ring and accumulation of negative charge in a delocalized system, comprising N1, C2 and C3, that is partially stabilized by proximity to the Sfh-I zinc centre. Stabilisation of anionic species **2**, generated upon fission of the β-lactam amide bond, by interaction with the metal ion in the MBL Zn2 site has been proposed to be important to MBL-catalysed hydrolysis of a

range of cephalosporin and carbapenem substrates (MCMANUS-MUNOZ and CROWDER, 1999; SPENCER *et al.*, 2005; TIONI *et al.*, 2008; WANG, Z. *et al.*, 1999). Freeze-quench EPR studies of meropenem hydrolysis by Co^{++}-substituted ImiS identified populated species with a 5 – co-ordinate metal centre, as proposed for this species, rather than the resting 4 – co-ordinate state (SHARMA *et al.*, 2006). This anionic species may then decay by up to three possible routes. Proton transfer to N1 from an incoming water molecule, most likely in the Wat2 position, will generate the expected hydrolysis product (Δ2 tautomer, **3**). An appropriately positioned water molecule, located very close to the Sfh-I Wat2 site, is observed in the CphA:biapenem complex (GARAU *et al.*, 2005). However, this structure also reveals hydrolysed biapenem to be present in an unanticipated cyclised form, suggesting that, for B2 MBLs, carbapenem hydrolysis may also involve an intramolecular rearrangement that requires abstraction of a proton from the C8 hydroxyl, its addition to C3, and subsequent attack of the nucleophile so generated upon C2 (**4**). Protonation at C3 could then also occur from an incoming water molecule, generating the hydrolysis product in the imine (Δ1) tautomer **5**. The role of zinc in B2 MBLs is then twofold: firstly binding substrate via interaction with the C2 carboxylate, and second in providing a means of stabilizing the negative charge that accumulates on N1 during and after cleavage of the β-lactam amide bond. In contrast to the binuclear enzymes of subclasses B1 and B3, the metal ion is not involved in activation of the water nucleophile.

Such a mechanism implies comparatively inefficient proton transfer to N1, a possible consequence of the occluded active site observed in the Sfh-I and CphA structures (Figure 6.6B), in which access of water molecules to the carbapenem-bound active site may be difficult. It would also predict that the anionic intermediate **2** can accumulate during carbapenem hydrolysis. Preliminary investigations of imipenem hydrolysis by Sfh-I under pre-steady-state conditions indeed indicate the existence of transiently populated intermediates during the catalytic cycle (Lisa, M.N. and Vila, A.J., personal communication).

The preference of Sfh-I, and other B2 MBLs, for carbapenem substrates then arises from a combination of factors- restricted access to the active site, likely to be particularly deleterious to binding of substrates with bulky substituents at the C6 (penicillin) or C7 (cephalosporin) positions; presence of the C2 = C3 double bond in carbapenems, enabling anionic species to be stabilized by conjugation as well as interaction with zinc; and the availability of the C8 hydroxyl group, permitting

resolution of the anionic intermediate **2** by intramolecular rearrangement, as in **4**. Limited activity, as is observed against some penicillin substrates, may be possible when some of these factors are absent, but only carbapenems satisfy all of these criteria. These are thus the preferred substrates for B2 MBLs.

6.3.4 Concluding remarks

The data presented here, from a divergent member of the B2 metallo-β-lactamase subclass, confirms that structural features such as the extended α3 helix and occluded active site cavity are likely to be common to this group of enzymes and distinguish them from other MBLs.

Most importantly, clear evidence is provided for an active site water molecule bound to His118, rather than Asp120, clarifying the means by which the nucleophile is activated for β-lactam hydrolysis in these enzymes.

In support of this contention it is shown that His118 occupies a distinct environment in B2 MBLs, consistent with a mechanistic function rather than a role as a zinc ligand. These results provide further evidence that B2 MBLs operate via a distinct catalytic mechanism and thus highlight the challenges associated with development of MBL inhibitors with activity against the full range of these enzymes.

7. General Discussion

7.1 Antibiotic resistance – the problem

Antibiotics have been successfully used since the 1940s and are essential drugs with which to treat patients who have infectious diseases. For the last 70 years antibiotic use has significantly reduced morbidity and mortality caused by infectious diseases. However, the wide and prolonged use of these drugs, initially seen as "magic bullets", promoted the evolution of the target infectious bacteria in order to overcome their action and make them ineffective (KUMARASAMY *et al.*, 2010; LIVERMORE, D., 2009). While some microorganisms are resistant to a single antibiotic or related class, others can develop resistance to several antibiotics. The later are known as multidrug resistant (MDR) strains (LIVERMORE, 2007). The continuing emergence, development and spread of drug-resistant pathogenic strains are a cause of increasing concern.

Antibiotic resistance is now one of the leading unresolved problems in public health whose consequences include high human and economic costs associated with the treatment of infectious diseases. Indeed, infections caused by drug-resistant strains require longer, resulting in potential spread of resistant microorganisms to others, and more expensive therapies, being associated with an increased risk of death (DE KRAKER *et al.*, 2011; NOSKIN *et al.*, 2005). Recently a study based on a sample of high-risk hospitalised adult patients, 13.5% of which had antibiotic resistant infections (ARIs), revealed that the medical cost attributable to ARIs ranged from $18,588 to $29,069 per patient, while the duration of hospital stay was extended by 6.4 to 12.7 days for affected patients (ROBERTS *et al.*, 2009). This study found that ARIs alone contribute to an excess mortality of 6.5 %, a death rate two times higher than in patients without ARIs. All together, these reports aim to be an alert for a better management of infections caused by antibiotic resistant strains and for an effective control and prevention of these infections.

However, bacteria resistant to several antibacterial agents now occur worldwide and are no longer limited to the nosocomial environment. Originally, most multidrug resistant pathogens emerged in hospitals, in which antibiotic use was prevalent, though antibiotic resistant strains are spreading and becoming more common in the community (DELEO *et al.*, 2010; ROONEY *et al.*, 2009). The widespread development of antibiotic resistance has weakened their value as treatments for bacterial infections. Moreover, there is paucity in the development of

new effective drugs, in particular against Gram-negative bacterial pathogens such as *A. baumannii* and *P. aeruginosa* (ABBANAT *et al.*, 2008). Since the 1990s, the number and effort of pharmaceutical companies conducting research to discover novel antimicrobials has decreased (PROJAN, 2003). This is possibly explained by the fact that antibacterial agents have a low rate of return on investment. Indeed, antibiotics are taken just for a few days/weeks, in comparison with other drugs that are used for life, they become useless after a while due to resistance, and also because it takes a long time and funds for a new drug to reach the market (PROJAN, 2003; SPELLBERG *et al.*, 2008).

7.2 Antibiotic resistance as a whole

As previously referred, bacteria resistant to multiple antibiotics represent a huge threat in the hospital setting and, consequently, the majority of the studies address the antibiotic resistance mechanisms of clinically important bacteria (PATERSON and BONOMO, 2005; RICE, 2009). Nonetheless these reports do not address the origin and sources of the resistance determinants that are of clinical significance at present. Moreover, it is clear that currently disseminated resistance mechanisms represent just a fraction of the total antibiotic resistance scenario.

A broader view of antibiotic resistance would involve all of the antibiotic resistance genes found in microorganisms, known as the resistome (WRIGHT, 2007). The resistome, a concept introduced by D'Costa *et al.* (2006), comprises not only resistance elements from pathogens but also those found in environmental organisms that are not usually associated with disease. It includes resistance genes from antibiotic-producing bacteria, and genes that are embedded in the bacterial chromosome and have some potential to have a role in resistance, termed cryptic genes. The resistome also comprises precursor genes encoding proteins with modest antibiotic resistance activity but that are able to evolve into effective resistance genes if the right selective pressure is applied (WRIGHT, 2007).

In recent years, several studies have drawn the attention of the scientific community to the fact that important resistance determinants that have emerged clinically are closely associated with mechanisms found in environmental organisms, whether antibiotic producers or not (ALLEN *et al.*, 2010; D'COSTA *et al.*, 2006;

DANTAS *et al.*, 2008). For example, β-lactam resistance by production of CTX-M β-lactamases is likely to have originated from environmental isolates of *Kluyvera* spp. (HUMENIUK *et al.*, 2002; POIREL *et al.*, 2002), while water-borne *Shewanella algae* and *Vibrionacea* species are the potential progenitors of the *qnr* quinolone resistance determinants, encoding proteins that protect DNA gyrase and topoisomerase IV from the inhibitory activity of quinolones (CATTOIR *et al.*, 2007; POIREL *et al.*, 2005). These reports show that it is essential to expand research into antibiotic resistance to include nonpathogenic organisms. Thus, an integrated view of resistance determinants may help researchers to better understand the evolution of antibiotic resistance and predict new resistance mechanisms prior to their emergence clinically (MARTINEZ, 2009; WRIGHT, 2010). The knowledge obtained can therefore be used to develop new therapeutic strategies to fight resistance before it reaches pathogenic bacteria (MARTINEZ, 2009; WRIGHT, 2010).

7.3 Study of carbapenemases from *S. fonticola* UTAD54

The overall purpose of this dissertation was to study the biochemical properties, and determine the structures of carbapenemases expressed by *Serratia fonticola* UTAD54, a naturally-occurring strain isolated from untreated drinking waters in the Northeastern Portugal. Previous studies have shown that carbapenem-resistant *S. fonticola* UTAD54 possesses chromosomal genes encoding two carbapenem-hydrolyzing β-lactamases, a class A enzyme and a subclass B2 metallo-protein (HENRIQUES *et al.*, 2004; SAAVEDRA *et al.*, 2003). These genes are absent from other *S. fonticola* strains and are phylogenetically distant from previously characterised related β-lactamases (HENRIQUES *et al.*, 2004; SAAVEDRA *et al.*, 2003). Carbapenems are the most powerful class of β-lactams and have a broad spectrum of activity against Gram-negative opportunist pathogens including both the Enterobacteriaceae and non-fermenting species such as *P. aeruginosa* and *A. baumannii* (BAUGHMAN, 2009). The spread of resistance to other antibiotics, including penicillins and cephalosporins, in these species, has severally reduced treatment options for these patients (LIVERMORE, D., 2009; MASTERTON, 2009). Therefore, *S. fonticola* UTAD54 is a potential source of new resistance mechanisms to antibiotics that are clinically used as last resort treatments for serious infections by Gram-negative organisms. Moreover, there is evidence that the carbapenem

resistance gene *bla*$_{Sfh-I}$ encoded on the chromosome of *S. fonticola* UTAD54 is embedded in mobile genetic elements (I Henriques and A. Correia, unpublished results), potentially enabling its dissemination into other bacteria.

In order to overcome resistance to β-lactam antibiotics it is fundamental to understand in detail the mechanisms of resistance and the mechanism of action of β-lactamases, so that new effective drugs and/or inhibitors can be developed. The results here presented can be seen as part of this global approach. This work is divided in two independent parts, each concerning the study of a carbapenemase from *S. fonticola* UTAD54. Thus, in the discussion I will consider each of these enzymes in turn.

7.3.1 SFC-1, an Ambler class A carbapenemase

SFC-1 is a Bush subgroup 2f β-lactamase that has been shown to be active against penicillins, cephalothin, and aztreonam with reduced susceptibility to the carbapenems meropenem and imipenem, and to be inhibited by clinically used inhibitors (HENRIQUES *et al.*, 2004). Although this resistance profile is typical for class A carbapenem-hydrolysing β-lactamases, the kinetic characterisation of SFC-1 revealed that this enzyme exhibits unique properties.

In this work it was shown that for SFC-1 the turnover rates for ceftazidime and cefoxitin are higher than those reported for IMI-1 and KPC-2. Previous studies have shown that a threonine at position 237, as displayed by SFC-1 and KPC, is involved in broadening the activity of class A carbapenemases to include extended-spectrum cephalosporins (MAJIDUDDIN and PALZKILL, 2005; SOUGAKOFF *et al.*, 1999). Additionally, a second substitution present in SFC-1 and KPC amino acid sequences but absent in the remaining enzymes of subgroup 2f, an Ala240Val mutation can also explain the increased activity against the extended-spectrum cephalosporins, as suggested for the ESBL TEM-149 (PERILLI *et al.*, 2008). Nonetheless, more studies are required to validate these hypotheses in SFC-1.

This study of SFC-1 also demonstrated that although this enzyme is inhibited by the typical class A β-lactamase inhibitors, the inhibition is weak (IC_{50} higher than 1 μM) when compared to carbapenemases IMI-1 and KPC (RASMUSSEN *et al.*, 1996; YIGIT *et al.*, 2001). These results show that SFC-1 is a class A β-lactamase with a

very broad substrate profile, able to hydrolyse carbapenems and extended-spectrum cephalosporins with reduced susceptibility to available β-lactamase inhibitors. Although the genetic context of bla_{SFC-1} does not include mobile genetic elements, unpublished results reveal a close proximity (within 10 Kb) of the bla_{SFC-1} and bla_{Sfh-I} genes on the chromosome of *S. fonticola* UTAD54. Therefore we cannot rule out the possibility that both genes are associated to mobile genetic elements. Moreover, these genes were found in *S. fonticola* UTAD54 (HENRIQUES *et al.,* 2004) but not in related strains, further supporting an exogenous origin.

Despite the availability of crystal structures for several class A carbapenemases (KE *et al.*, 2007; SOUGAKOFF *et al.*, 2002; SWARÉN *et al.*, 1998), the structural basis for β-lactam resistance mediated by these enzymes remains elusive. In an attempt to attain more information on the interaction between β-lactamases and β-lactams, especially carbapenems, crystal structures of the carbapenemase SFC-1, the acylation-deficient S70A mutant and the deacylation-deficient E166A mutant in complex with the carbapenem meropenem, were solved during this work. As reported for other class A carbapenemases, the structure of native SFC-1 is very similar to those of class A β-lactamases, such as TEM-1 (STEC *et al.*, 2005) and SHV-1 (KUZIN *et al.*, 1999), but with the disulphide bridge between Cys69 and Cys238 that distinguishes class A carbapenemases (WALTHER-RASMUSSEN and HOIBY, 2007). The structure of wild-type SFC-1 alone does not offer a clear explanation for its broad spectrum of activity. However, the presence of a proline residue at position 104 and the orientation of His105 may contribute to the expansion of the catalytic cavity. The opened cavity can then accommodate the bulky side chains of extended-spectrum cephalosporins, avoiding steric constraints that could arise from bulkier or more flexible residues at positions 104 and 105 (BETHEL *et al.*, 2006; DOUCET *et al.*, 2004). A study concerning the role of the residue at position 104 in SHV supports these results, providing indication that the Asp104Pro substitution increases β-lactam resistance, according to reported MIC values (BETHEL *et al.*, 2006). However, in a similar investigation using β-lactamase SME-1, the Tyr104Pro mutant only maintained high levels of resistance to imipenem, exhibiting a decrease in resistance to ampicillin and, to a lesser extent, cefotaxime (MAJIDUDDIN and PALZKILL, 2005). These studies demonstrate that is difficult to assign substrate specificity in many β-lactamases to a single position, and most

likely this property results from the interaction of several residues and its influence in the active site of these enzymes.

The X-ray crystal structure of the SFC-1 S70A mutant in complex with meropenem has shown that the β-lactam carbonyl oxygen of the substrate is completely bound in the oxyanion hole, a result that clearly differs from earlier observations of other class A β-lactamases (MAVEYRAUD *et al.*, 1998; NUKAGA *et al.*, 2008). It was also observed that bound meropenem establishes contacts with the amide nitrogens of Thr237 and Ala70, and Ser130 is close to the meropenem amide nitrogen, consistent with a role in the protonation of the β-lactam nitrogen.

The structure of the E166A acylenzyme shows that a number of modifications occur upon acylation of the SFC-1 β-lactamase. Among these are: the positioning of the β-lactam ring carbonyl oxygen in close proximity to the amide nitrogens of both Ser70 and Thr237, the substrate carboxylate is nearer to the side chain hydroxyls of Thr237 and Thr235 than in the substrate complex, while the hydrogen bond between the meropenem carboxylate and Ser130 is missing. Also, the 6α-hydroxyethyl substituent of meropenem is rotated and no longer interacts with the catalytic water molecule, a result that distinguishes the acylenzyme of SFC-1 from carbapenem acylenzymes of TEM-1 and SHV-1 (MAVEYRAUD *et al.*, 1998; NUKAGA *et al.*, 2008). In the later enzymes, the 6α-hydroxyethyl carbapenem substituent is hydrogen bonded to the hydrolytic water, possibly explaining the longevity of carbapenem acylenzymes in the active sites of these β-lactamases.

Another important observation, arising from the structures of SFC-1, refers to the position adopted by Ser130 in class A carbapenemases. In TEM-1 and SHV-1, both non-carbapenemases, Ser130 is reoriented in the presence of the substrate, pointing its hydroxyl group towards the amino group of Lys234 instead of Lys73, as seen in the apo structure (MAVEYRAUD *et al.*, 1998; NUKAGA *et al.*, 2008). By contrast, in SFC-1 the Ser130 hydroxyl assumes the same position as in the apo structures of other class A β-lactamases. This arrangement allows interaction with Lys73 and Lys234, as well as the amide nitrogen (N4) of meropenem in the SFC-1 acylenzyme, suggesting that Ser130 also helps to position meropenem in a favorable orientation for deacylation. A close interaction of the acylenzyme amide nitrogen with Ser130 may also prevent tautomerisation to the less reactive imine (delta-1 tautomer) form.

7.3.2 Sfh-I, a subclass B2 metallo-β-lactamase

Sfh-I is the first subgroup B2 metallo-β-lactamase to be identified in a genus other than *Aeromonas*. The gene coding for Sfh-I is present on the chromosome of *S. fonticola* UTAD54 (SAAVEDRA *et al.*, 2003). However unpublished results from our group (I. Henriques and A. Correia, personal communication) provide evidence that $bla_{Sfh\text{-}I}$ is flanked by transposable elements, suggesting a potential horizontal transfer of this genetic determinant from/into other isolates in the environment.

In this work it was demonstrated that Sfh-I, like CphA and ImiS, has a preference for carbapenem substrates and displays high activity when coordinating one equivalent of Zn(II) (Chapter 5). Other groups of metallo-β-lactamases have a broad substrate profile but require two Zn(II) ions for optimal activity (CROWDER *et al.*, 2006).

Previous studies have shown that B2 MBLs are able to bind a second zinc ion, but their enzymatic activity is noncompetitively inhibited in this situation (CRAWFORD *et al.*, 2004; VALLADARES *et al.*, 1997). Sfh-I, however, is revealed to be a singular B2 MBL that exhibits a substrate-dependent behaviour upon binding of a second zinc ion (Chapter 5). No inhibition was detected when a good substrate (imipenem) was assayed, but nitrocefinase activity increased in the presence of a second zinc ion. Bebrone *et al.*, (2005) reported no influence of added zinc on CphA activity when nitrocefin was used as substrate. In this investigation a CphA mutant, N116H/N220G, was engineered, whose di-zinc form is more active against nitrocefin (among other β-lactam antibiotics) than the mono-zinc form. With imipenem the activity decreases by binding of a second zinc ion (BEBRONE *et al.*, 2005). A similar result has been observed for the CphA mutant N116H (VANHOVE *et al.*, 2003). Based on these results the authors proposed that a slightly different mechanism would be used by these mutants to hydrolyse carbapenem, and some cephalosporin, substrates (BEBRONE *et al.*, 2005). Our results on the effect of added zinc on Sfh-I activity thus emphasize the divergence between this enzyme and previously characterised B2 MBLs. Another distinctive property of Sfh-I is its ability to hydrolyse cefepime (Chapter 5), a fourth generation cephalosporin displaying enhanced *in vitro* activity against Gram-positive pathogens, along with Gram-negative bacteria producing ESBLs (SADER *et al.*, 2005). To our knowledge, this is the first description of cefepime hydrolysis by a subgroup B2 MBL; this

cephalosporin was not recognised as a substrate by CphA (FELICI and AMICOSANTE, 1995).

The studies conducted along this dissertation provided evidence that Sfh-I binds up to three zinc ions if enough zinc is added to the enzyme's milieu (Chapter 5), although the binding affinities for the different zinc ions vary hugely. We were unable to determine the binding affinity for the first zinc ion but we believe it to be high, as reported for related enzymes (VALLADARES *et al.*, 1997) and evidenced by its high occupancy in our crystal structures. However, the second zinc binds with an affinity (K_{d2}) similar to that reported for CphA (VALLADARES *et al.*, 1997). Sfh-I binds a third zinc equivalent but very loosely (K_{d3} > 1 mM), and we consider this metal ion unlikely to play a role in the enzyme's activity. This result is in agreement with the crystal structure of CphA determined in the presence of excess zinc, where a third zinc ion was observed on the surface of the protein, away from the catalytic cavity (BEBRONE *et al.*, 2009).

To understand how β-lactams are hydrolysed by metallo-β-lactamases and hence make possible the design of new β-lactams, and/or inhibitors with decreased susceptibility to these enzymes, it is essential to determine the exact molecular mechanism that underlies the turnover of most β-lactams.

Mechanistic and structural data is particularly scarce for subclass B2 metallo-β-lactamases. Until now, the only crystal structures available for a B2 MBL are of CphA from *A. hydrophila* containing small molecules in the active site (BEBRONE *et al.*, 2009; GARAU *et al.*, 2005). No unliganded structure is accessible for subclass B2 MBLs. Moreover, there is no consensus about the catalytic mechanism employed by these enzymes, although crystallographic (GARAU *et al.*, 2005), spectroscopic (SHARMA *et al.*, 2006) and molecular modelling (SIMONA *et al.*, 2009; XU *et al.*, 2006) studies addressed this subject. The most important issue to be unambiguously clarified refers to the identity of the general base responsible for the activation of nucleophilic water, proposed to be either Asp120 (XU *et al.*, 2006) or His118 (SIMONA *et al.*, 2009).

In this work, the crystal structure of Sfh-I from *S. fonticola* UTAD54 was solved. The overall fold was shown to be very similar to the previously determined structure of CphA from *A. hydrophila* (Chapter 6). The structure of Sfh-I is the first for an unliganded subclass B2 MBL, explicitly revealing the position of two water molecules in the active site. In the Sfh-I structure, the fourth zinc ligand is a water

molecule (Wat1) in contrast with the CphA structure where a carbonate ion occupies this position (GARAU *et al.*, 2005). The involvement of a second water molecule (Wat2) in the catalytic mechanism of CphA was previously predicted by computational methods (SIMONA *et al.*, 2009). However, no structural data to support this calculation was available. The observed bound water molecules in the Sfh-I active site-pocket thus provide new insights into the catalytic mechanism of subclass B2 MBLs. In fact, the structural data obtained on Sfh-I, suggest Wat2 to be the most likely nucleophile. Wat2 is positioned closer to His118 when compared to Asp120, the strongest candidates to act as the general base, and therefore, it is proposed that Wat2 is activated by His118, rather than by Asp120 as has been suggested for CphA (XU *et al.*, 2006).

7.4 Conclusions

The work developed and described along this dissertation, through characterisation of the unique β-lactamases SFC-1 and Sfh-I found in *S. fonticola* UTAD54, provides new information on the interaction and hydrolysis of β-lactam antibiotics by Ambler class A carbapenemases and subclass B2 metallo-β-lactamases. The main conclusions that can be extracted from the study here presented are as follows:

1. As expressed in *E. coli*, SFC-1 is an enzyme with a very broad substrate profile, including penicillins, oxyimino-cephalosporins (ceftazidime and cefotaxime), cephamycins (cefoxitin), carbapenems (imipenem, meropenem) and the β-lactamase inhibitors (clavulanic acid, sulbactam and tazobactam);
2. When compared to other class A carbapenemases, SFC-1 is more resistant to extended-spectrum cephalosporins and β-lactamase inhibitors;
3. The crystal structure of SFC-1 reveals an overall fold that is essentially identical to those of other class A β-lactamases;
4. The determination of atomic resolution structures of SFC-1 point mutants in complex with bound meropenem provided, for the first time,

information on the recognition and hydrolysis of carbapenems by class A carbapenemases;

5. Recombinant Sfh-I produced from *E. coli* is a mono-zinc subclass B2 MBL with a strong preference for carbapenem substrates, that is typical of such enzymes. Nonetheless, Sfh-I is able to hydrolyse cefepime and sulbactam, substrates not recognised by related enzymes;

6. In the presence of added zinc Sfh-I was shown to behave differently from previously characterised B2 MBLs, since Sfh-I carbapenemase activity was not inhibited by elevated zinc concentrations;

7. Despite the unique properties revealed by the kinetic characterisation of Sfh-I, the structure of this enzyme closely resembles that of CphA from *A. hydrophila.* Thus the differences in specificity exhibited by Sfh-I cannot be inferred from the structure alone;

8. Of most importance, the structure of Sfh-I, the first for an unliganded B2 MBL, provides important information on the catalytic mechanism of these enzymes, for example the identity of the nucleophile species (Wat2) and the way it is activated (His118).

7.5 Future studies

The overall goal of this project was to characterise the carbapenem-hydrolysing β-lactamases SFC-1 and Sfh-I from *S. fonticola* UTAD54. To continue pursuit of these objectives, further studies are suggested.

In the work presented here, it was not possible to offer a clear explanation for the increased activity against oxyimino-cephalosporins, and the inhibitor resistance, displayed by SFC-1, when compared to other class A carbapenemases. To address this question it would be interesting to use site-directed mutagenesis, targeting residues at positions 237 and 240. Positions 237 and 240 are suggested to be involved in the activity of KPCs and TEM-149 against oxyimino-cephalosporins (PAPP-WALLACE *et al.*, 2010b; PERILLI *et al.*, 2008), respectively, while Thr at position 237 is also thought to play a role in inhibitor resistance in KPC (PAPP-WALLACE *et al.*, 2010b). Protein crystallography can also be used to unravel how

SFC-1 and related β-lactamases (e.g. KPCs) hydrolyse extended-spectrum cephalosporins.

This project also raises a number of questions regarding the activity of Sfh-I. For example, the mechanism of inactivation of Sfh-I by cephalothin remains to be fully elucidated. Despite several attempts to co-crystallise Sfh-I with cephalothin, and the use of mass spectrometry in attempts to identify the modified peptide, no conclusive answer was obtained. The interaction between Sfh-I and cephalothin can also be examined by molecular modelling methods using the structure of Sfh-I. The same techniques can be used to describe the hydrolysis of cefepime by Sfh-I MBL.

Further investigations to understand the effect of added zinc on the carbapenemase activity of Sfh-I are required. As crystals of Sfh-I in the presence of a high concentration of zinc proved to be difficult to obtain, the information about the metal binding sites can be achieved using spectroscopic techniques such as EXAFS (COSTELLO *et al.*, 2006; CRAWFORD *et al.*, 2005).

8. References

ABBANAT, D., MORROW, B., and BUSH, K. (2008). New agents in development for the treatment of bacterial infections. Current Opinion in Pharmacology. Vol. 8 (5), p. 582-592. DOI: 10.1016/j.coph.2008.08.001.

ABRAHAM, E., and CHAIN, E. (1940). An enzyme from bacteria able to destroy penicillin. Nature. Vol. 146 (3713), p. 837. DOI: 10.1038/146837a0.

ADACHI, H., OHTA, T., and MATSUZAWA, H. (1991). Site-directed mutants, at position 166, of RTEM-1 β-lactamase that form a stable acyl-enzyme intermediate with penicillin. Journal of Biological Chemistry. Vol. 266 (5), p. 3186-3191.

ALLEN, H. K., DONATO, J., WANG, H. H., CLOUD-HANSEN, K. A., DAVIES, J., and HANDELSMAN, J. (2010). Call of the wild: antibiotic resistance genes in natural environments. Nat Rev Microbiol. Vol. 8 (4), p. 251-259. DOI: 10.1038/nrmicro2312.

AMBLER, R. P. (1980). The structure of β-lactamases. Philos Trans R Soc Lond B Biol Sci. Vol. 289 (1036), p. 321-331. DOI: 10.1098/rstb.1980.0049

AMBLER, R. P., COULSON, A. F., FRERE, J. M., GHUYSEN, J. M., JORIS, B., FORSMAN, M., LEVESQUE, R. C., TIRABY, G., and WALEY, S. G. (1991). A standard numbering scheme for the class A β-lactamases. Biochem J. Vol. 276 (Pt 1), p. 269-270.

AUBRON, C., POIREL, L., ASH, R. J., and NORDMANN, P. (2005). Carbapenemase-producing Enterobacteriaceae, U.S. rivers. Emerg Infect Dis. Vol. 11 (2), p. 260-264.

BADARAU, A., LLINAS, A., LAWS, A. P., DAMBLON, C., and PAGE, M. I. (2005). Inhibitors of metallo-β-lactamase generated from β-lactam antibiotics. Biochemistry. Vol. 44 (24), p. 8578-8589. DOI: 10.1021/bi050302j.

BANEYX, F., and MUJACIC, M. (2004). Recombinant protein folding and misfolding in *Escherichia coli*. Nat Biotech. Vol. 22 (11), p. 1399-1408. DOI: 10.1038/nbt1029.

BARBER, M. (1947). Staphylococcal infection due to penicillin-resistant strains. Br Med J. Vol. 2 (4534), p. 863-865.

BAUGHMAN, R. P. (2009). The use of carbapenems in the treatment of serious infections. J Intensive Care Med. Vol. 24 (4), p. 230-241. DOI: 10.1177/0885066609335660.

BAYLES, K. W. (2000). The bactericidal action of penicillin: new clues to an unsolved mystery. Trends in Microbiology. Vol. 8 (6), p. 274-278. DOI: 10.1016/S0966-842X(00)01762-5.

BEADLE, B. M., and SHOICHET, B. K. (2002). Structural Basis for Imipenem Inhibition of Class C β-Lactamases. Antimicrob. Agents Chemother. Vol. 46 (12), p. 3978-3980. DOI: 10.1128/aac.46.12.3978-3980.2002.

BEBEAR, C. M., and PEREYRE, S. (2005). Mechanisms of Drug Resistance in *Mycoplasma pneumoniae*. Current Drug Targets - Infectious Disorders. Vol. 5 (3), p. 263-271.

BEBRONE, C. (2007). Metallo-β-lactamases (classification, activity, genetic organization, structure, zinc coordination) and their superfamily. Biochem Pharmacol. Vol. 74 (12), p. 1686-1701. DOI: 10.1016/j.bcp.2007.05.021.

BEBRONE, C., ANNE, C., DE VRIENDT, K., DEVREESE, B., ROSSOLINI, G. M., VAN BEEUMEN, J., FRERE, J. M., and GALLENI, M. (2005). Dramatic broadening of the substrate profile of the *Aeromonas hydrophila* CphA metallo-β-lactamase by site-directed mutagenesis. J Biol Chem. Vol. 280 (31), p. 28195-28202. DOI: 10.1074/jbc.M414052200.

BEBRONE, C., ANNE, C., KERFF, F., GARAU, G., DE VRIENDT, K., LANTIN, R., DEVREESE, B., VAN BEEUMEN, J., DIDEBERG, O., FRERE, J. M*., et al.* (2008). Mutational analysis of the zinc- and substrate-binding sites in the CphA metallo-β-lactamase from *Aeromonas hydrophila*. Biochem J. Vol. 414 (1), p. 151-159. DOI: 10.1042/BJ20080375.

BEBRONE, C., DELBRUCK, H., KUPPER, M. B., SCHLOMER, P., WILLMANN, C., FRERE, J. M., FISCHER, R., GALLENI, M., and HOFFMANN, K. M. (2009). The structure of the dizinc subclass B2 metallo-β-lactamase CphA reveals that the second inhibitory zinc ion binds in the histidine site. Antimicrob Agents Chemother. Vol. 53 (10), p. 4464-4471. DOI: 10.1128/AAC.00288-09.

BELLAIS, S., AUBERT, D., NAAS, T., and NORDMANN, P. (2000). Molecular and Biochemical Heterogeneity of Class B Carbapenem-Hydrolyzing β-Lactamases in *Chryseobacterium meningosepticum*. Antimicrob. Agents Chemother. Vol. 44 (7), p. 1878-1886. DOI: 10.1128/aac.44.7.1878-1886.2000.

BENNETT, P. M. (2008). Plasmid encoded antibiotic resistance: acquisition and transfer of antibiotic resistance genes in bacteria. Br J Pharmacol. Vol. 153 (Suppl 1), p. S347-S357. DOI: 10.1038/sj.bjp.0707607.

BERTINI, A., GIORDANO, A., VARESI, P., VILLA, L., MANCINI, C., and CARATTOLI, A. (2006). First Report of the Carbapenem-Hydrolyzing Oxacillinase OXA-58 in *Acinetobacter baumannii* Isolates in Italy. Antimicrob. Agents Chemother. Vol. 50 (6), p. 2268-2269. DOI: 10.1128/aac.00166-06.

BETHEL, C. R., HUJER, A. M., HUJER, K. M., THOMSON, J. M., RUSZCZYCKY, M. W., ANDERSON, V. E., PUSZTAI-CAREY, M., TARACILA, M., HELFAND, M. S., and BONOMO, R. A. (2006). Role of Asp104 in the SHV β-lactamase. Antimicrobial Agents and Chemotherapy. Vol. 50 (12), p. 4124-4131. DOI: 10.1128/AAC.00848-06.

BETRIU, C., GÓMEZ, M., LÓPEZ-FABAL, F., CULEBRAS, E., RODRÍGUEZ-AVIAL, I., and PICAZO, J. (2010). Activity of doripenem against extended-spectrum β-lactamase-producing Enterobacteriaceae and *Pseudomonas aeruginosa* isolates. European Journal of Clinical Microbiology & Infectious Diseases. Vol. 29 (9), p. 1179-1181. DOI: 10.1007/s10096-010-0974-3.

BIRNBAUM, J., KAHAN, F. M., KROPP, H., and MACDONALD, J. S. (1985). Carbapenems, a new class of beta-lactam antibiotics. Discovery and development of imipenem/cilastatin. Am J Med. Vol. 78 (6A), p. 3-21.

BOLLET, C., GAINNIER, M., SAINTY, J. M., ORHESSER, P., and DE MICCO, P. (1991). *Serratia fonticola* isolated from a leg abscess. J Clin Microbiol. Vol. 29 (4), p. 834-835.

BONFIGLIO, G., RUSSO, G., and NICOLETTI, G. (2002). Recent developments in carbapenems. Expert Opin Investig Drugs. Vol. 11 (4), p. 529-544. DOI: 10.1517/13543784.11.4.529.

BONNET, R. (2004). Growing group of extended-spectrum β-lactamases: the CTX-M enzymes. Antimicrob Agents Chemother. Vol. 48 (1), p. 1-14. DOI: 10.1128/AAC.48.1.1-14.2004.

BONOMO, R. A., and SZABO, D. (2006). Mechanisms of Multidrug Resistance in *Acinetobacter* Species and *Pseudomonas aeruginosa*. Clinical Infectious Diseases. Vol. 43 (Supplement 2), p. S49-S56. DOI: 10.1086/504477.

BOSCHI, L., MERCURI, P. S., RICCIO, M. L., AMICOSANTE, G., GALLENI, M., FRERE, J.-M., and ROSSOLINI, G. M. (2000). The *Legionella* (*Fluoribacter*) *gormanii* Metallo-β-Lactamase: a New Member of the Highly Divergent Lineage of Molecular-Subclass B3 β-Lactamases. Antimicrob. Agents Chemother. Vol. 44 (6), p. 1538-1543. DOI: 10.1128/aac.44.6.1538-1543.2000.

BROWN, A., BUTTERWORTH, D., COLE, M., HANSCOMB, G., HOOD, J., READING, C., and ROLINSON, G. (1976). Naturally-occurring β-lactamase inhibitors with antibacterial activity. The Journal of antibiotics. Vol. 29 (6), p. 668-669.

BUSH, K. (1989). Characterization of β-lactamases. Antimicrob Agents Chemother. Vol. 33 (3), p. 259-263.

BUSH, K. (2002). The impact of β-lactamases on the development of novel antimicrobial agents. Curr Opin Investig Drugs. Vol. 3 (9), p. 1284-1290.

BUSH, K. (2010). Alarming β-lactamase-mediated resistance in multidrug-resistant *Enterobacteriaceae*. Current Opinion in Microbiology. Vol. 13 (5), p. 558-564. DOI: 10.1016/j.mib.2010.09.006.

BUSH, K., and JACOBY, G. A. (2010). Updated functional classification of β-lactamases. Antimicrob Agents Chemother. Vol. 54 (3), p. 969-976. DOI: 10.1128/AAC.01009-09.

BUSH, K., JACOBY, G. A., and MEDEIROS, A. A. (1995). A functional classification scheme for β-lactamases and its correlation with molecular structure. Antimicrob Agents Chemother. Vol. 39 (6), p. 1211-1233.

BUYNAK, J. D. (2006). Understanding the longevity of the β-lactam antibiotics and of antibiotic/β-lactamase inhibitor combinations. Biochemical Pharmacology. Vol. 71 (7), p. 930-940. DOI: 10.1016/j.bcp.2005.11.012.

CANTON, R., and COQUE, T. M. (2006). The CTX-M β-lactamase pandemic. Curr Opin Microbiol. Vol. 9 (5), p. 466-475. DOI: 10.1016/j.mib.2006.08.011.

CANTU, C., and PALZKILL, T. (1998). The Role of Residue 238 of TEM-1 β-Lactamase in the Hydrolysis of Extended-spectrum Antibiotics. Journal of Biological Chemistry. Vol. 273 (41), p. 26603-26609. DOI: 10.1074/jbc.273.41.26603.

CARENBAUER, A., GARRITY, J., PERIYANNAN, G., YATES, R., and CROWDER, M. (2002). Probing substrate binding to Metallo-β-Lactamase L1 from *Stenotrophomonas maltophilia* by using site-directed mutagenesis. BMC Biochemistry. Vol. 3 (1), p. 4. DOI: 10.1186/1471-2091-3-4.

CARFI, A., PARES, S., DUEE, E., GALLENI, M., DUEZ, C., FRERE, J. M., and DIDEBERG, O. (1995). The 3-D structure of a zinc metallo-β-lactamase from *Bacillus cereus* reveals a new type of protein fold. EMBO J. Vol. 14 (20), p. 4914-4921.

CARRER, A., POIREL, L., YILMAZ, M., AKAN, O. A., FERIHA, C., CUZON, G., MATAR, G., HONDERLICK, P., and NORDMANN, P. (2010). Spread of OXA-48-Encoding Plasmid in Turkey and Beyond. Antimicrob. Agents Chemother. Vol. 54 (3), p. 1369-1373. DOI: 10.1128/aac.01312-09.

CARTWRIGHT, S. J., and COULSON, A. F. W. (1979). A semi-synthetic penicillinase inactivator. Nature. Vol. 278 (5702), p. 360-361. DOI: 10.1038/278360a0.

CASTANHEIRA, M., JONES, R. N., and LIVERMORE, D. M. (2009). Antimicrobial activities of doripenem and other carbapenems against *Pseudomonas aeruginosa*, other nonfermentative bacilli, and *Aeromonas* spp. Diagnostic Microbiology and Infectious Disease. Vol. 63 (4), p. 426-433. DOI: 10.1016/j.diagmicrobio.2009.01.026.

CASTANHEIRA, M., TOLEMAN, M. A., JONES, R. N., SCHMIDT, F. J., and WALSH, T. R. (2004). Molecular Characterization of a β-Lactamase Gene, blaGIM-1, Encoding a New Subclass of Metallo-β-Lactamase. Antimicrob. Agents Chemother. Vol. 48 (12), p. 4654-4661. DOI: 10.1128/aac.48.12.4654-4661.2004.

CATTOIR, V., POIREL, L., MAZEL, D., SOUSSY, C.-J., and NORDMANN, P. (2007). *Vibrio splendidus* as the Source of Plasmid-Mediated QnrS-Like Quinolone Resistance Determinants. Antimicrob. Agents Chemother. Vol. 51 (7), p. 2650-2651. DOI: 10.1128/aac.00070-07.

CHAIN, E., FLOREY, H. W., GARDNER, A. D., HEATLEY, N. G., JENNINGS, M. A., ORR-EWING, J., and SANDERS, A. G. (1940). PENICILLIN AS A CHEMOTHERAPEUTIC AGENT. The Lancet. Vol. 236 (6104), p. 226-228. DOI: 10.1016/S0140-6736(01)08728-1.

CHEN, C. C., SMITH, T. J., KAPADIA, G., WASCH, S., ZAWADZKE, L. E., COULSON, A., and HERZBERG, O. (1996). Structure and Kinetics of the β-Lactamase Mutants S70A and K73H from *Staphylococcus aureus* PC1. Biochemistry. Vol. 35 (38), p. 12251-12258. DOI: 10.1021/bi961153v.

CHEN, C. C. H., and HERZBERG, O. (2001). Structures of the Acyl−Enzyme Complexes of the *Staphylococcus aureus* β-Lactamase Mutant Glu166Asp:Asn170Gln with Benzylpenicillin and Cephaloridine. Biochemistry. Vol. 40 (8), p. 2351-2358. DOI: 10.1021/bi002277h.

CHEN, V. B., ARENDALL, W. B., III, HEADD, J. J., KEEDY, D. A., IMMORMINO, R. M., KAPRAL, G. J., MURRAY, L. W., RICHARDSON, J. S., and RICHARDSON, D. C. (2010). MolProbity: all-atom structure validation for macromolecular crystallography. Acta Crystallographica Section D. Vol. 66 (1), p. 12-21. DOI: 10.1107/S0907444909042073.

CHEN, Y., BONNET, R., and SHOICHET, B. K. (2007). The Acylation Mechanism of CTX-M β-Lactamase at 0.88 Å Resolution. Journal of the American Chemical Society. Vol. 129 (17), p. 5378-5380. DOI: 10.1021/ja0712064.

CHEN, Y., DELMAS, J., SIROT, J., SHOICHET, B., and BONNET, R. (2005). Atomic Resolution Structures of CTX-M β-Lactamases: Extended Spectrum Activities from Increased Mobility and Decreased Stability. Journal of Molecular Biology. Vol. 348 (2), p. 349-362. DOI: 10.1016/j.jmb.2005.02.010.

CHEN, Y., MINASOV, G., ROTH, T. A., PRATI, F., and SHOICHET, B. K. (2006). The Deacylation Mechanism of AmpC β-Lactamase at Ultrahigh Resolution. Journal of the American Chemical Society. Vol. 128 (9), p. 2970-2976. DOI: 10.1021/ja056806m.

CHIA, J. H., SU, L. H., LEE, M. H., KUO, A. J., SHIH, N. Y., SIU, L. K., and WU, T. L. (2010). Development of High-Level Carbapenem Resistance in *Klebsiella pneumoniae* Among

Patients with Prolonged Hospitalization and Carbapenem Exposure. Microb Drug Resist. DOI: 10.1089/mdr.2009.0048.

CLARDY, J., FISCHBACH, M. A., and WALSH, C. T. (2006). New antibiotics from bacterial natural products. Nat Biotech. Vol. 24 (12), p. 1541-1550. DOI: 10.1038/nbt1266.

COLLABORATIVE COMPUTATIONAL PROJECT, N. (1994). The CCP4 suite: programs for protein crystallography. Acta Crystallographica Section D. Vol. 50 (5), p. 760-763. DOI: doi:10.1107/S0907444994003112.

COLLIGNON, P. (2004). Antibiotic growth promoters. J. Antimicrob. Chemother. Vol. 54 (1), p. 272. DOI: 10.1093/jac/dkh266.

CONCHA, N. O., JANSON, C. A., ROWLING, P., PEARSON, S., CHEEVER, C. A., CLARKE, B. P., LEWIS, C., GALLENI, M., FRERE, J. M., PAYNE, D. J*., et al.* (2000). Crystal structure of the IMP-1 metallo β-lactamase from *Pseudomonas aeruginosa* and its complex with a mercaptocarboxylate inhibitor: binding determinants of a potent, broad-spectrum inhibitor. Biochemistry. Vol. 39 (15), p. 4288-4298. DOI: bi992569m

CONCHA, N. O., RASMUSSEN, B. A., BUSH, K., and HERZBERG, O. (1996). Crystal structure of the wide-spectrum binuclear zinc β-lactamase from *Bacteroides fragilis*. Structure. Vol. 4 (7), p. 823-836. DOI: 10.1016/S0969-2126(96)00089-5

COSTELLO, A. L., SHARMA, N. P., YANG, K. W., CROWDER, M. W., and TIERNEY, D. L. (2006). X-ray absorption spectroscopy of the zinc-binding sites in the class B2 metallo-β-lactamase ImiS from *Aeromonas veronii* bv. *sobria*. Biochemistry. Vol. 45 (45), p. 13650-13658. DOI: 10.1021/bi061547e.

CRAWFORD, P. A., SHARMA, N., CHANDRASEKAR, S., SIGDEL, T., WALSH, T. R., SPENCER, J., and CROWDER, M. W. (2004). Over-expression, purification, and characterization of metallo-β-lactamase ImiS from *Aeromonas veronii* bv. *sobria*. Protein Expr Purif. Vol. 36 (2), p. 272-279. DOI: 10.1016/j.pep.2004.04.017

CRAWFORD, P. A., YANG, K. W., SHARMA, N., BENNETT, B., and CROWDER, M. W. (2005). Spectroscopic studies on cobalt(II)-substituted metallo-β-lactamase ImiS from *Aeromonas veronii* bv. *sobria*. Biochemistry. Vol. 44 (13), p. 5168-5176. DOI: 10.1021/bi047463s.

CROWDER, M. W., SPENCER, J., and VILA, A. J. (2006). Metallo-β-lactamases: Novel Weaponry for Antibiotic Resistance in Bacteria. Accounts of Chemical Research. Vol. 39 (10), p. 721-728. DOI: 10.1021/ar0400241.

CROWDER, M. W., WALSH, T. R., BANOVIC, L., PETTIT, M., and SPENCER, J. (1998). Over-expression, Purification, and Characterization of the Cloned Metallo-β-Lactamase L1 from *Stenotrophomonas maltophilia*. Antimicrob. Agents Chemother. Vol. 42 (4), p. 921-926.

D'COSTA, V., MCGRANN, K., HUGHES, D., and WRIGHT, G. (2006). Sampling the antibiotic resistome. Science. Vol. 311 (5759), p. 374-377. DOI: 10.1126/science.1120800

DAL PERARO, M., VILA, A. J., CARLONI, P., and KLEIN, M. L. (2007). Role of Zinc Content on the Catalytic Efficiency of B1 Metallo β-Lactamases. Journal of the American Chemical Society. Vol. 129 (10), p. 2808-2816. DOI: 10.1021/ja0657556.

DALBADIE-MCFARLAND, G., NEITZEL, J. J., and RICHARDS, J. H. (1986). Active-site mutants of β-lactamase: use of an inactive double mutant to study requirements for catalysis. Biochemistry. Vol. 25 (2), p. 332-338. DOI: 10.1021/bi00350a008.

DANTAS, G., SOMMER, M. O. A., OLUWASEGUN, R. D., and CHURCH, G. M. (2008). Bacteria Subsisting on Antibiotics. Science. Vol. 320 (5872), p. 100-103. DOI: 10.1126/science.1155157.

DAVIES, J. (1994). Inactivation of antibiotics and the dissemination of resistance genes. Science. Vol. 264 (5157), p. 375-382. DOI: 10.1126/science.8153624.

DE KRAKER, M. E. A., WOLKEWITZ, M., DAVEY, P. G., KOLLER, W., BERGER, J., NAGLER, J., ICKET, C., KALENIC, S., HORVATIC, J., SEIFERT, H*., et al.* (2011). Burden of antimicrobial resistance in European hospitals: excess mortality and length of hospital stay associated with bloodstream infections due to *Escherichia coli* resistant to third-generation cephalosporins. Journal of Antimicrobial Chemotherapy. Vol. 66 (2), p. 398-407. DOI: 10.1093/jac/dkq412.

DE LENCASTRE, H., DE JONGE, B. L., MATTHEWS, P. R., and TOMASZ, A. (1994). Molecular aspects of methicillin resistance in *Staphylococcus aureus*. J Antimicrob Chemother. Vol. 33 (1), p. 7-24. DOI: 10.1093/jac/33.1.7.

DELAIRE, M., LENFANT, F., LABIA, R., and MASSON, J.-M. (1991). Site-directed mutagenesis on TEM-1 β-lactamase: role of Glul66 in catalysis and substrate binding. Protein Engineering. Vol. 4 (7), p. 805-810. DOI: 10.1093/protein/4.7.805.

DELANO, W. (2008). The PyMOL molecular graphics system. DeLano Scientific LLC, Palo Alto, CA, USA.

DELEO, F. R., OTTO, M., KREISWIRTH, B. N., and CHAMBERS, H. F. (2010). Community-associated meticillin-resistant *Staphylococcus aureus*. The Lancet. Vol. 375 (9725), p. 1557-1568. DOI: 10.1016/s0140-6736(09)61999-1.

DELMAS, J., CHEN, Y., PRATI, F., ROBIN, F., SHOICHET, B. K., and BONNET, R. (2008). Structure and Dynamics of CTX-M Enzymes Reveal Insights into Substrate Accommodation by Extended-spectrum β-Lactamases. Journal of Molecular Biology. Vol. 375 (1), p. 192-201. DOI: 10.1016/j.jmb.2007.10.026.

DEMAIN, A. L., and ELANDER, R. P. (1999). The β-lactam antibiotics: past, present, and future. Antonie Van Leeuwenhoek. Vol. 75 (1), p. 5-19. DOI: 10.1023/a:1001738823146.

DIDEBERG, O., CHARLIER, P., WERY, J. P., DEHOTTAY, P., DUSART, J., ERPICUM, T., FRERE, J. M., and GHUYSEN, J. M. (1987). The crystal structure of the β-lactamase of *Streptomyces albus* G at 0.3 nm resolution. Biochem J. Vol. 245 (3), p. 911-913.

DOCQUIER, J.-D., BENVENUTI, M., CALDERONE, V., STOCZKO, M., MENCIASSI, N., ROSSOLINI, G. M., and MANGANI, S. (2010). High-Resolution Crystal Structure of the Subclass B3 Metallo-β-Lactamase BJP-1: Rational Basis for Substrate Specificity and Interaction with Sulfonamides. Antimicrob. Agents Chemother. Vol. 54 (10), p. 4343-4351. DOI: 10.1128/aac.00409-10.

DOCQUIER, J.-D., PANTANELLA, F., GIULIANI, F., THALLER, M. C., AMICOSANTE, G., GALLENI, M., FRERE, J.-M., BUSH, K., and ROSSOLINI, G. M. (2002). CAU-1, a Subclass B3 Metallo-β-Lactamase of Low Substrate Affinity Encoded by an Ortholog Present in the *Caulobacter crescentus* Chromosome. Antimicrob. Agents Chemother. Vol. 46 (6), p. 1823-1830. DOI: 10.1128/aac.46.6.1823-1830.2002.

DONADIO, S., MAFFIOLI, S., MONCIARDINI, P., SOSIO, M., and JABES, D. (2010). Sources of novel antibiotics—aside the common roads. Applied Microbiology and Biotechnology. Vol. 88 (6), p. 1261-1267. DOI: 10.1007/s00253-010-2877-8.

DOUCET, N., DE WALS, P. Y., and PELLETIER, J. N. (2004). Site-saturation mutagenesis of Tyr-105 reveals its importance in substrate stabilization and discrimination in TEM-1 β-lactamase. Journal of Biological Chemistry. Vol. 279 (44), p. 46295-46303. DOI: 10.1074/jbc.M407606200.

DRAWZ, S. M., and BONOMO, R. A. (2010). Three Decades of β-Lactamase Inhibitors. Clin. Microbiol. Rev. Vol. 23 (1), p. 160-201. DOI: 10.1128/cmr.00037-09.

DUPONT, M., PAGÈS, J.-M., LAFITTE, D., SIROY, A., and BOLLET, C. (2005). Identification of an OprD Homologue in *Acinetobacter baumannii*. Journal of Proteome Research. Vol. 4 (6), p. 2386-2390. DOI: 10.1021/pr050143q.

EASTON, C. J., and KNOWLES, J. R. (1982). Inhibition of the RTEM β–lactamase from *Escherichia coli*. Interaction of the enzyme with derivatives of olivanic acid. Biochemistry. Vol. 21 (12), p. 2857-2862. DOI: 10.1021/bi00541a008.

EMSLEY, P., LOHKAMP, B., SCOTT, W. G., and COWTAN, K. (2010). Features and development of Coot. Acta Crystallographica Section D. Vol. 66 (4), p. 486-501. DOI: 10.1107/S0907444910007493.

ENGLISH, A. R., RETSEMA, J. A., GIRARD, A. E., LYNCH, J. E., and BARTH, W. E. (1978). CP-45,899, a Beta-Lactamase Inhibitor That Extends the Antibacterial Spectrum of β-Lactams: Initial Bacteriological Characterization. Antimicrob. Agents Chemother. Vol. 14 (3), p. 414-419. DOI: 10.1128/aac.

ESCOBAR, W. A., TAN, A. K., and FINK, A. L. (1991). Site-directed mutagenesis of β-lactamase leading to accumulation of a catalytic intermediate. Biochemistry. Vol. 30 (44), p. 10783-10787. DOI: 10.1021/bi00108a025.

EVANS, P. (2006). Scaling and assessment of data quality. Acta Crystallographica Section D. Vol. 62 (1), p. 72-82. DOI: 10.1107/S0907444905036693.

FABIANE, S. M., SOHI, M. K., WAN, T., PAYNE, D. J., BATESON, J. H., MITCHELL, T., and SUTTON, B. J. (1998). Crystal structure of the zinc-dependent β-lactamase from *Bacillus cereus* at 1.9 A resolution: binuclear active site with features of a mononuclear enzyme. Biochemistry. Vol. 37 (36), p. 12404-12411. DOI: 10.1021/bi980506i.

FARMER, J. J., DAVIS, B. R., HICKMAN-BRENNER, F. W., MCWHORTER, A., HUNTLEY-CARTER, G. P., ASBURY, M. A., RIDDLE, C., WATHEN-GRADY, H. G., ELIAS, C., and FANNING, G. R. (1985). Biochemical identification of new species and biogroups of Enterobacteriaceae isolated from clinical specimens. J Clin Microbiol. Vol. 21 (1), p. 46-76.

FELICI, A., and AMICOSANTE, G. (1995). Kinetic analysis of extension of substrate specificity with *Xanthomonas maltophilia*, *Aeromonas hydrophila*, and *Bacillus cereus* metallo-β-lactamases. Antimicrob Agents Chemother. Vol. 39 (1), p. 192-199.

FELICI, A., AMICOSANTE, G., ORATORE, A., STROM, R., LEDENT, P., JORIS, B., FANUEL, L., and FRERE, J. M. (1993). An overview of the kinetic parameters of class B β-lactamases. Biochem J. Vol. 291 (Pt 1), p. 151-155.

FISHER, J. F., MEROUEH, S. O., and MOBASHERY, S. (2005). Bacterial resistance to β-lactam antibiotics: compelling opportunism, compelling opportunity. Chem Rev. Vol. 105 (2), p. 395-424. DOI: 10.1021/cr030102i.

FISHER, J. F., and MOBASHERY, S. (2009). Three decades of the class A β-lactamase acyl-enzyme. Curr Protein Pept Sci. Vol. 10 (5), p. 401-407.

FLEMING, A. (1929). On the antimicrobial action of cultures of a penicillium with special reference to their use in the isolation of B. influenzae. British Journal of Experimental Pathology. Vol. 10, p. 226-236.

FONSECA, F., SARMENTO, A. C., HENRIQUES, I., SAMYN, B., VAN BEEUMEN, J., DOMINGUES, P., DOMINGUES, M. R., SAAVEDRA, M. J., and CORREIA, A. (2007). Biochemical Characterization of SFC-1, a Class A Carbapenem-Hydrolyzing β-Lactamase. Antimicrob. Agents Chemother. Vol. 51 (12), p. 4512-4514. DOI: 10.1128/aac.00491-07.

FRASE, H., SMITH, C. A., TOTH, M., CHAMPION, M. M., MOBASHERY, S., and VAKULENKO, S. B. (2011). Identification of products of inhibition of GES-2 β-lactamase by tazobactam by x-ray crystallography and spectrometry. Journal of Biological Chemistry. DOI: 10.1074/jbc.M110.208744.

FROST, L. S., LEPLAE, R., SUMMERS, A. O., and TOUSSAINT, A. (2005). Mobile genetic elements: the agents of open source evolution. Nat Rev Micro. Vol. 3 (9), p. 722-732.

FUDA, C. C., FISHER, J. F., and MOBASHERY, S. (2005). β-lactam resistance in *Staphylococcus aureus*: the adaptive resistance of a plastic genome. Cell Mol Life Sci. Vol. 62 (22), p. 2617-2633. DOI: 10.1007/s00018-005-5148-6.

GALLENI, M., LAMOTTE-BRASSEUR, J., ROSSOLINI, G. M., SPENCER, J., DIDEBERG, O., and FRERE, J.-M. (2001). Standard Numbering Scheme for Class B β-Lactamases. Antimicrob. Agents Chemother. Vol. 45 (3), p. 660-663. DOI: 10.1128/aac.45.3.660-663.2001.

GARAU, G., BEBRONE, C., ANNE, C., GALLENI, M., FRERE, J. M., and DIDEBERG, O. (2005). A metallo-β-lactamase enzyme in action: crystal structures of the monozinc carbapenemase CphA and its complex with biapenem. Journal of Molecular Biology. Vol. 345 (4), p. 785-795. DOI: 10.1016/j.jmb.2004.10.070.

GARAU, G., GARCIA-SAEZ, I., BEBRONE, C., ANNE, C., MERCURI, P., GALLENI, M., FRERE, J. M., and DIDEBERG, O. (2004). Update of the standard numbering scheme for class B β-lactamases. Antimicrob Agents Chemother. Vol. 48 (7), p. 2347-2349. DOI: 10.1128/AAC.48.7.2347-2349.2004.

GARCIA-FERNANDEZ, A., MIRIAGOU, V., PAPAGIANNITSIS, C. C., GIORDANO, A., VENDITTI, M., MANCINI, C., and CARATTOLI, A. (2010). An Ertapenem-Resistant Extended-Spectrum-β-Lactamase-Producing *Klebsiella pneumoniae* Clone Carries a Novel OmpK36 Porin Variant. Antimicrob. Agents Chemother. Vol. 54 (10), p. 4178-4184. DOI: 10.1128/aac.01301-09.

GARCIA-SAEZ, I., DOCQUIER, J. D., ROSSOLINI, G. M., and DIDEBERG, O. (2008). The three-dimensional structure of VIM-2, a Zn-β-lactamase from *Pseudomonas aeruginosa* in its reduced and oxidised form. Journal of Molecular Biology. Vol. 375 (3), p. 604-611. DOI: 10.1016/j.jmb.2007.11.012.

GARCÍA-SÁEZ, I., HOPKINS, J., PAPAMICAEL, C., FRANCESCHINI, N., AMICOSANTE, G., ROSSOLINI, G. M., GALLENI, M., FRÈRE, J.-M., and DIDEBERG, O. (2003). The 1.5-Å Structure of Chryseobacterium meningosepticum Zinc β-Lactamase in Complex with the Inhibitor, D-Captopril. Journal of Biological Chemistry. Vol. 278 (26), p. 23868-23873. DOI: 10.1074/jbc.M301062200.

GARCIA-SAEZ, I., MERCURI, P. S., PAPAMICAEL, C., KAHN, R., FRÈRE, J. M., GALLENI, M., ROSSOLINI, G. M., and DIDEBERG, O. (2003). Three-dimensional Structure of FEZ-1, a Monomeric Subclass B3 Metallo-β-lactamase from *Fluoribacter gormanii*, in Native Form and in Complex with d-Captopril. Journal of Molecular Biology. Vol. 325 (4), p. 651-660. DOI: 10.1016/S0022-2836(02)01271-8.

GARRITY, J. D., BENNETT, B., and CROWDER, M. W. (2004). Direct Evidence That the Reaction Intermediate of Metallo-β-lactamase L1 Is Metal Bound. Biochemistry. Vol. 44 (3), p. 1078-1087. DOI: 10.1021/bi048385b.

GAVINI, F., FERRAGUT, C., IZARD, D., TRINEL, P. A., LECLERC , H., LEFEBVRE, B., and MOSSEL, D. A. A. (1979). *Serratia fonticola*, a New Species from Water. Int J Syst Bacteriol. Vol. 29 (2), p. 92-101. DOI: 10.1099/00207713-29-2-92.

GEORGOPAPADAKOU, N. H. (1993). Penicillin-binding proteins and bacterial resistance to β-lactams. Antimicrob. Agents Chemother. Vol. 37 (10), p. 2045-2053. DOI: 10.1128/aac.

GIANI, T., D'ANDREA, M. M., PECILE, P., BORGIANNI, L., NICOLETTI, P., TONELLI, F., BARTOLONI, A., and ROSSOLINI, G. M. (2009). Emergence in Italy of *Klebsiella pneumoniae* Sequence Type 258 Producing KPC-3 Carbapenemase. J. Clin. Microbiol. Vol. 47 (11), p. 3793-3794. DOI: 10.1128/jcm.01773-09.

GILL, S. C., and VON HIPPEL, P. H. (1989). Calculation of protein extinction coefficients from amino acid sequence data. Analytical Biochemistry. Vol. 182 (2), p. 319-326. DOI: 10.1016/0003-2697(89)90602-7

GIRLICH, D., NAAS, T., and NORDMANN, P. (2004). Biochemical Characterization of the Naturally Occurring Oxacillinase OXA-50 of *Pseudomonas aeruginosa*. Antimicrob. Agents Chemother. Vol. 48 (6), p. 2043-2048. DOI: 10.1128/aac.48.6.2043-2048.2004.

GIRLICH, D., POIREL, L., and NORDMANN, P. (2010). Novel Ambler Class A Carbapenem-Hydrolyzing β-Lactamase from a *Pseudomonas fluorescens* Isolate from the Seine River,

Paris, France. Antimicrob. Agents Chemother. Vol. 54 (1), p. 328-332. DOI: 10.1128/aac.00961-09.

GOLDSTEIN, E. J. C., and CITRON, D. M. (2009). Activity of a novel carbapenem, doripenem, against anaerobic pathogens. Diagnostic Microbiology and Infectious Disease. Vol. 63 (4), p. 447-454. DOI: 10.1016/j.diagmicrobio.2009.01.022

GOLEMI, D., MAVEYRAUD, L., VAKULENKO, S., SAMAMA, J.-P., and MOBASHERY, S. (2001). Critical involvement of a carbamylated lysine in catalytic function of class D β-lactamases. Proceedings of the National Academy of Sciences of the United States of America. Vol. 98 (25), p. 14280-14285. DOI: 10.1073/pnas.241442898.

GORRET, J., CHEVALIER, J., GASCHET, A., FRAISSE, B., VIOLAS, P., CHAPUIS, M., and JOLIVET-GOUGEON, A. (2009). Childhood delayed septic arthritis of the knee caused by *Serratia fonticola*. Knee. Vol. 16 (6), p. 512-514. DOI: 10.1016/j.knee.2009.02.008

GREBE, T., and HAKENBECK, R. (1996). Penicillin-binding proteins 2b and 2x of *Streptococcus pneumoniae* are primary resistance determinants for different classes of β-lactam antibiotics. Antimicrob Agents Chemother. Vol. 40 (4), p. 829-834.

GRUNE, T. (2008). mtz2sca and mtz2hkl: facilitated transition from CCP4 to the SHELX program suite. Journal of Applied Crystallography. Vol. 41 (1), p. 217-218. DOI: doi:10.1107/S0021889807050054.

GUILLAUME, G., VANHOVE, M., LAMOTTE-BRASSEUR, J., LEDENT, P., JAMIN, M., JORIS, B., and FRERE, J. M. (1997). Site-directed mutagenesis of glutamate 166 in two β-lactamases. Kinetic and molecular modeling studies. J Biol Chem. Vol. 272 (9), p. 5438-5444. DOI: 10.1074/jbc.272.9.5438.

GÜLMEZ, D., WOODFORD, N., PALEPOU, M.-F. I., MUSHTAQ, S., METAN, G., YAKUPOGULLARI, Y., KOCAGOZ, S., UZUN, O., HASCELIK, G., and LIVERMORE, D. M. (2008). Carbapenem-resistant *Escherichia coli* and *Klebsiella pneumoniae* isolates from Turkey with OXA-48-like carbapenemases and outer membrane protein loss. International Journal of Antimicrobial Agents. Vol. 31 (6), p. 523-526. DOI: 10.1016/j.ijantimicag.2008.01.017

HAKENBECK, R., BALMELLE, N., WEBER, B., GARDES, C., KECK, W., and DE SAIZIEU, A. (2001). Mosaic Genes and Mosaic Chromosomes: Intra- and Interspecies Genomic Variation of *Streptococcus pneumoniae*. Infect. Immun. Vol. 69 (4), p. 2477-2486. DOI: 10.1128/iai.69.4.2477-2486.2001.

HALL, R. M., and COLLIS, C. M. (1998). Antibiotic resistance in gram-negative bacteria: the role of gene cassettes and integrons. Drug Resistance Updates. Vol. 1 (2), p. 109-119. DOI: 10.1016/S1368-7646(98)80026-5.

HARTMAN, B. J., and TOMASZ, A. (1984). Low-affinity penicillin-binding protein associated with β-lactam resistance in *Staphylococcus aureus*. J Bacteriol. Vol. 158 (2), p. 513-516.

HAWKEY, P. M., and JONES, A. M. (2009). The changing epidemiology of resistance. J Antimicrob Chemother. Vol. 64 (Suppl 1), p. i3-i10. DOI: 10.1093/jac/dkp256.

HENQUELL, C., CHANAL, C., SIROT, D., LABIA, R., and SIROT, J. (1995). Molecular characterization of nine different types of mutants among 107 inhibitor-resistant TEM β-lactamases from clinical isolates of *Escherichia coli*. Antimicrob. Agents Chemother. Vol. 39 (2), p. 427-430.

HENRIQUES, I., MOURA, A., ALVES, A., SAAVEDRA, M. J., and CORREIA, A. (2004). Molecular Characterization of a Carbapenem-Hydrolyzing Class A β-Lactamase, SFC-1, from *Serratia fonticola* UTAD54. Antimicrob. Agents Chemother. Vol. 48 (6), p. 2321-2324. DOI: 10.1128/aac.48.6.2321-2324.2004.

HERITIER, C., POIREL, L., AUBERT, D., and NORDMANN, P. (2003). Genetic and Functional Analysis of the Chromosome-Encoded Carbapenem-Hydrolyzing Oxacillinase OXA-40 of *Acinetobacter baumannii*. Antimicrob. Agents Chemother. Vol. 47 (1), p. 268-273. DOI: 10.1128/aac.47.1.268-273.2003.

HERITIER, C., POIREL, L., LAMBERT, T., and NORDMANN, P. (2005). Contribution of Acquired Carbapenem-Hydrolyzing Oxacillinases to Carbapenem Resistance in *Acinetobacter baumannii*. Antimicrob. Agents Chemother. Vol. 49 (8), p. 3198-3202. DOI: 10.1128/aac.49.8.3198-3202.2005.

HERMANN, J. C., PRADON, J., HARVEY, J. N., and MULHOLLAND, A. J. (2009). High Level QM/MM Modeling of the Formation of the Tetrahedral Intermediate in the Acylation of Wild Type and K73A Mutant TEM-1 Class A β-Lactamase. The Journal of Physical Chemistry A. Vol. 113 (43), p. 11984-11994. DOI: 10.1021/jp9037254.

HERZBERG, O., and MOULT, J. (1987). Bacterial resistance to β-lactam antibiotics: crystal structure of β-lactamase from *Staphylococcus aureus* PC1 at 2.5 A resolution. Science. Vol. 236 (4802), p. 694-701. DOI: 10.1126/science.3107125

HODGKIN, D. C. (1949). The X-ray analysis of the structure of penicillin. Adv Sci. Vol. 6 (22), p. 85-89.

HU, Z., and ZHAO, W.-H. (2009). Identification of plasmid- and integron-borne blaIMP-1 and blaIMP-10 in clinical isolates of *Serratia marcescens*. J Med Microbiol. Vol. 58 (2), p. 217-221. DOI: 10.1099/jmm.0.006874-0.

HULETSKY, A., KNOX, J. R., and LEVESQUE, R. C. (1993). Role of Ser-238 and Lys-240 in the hydrolysis of third-generation cephalosporins by SHV-type β-lactamases probed by site-directed mutagenesis and three-dimensional modeling. Journal of Biological Chemistry. Vol. 268 (5), p. 3690-3697.

HUMENIUK, C., ARLET, G., GAUTIER, V., GRIMONT, P., LABIA, R., and PHILIPPON, A. (2002). β-Lactamases of *Kluyvera ascorbata*, Probable Progenitors of Some Plasmid-Encoded CTX-M Types. Antimicrobial Agents and Chemotherapy. Vol. 46 (9), p. 3045. DOI: 10.1128/AAC.46.9.3045-3049.2002.

HUOVINEN, P., HUOVINEN, S., and JACOBY, G. A. (1988). Sequence of PSE-2 β-lactamase. Antimicrob Agents Chemother. Vol. 32 (1), p. 134-136.

HUSSAIN, M., CARLINO, A., MADONNA, M. J., and LAMPEN, J. O. (1985). Cloning and sequencing of the metallothioprotein β-lactamase II gene of *Bacillus cereus* 569/H in *Escherichia coli*. J. Bacteriol. Vol. 164 (1), p. 223-229.

IBUKA, A., TAGUCHI, A., ISHIGURO, M., FUSHINOBU, S., ISHII, Y., KAMITORI, S., OKUYAMA, K., YAMAGUCHI, K., KONNO, M., and MATSUZAWA, H. (1999). Crystal structure of the E166A mutant of extended-spectrum β-lactamase toho-1 at 1.8 Å resolution. Journal of Molecular Biology. Vol. 285 (5), p. 2079-2087. DOI: 10.1006/jmbi.1998.2432.

JACOBY, G. A., and MUNOZ-PRICE, L. S. (2005). The new β-lactamases. N Engl J Med. Vol. 352 (4), p. 380-391. DOI: 10.1056/NEJMra041359.

JANCARIK, J., and KIM, S.-H. (1991). Sparse matrix sampling: a screening method for crystallization of proteins. Journal of Applied Crystallography. Vol. 24 (4), p. 409-411. DOI: 10.1107/S0021889891004430.

JAURIN, B., and GRUNDSTROM, T. (1981). ampC cephalosporinase of *Escherichia coli* K-12 has a different evolutionary origin from that of β-lactamases of the penicillinase type. Proc Natl Acad Sci U S A. Vol. 78 (8), p. 4897-4901.

JEAN-MARIE, G. (1997). Penicillin-binding proteins. Wall peptidoglycan assembly and resistance to penicillin: facts, doubts and hopes. International Journal of Antimicrobial Agents. Vol. 8 (1), p. 45-60. DOI: doi:10.1016/S0924-8579(96)00358-5

JELSCH, C., LENFANT, F., MASSON, J. M., and SAMAMA, J. P. (1992). β-lactamase TEM1 of *E. coli* Crystal structure determination at 2.5 Å resolution. FEBS Letters. Vol. 299 (2), p. 135-142.

JELSCH, C., MOUREY, L., MASSON, J. M., and SAMAMA, J. P. (1993). Crystal structure of *Escherichia coli* TEM1 β-lactamase at 1.8 Å resolution. Proteins: Structure, Function, and Bioinformatics. Vol. 16 (4), p. 364-383. DOI: 10.1002/prot.340160406.

JEVONS, M. P. (1961). Celbenin - resistant Staphylococci. British Medical Journal. Vol. 1 (521), p. 124-125.

KALP, M., and CAREY, P. R. (2008). Carbapenems and SHV-1 β-Lactamase Form Different Acyl-Enzyme Populations in Crystals and Solution. Biochemistry. Vol. 47 (45), p. 11830-11837. DOI: 10.1021/bi800833u.

KE, W., BETHEL, C. R., THOMSON, J. M., BONOMO, R. A., and VAN DEN AKKER, F. (2007). Crystal Structure of KPC-2: Insights into Carbapenemase Activity in Class A β-Lactamases. Biochemistry. Vol. 46 (19), p. 5732-5740. DOI: 10.1021/bi700300u.

KIM, J. Y., JUNG, H. I., AN, Y. J., LEE, J. H., KIM, S. J., JEONG, S. H., LEE, K. J., SUH, P.-G., LEE, H.-S., LEE, S. H.*, et al.* (2006). Structural basis for the extended substrate spectrum of CMY-10, a plasmid-encoded class C β-lactamase. Molecular Microbiology. Vol. 60 (4), p. 907-916. DOI: 10.1111/j.1365-2958.2006.05146.x.

KNOX, J. R. (1995). Extended-spectrum and inhibitor-resistant TEM-type β-lactamases: mutations, specificity, and three-dimensional structure. Antimicrob Agents Chemother. Vol. 39 (12), p. 2593-2601.

KNOX, J. R., MOEWS, P. C., and FRERE, J.-M. (1996). Molecular evolution of bacterial β–lactam resistance. Chemistry & Biology. Vol. 3 (11), p. 937-947.

KOTRA, L. P., and MOBASHERY, S. (1999). Mechanistic and clinical aspects of β-lactam antibiotics and β-lactamases. Arch Immunol Ther Exp (Warsz). Vol. 47 (4), p. 211-216.

KRISSINEL, E., and HENRICK, K. (2004). Secondary-structure matching (SSM), a new tool for fast protein structure alignment in three dimensions. Acta Crystallographica Section D. Vol. 60 (12 Part 1), p. 2256-2268. DOI: doi:10.1107/S0907444904026460.

KUMAR, A., and SCHWEIZER, H. P. (2005). Bacterial resistance to antibiotics: Active efflux and reduced uptake. Advanced Drug Delivery Reviews. Vol. 57 (10), p. 1486-1513. DOI: 10.1016/j.addr.2005.04.004.

KUMARASAMY, K. K., TOLEMAN, M. A., WALSH, T. R., BAGARIA, J., BUTT, F., BALAKRISHNAN, R., CHAUDHARY, U., DOUMITH, M., GISKE, C. G., IRFAN, S.*, et al.* (2010). Emergence of a new antibiotic resistance mechanism in India, Pakistan, and the UK: a molecular, biological, and

epidemiological study. The Lancet Infectious Diseases. Vol. 10 (9), p. 597-602. DOI: 10.1016/S1473-3099(10)70143-2

KUZIN, A. P., NUKAGA, M., NUKAGA, Y., HUJER, A. M., BONOMO, R. A., and KNOX, J. R. (1999). Structure of the SHV-1 β-Lactamase. Biochemistry. Vol. 38 (18), p. 5720-5727. DOI: 10.1021/bi990136d.

LAEMMLI, U. K. (1970). Cleavage of Structural Proteins during the Assembly of the Head of Bacteriophage T4. Nature. Vol. 227 (5259), p. 680-685.

LAIBLE, G., SPRATT, B. G., and HAKENBECK, R. (1991). Interspecies recombinational events during the evolution of altered PBP 2x genes in penicillin-resistant clinical isolates of *Streptococcus pneumoniae*. Mol Microbiol. Vol. 5 (8), p. 1993-2002.

LAMBERT, P. A. (2005). Bacterial resistance to antibiotics: Modified target sites. Advanced Drug Delivery Reviews. Vol. 57 (10), p. 1471-1485. DOI: 10.1016/j.addr.2005.04.003

LAMOTTE-BRASSEUR, J., DIVE, G., DIDEBERG, O., CHARLIER, P., FRERE, J. M., and GHUYSEN, J. M. (1991). Mechanism of acyl transfer by the class A serine β-lactamase of *Streptomyces albus* G. Biochem J. Vol. 279 (Pt 1), p. 213-221.

LARAKI, N., FRANCESCHINI, N., ROSSOLINI, G. M., SANTUCCI, P., MEUNIER, C., DE PAUW, E., AMICOSANTE, G., FRERE, J. M., and GALLENI, M. (1999). Biochemical characterization of the *Pseudomonas aeruginosa* 101/1477 metallo-β-lactamase IMP-1 produced by *Escherichia coli*. Antimicrob Agents Chemother. Vol. 43 (4), p. 902-906.

LASKOWSKI, R. A., MACARTHUR, M. W., MOSS, D. S., and THORNTON, J. M. (1993). PROCHECK: a program to check the stereochemical quality of protein structures. Journal of Applied Crystallography. Vol. 26 (2), p. 283-291. DOI: 10.1107/S0021889892009944.

LAURETTI, L., RICCIO, M. L., MAZZARIOL, A., CORNAGLIA, G., AMICOSANTE, G., FONTANA, R., and ROSSOLINI, G. M. (1999). Cloning and Characterization of blaVIM, a New Integron-Borne Metallo-β-Lactamase Gene from a *Pseudomonas aeruginosa* Clinical Isolate. Antimicrob. Agents Chemother. Vol. 43 (7), p. 1584-1590.

LEE, W., MCDONOUGH, M. A., KOTRA, L. P., LI, Z.-H., SILVAGGI, N. R., TAKEDA, Y., KELLY, J. A., and MOBASHERY, S. (2001). A 1.2-Å snapshot of the final step of bacterial cell wall biosynthesis. Proceedings of the National Academy of Sciences of the United States of America. Vol. 98 (4), p. 1427-1431. DOI: 10.1073/pnas.98.4.1427

LEE, Y., YUM, J. H., KIM, C.-K., YONG, D., JEON, E. H., JEONG, S. H., AHN, J. Y., and LEE, K. (2010). Role of OXA-23 and AdeABC Efflux Pump for Acquiring Carbapenem Resistance in an

Acinetobacter baumannii Strain Carrying the blaOXA-66 Gene. Ann Clin Lab Sci. Vol. 40 (1), p. 43-48.

LEFLON-GUIBOUT, V., SPELDOOREN, V., HEYM, B., and NICOLAS-CHANOINE, M.-H. (2000). Epidemiological Survey of Amoxicillin-Clavulanate Resistance and Corresponding Molecular Mechanisms in *Escherichia coli* Isolates in France: New Genetic Features of bla_{TEM} Genes. Antimicrob. Agents Chemother. Vol. 44 (10), p. 2709-2714. DOI: 10.1128/aac.44.10.2709-2714.2000.

LESLIE, A. (2006). The integration of macromolecular diffraction data. Acta Crystallographica Section D. Vol. 62 (1), p. 48-57. DOI: doi:10.1107/S0907444905039107.

LEVY, S. B., and MARSHALL, B. (2004). Antibacterial resistance worldwide: causes, challenges and responses. Nat Med. DOI: 10.1038/nm1145

LI, X., NIKAIDO, H., and POOLE, K. (1995). Role of mexA-mexB-oprM in antibiotic efflux in *Pseudomonas aeruginosa*. Antimicrob. Agents Chemother. Vol. 39 (9), p. 1948-1953.

LIETZ, E. J., TRUHER, H., KAHN, D., HOKENSON, M. J., and FINK, A. L. (2000). Lysine-73 Is Involved in the Acylation and Deacylation of β-Lactamase. Biochemistry. Vol. 39 (17), p. 4971-4981. DOI: 10.1021/bi992681k.

LIMANSKY, A. S., MUSSI, M. A., and VIALE, A. M. (2002). Loss of a 29-Kilodalton Outer Membrane Protein in *Acinetobacter baumannii* Is Associated with Imipenem Resistance. J. Clin. Microbiol. Vol. 40 (12), p. 4776-4778. DOI: 10.1128/jcm.40.12.4776-4778.2002.

LIN, Y.-F., WALMSLEY, A. R., and ROSEN, B. P. (2006). An arsenic metallochaperone for an arsenic detoxification pump. Proceedings of the National Academy of Sciences. Vol. 103 (42), p. 15617-15622. DOI: 10.1073/pnas.0603974103.

LIN, Y. L., LEE, Y. M., and LIM, C. (2005). Differential effects of the Zn-His-Bkb vs Zn-His-[Asp/Glu] triad on Zn-core stability and reactivity. J Am Chem Soc. Vol. 127 (32), p. 11336-11347. DOI: 10.1021/ja051304u.

LINE, K., ISUPOV, M. N., and LITTLECHILD, J. A. (2004). The Crystal Structure of a (-) γ–Lactamase from an *Aureobacterium* Species Reveals a Tetrahedral Intermediate in the Active Site. Journal of Molecular Biology. Vol. 338 (3), p. 519-532. DOI: 10.1016/j.jmb.2004.03.001.

LIVERMORE, D. (2009). Has the era of untreatable infections arrived? Journal of Antimicrobial Chemotherapy. Vol. 64 (Supplement 1), p. i29-i36. DOI: 10.1093/jac/dkp255.

LIVERMORE, D. M. (2007). Introduction: the challenge of multiresistance. International Journal of Antimicrobial Agents. Vol. 29 (Supplement 3), p. S1-S7.

LIVERMORE, D. M. (2009). β-Lactamases- the Threat Renews. Curr Protein Pept Sci. Vol. 10 (5), p. 397-400. DOI: 10.2174/138920309789351994.

LIVERMORE, D. M., and WOODFORD, N. (2006). The β-lactamase threat in Enterobacteriaceae, *Pseudomonas* and *Acinetobacter*. Trends Microbiol. Vol. 14 (9), p. 413-420. DOI: 10.1016/j.tim.2006.07.008.

LLANES, C., HOCQUET, D., VOGNE, C., BENALI-BAITICH, D., NEUWIRTH, C., and PLESIAT, P. (2004). Clinical Strains of *Pseudomonas aeruginosa* Overproducing MexAB-OprM and MexXY Efflux Pumps Simultaneously. Antimicrob. Agents Chemother. Vol. 48 (5), p. 1797-1802. DOI: 10.1128/aac.48.5.1797-1802.2004.

LLARRULL, L. I., FABIANE, S. M., KOWALSKI, J. M., BENNETT, B., SUTTON, B. J., and VILA, A. J. (2007). Asp-120 locates Zn2 for optimal metallo-β-lactamase activity. J Biol Chem. Vol. 282 (25), p. 18276-18285. DOI: 10.1074/jbc.M700742200.

MACHEBOEUF, P., CONTRERAS-MARTEL, C., JOB, V., DIDEBERG, O., and DESSEN, A. (2006). Penicillin Binding Proteins: key players in bacterial cell cycle and drug resistance processes. FEMS Microbiology Reviews. Vol. 30 (5), p. 673-691. DOI: 10.1111/j.1574-6976.2006.00024.x.

MAJIDUDDIN, F. K., and PALZKILL, T. (2003). Amino Acid Sequence Requirements at Residues 69 and 238 for the SME-1 β-Lactamase To Confer Resistance to β-Lactam Antibiotics. Antimicrob. Agents Chemother. Vol. 47 (3), p. 1062-1067. DOI: 10.1128/aac.47.3.1062-1067.2003.

MAJIDUDDIN, F. K., and PALZKILL, T. (2005). Amino acid residues that contribute to substrate specificity of class A β-lactamase SME-1. Antimicrob Agents Chemother. Vol. 49 (8), p. 3421-3427. DOI: 10.1128/AAC.49.8.3421-3427.2005.

MAMMERI, H., NORDMANN, P., BERKANI, A., and EB, F. (2008). Contribution of extended-spectrum AmpC (ESAC) β-lactamases to carbapenem resistance in *Escherichia coli*. FEMS Microbiology Letters. Vol. 282 (2), p. 238-240. DOI: 10.1111/j.1574-6968.2008.01126.x.

MANDELL, L. (2009). Doripenem: a new carbapenem in the treatment of nosocomial infection. Clin Infect Dis. Vol. 49 Suppl 1, p. S1-3. DOI: 10.1086/599809.

MARIOTTE-BOYER, S., NICOLAS-CHANOINE, M. H., and LABIA, R. (1996). A kinetic study of NMC-A β-lactamase, an Ambler class A carbapenemase also hydrolyzing cephamycins. FEMS Microbiology Letters. Vol. 143 (1), p. 29-33. DOI: 10.1111/j.1574-6968.1996.tb08457.x.

MARTINEZ, J. L. (2009). The role of natural environments in the evolution of resistance traits in pathogenic bacteria. Proceedings of the Royal Society B: Biological Sciences. Vol. 276 (1667), p. 2521-2530. DOI: 10.1098/rspb.2009.0320.

MARTINEZ, J. L., SÁNCHEZ, M. B., MARTÍNEZ-SOLANO, L., HERNANDEZ, A., GARMENDIA, L., FAJARDO, A., and ALVAREZ-ORTEGA, C. (2009). Functional role of bacterial multidrug efflux pumps in microbial natural ecosystems. FEMS Microbiology Reviews. Vol. 33 (2), p. 430-449. DOI: 10.1111/j.1574-6976.2008.00157.x.

MASSIDDA, O., ROSSOLINI, G. M., and SATTA, G. (1991). The *Aeromonas hydrophila* cphA gene: molecular heterogeneity among class B metallo-β-lactamases. J. Bacteriol. Vol. 173 (15), p. 4611-4617.

MASSOVA, I., and MOBASHERY, S. (1998). Kinship and Diversification of Bacterial Penicillin-Binding Proteins and β-Lactamases. Antimicrob. Agents Chemother. Vol. 42 (1), p. 1-17.

MASTERTON, R. G. (2009). The new treatment paradigm and the role of carbapenems. International Journal of Antimicrobial Agents. Vol. 33 (2), p. 105.e101-105.e108.

MASUDA, N., SAKAGAWA, E., OHYA, S., GOTOH, N., TSUJIMOTO, H., and NISHINO, T. (2000). Substrate Specificities of MexAB-OprM, MexCD-OprJ, and MexXY-OprM Efflux Pumps in *Pseudomonas aeruginosa*. Antimicrob. Agents Chemother. Vol. 44 (12), p. 3322-3327. DOI: 10.1128/aac.44.12.3322-3327.2000.

MATAGNE, A., LAMOTTE-BRASSEUR, J., and FRERE, J. M. (1998). Catalytic properties of class A β-lactamases: efficiency and diversity. Biochem J. Vol. 330 (Pt 2), p. 581-598.

MATERON, I. C., and PALZKILL, T. (2001). Identification of residues critical for metallo-β-lactamase function by codon randomization and selection. Protein Science. Vol. 10 (12), p. 2556-2565. DOI: 10.1110/ps.40884.

MAVEYRAUD, L., GOLEMI-KOTRA, D., ISHIWATA, A., MEROUEH, O., MOBASHERY, S., and SAMAMA, J.-P. (2002). High-Resolution X-ray Structure of an Acyl-Enzyme Species for the Class D OXA-10 β-Lactamase. Journal of the American Chemical Society. Vol. 124 (11), p. 2461-2465. DOI: 10.1021/ja016736t.

MAVEYRAUD, L., GOLEMI, D., KOTRA, L. P., TRANIER, S., VAKULENKO, S., MOBASHERY, S., and SAMAMA, J.-P. (2000). Insights into Class D β-Lactamases Are Revealed by the Crystal

Structure of the OXA10 Enzyme from *Pseudomonas aeruginosa*. Structure. Vol. 8 (12), p. 1289-1298. DOI: 10.1016/s0969-2126(00)00534-7.

MAVEYRAUD, L., MOUREY, L., KOTRA, L. P., PEDELACQ, J.-D., GUILLET, V., MOBASHERY, S., and SAMAMA, J.-P. (1998). Structural Basis for Clinical Longevity of Carbapenem Antibiotics in the Face of Challenge by the Common Class A β-Lactamases from the Antibiotic-Resistant Bacteria. Journal of the American Chemical Society. Vol. 120 (38), p. 9748-9752. DOI: 10.1021/ja9818001.

MAZEL, D., and DAVIES, J. (1999). Antibiotic resistance in microbes. Cellular and Molecular Life Sciences. Vol. 56 (9), p. 742-754. DOI: 10.1007/s000180050021.

MCCOY, A. J., GROSSE-KUNSTLEVE, R. W., ADAMS, P. D., WINN, M. D., STORONI, L. C., and READ, R. J. (2007). Phaser crystallographic software. Journal of Applied Crystallography. Vol. 40 (4), p. 658-674. DOI: 10.1107/S0021889807021206.

MCMANUS-MUNOZ, S., and CROWDER, M. W. (1999). Kinetic mechanism of metallo-β-lactamase L1 from *Stenotrophomonas maltophilia*. Biochemistry. Vol. 38 (5), p. 1547-1553. DOI: 10.1021/bi9826512.

MINASOV, G., WANG, X., and SHOICHET, B. K. (2002). An Ultrahigh Resolution Structure of TEM-1 β-Lactamase Suggests a Role for Glu166 as the General Base in Acylation. Journal of the American Chemical Society. Vol. 124 (19), p. 5333-5340. DOI: 10.1021/ja0259640.

MOALI, C., ANNE, C., LAMOTTE-BRASSEUR, J., GROSLAMBERT, S., DEVREESE, B., VAN BEEUMEN, J., GALLENI, M., and FRÈRE, J.-M. (2003). Analysis of the Importance of the Metallo-β-Lactamase Active Site Loop in Substrate Binding and Catalysis. Chemistry & Biology. Vol. 10 (4), p. 319-329. DOI: 10.1016/S1074-5521(03)00070-X.

MOEWS, P. C., KNOX, J. R., DIDEBERG, O., CHARLIER, P., and FRERE, J. M. (1990). β-lactamase of *Bacillus licheniformis* 749/C at 2 A resolution. Proteins. Vol. 7 (2), p. 156-171. DOI: 10.1002/prot.340070205.

MOLSTAD, S., LUNDBORG, C. S., KARLSSON, A. K., and CARS, O. (2002). Antibiotic prescription rates vary markedly between 13 European countries. Scand J Infect Dis. Vol. 34 (5), p. 366-371.

MOURA, A., HENRIQUES, I., SMALLA, K., and CORREIA, A. (2010). Wastewater bacterial communities bring together broad-host range plasmids, integrons and a wide diversity of uncharacterized gene cassettes. Research in Microbiology. Vol. 161 (1), p. 58-66.

MÜLLER, H. E., FANNING, G. R., and BRENNER, D. J. (1995). Isolation of *Serratia fonticola* from mollusks. Syst Appl Microbiol. Vol. 18 (2), p. 279-284.

MÜLLER, H. E., STEIGERWALT, A. G., and BRENNER, D. J. (1986). Isolation of *Serratia fonticola* from birds. Zentralbl Bakteriol Mikrobiol Hyg A. Vol. 261 (2), p. 212-218.

MURPHY, T. A., CATTO, L. E., HALFORD, S. E., HADFIELD, A. T., MINOR, W., WALSH, T. R., and SPENCER, J. (2006). Crystal Structure of *Pseudomonas aeruginosa* SPM-1 Provides Insights into Variable Zinc Affinity of Metallo-β-lactamases. Journal of Molecular Biology. Vol. 357 (3), p. 890-903.

MURSHUDOV, G. N., VAGIN, A. A., and DODSON, E. J. (1997). Refinement of Macromolecular Structures by the Maximum-Likelihood Method. Acta Crystallographica Section D. Vol. 53 (3), p. 240-255. DOI: 10.1107/S0907444996012255.

MUSSI, M. A., LIMANSKY, A. S., and VIALE, A. M. (2005). Acquisition of Resistance to Carbapenems in Multidrug-Resistant Clinical Strains of *Acinetobacter baumannii*: Natural Insertional Inactivation of a Gene Encoding a Member of a Novel Family of β-Barrel Outer Membrane Proteins. Antimicrob. Agents Chemother. Vol. 49 (4), p. 1432-1440. DOI: 10.1128/aac.49.4.1432-1440.2005.

NAAS, T., LIVERMORE, D. M., and NORDMANN, P. (1995). Characterization of an LysR family protein, SmeR from *Serratia marcescens* S6, its effect on expression of the carbapenem-hydrolyzing β-lactamase Sme-1, and comparison of this regulator with other β-lactamase regulators. Antimicrob Agents Chemother. Vol. 39 (3), p. 629-637.

NAAS, T., and NORDMANN, P. (1994). Analysis of a carbapenem-hydrolyzing class A β-lactamase from *Enterobacter cloacae* and of its LysR-type regulatory protein. Proc Natl Acad Sci U S A. Vol. 91 (16), p. 7693-7697.

NAGARAJAN, R., BOECK, L. D., GORMAN, M., HAMILL, R. L., HIGGENS, C. E., HOEHN, M. M., STARK, W. M., and WHITNEY, J. G. (1971). β-Lactam antibiotics from *Streptomyces*. Journal of the American Chemical Society. Vol. 93 (9), p. 2308-2310. DOI: 10.1021/ja00738a035.

NAVAZA, J. (2001). Implementation of molecular replacement in AMoRe. Acta Crystallogr D Biol Crystallogr. Vol. 57 (Pt 10), p. 1367-1372.

NEWMAN, J., EGAN, D., WALTER, T. S., MEGED, R., BERRY, I., JELLOUL, B., SUSSMAN, J. L., STUART, D. I., and PERRAKIS, A. (2005). Towards rationalization of crystallization screening for small- to medium-sized academic laboratories: the PACT/JCSG+ strategy. Acta Crystallographica Section D: Biological Crystallography. Vol. 61 (10), p. 1426-1431.

NIKAIDO, H. (2003). Molecular basis of bacterial outer membrane permeability revisited. Microbiol Mol Biol Rev. Vol. 67 (4), p. 593-656.

NORDMANN, P., CUZON, G., and NAAS, T. (2009). The real threat of *Klebsiella pneumoniae* carbapenemase-producing bacteria. The Lancet Infectious Diseases. Vol. 9 (4), p. 228-236. DOI: 10.1016/s1473-3099(09)70054-4.

NORDMANN, P., MARIOTTE, S., NAAS, T., LABIA, R., and NICOLAS, M. H. (1993). Biochemical properties of a carbapenem-hydrolyzing β-lactamase from *Enterobacter cloacae* and cloning of the gene into *Escherichia coli*. Antimicrob Agents Chemother. Vol. 37 (5), p. 939-946.

NORDMANN, P., POIREL, L., TOLEMAN, M. A., and WALSH, T. R. (2011). Does broad-spectrum β-lactam resistance due to NDM-1 herald the end of the antibiotic era for treatment of infections caused by Gram-negative bacteria? Journal of Antimicrobial Chemotherapy. Vol. 66 (4), p. 689-692. DOI: 10.1093/jac/dkq520.

NOSKIN, G. A., RUBIN, R. J., SCHENTAG, J. J., KLUYTMANS, J., HEDBLOM, E. C., SMULDERS, M., LAPETINA, E., and GEMMEN, E. (2005). The Burden of *Staphylococcus aureus* Infections on Hospitals in the United States: An Analysis of the 2000 and 2001 Nationwide Inpatient Sample Database. Arch Intern Med. Vol. 165 (15), p. 1756-1761. DOI: 10.1001/archinte.165.15.1756.

NUKAGA, M., ABE, T., VENKATESAN, A. M., MANSOUR, T. S., BONOMO, R. A., and KNOX, J. R. (2003a). Inhibition of Class A and Class C β-Lactamases by Penems: Crystallographic Structures of a Novel 1,4-Thiazepine Intermediate. Biochemistry. Vol. 42 (45), p. 13152-13159. DOI: 10.1021/bi034986b.

NUKAGA, M., BETHEL, C. R., THOMSON, J. M., HUJER, A. M., DISTLER, A., ANDERSON, V. E., KNOX, J. R., and BONOMO, R. A. (2008). Inhibition of Class A β-Lactamases by Carbapenems: Crystallographic Observation of Two Conformations of Meropenem in SHV-1. Journal of the American Chemical Society. Vol. 130 (38), p. 12656-12662. DOI: 10.1021/ja7111146.

NUKAGA, M., MAYAMA, K., HUJER, A. M., BONOMO, R. A., and KNOX, J. R. (2003b). Ultrahigh Resolution Structure of a Class A β-Lactamase: On the Mechanism and Specificity of the Extended-spectrum SHV-2 Enzyme. Journal of Molecular Biology. Vol. 328 (1), p. 289-301. DOI: 10.1016/S0022-2836(03)00210-9.

OCHIAI, S., SEKIGUCHI, S., HAYASHI, A., SHIMADZU, M., ISHIKO, H., MATSUSHIMA-NISHIWAKI, R., KOZAWA, O., YASUDA, M., and DEGUCHI, T. (2007). Decreased affinity of mosaic-structure recombinant penicillin-binding protein 2 for oral cephalosporins in *Neisseria gonorrhoeae*. Journal of Antimicrobial Chemotherapy. Vol. 60 (1), p. 54-60. DOI: 10.1093/jac/dkm166.

OEFNER, C., D'ARCY, A., DALY, J. J., GUBERNATOR, K., CHARNAS, R. L., HEINZE, I., HUBSCHWERLEN, C., and WINKLER, F. K. (1990). Refined crystal structure of β-lactamase from *Citrobacter freundii* indicates a mechanism for β-lactam hydrolysis. Nature. Vol. 343 (6255), p. 284-288.

OHNISHI, M., WATANABE, Y., ONO, E., TAKAHASHI, C., OYA, H., KUROKI, T., SHIMUTA, K., OKAZAKI, N., NAKAYAMA, S., and WATANABE, H. (2010). Spread of a chromosomal cefixime-resistant penA gene among different *Neisseria gonorrhoeae* lineages. Antimicrobial agents and chemotherapy. Vol. 54 (3), p. 1060-1067. DOI: 10.1128/AAC.01010-09.

OKAMOTO, K., GOTOH, N., and NISHINO, T. (2001). *Pseudomonas aeruginosa* Reveals High Intrinsic Resistance to Penem Antibiotics: Penem Resistance Mechanisms and Their Interplay. Antimicrob. Agents Chemother. Vol. 45 (7), p. 1964-1971. DOI: 10.1128/aac.45.7.1964-1971.2001.

ORENCIA, M. C., YOON, J. S., NESS, J. E., STEMMER, W. P., and STEVENS, R. C. (2001). Predicting the emergence of antibiotic resistance by directed evolution and structural analysis. Nat Struct Biol. Vol. 8 (3), p. 238-242. DOI: 10.1038/84981.

OTWINOWSKI, Z., and MINOR, W. (1997). Processing of X-ray diffraction data collected in oscillation mode. Macromolecular Crystallography, Pt A. Vol. 276, p. 307-326.

OUELLETTE, M., BISSONNETTE, L., and ROY, P. H. (1987). Precise insertion of antibiotic resistance determinants into Tn21-like transposons: nucleotide sequence of the OXA-1 β-lactamase gene. Proc Natl Acad Sci U S A. Vol. 84 (21), p. 7378-7382.

PADAYATTI, P. S., HELFAND, M. S., TOTIR, M. A., CAREY, M. P., HUJER, A. M., CAREY, P. R., BONOMO, R. A., and VAN DEN AKKER, F. (2004). Tazobactam Forms a Stoichiometric trans-Enamine Intermediate in the E166A Variant of SHV-1 β-Lactamase: 1.63 Å Crystal Structure. Biochemistry. Vol. 43 (4), p. 843-848. DOI: 10.1021/bi035985m.

PADILLA, E., LLOBET, E., DOMENECH-SANCHEZ, A., MARTINEZ-MARTINEZ, L., BENGOECHEA, J. A., and ALBERTI, S. (2010). *Klebsiella pneumoniae* AcrAB Efflux Pump Contributes to Antimicrobial Resistance and Virulence. Antimicrob. Agents Chemother. Vol. 54 (1), p. 177-183. DOI: 10.1128/aac.00715-09.

PAGES, J.-M., LAVIGNE, J.-P., LEFLON-GUIBOUT, V., MARCON, E., BERT, F., NOUSSAIR, L., and NICOLAS-CHANOINE, M.-H. (2009). Efflux Pump, the Masked Side of β-Lactam Resistance in *Klebsiella pneumoniae* Clinical Isolates. PLoS One. Vol. 4 (3), p. e4817. DOI: 10.1371/journal.pone.0004817.

PANG, Y., BROWN, B. A., STEINGRUBE, V. A., WALLACE, R. J., JR, and ROBERTS, M. C. (1994). Tetracycline resistance determinants in *Mycobacterium* and *Streptomyces* species. Antimicrob. Agents Chemother. Vol. 38 (6), p. 1408-1412. DOI: 10.1128/aac.

PAPP-WALLACE, K. M., BETHEL, C. R., DISTLER, A. M., KASUBOSKI, C., TARACILA, M., and BONOMO, R. A. (2010a). Inhibitor Resistance in the KPC-2 β-Lactamase, a Preeminent Property of This Class A β-Lactamase. Antimicrob. Agents Chemother. Vol. 54 (2), p. 890-897. DOI: 10.1128/aac.00693-09.

PAPP-WALLACE, K. M., TARACILA, M., HORNICK, J. M., HUJER, A. M., HUJER, K. M., DISTLER, A. M., ENDIMIANI, A., and BONOMO, R. A. (2010b). Substrate Selectivity and a Novel Role in Inhibitor Discrimination by Residue 237 in the KPC-2 β-Lactamase. Antimicrob. Agents Chemother. Vol. 54 (7), p. 2867-2877. DOI: 10.1128/aac.00197-10.

PATERSON, D. L., and BONOMO, R. A. (2005). Extended-spectrum β-lactamases: a clinical update. Clin Microbiol Rev. Vol. 18 (4), p. 657-686. DOI: 10.1128/CMR.18.4.657-686.2005.

PEDUZZI, J., FARZANEH, S., REYNAUD, A., BARTHELEMY, M., and LABIA, R. (1997). Characterization and amino acid sequence analysis of a new oxyimino cephalosporin-hydrolyzing class A β-lactamase from *Serratia fonticola* CUV. Biochim Biophys Acta. Vol. 1341 (1), p. 58-70.

PELEG, A. Y., and HOOPER, D. C. (2010). Hospital-Acquired Infections Due to Gram-Negative Bacteria. New England Journal of Medicine. Vol. 362 (19), p. 1804-1813. DOI: 10.1056/NEJMra0904124.

PEREZ, F., ENDIMIANI, A., HUJER, K. M., and BONOMO, R. A. (2007). The continuing challenge of ESBLs. Curr Opin Pharmacol. Vol. 7 (5), p. 459-469. DOI: 10.1016/j.coph.2007.08.003.

PERILLI, M., CELENZA, G., DE SANTIS, F., PELLEGRINI, C., FORCELLA, C., ROSSOLINI, G. M., STEFANI, S., and AMICOSANTE, G. (2008). E240V Substitution Increases Catalytic Efficiency toward Ceftazidime in a New Natural TEM-Type Extended-Spectrum β-Lactamase, TEM-149, from *Enterobacter aerogenes* and *Serratia marcescens* Clinical Isolates. Antimicrob. Agents Chemother. Vol. 52 (3), p. 915-919. DOI: 10.1128/aac.01028-07.

PFYFFER, G. E. (1992). *Serratia fonticola* as an infectious agent. Eur J Clin Microbiol Infect Dis. Vol. 11 (2), p. 199-200.

POIREL, L., HERITIER, C., and NORDMANN, P. (2004a). Chromosome-Encoded Ambler Class D β-Lactamase of *Shewanella oneidensis* as a Progenitor of Carbapenem-Hydrolyzing Oxacillinase. Antimicrob. Agents Chemother. Vol. 48 (1), p. 348-351. DOI: 10.1128/aac.48.1.348-351.2004.

POIREL, L., HERITIER, C., TOLUN, V., and NORDMANN, P. (2004b). Emergence of Oxacillinase-Mediated Resistance to Imipenem in *Klebsiella pneumoniae*. Antimicrob. Agents Chemother. Vol. 48 (1), p. 15-22. DOI: 10.1128/aac.48.1.15-22.2004.

POIREL, L., KÄMPFER, P., and NORDMANN, P. (2002). Chromosome-encoded Ambler class A β-lactamase of *Kluyvera georgiana*, a probable progenitor of a subgroup of CTX-M extended-spectrum β–lactamases. Antimicrobial agents and chemotherapy. Vol. 46 (12), p. 4038.

POIREL, L., LAGRUTTA, E., TAYLOR, P., PHAM, J., and NORDMANN, P. (2010a). Emergence of Metallo-β-Lactamase NDM-1-Producing Multidrug-Resistant *Escherichia coli* in Australia. Antimicrob. Agents Chemother. Vol. 54 (11), p. 4914-4916. DOI: 10.1128/aac.00878-10.

POIREL, L., LE THOMAS, I., NAAS, T., KARIM, A., and NORDMANN, P. (2000). Biochemical sequence analyses of GES-1, a novel class A extended-spectrum β-lactamase, and the class 1 integron In52 from *Klebsiella pneumoniae*. Antimicrob Agents Chemother. Vol. 44 (3), p. 622-632. DOI: 10.1128/aac.44.3.622-632.2000.

POIREL, L., and NORDMANN, P. (2002). Acquired carbapenem-hydrolyzing β-lactamases and their genetic support. Curr Pharm Biotechnol. Vol. 3 (2), p. 117-127.

POIREL, L., RODRIGUEZ-MARTINEZ, J.-M., AL NAIEMI, N., DEBETS-OSSENKOPP, Y. J., and NORDMANN, P. (2010b). Characterization of DIM-1, an Integron-Encoded Metallo-β-Lactamase from a *Pseudomonas stutzeri* Clinical Isolate in the Netherlands. Antimicrob. Agents Chemother. Vol. 54 (6), p. 2420-2424. DOI: 10.1128/aac.01456-09.

POIREL, L., RODRIGUEZ-MARTINEZ, J.-M., MAMMERI, H., LIARD, A., and NORDMANN, P. (2005). Origin of Plasmid-Mediated Quinolone Resistance Determinant QnrA. Antimicrob. Agents Chemother. Vol. 49 (8), p. 3523-3525. DOI: 10.1128/aac.49.8.3523-3525.2005.

POIREL, L., WELDHAGEN, G. F., NAAS, T., DE CHAMPS, C., DOVE, M. G., and NORDMANN, P. (2001). GES-2, a Class A β-Lactamase from *Pseudomonas aeruginosa* with Increased Hydrolysis of Imipenem. Antimicrob. Agents Chemother. Vol. 45 (9), p. 2598-2603. DOI: 10.1128/aac.45.9.2598-2603.2001.

POOLE, K. (2007). Efflux pumps as antimicrobial resistance mechanisms. Ann Med. Vol. 39 (3), p. 162-176. DOI: 10.1080/07853890701195262.

POTTERTON, E., BRIGGS, P., TURKENBURG, M., and DODSON, E. (2003). A graphical user interface to the CCP4 program suite. Acta Crystallographica Section D. Vol. 59 (7), p. 1131-1137. DOI: 10.1107/S0907444903008126.

POTTERTON, L., MCNICHOLAS, S., KRISSINEL, E., GRUBER, J., COWTAN, K., EMSLEY, P., MURSHUDOV, G. N., COHEN, S., PERRAKIS, A., and NOBLE, M. (2004). Developments in the

CCP4 molecular-graphics project. Acta Crystallogr D Biol Crystallogr. Vol. 60 (Part 12 Sp. Iss. 1), p. 2288-2294.

POURNARAS, S., POULOU, A., VOULGARI, E., VRIONI, G., KRISTO, I., and TSAKRIS, A. (2010). Detection of the new metallo-β-lactamase VIM-19 along with KPC-2, CMY-2 and CTX-M-15 in. Journal of Antimicrobial Chemotherapy. Vol. 65 (8), p. 1604-1607. DOI: 10.1093/jac/dkq190.

PROJAN, S. J. (2003). Why is big Pharma getting out of antibacterial drug discovery? Current Opinion in Microbiology. Vol. 6 (5), p. 427-430. DOI: 10.1016/j.mib.2003.08.003.

QIN, X., RAZIA, Y., JOHNSON, J. R., STAPP, J. R., BOSTER, D. R., TSOSIE, T., SMITH, D. L., BRADEN, C. R., GAY, K., ANGULO, F. J*., et al.* (2006). Ciprofloxacin-Resistant Gram-Negative Bacilli in the Fecal Microflora of Children. Antimicrob. Agents Chemother. Vol. 50 (10), p. 3325-3329. DOI: 10.1128/aac.00548-06.

QUALE, J., BRATU, S., GUPTA, J., and LANDMAN, D. (2006). Interplay of Efflux System, ampC, and oprD Expression in Carbapenem Resistance of *Pseudomonas aeruginosa* Clinical Isolates. Antimicrob. Agents Chemother. Vol. 50 (5), p. 1633-1641. DOI: 10.1128/aac.50.5.1633-1641.2006.

QUEENAN, A. M., and BUSH, K. (2007). Carbapenemases: the Versatile β-Lactamases. Clin. Microbiol. Rev. Vol. 20 (3), p. 440-458. DOI: 10.1128/cmr.00001-07.

QUEENAN, A. M., SHANG, W., SCHRECKENBERGER, P., LOLANS, K., BUSH, K., and QUINN, J. (2006). SME-3, a novel member of the *Serratia marcescens* SME family of carbapenem-hydrolyzing β-lactamases. Antimicrob Agents Chemother. Vol. 50 (10), p. 3485-3487. DOI: 10.1128/AAC.00363-06.

QUEENAN, A. M., TORRES-VIERA, C., GOLD, H. S., CARMELI, Y., ELIOPOULOS, G. M., MOELLERING, R. C., JR., QUINN, J. P., HINDLER, J., MEDEIROS, A. A., and BUSH, K. (2000). SME-type carbapenem-hydrolyzing class A β-lactamases from geographically diverse *Serratia marcescens* strains. Antimicrob Agents Chemother. Vol. 44 (11), p. 3035-3039.

RAQUET, X., LAMOTTE-BRASSEUR, J., BOUILLENNE, F., and FRERE, J. M. (1997). A disulfide bridge near the active site of carbapenem-hydrolyzing class A β-lactamases might explain their unusual substrate profile. Proteins. Vol. 27 (1), p. 47-58. DOI: 10.1002/(SICI)1097-0134(199701)27:1<47::AID-PROT6>3.0.CO;2-K.

RASIA, R. M., and VILA, A. J. (2004). Structural determinants of substrate binding to *Bacillus cereus* metallo-β-lactamase. J Biol Chem. Vol. 279 (25), p. 26046-26051. DOI: 10.1074/jbc.M311373200.

RASMUSSEN, B. A., and BUSH, K. (1997). Carbapenem-hydrolyzing β-lactamases. Antimicrob Agents Chemother. Vol. 41 (2), p. 223-232.

RASMUSSEN, B. A., BUSH, K., KEENEY, D., YANG, Y., HARE, R., O'GARA, C., and MEDEIROS, A. A. (1996). Characterization of IMI-1 β-lactamase, a class A carbapenem-hydrolyzing enzyme from *Enterobacter cloacae*. Antimicrob Agents Chemother. Vol. 40 (9), p. 2080-2086.

RASMUSSEN, B. A., GLUZMAN, Y., and TALLY, F. P. (1990). Cloning and sequencing of the class B β-lactamase gene (ccrA) from *Bacteroides fragilis* TAL3636. Antimicrob. Agents Chemother. Vol. 34 (8), p. 1590-1592. DOI: 10.1128/aac.

RHODES, G., HUYS, G., SWINGS, J., MCGANN, P., HINEY, M., SMITH, P., and PICKUP, R. W. (2000). Distribution of Oxytetracycline Resistance Plasmids between Aeromonads in Hospital and Aquaculture Environments: Implication of Tn1721 in Dissemination of the Tetracycline Resistance Determinant Tet A. Appl. Environ. Microbiol. Vol. 66 (9), p. 3883-3890. DOI: 10.1128/aem.66.9.3883-3890.2000.

RICE, L. B. (2009). The clinical consequences of antimicrobial resistance. Current Opinion in Microbiology. Vol. 12 (5), p. 476-481. DOI: 10.1016/j.mib.2009.08.001.

RICHMOND, M. H. (1963). Purification and Properties of the Exopenicillinase from *Staphylococcus aureus*. Biochem J. Vol. 88, p. 452-459.

RICHMOND, M. H., and SYKES, R. B. (1973). The β-lactamases of Gram-negative bacteria and their possible physiological role. Adv Microb Physiol. Vol. 9, p. 31-88.

ROBERTS, R. R., HOTA, B., AHMAD, I., SCOTT, R. D., FOSTER, S. D., ABBASI, F., SCHABOWSKI, S., KAMPE, L. M., CIAVARELLA, G. G., SUPINO, M*., et al.* (2009). Hospital and Societal Costs of Antimicrobial-Resistant Infections in a Chicago Teaching Hospital: Implications for Antibiotic Stewardship. Clinical Infectious Diseases. Vol. 49 (8), p. 1175-1184. DOI: 10.1086/605630.

ROBLEDO, I. E., AQUINO, E. E., SANTE, M. I., SANTANA, J. L., OTERO, D. M., LEON, C. F., and VAZQUEZ, G. J. (2010). Detection of KPC in *Acinetobacter* spp. in Puerto Rico. Antimicrob. Agents Chemother. Vol. 54 (3), p. 1354-1357. DOI: 10.1128/aac.00899-09.

RODRIGUEZ-MARTINEZ, J. M., POIREL, L., and NORDMANN, P. (2009). Molecular epidemiology and mechanisms of carbapenem resistance in *Pseudomonas aeruginosa*. Antimicrob Agents Chemother. Vol. 53 (11), p. 4783-4788. DOI: 10.1128/AAC.00574-09.

ROONEY, P. J., O'LEARY, M. C., LOUGHREY, A. C., MCCALMONT, M., SMYTH, B., DONAGHY, P., BADRI, M., WOODFORD, N., KARISIK, E., and LIVERMORE, D. M. (2009). Nursing homes as a reservoir of extended-spectrum β-lactamase (ESBL)-producing ciprofloxacin-resistant

Escherichia coli. Journal of Antimicrobial Chemotherapy. Vol. 64 (3), p. 635-641. DOI: 10.1093/jac/dkp220.

ROSSOLINI, G. M., CONDEMI, M. A., PANTANELLA, F., DOCQUIER, J.-D., AMICOSANTE, G., and THALLER, M. C. (2001). Metallo-β-Lactamase Producers in Environmental Microbiota: New Molecular Class B Enzyme in *Janthinobacterium lividum*. Antimicrob. Agents Chemother. Vol. 45 (3), p. 837-844. DOI: 10.1128/aac.45.3.837-844.2001.

ROSSOLINI, G. M., FRANCESCHINI, N., RICCIO, M. L., MERCURI, P. S., PERILLI, M., GALLENI, M., FRERE, J. M., and AMICOSANTE, G. (1998). Characterization and sequence of the *Chryseobacterium* (*Flavobacterium*) *meningosepticum* carbapenemase: a new molecular class B β-lactamase showing a broad substrate profile. Biochem. J. Vol. 332 (1), p. 145-152.

RUSSO, T. A., MACDONALD, U., BEANAN, J. M., OLSON, R., MACDONALD, I. J., SAUBERAN, S. L., LUKE, N. R., SCHULTZ, L. W., and UMLAND, T. C. (2009). Penicillin-binding protein 7/8 contributes to the survival of *Acinetobacter baumannii* in vitro and in vivo. J Infect Dis. Vol. 199 (4), p. 513-521. DOI: 10.1086/596317.

SAAVEDRA, M. J., PEIXE, L., SOUSA, J. C., HENRIQUES, I., ALVES, A., and CORREIA, A. (2003). Sfh-I, a subclass B2 metallo-β-lactamase from a *Serratia fonticola* environmental isolate. Antimicrob Agents Chemother. Vol. 47 (7), p. 2330-2333.

SABATH, L. D., and ABRAHAM, E. P. (1966). Zinc as a cofactor for cephalosporinase from *Bacillus cereus* 569. Biochem J. Vol. 98 (1), p. 11C-13C.

SADER, H. S., FRITSCHE, T. R., and JONES, R. N. (2005). Potency and spectrum trends for cefepime tested against 65746 clinical bacterial isolates collected in North American medical centers: results from the SENTRY Antimicrobial Surveillance Program (1998-2003). Diagnostic Microbiology and Infectious Disease. Vol. 52 (3), p. 265-273. DOI: 10.1016/j.diagmicrobio.2005.02.003.

SAMUELSEN, Ø., CASTANHEIRA, M., WALSH, T. R., and SPENCER, J. (2008). Kinetic characterization of VIM-7, a divergent member of the VIM metallo-beta-lactamase family. Antimicrob Agents Chemother. Vol. 52 (8), p. 2905-2908.

SAVES, I., BURLET-SCHILTZ, O., SWARN, P., LEFVRE, F., MASSON, J.-M., PROM, J.-C., and SAMAMA, J.-P. (1995). The Asparagine to Aspartic Acid Substitution at Position 276 of TEM-35 and TEM-36 Is Involved in the β−Lactamase Resistance to Clavulanic Acid. Journal of Biological Chemistry. Vol. 270 (31), p. 18240-18245. DOI: 10.1074/jbc.270.31.18240.

SCHLEIFER, K. H., and KANDLER, O. (1972). Peptidoglycan types of bacterial cell walls and their taxonomic implications. Microbiol. Mol. Biol. Rev. Vol. 36 (4), p. 407-477.

SCHUTTELKOPF, A. W., and VAN AALTEN, D. M. F. (2004). PRODRG: a tool for high-throughput crystallography of protein-ligand complexes. Acta Crystallographica Section D. Vol. 60 (8), p. 1355-1363. DOI: 10.1107/S0907444904011679.

SEGATORE, B., MASSIDDA, O., SATTA, G., SETACCI, D., and AMICOSANTE, G. (1993). High specificity of cphA-encoded metallo-β-lactamase from *Aeromonas hydrophila* AE036 for carbapenems and its contribution to β-lactam resistance. Antimicrob Agents Chemother. Vol. 37 (6), p. 1324-1328.

SHARMA, N. P., HAJDIN, C., CHANDRASEKAR, S., BENNETT, B., YANG, K. W., and CROWDER, M. W. (2006). Mechanistic studies on the mononuclear ZnII-containing metallo-β-lactamase ImiS from *Aeromonas sobria*. Biochemistry. Vol. 45 (35), p. 10729-10738.

SHELDRICK, G. (2008). A short history of SHELX. Acta Crystallographica Section A. Vol. 64 (1), p. 112-122. DOI: doi:10.1107/S0108767307043930.

SHIMAMURA, T., IBUKA, A., FUSHINOBU, S., WAKAGI, T., ISHIGURO, M., ISHII, Y., and MATSUZAWA, H. (2002). Acyl-intermediate Structures of the Extended-spectrum Class A β-Lactamase, Toho-1, in Complex with Cefotaxime, Cephalothin, and Benzylpenicillin. Journal of Biological Chemistry. Vol. 277 (48), p. 46601-46608. DOI: 10.1074/jbc.M207884200.

SIMM, A. M., HIGGINS, C. S., PULLAN, S. T., AVISON, M. B., NIUMSUP, P., ERDOZAIN, O., BENNETT, P. M., and WALSH, T. R. (2001). A novel metallo-β-lactamase, Mbl1b, produced by the environmental bacterium *Caulobacter crescentus*. FEBS Letters. Vol. 509 (3), p. 350-354.

SIMONA, F., MAGISTRATO, A., DAL PERARO, M., CAVALLI, A., VILA, A. J., and CARLONI, P. (2009). Common mechanistic features among metallo-β-lactamases: a computational study of *Aeromonas hydrophila* CphA enzyme. J Biol Chem. Vol. 284 (41), p. 28164-28171. DOI: 10.1074/jbc.M109.049502.

SMITH, A. M., FELDMAN, C., MASSIDDA, O., MCCARTHY, K., NDIWENI, D., and KLUGMAN, K. P. (2005). Altered PBP 2A and its role in the development of penicillin, cefotaxime, and ceftriaxone resistance in a clinical isolate of *Streptococcus pneumoniae*. Antimicrob Agents Chemother. Vol. 49 (5), p. 2002-2007. DOI: 10.1128/AAC.49.5.2002-2007.2005.

SMITH MOLAND, E., HANSON, N. D., HERRERA, V. L., BLACK, J. A., LOCKHART, T. J., HOSSAIN, A., JOHNSON, J. A., GOERING, R. V., and THOMSON, K. S. (2003). Plasmid-mediated, carbapenem-hydrolysing β-lactamase, KPC-2, in *Klebsiella pneumoniae* isolates. J Antimicrob Chemother. Vol. 51 (3), p. 711-714.

SONG, W., SUH, B., CHOI, J. Y., JEONG, S. H., JEON, E. H., LEE, Y. K., HONG, S. G., and LEE, K. (2009). In vivo selection of carbapenem-resistant *Klebsiella pneumoniae* by OmpK36 loss during

meropenem treatment. Diagn Microbiol Infect Dis. Vol. 65 (4), p. 447-449. DOI: 10.1016/j.diagmicrobio.2009.08.010.

SOUGAKOFF, W., L'HERMITE, G., PERNOT, L., NAAS, T., GUILLET, V., NORDMANN, P., JARLIER, V., and DELETTRE, J. (2002). Structure of the imipenem-hydrolyzing class A β–lactamase SME-1 from *Serratia marcescens*. Acta Crystallographica Section D. Vol. 58 (2), p. 267-274. DOI: doi:10.1107/S0907444901019606.

SOUGAKOFF, W., NAAS, T., NORDMANN, P., COLLATZ, E., and JARLIER, V. (1999). Role of Ser-237 in the substrate specificity of the carbapenem-hydrolyzing class A β-lactamase Sme-1. Biochim Biophys Acta. Vol. 1433 (1-2), p. 153-158. DOI: S0167-4838(99)00138-7.

SPELLBERG, B., GUIDOS, R., GILBERT, D., BRADLEY, J., BOUCHER, H. W., SCHELD, W. M., BARTLETT, J. G., EDWARDS, J., and AMERICA, T. I. D. S. O. (2008). The Epidemic of Antibiotic-Resistant Infections: A Call to Action for the Medical Community from the Infectious Diseases Society of America. Clinical Infectious Diseases. Vol. 46 (2), p. 155-164. DOI: 10.1086/524891.

SPENCER, J., CLARKE, A. R., and WALSH, T. R. (2001). Novel mechanism of hydrolysis of therapeutic β-lactams by *Stenotrophomonas maltophilia* L1 metallo-β-lactamase. J Biol Chem. Vol. 276 (36), p. 33638-33644. DOI: 10.1074/jbc.M105550200.

SPENCER, J., READ, J., SESSIONS, R. B., HOWELL, S., BLACKBURN, G. M., and GAMBLIN, S. J. (2005). Antibiotic Recognition by Binuclear Metallo-β-Lactamases Revealed by X-ray Crystallography. Journal of the American Chemical Society. Vol. 127 (41), p. 14439-14444. DOI: 10.1021/ja0536062.

STEC, B., HOLTZ, K. M., WOJCIECHOWSKI, C. L., and KANTROWITZ, E. R. (2005). Structure of the wild-type TEM-1 β-lactamase at 1.55 A and the mutant enzyme Ser70Ala at 2.1 A suggest the mode of noncovalent catalysis for the mutant enzyme. Acta Crystallographica Section D. Vol. 61 (8), p. 1072-1079. DOI: 10.1107/S0907444905014356.

STOCK, I., BURAK, S., SHERWOOD, K. J., GRUGER, T., and WIEDEMANN, B. (2003). Natural antimicrobial susceptibilities of strains of 'unusual' *Serratia* species: *S. ficaria*, *S. fonticola*, *S. odorifera*, *S. plymuthica* and *S. rubidaea*. J Antimicrob Chemother. Vol. 51 (4), p. 865-885. DOI: 10.1093/jac/dkg156.

STOCZKO, M., FRERE, J.-M., ROSSOLINI, G. M., and DOCQUIER, J.-D. (2006). Postgenomic Scan of Metallo-β-Lactamase Homologues in Rhizobacteria: Identification and Characterization of BJP-1, a Subclass B3 Ortholog from *Bradyrhizobium japonicum*. Antimicrob. Agents Chemother. Vol. 50 (6), p. 1973-1981. DOI: 10.1128/aac.01551-05.

STRYNADKA, N. C. J., ADACHI, H., JENSEN, S. E., JOHNS, K., SIELECKI, A., BETZEL, C., SUTOH, K., and JAMES, M. N. G. (1992). Molecular structure of the acyl-enzyme intermediate in β-lactam hydrolysis at 1.7 A resolution. Nature. Vol. 359 (6397), p. 700-705.

SWARÉN, P., MAVEYRAUD, L., RAQUET, X., CABANTOUS, S., DUEZ, C., PÉDELACQ, J.-D., MARIOTTE-BOYER, S., MOUREY, L., LABIA, R., NICOLAS-CHANOINE, M.-H*., et al.* (1998). X-ray Analysis of the NMC-A β-Lactamase at 1.64-Å Resolution, a Class A Carbapenemase with Broad Substrate Specificity. Journal of Biological Chemistry. Vol. 273 (41), p. 26714-26721. DOI: 10.1074/jbc.273.41.26714.

SYKES, R. (2010). The 2009 Garrod Lecture: The evolution of antimicrobial resistance: a Darwinian perspective. Journal of Antimicrobial Chemotherapy. Vol. 65 (9), p. 1842-1852. DOI: 10.1093/jac/dkq217.

SYKES, R. B., CIMARUSTI, C. M., BONNER, D. P., BUSH, K., FLOYD, D. M., GEORGOPAPADAKOU, N. H., KOSTER, W. H., LIU, W. C., PARKER, W. L., PRINCIPE, P. A*., et al.* (1981). Monocyclic β-lactam antibiotics produced by bacteria. Nature. Vol. 291 (5815), p. 489-491.

SYKES, R. B., and MATTHEW, M. (1976). The β-lactamases of Gram-negative bacteria and their role in resistance to β-lactam antibiotics. J Antimicrob Chemother. Vol. 2 (2), p. 115-157.

TAHLAN, K., AHN, S. K., SING, A., BODNARUK, T. D., WILLEMS, A. R., DAVIDSON, A. R., and NODWELL, J. R. (2007). Initiation of actinorhodin export in *Streptomyces coelicolor*. Molecular Microbiology. Vol. 63 (4), p. 951-961. DOI: 10.1111/j.1365-2958.2006.05559.x.

TATO, M., COQUE, T. M., BAQUERO, F., and CANTON, R. (2010). Dispersal of Carbapenemase blaVIM-1 Gene Associated with Different Tn402 Variants, Mercury Transposons, and Conjugative Plasmids in Enterobacteriaceae and *Pseudomonas aeruginosa*. Antimicrob. Agents Chemother. Vol. 54 (1), p. 320-327. DOI: 10.1128/aac.00783-09.

THERRIEN, C., and LEVESQUE, R. C. (2000). Molecular basis of antibiotic resistance and β-lactamase inhibition by mechanism-based inactivators: perspectives and future directions. FEMS Microbiology Reviews. Vol. 24 (3), p. 251-262. DOI: 10.1111/j.1574-6976.2000.tb00541.x.

THOMSON, J. M., and BONOMO, R. A. (2005). The threat of antibiotic resistance in Gram-negative pathogenic bacteria: β-lactams in peril! Current Opinion in Microbiology. Vol. 8 (5), p. 518-524.

TIONI, M. F., LLARRULL, L. I., POEYLAUT-PALENA, A. A., MARTI, M. A., SAGGU, M., PERIYANNAN, G. R., MATA, E. G., BENNETT, B., MURGIDA, D. H., and VILA, A. J. (2008). Trapping and characterization of a reaction intermediate in carbapenem hydrolysis by *B. cereus* metallo-β-lactamase. J Am Chem Soc. Vol. 130 (47), p. 15852-15863. DOI: 10.1021/ja801169j.

TIPPER, D. J., and STROMINGER, J. L. (1965). Mechanism of action of penicillins: a proposal based on their structural similarity to acyl-D-alanyl-D-alanine. Proceedings of the National Academy of Sciences of the United States of America. Vol. 54 (4), p. 1133-1141.

TOLEMAN, M. A., BENNETT, P. M., and WALSH, T. R. (2006). ISCR Elements: Novel Gene-Capturing Systems of the 21st Century? Microbiol. Mol. Biol. Rev. Vol. 70 (2), p. 296-316. DOI: 10.1128/mmbr.00048-05.

TOLEMAN, M. A., SIMM, A. M., MURPHY, T. A., GALES, A. C., BIEDENBACH, D. J., JONES, R. N., and WALSH, T. R. (2002). Molecular characterization of SPM-1, a novel metallo-β-lactamase isolated in Latin America: report from the SENTRY antimicrobial surveillance programme. Journal of Antimicrobial Chemotherapy. Vol. 50 (5), p. 673-679. DOI: 10.1093/jac/dkf210.

TOMAS, M. D. M., BECEIRO, A., PEREZ, A., VELASCO, D., MOURE, R., VILLANUEVA, R., MARTINEZ-BELTRAN, J., and BOU, G. (2005). Cloning and Functional Analysis of the Gene Encoding the 33- to 36-Kilodalton Outer Membrane Protein Associated with Carbapenem Resistance in *Acinetobacter baumannii*. Antimicrob. Agents Chemother. Vol. 49 (12), p. 5172-5175. DOI: 10.1128/aac.49.12.5172-5175.2005.

TREMBLAY, L. W., XU, H., and BLANCHARD, J. S. (2010). Structures of the Michaelis Complex (1.2 Å) and the Covalent Acyl Intermediate (2.0 Å) of Cefamandole Bound in the Active Sites of the *Mycobacterium tuberculosis* β-Lactamase K73A and E166A Mutants. Biochemistry. Vol. 49 (45), p. 9685-9687. DOI: 10.1021/bi1015088.

ULLAH, J. H., WALSH, T. R., TAYLOR, I. A., EMERY, D. C., VERMA, C. S., GAMBLIN, S. J., and SPENCER, J. (1998). The crystal structure of the L1 metallo-β-lactamase from *Stenotrophomonas maltophilia* at 1.7 A resolution. J Mol Biol. Vol. 284 (1), p. 125-136. DOI: 10.1006/jmbi.1998.2148.

VALLADARES, M. H., FELICI, A., WEBER, G., ADOLPH, H. W., ZEPPEZAUER, M., ROSSOLINI, G. M., AMICOSANTE, G., FRERE, J. M., and GALLENI, M. (1997). Zn(II) dependence of the *Aeromonas hydrophila* AE036 metallo-β-lactamase activity and stability. Biochemistry. Vol. 36 (38), p. 11534-11541. DOI: 10.1021/bi971056h.

VANHOVE, M., ZAKHEM, M., DEVREESE, B., FRANCESCHINI, N., ANNE, C., BEBRONE, C., AMICOSANTE, G., ROSSOLINI, G. M., VAN BEEUMEN, J., FRERE, J. M.*, et al.* (2003). Role of Cys221 and Asn116 in the zinc-binding sites of the *Aeromonas hydrophila* metallo-β-lactamase. Cell Mol Life Sci. Vol. 60 (11), p. 2501-2509. DOI: 10.1007/s00018-003-3092-x.

VENKATACHALAM, K. V., HUANG, W., LAROCCO, M., and PALZKILL, T. (1994). Characterization of TEM-1 β-lactamase mutants from positions 238 to 241 with increased catalytic efficiency for ceftazidime. Journal of Biological Chemistry. Vol. 269 (38), p. 23444-23450.

VILLAVERDE, A., and MAR CARRIÓ, M. (2003). Protein aggregation in recombinant bacteria: biological role of inclusion bodies. Biotechnology Letters. Vol. 25 (17), p. 1385-1395. DOI: 10.1023/a:1025024104862.

VILLEGAS, M. V., LOLANS, K., CORREA, A., KATTAN, J. N., LOPEZ, J. A., QUINN, J. P., and AND THE COLOMBIAN NOSOCOMIAL RESISTANCE STUDY GROUP. (2007). First Identification of *Pseudomonas aeruginosa* Isolates Producing a KPC-Type Carbapenem-Hydrolyzing β-Lactamase. Antimicrob. Agents Chemother. Vol. 51 (4), p. 1553-1555. DOI: 10.1128/aac.01405-06.

VOLLMER, W., BLANOT, D., and DE PEDRO, M. A. (2008). Peptidoglycan structure and architecture. FEMS Microbiol Rev. Vol. 32 (2), p. 149-167. DOI: 10.1111/j.1574-6976.2007.00094.x.

VOURLI, S., GIAKKOUPI, P., MIRIAGOU, V., TZELEPI, E., VATOPOULOS, A. C., and TZOUVELEKIS, L. S. (2004). Novel GES/IBC extended-spectrum β-lactamase variants with carbapenemase activity in clinical enterobacteria. FEMS Microbiology Letters. Vol. 234 (2), p. 209-213. DOI: 10.1111/j.1574-6968.2004.tb09535.x.

WACHINO, J.-I., DOI, Y., YAMANE, K., SHIBATA, N., YAGI, T., KUBOTA, T., and ARAKAWA, Y. (2004). Molecular Characterization of a Cephamycin-Hydrolyzing and Inhibitor-Resistant Class A β-Lactamase, GES-4, Possessing a Single G170S Substitution in the Omega-Loop. Antimicrob. Agents Chemother. Vol. 48 (8), p. 2905-2910. DOI: 10.1128/aac.48.8.2905-2910.2004.

WALSH, C. (2000). Molecular mechanisms that confer antibacterial drug resistance. Nature. Vol. 406 (6797), p. 775-781.

WALSH, T. R. (2008). Clinically significant carbapenemases: an update. Current Opinion in Infectious Diseases. Vol. 21 (4), p. 367-371 DOI: 10.1097/QCO.0b013e328303670b.

WALSH, T. R., GAMBLIN, S., EMERY, D. C., MACGOWAN, A. P., and BENNETT, P. M. (1996). Enzyme kinetics and biochemical analysis of ImiS, the metallo-β-lactamase from *Aeromonas sobria* 163a. J Antimicrob Chemother. Vol. 37 (3), p. 423-431.

WALSH, T. R., HALL, L., ASSINDER, S. J., NICHOLS, W. W., CARTWRIGHT, S. J., MACGOWAN, A. P., and BENNETT, P. M. (1994). Sequence analysis of the L1 metallo-β-lactamase from *Xanthomonas maltophilia*. Biochimica et Biophysica Acta (BBA) - Gene Structure and Expression. Vol. 1218 (2), p. 199-201.

WALSH, T. R., NEVILLE, W. A., HARAN, M. H., TOLSON, D., PAYNE, D. J., BATESON, J. H., MACGOWAN, A. P., and BENNETT, P. M. (1998). Nucleotide and amino acid sequences of the metallo-β-lactamase, ImiS, from *Aeromonas veronii* bv. *sobria*. Antimicrob Agents Chemother. Vol. 42 (2), p. 436-439.

WALSH, T. R., TOLEMAN, M. A., POIREL, L., and NORDMANN, P. (2005). Metallo-β-lactamases: the quiet before the storm? Clin Microbiol Rev. Vol. 18 (2), p. 306-325. DOI: 10.1128/CMR.18.2.306-325.2005.

WALTHER-RASMUSSEN, J., and HOIBY, N. (2007). Class A carbapenemases. J Antimicrob Chemother. Vol. 60 (3), p. 470-482. DOI: 10.1093/jac/dkm226.

WALTHER-RASMUSSEN, J., and HØIBY, N. (2006). OXA-type carbapenemases. Journal of Antimicrobial Chemotherapy. Vol. 57 (3), p. 373-383. DOI: 10.1093/jac/dki482.

WALTHER-RASMUSSEN, J., JOHNSEN, A. H., and HOIBY, N. (1999). Terminal truncations in amp C β-lactamase from a clinical isolate of *Pseudomonas aeruginosa*. Eur J Biochem. Vol. 263 (2), p. 478-485.

WANG, J., ZHOU, J. Y., QU, T. T., SHEN, P., WEI, Z. Q., YU, Y. S., and LI, L. J. (2010). Molecular epidemiology and mechanisms of carbapenem resistance in *Pseudomonas aeruginosa* isolates from Chinese hospitals. Int J Antimicrob Agents. Vol. 35 (5), p. 486-491. DOI: 10.1016/j.ijantimicag.2009.12.014.

WANG, Z., FAST, W., and BENKOVIC, S. J. (1999). On the Mechanism of the Metallo-β-lactamase from *Bacteroides fragilis*. Biochemistry. Vol. 38 (31), p. 10013-10023. DOI: 10.1021/bi990356r.

WANG, Z., FAST, W., VALENTINE, A. M., and BENKOVIC, S. J. (1999). Metallo-β-lactamase: structure and mechanism. Curr Opin Chem Biol. Vol. 3 (5), p. 614-622. DOI: S1367-5931(99)00017-4.

WATANABE, M., IYOBE, S., INOUE, M., and MITSUHASHI, S. (1991). Transferable imipenem resistance in *Pseudomonas aeruginosa*. Antimicrob Agents Chemother. Vol. 35 (1), p. 147-151.

WEGENER, H. C. (2003). Antibiotics in animal feed and their role in resistance development. Curr Opin Microbiol. Vol. 6 (5), p. 439-445. DOI: S1369527403001206.

WITTE, W. (1998). Medical consequences of antibiotic use in agriculture. Science. Vol. 279 (5353), p. 996-997.

WOODFORD, N., TIERNO, P. M., JR., YOUNG, K., TYSALL, L., PALEPOU, M. F., WARD, E., PAINTER, R. E., SUBER, D. F., SHUNGU, D., SILVER, L. L.*, et al.* (2004). Outbreak of *Klebsiella pneumoniae* producing a new carbapenem-hydrolyzing class A β-lactamase, KPC-3, in a New York Medical Center. Antimicrob Agents Chemother. Vol. 48 (12), p. 4793-4799. DOI: 10.1128/AAC.48.12.4793-4799.2004.

WRIGHT, G. D. (2007). The antibiotic resistome: the nexus of chemical and genetic diversity. Nat Rev Micro. Vol. 5 (3), p. 175-186.

WRIGHT, G. D. (2010). Antibiotic resistance in the environment: a link to the clinic? Current Opinion in Microbiology. Vol. 13 (5), p. 589-594. DOI: DOI: 10.1016/j.mib.2010.08.005.

WRIGHT, G. D., and BEGLEY, T. P. (2007). *Antibiotics: Bacterial Resistance*: John Wiley & Sons, Inc.

XI, C., ZHANG, Y., MARRS, C. F., YE, W., SIMON, C., FOXMAN, B., and NRIAGU, J. (2009). Prevalence of Antibiotic Resistance in Drinking Water Treatment and Distribution Systems. Appl. Environ. Microbiol. Vol. 75 (17), p. 5714-5718. DOI: 10.1128/aem.00382-09.

XU, D., XIE, D., and GUO, H. (2006). Catalytic mechanism of class B2 metallo-β-lactamase. J Biol Chem. Vol. 281 (13), p. 8740-8747. DOI: 10.1074/jbc.M512517200.

YAMAGUCHI, Y., TAKASHIO, N., WACHINO, J.-I., YAMAGATA, Y., ARAKAWA, Y., MATSUDA, K., and KUROSAKI, H. (2010). Structure of metallo-β-lactamase IND-7 from a *Chryseobacterium indologenes* clinical isolate at 1.65-Å resolution. Journal of Biochemistry. Vol. 147 (6), p. 905-915. DOI: 10.1093/jb/mvq029.

YANG, Q., WANG, H., SUN, H., CHEN, H., XU, Y., and CHEN, M. (2010). Phenotypic and Genotypic Characterization of Enterobacteriaceae with Decreased Susceptibility to Carbapenems: Results from Large Hospital-Based Surveillance Studies in China. Antimicrob. Agents Chemother. Vol. 54 (1), p. 573-577. DOI: 10.1128/aac.01099-09.

YANG, Y., and BUSH, K. (1996). Biochemical characterization of the carbapenem-hydrolyzing β-lactamase AsbM1 from Aeromonas sobria AER 14M: a member of a novel subgroup of metallo-β-lactamases. FEMS Microbiology Letters. Vol. 137 (2-3), p. 193-200. DOI: 10.1111/j.1574-6968.1996.tb08105.x.

YANG, Y. J., WU, P. J., and LIVERMORE, D. M. (1990). Biochemical characterization of a β-lactamase that hydrolyzes penems and carbapenems from two *Serratia marcescens* isolates. Antimicrob Agents Chemother. Vol. 34 (5), p. 755-758.

YIGIT, H., QUEENAN, A. M., ANDERSON, G. J., DOMENECH-SANCHEZ, A., BIDDLE, J. W., STEWARD, C. D., ALBERTI, S., BUSH, K., and TENOVER, F. C. (2001). Novel carbapenem-hydrolyzing β-lactamase, KPC-1, from a carbapenem-resistant strain of *Klebsiella pneumoniae*. Antimicrob Agents Chemother. Vol. 45 (4), p. 1151-1161. DOI: 10.1128/AAC.45.4.1151-1161.2001.

YIGIT, H., QUEENAN, A. M., RASHEED, J. K., BIDDLE, J. W., DOMENECH-SANCHEZ, A., ALBERTI, S., BUSH, K., and TENOVER, F. C. (2003). Carbapenem-Resistant Strain of *Klebsiella oxytoca* Harboring Carbapenem-Hydrolyzing β-Lactamase KPC-2. Antimicrob. Agents Chemother. Vol. 47 (12), p. 3881-3889. DOI: 10.1128/aac.47.12.3881-3889.2003.

YONG, D., TOLEMAN, M. A., GISKE, C. G., CHO, H. S., SUNDMAN, K., LEE, K., and WALSH, T. R. (2009). Characterization of a New Metallo-β-Lactamase Gene, blaNDM-1, and a Novel Erythromycin Esterase Gene Carried on a Unique Genetic Structure in *Klebsiella pneumoniae* Sequence Type 14 from India. Antimicrob. Agents Chemother. Vol. 53 (12), p. 5046-5054. DOI: 10.1128/aac.00774-09.

YU, Y.-S., DU, X.-X., ZHOU, Z.-H., CHEN, Y.-G., and LI, L.-J. (2006). First Isolation of blaIMI-2 in an *Enterobacter cloacae* Clinical Isolate from China. Antimicrob. Agents Chemother. Vol. 50 (4), p. 1610-1611. DOI: 10.1128/aac.50.4.1610-1611.2006.

ZAFARALLA, G., and MOBASHERY, S. (1992). Facilitation of the Δ^2 to Δ^1 pyrroline tautomerization of carbapenem antibiotics by the highly conserved arginine-244 of class A β-lactamases during the course of turnover. Journal of the American Chemical Society. Vol. 114 (4), p. 1505-1506. DOI: 10.1021/ja00030a070.

ZAMORANO, L., MOYA, B., JUAN, C., and OLIVER, A. (2010). Differential β-lactam resistance response driven by ampD or dacB (PBP4) inactivation in genetically diverse *Pseudomonas aeruginosa* strains. J Antimicrob Chemother. Vol. 65 (7), p. 1540-1542. DOI: 10.1093/jac/dkq142.

ZERVOSEN, A., VALLADARES, M. H., DEVREESE, B., PROSPERI-MEYS, C., ADOLPH, H. W., MERCURI, P. S., VANHOVE, M., AMICOSANTE, G., VAN BEEUMEN, J., FRERE, J. M.*, et al.* (2001). Inactivation of *Aeromonas hydrophila* metallo-β-lactamase by cephamycins and moxalactam. Eur J Biochem. Vol. 268 (13), p. 3840-3850.

ZHOU, X. Y., BORDON, F., SIROT, D., KITZIS, M. D., and GUTMANN, L. (1994). Emergence of clinical isolates of *Escherichia coli* producing TEM-1 derivatives or an OXA-1 β-lactamase conferring resistance to β-lactamase inhibitors. Antimicrob. Agents Chemother. Vol. 38 (5), p. 1085-1089. DOI: 10.1128/aac.